Towards Defence In Depth In Diabetes Glucose Self-Management

Ståhl, Fredrik

2015

Document Version:
Publisher's PDF, also known as Version of record

Towards Defence In Depth In Diabetes Glucose Self-Management

Fredrik Ståhl

LUND
UNIVERSITY

Department of Automatic Control

Cover page: The blue circle is the international symbol for diabetes.

PhD Thesis
ISRN LUTFD2/TFRT--1111--SE
ISBN 978-91-7623-575-1 (print)
ISBN 978-91-7623-576-8 (web)
ISSN 0280–5316

Department of Automatic Control
Lund University
Box 118
SE-221 00 LUND
Sweden

Printed in Sweden by Media-Tryck.
Lund 2015

Abstract

Diabetes is a disease characterized by insufficient capacity to regulate the blood glucose level. In insulin-dependent diabetes, multiple daily injections of insulin have to be administered. In-between scheduled visits to the care provider, the patient has to manage the glucose control independently. Insulin dosing is a non-trivial task and many patients find it difficult. This is reflected in the health statistics, that indicate that a majority of patients with diabetes have poor metabolic control with associate risks of several short and long term complications.

In this thesis, building blocks of a defence-in-depth approach to glucose self-management in insulin-dependent diabetes are investigated. Defence-in-depth is a concept where technical and administrative systems work in cohort to divert potentially dangerous conditions and events. In the context of insulin-dependent diabetes this amounts to avoiding low (hypoglycemia) and high (hyperglycemia) glucose values. Data from the European DIADvisor project and from a local trial conducted with patients from Skåne University Hospital were used in the thesis.

A basis for improved glucose control is understanding and knowledge of the glucose-lowering effect of insulin, the insulin action, and the corresponding glucose-elevating effect produced by meal intake. Individualized models of these impacts, and methods to improve the predictive capacity of these models, were developed. Interesting properties, such as, time-variability and nonlinear effects, were found. The models allow for the glucose level to be predicted and different meal and bolus scenarios to be simulated. Using the models, the possibility to foresee and prevent nocturnal hypoglycemia was validated with good performance in a retrospective analysis on the collected data.

Recent advances in sensor technology have allowed for commercial systems where the glucose level is measured with a high sampling rate in the interstitial fluid. However, a known deficiency with this approach is the measurement lag introduced by equilibrium dynamics between the blood and

interstitial compartments. A Kalman filter based approach to resolving this issue was developed and successfully validated in a case study.

Diabetes glucose dynamics is known to comprise both short and more long term time-variability. Merging different diversified models may prove to be a successful approach, as a means to improve performance and robustness under such conditions. A novel merging algorithm based in a Bayesian setting was developed. The suggested method admits for soft switching and interpolation between the different models based on an evaluation of the different predictors' recent performance, using a sliding data window, and by looking for data features identified to be correlated to switching. Different aspects of the merging approach were investigated, using a simulated dataset, and the concept was thereafter successfully validated, showing improved robustness to the prediction performance in comparison to relying on the individual prediction models.

Meal impact models were estimated for 56 different meal types, and a clustering analysis showed that a majority of these models could be represented by three base models. Cross-validation confirmed good predictive capacity. The insulin action and meal impact models were further used to assess whether clinical recommendations on postprandial glucose levels, issued by international patient and professional organizations, are realistic and achievable. An important finding was that the postprandial excursion of meals with rapid postprandial response may be impossible to restrain within the recommended boundaries for even moderate meal sizes. This difficulty is exaggerated for persons with slower than normal insulin action.

The above methods and models could contribute to improving already available technology in diabetes self-management such as, e.g., bolus dose guides in insulin pumps, warning systems in continuous glucose monitoring systems or in interpretation and implementation of postprandial recommendations.

Acknowledgements

First of all, I would like to express my gratitude towards my supervisor, professor Rolf Johansson, for introducing me to graduate studies and the DIAdvisor project, which he initiated, and for his encouragement over the last years. I would also like to thank the co-supervisors Per Hagander and Tore Hägglund.

I am very grateful to all the participants in both the DIAdvisor trials and the ULund trial, who willingly shared their time and data. Without these empirical data, this thesis would not have been written. Thanks to Linkura for allowing the use of their software for diet data collection.

The department is an interesting and fun workplace and I would like to thank all my colleagues for making it so. A special call-out goes to the administrative staff.

Proof-reading has been provided by Rolf Johansson, Kristian Soltesz, Tore Hägglund and Carolina Lidström, to whom I am in debt. Leif Andersson is a solid source for LaTeX advise, and without his help the thesis would have looked far worse.

The DIAdvisor project has been a very exciting project, giving me the opportunity to work in a cross-disciplinary and cross-cultural context, with a subject matter of high personal interest. It has been a pleasure collaborating with our European colleagues and enjoying the hospitality of these partners. During this project I have also been fortunate to have been working with my highly praised colleagues Marzia Cescon and Meike Stemmann, with whom I have enjoyed many rewarding moments.

Over these years, I have also had many fruitful collaborations and discussions with the clinical researcher professor Mona Landin-Olsson at the Endocrinology Department.

The person to whom I owe the most though is my wife, Åsa, whose support, love and friendship formed the foundation for this endeavour.

Financial Support

Financial support was provided by the E.U. through the DIAdvisor project, the Swedish Research Council through the LCCC and ELLIT research excellence centers, and the ULund trial was enabled thanks to support from Vinnova.

Preface

The audience of this thesis are clinicians, patients and their relatives, interested in how technology can be used to improve diabetes self-management and patient empowerment, and scientist and engineers who want to work together with the former to transform these goals into reality. While some more technical parts may be more inaccessible to someone lacking an engineering background, most of the results, discussions and conclusions should be readable to anyone with an interest in glucose self-management.

Several landmark technological and pharmacological achievements, primarily the rapid-acting and long-acting insulin analogs, the insulin pump and the continuous glucose sensor, are indispensable in this venture. Looking back, we are moving from an inflexible therapy centred around compliance, infrequent feedback and guess-work, into an agile, knowledge- and information-oriented care with higher level of patient empowerment. Within the research community, several groups are working on both the open- and closed-loop approach—the artificial pancreas. The steady progress, visible in the number of studies moving the research from the hospital bed into real-world home free-living conditions, is encouraging. In parallel, patient-driven groups such as Nightscout, often spearheaded by enthusiastic and frustrated parents of children with insulin-dependent diabetes, push the envelope of making continuous glucose monitoring more accessible and useful, by allowing sharing of the data over the cloud and on different platforms. All put together, these groups can help transform diabetes care into preventive, rather than reactive, care. This is my contribution.

Contents

1

Introduction

1.1 Motivation

Diabetes Mellitus is a chronic metabolic disease where the affected patients have disturbed glucose regulation which if left untreated, results in elevated blood glucose levels. The disease is divided into two categories; type 1 diabetes (T1DM) and type 2 diabetes (T2DM). In T1DM, the pancreatic insulin producing β-cell are destroyed due to an auto-immune response. T2DM is a common diagnosis for several different underlying causes to deteriorating glucose control, such as reduced insulin sensitivity and prolonged or deteriorated pancreatic insulin response. There is a strong genetic component to the risk of both T1DM and T2DM. The etiology behind the sudden auto-immune attack leading to type 1 is still obscured, but some evidence point to that viral infections may play a key role in the triggering mechanism [Christen et al., 2012]. Type 2 diabetes typically evolves over a number of years before diagnosis, and is strongly connected to sedentary life-style and overweight, but the incidence also increases with age.

The incidence of both types of diabetes, especially T2DM, increases at an alarming rate on a global scale. In year 2000, WHO estimated 171 million to be affected [Wild et al., 2004], and in 2014 the International Diabetes Federation (IDF) estimated the number to 387 million (of which 179 million are undiagnosed) [IDF, 2014], already exceeding the 2030 forecast from WHO in 2000. By 2035, the expected number closes in on 600 million in IDF's recent analysis [IDF, 2014]. In Sweden, the total number is about 365.000, of which about 40.000 are T1DM [The Swedish National Board of Health and Welfare, 2009a]. In general, about 10% of the patients are of T1DM. Along with the increasing numbers of affected, the total costs to society increase dramatically. In Sweden, the total direct cost of diabetes treatment was estimated to 7 billion SEK in 1998, considering only T2DM patients [Henriksson et al., 2000]. Globally, figures of 612 billion USD have been stated, amounting to 11% of the total healthcare expenditure for adults (20-79 years old) [IDF, 2014]. The main cost drivers are costs related to treatment of acute and late

Table 1.1 Comparison of the cost structure for an average patient and a patient with both micro and macrovascular complications. Costs in SEK per year (1998) [Henriksson et al., 2000].

	Average Patient	Patient with both micro- and macro-vascular complications
Hospitalization	10 599	29 555
Ambulatory Care	7 719	11 053
Drugs	6 665	9 520
Total	24 983	50 128

complications resulting from poor glycemic control [Henriksson et al., 2000], see Table 1.1, and the indirect costs, related to loss of productivity resulting from mortality and disability from these complications—in Sweden estimated to 5.4 billion SEK [Bolin et al., 2009].

These complications spring from either too low glucose levels, hypoglycemia, or too high blood glucose concentrations, hyperglycemia. Hypoglycemia may result in acute seizure, coma and even death in severe cases due to insufficient energy supply to the brain. Glycated haemoglobin (HbA1c) reflects elevated glucose levels over a longer time period (2-3 months), and prolonged raised HbA1c has been shown in large multi-center trials to be linked to increased risk of micro and macro cardiovascular implications, and result in, e.g., renal failure, amputation and blindness [DCCT Group, 1993; DCCT/EDIC Group, 2005]. Records show that almost half of the diabetic population in Sweden have a mean glucose level, measured as HbA1c, above the guideline value, implying a significantly increased risk of the aforementioned long-term complications [The Swedish National Board of Health and Welfare, 2009b], and there is good reason to believe that these numbers translate globally. Thus, means to improve the metabolic control for these patients are seminal to cut back the dismaying growth rate of monetary and physiological costs of this disease, and to lighten the heavy burden this implies on the healthcare programmes and institutions. For non-insulin dependent (NIDDM) T2DM, insulin sensitivity promoting oral agent, together with changes in lifestyle, may suffice to improve the metabolic control. In insulin-dependent *diabetes mellitus* (IDDM) covering T1DM and insulin-treated T2DM patients, the conditions are very different. For IDDM, the appropriate amount of insulin to administer is often hard to estimate and steep changes of the glucose level may suddenly arise. An undesirable, or even dangerous, situation may thereby quickly arise, calling for new treatment decisions. In comparison to NIDDM, the variations are faster, the number of decision points over the day more frequent and different, and the acute risks more pronounced. The need, prerequisites and type of decision support or

automatic control is therefore very different between these two groups. For the IDDM, continuous support to optimize the insulin regime may have a profound effect on the possibility to maintain normal glucose levels, whereas management of diet, exercise and other lifestyle-related changes, and long-term follow-up thereof, is the core to improved NIDDM T2DM metabolic control.

In order to contribute to means to improved glycemic control, this thesis investigates methods and models that may be used in glucose self management for persons with IDDM. Some of the fundamental questions, as well as more practically oriented aspects of glucose control, will be addressed:

- Can the insulin action, i.e., the glucose-lowering effect, of rapid-acting insulin be estimated for a specific individual?
- Is there time-variability in the glucose dynamics, and can changes in insulin requirement related thereto be estimated?
- Can nocturnal hypoglycemia be predicted in advance, and if so, can preventive actions be taken to circumvent such an event?
- How do different meal types impact the glucose level?
- What are the optimal bolus approach to different meal types?
- Are the clinical guidelines regarding postprandial response realistic and achievable for all patients and all meal types?
- Can the sensor lag introduced by the continuous glucose monitor systems be circumvented?

The research was based on data from the European FP7 IP research project DIAdvisor [DIAdvisor, 2012] and from data collected in a clinical trial conducted at the Endocrinology Department at the Skåne University Hospital.

1.2 Outline of the Thesis and Summary of Contributions

Chapter 2. Background

In this chapter a background of diabetes physiology and technology used in diabetes therapy is given. This covers an overview of some of the most important and influential physiological and data-driven models used in diabetes technology research. The concept of defence-in-depth, and how it relates to diabetes management is also explained.

Chapter 3. Data and Data Characteristics

The basis for this thesis are the empirical data collected over several trials. Here, we present the Diadvisor and ULund trials and some data characteristics that were recognized. The chapter is partly based on the following publications:

- Ståhl F. Diabetes Mellitus Glucose Prediction by Linear and Bayesian Ensemble Modeling. Licentiate Thesis, TFRT--3255--SE, Department of Automatic Control, Lund University, Sweden, December 2012.
- Ståhl F and Johansson R. Diabetes Mellitus Modeling and Short-Term Prediction Based on Blood Glucose Measurements. In *Mathematical Biosciences*, 217(101-117), Jan 2009.

The first publication is the licentiate thesis by the author. Fredrik Ståhl was the main author of the second paper. The co-author contributed with assembling of the paper and with valuable comments and discussions regarding the methods and results. Regarding the ULund trial, the author designed the study, and wrote the application to the ethical committee together with Mona Landin Olsson.

Chapter 4. Modeling Insulin Action

Insulin action is the glucose-lowering effect of insulin. In this chapter, a non-parametric finite impulse response model was used to describe this phenomenon and the model's ability to reproduce overnight glucose data was tested for the ULund Trial data. The estimated duration and total glucose-lowering effect was compared to the patients' pump settings. Noteworthy is the heterogeneous properties of the model across the glucose range and the description of changes in insulin demand during the night. The chapter is based on the following publication:

- Ståhl F, Lindström E., Landin Olsson M and Johansson R. Kernel-based Estimate of the Insulin Action of Rapid-Acting Insulin in Home-Monitored Data. Accepted to 17th IFAC Symposium on System Identification (SYSID 2015), Beijing, China, Oct 19-21, 2015.

Fredrik Ståhl was the main author of the paper. The co-authors contributed with valuable comments and discussions regarding the methods and results.

Chapter 5. Nocturnal Hypoglycemia Prediction

Using the model developed in Chapter 4, the important application of detecting and preventing nocturnal hypoglycemia is evaluated. Pairing the model with a Kalman filter approach, validation on nocturnal hypoglycemic

episodes was conducted on the ULund Trial data. The chapter is based on the following publication:

- Ståhl F, Johansson R. and Landin Olsson M. Predicting Nocturnal Hypoglycemia Using a Non-Parametric Insulin Action Model. Accepted to 2015 IEEE International Conference on Systems, Man, and Cybernetics (SMC2015), Hong Kong, China, Oct 9-12, 2015.

Fredrik Ståhl was the main author of the paper. The co-authors contributed with valuable comments and discussions regarding the methods and results.

Chapter 6. Meal Impact Identification

In this chapter we turn to the impact of the most significant disturbance to glycemic homoeostasis—the meal intake. Continuing the outlined approach for the insulin impact we also modeled the postprandial impact of meals with a finite impulse response model. Recognizing that the composition of the meal plays a key role, the meals were divided into different recipes, and each recipe was modelled separately. The models were validated on the ULund trial data in terms of ability to reproduce the glucose excursion following a meal in the postprandial phase. Cluster analysis was conducted, showing that a majority of the identified meal impact models could be represented by three different base models. The chapter is based on the following publication:

- Ståhl, F. A novel model of the postprandial response in insulin-dependent diabetes. Submitted to *Medical & Biological Engineering & Computing*.

Chapter 7. Meal Bolus Optimization

In this chapter the models of insulin action and meal impact were combined with an optimization method to determine optimal meal bolus doses for each recipe identified in Chapter 6. Using these dosing strategies, it was investigated whether the different recommendations on the postprandial glucose response issued by international patient and professional organizations, such as the American Diabetes Association (ADA), International Diabetes Federation (IDF) and the American Association of Clinical Endocrinologists (AACE) always are achievable. An important finding was that for some individual with severe mismatch between the dynamics of the insulin action and the meal impacts, only small meal sizes can be digested without violating the recommendations, regardless of dosing strategy.

Chapter 8. Sensor Lag Compensation

Continuous glucose measurement in interstitial fluid is known to be lagging in relation to capillary glucose measurements. This chapter presents

an augmented model of the glucose-insulin interaction, including a model of measurement dynamics. The concept is evaluated for reduced lagging of the short-term prediction on one patient data set from the first trial of the DIAdvisor project. The chapter is based on the following publications:

- Ståhl F. and Johansson R., Observer Based Plasma Glucose Prediction in Type 1 Diabetes, In *Proc. 3rd IEEE Conf. on Systems and Control*, pp. 1620-1625, Yokohama, Japan, 8-10 Sept, 2010.

Fredrik Ståhl was the main author of the paper. The co-author contributed with valuable comments and discussions regarding the methods and results.

Chapter 9. Ensemble Prediction

Here, a novel algorithm for ensemble prediction is introduced, using several models derived for short-term glucose prediction. The suggested method admits for soft switching and interpolation between the different models based on an evaluation of the different predictors' recent performance, using a sliding data window, and by looking for data feature identified to be correlated to switching. The suggested method was validated on simulated data, as well as 12 patient data sets from the second DIAdvisor trial, showing improved robustness to the prediction performance in comparison to relying on the individual prediction models. The chapter is based on the following publications:

- Ståhl F and Johansson R. and Renard E. Ensemble Glucose Prediction in Insulin-Dependent Diabetes, in Data-driven Modeling for Diabetes, Lecture Notes in Bioengineering, Springer Verlag, 2014.
- Ståhl F, Johansson R. and Renard E. Bayesian Combination of Multiple Plasma Glucose Predictors. In *Proc. 34th Annual International IEEE EMBS Conference (EMBC 2012)*, pp. 2839-2844, San Diego, CA, U.S, Aug 28-Sept 1 2012.
- Ståhl F. and Johansson R. Receding Horizon Prediction by Bayesian Combination of Multiple Predictors. In *Proc. 51st Annual IEEE Conf. on Decision and Control (CDC2012)*, pp. 5278-5285, Maui, Hawaii, U.S, Dec. 10-13, 2012.

Fredrik Ståhl was the main author of all three publications. The co-authors contributed with valuable comments and discussions regarding the methods and results.

Chapter 10. Conclusions and Future Research

The most important contributions and conclusions of the thesis are summarized in this chapter and some directions for future research are outlined.

1.3 Other Publications

Other publications on the topic by the author:

Ståhl F, Johansson R. and Landin-Olsson M. Individualized Rapid-Acting Insulin Action Estimation From Insulin Pump and CGM Data, In *J. Diab. Sci. Technol.*, Vol. 9, Nr. 2, March 2015, A118.

Ståhl F, Johansson R. and Renard E. Intrapersonal variability in post-prandial response based on meal categorization, at *Diabetes Technology Meeting*, San Francisco, U.S., Oct 30-Nov 2, 2013.

Ståhl F, Johansson R. and Renard E. Investigation of the difference in post-prandial glucose excursion based on meal categorization, at Diabetes Technology Meeting, San Francisco, U.S., Oct 30-Nov 2, 2013.

Ståhl F, Johansson R. and Renard E. Model-Based Estimates of the Post-Prandial Response to Carbohydrate and Insulin and of the Carbohydrate-to-Insulin Ratio, In *Diabetes*, Vol. 62, A217, July 2013.

Ståhl F, Johansson R. and Renard E. Investigation of the relationship between elevated levels of insulin antibodies and prolonged insulin action. In *Diab. Technol & Therap.*, Vol. 15, Suppl. 1, A115, February 2013.

Ståhl F, Johansson R and Renard E. Can blood glucose drops during exercise be predicted from Heart Rate data?. In *J. Diab. Sci. Technol.*, Vol. 6, Nr. 2, March 2012, A175.

Ståhl F., Johansson R. and Renard E. Post-prandial Plasma Glucose Prediction in Type I Diabetes Based on Impulse Response Models. In *Proc. 32nd Annual International IEEE EMBS Conference (EMBC 2010)*, pp. 1324-1327, Buenos Aires, Aug 31 - Sept 4, 2010.

Stemmann M, Ståhl F, Lallemand J, Renard E, Johansson R. Sensor Calibration Models for a Non-Invasive Blood Glucose Measurement Sensor. In *Proc. 32nd Annual International IEEE EMBS Conference (EMBC 2010)*, pp. 4979-82, Buenos Aires, Aug 31 - Sept 4, 2010.

Ståhl F, Cescon M, Johansson R and Renard E. Infinite Horizon Prediction of Post-prandial Breakfast Glucose Excursion. In *J. Diab. Sci. Technol.*, Vol. 4, Nr. 2, A163, March 2010.

Cescon M, Ståhl F and Johansson R. Subspace-Based Model Identification of Diabetic Blood Glucose Dynamics. In *Proc. 15th IFAC Symposium on System Identification*, pp. 233–38, Saint-Malo, France, July 6 - 8, 2009.

Ståhl F and Johansson R. Short-Term Diabetes Blood Glucose Prediction Based On Blood Glucose Measurements. In *Proc. 30th Annual International IEEE EMBS Conference (EMBC 2008)*, pp. 291-294, Vancouver, Aug 20-24, 2008.

2

Background

2.1 Diabetes Type 1 and the Glucoregulatory System

Diabetes type 1 is a chronic disease where the β-cells of the pancreas have stopped to produce insulin. This is in most cases due to an auto-immune attack, but may in rare cases also be caused by sustained injuries from accidents or pancreatic cancer. In order to understand the disease, a brief overview of the glucoregulatory system is presented, see, e.g., [Nussey and Whitehead, 2001] for a more extensive review.

The Glucoregulatory System

The glucoregulatory system is concerned with glucose metabolism and the insulin/glucose mechanisms needed to maintain normoglycemia. Figure 2.1

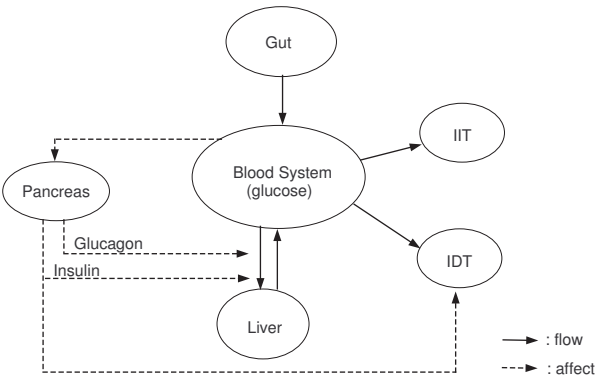

Figure 2.1 Overview of the glucoregulatory system describing the relationship between the flux from the gut into blood system and the interaction with the insulin-dependent tissue (IDT), the insulin-independent tissue (IIT), the pancreas and the liver.

presents a simplified overview of the flow of glucose between the most important organs relevant for this system. Below, a short description of these organs and their role in the so-called absorptive state and the post-absorptive state, the two parts that make up the metabolic cycle, is given. A brief description of insulin absorption from insulin injections will also be presented. Emphasis will be put on the digestive system and insulin absorption from injections.

The absorptive state is the time following a meal during which the ingested carbohydrates are digested and absorbed. During this period, excess glucose is absorbed and stored for later use. The post-absorptive state is the time after a meal when the gastro-intestinal tract is empty and energy has to be provided by the body's own storages.

During the absorptive stage, glucose is converted and stored as the polysaccharide glycogen, in the liver as well as directly in the muscle cells. This process is stimulated by insulin. During the post-absorptive stage, the liver glycogen storage is broken down to glucose and released into the blood stream, providing energy for the body cells. This process is stimulated by glucagon and inhibited by insulin. Apart from converting glycogen to glucose, new glucose can be formed from protein and fat by gluconeogenesis. The metabolism of consumed alcohol inhibits this process [Siler et al., 1998], which may result in severe hypoglycemia in IDDM patients [Turner et al., 2001].

In the pancreas, two important hormones relevant to the glucoregulatory system are synthesized, namely insulin and glucagon. Insulin release is mainly stimulated by elevated blood glucose concentration. Therefore, substantial amounts are released in the absorptive stage, when the glucose level is raised due to the absorption from the gut. Glugacon, which has the opposite effect on the hepatic balance, is accordingly released when the blood glucose concentration falls. These two hormones are thus in a feedback arrangement with the blood glucose concentration—controlling the glucose metabolism. Another hormone group of importance during the absorptive stage is the incretine gut hormone group. Incretine is secreted during meal uptake and stimulates pancreatic insulin release and inhibits the glucose flux from the gut into the blood stream. Impaired incretine function is believed to play an important role to the reduced and impaired insulin response of T2DM patients [Nauck et al., 2004].

Insulin-dependent tissue (IDT) is dependent on insulin to utilize glucose. This mechanism is discussed in the insulin section below. A significant portion of the insulin-dependent tissue is made up of skeletal muscles. In the absorptive state, skeletal muscle cells not only consume the glucose directly, but also convert some to glycogen, providing an energy storage for later use in a local depot.

Insulin independent tissue (IIT), such as the brain and the central nervous

system, do not need insulin to utilize glucose, but use insulin-independent glucose transporters such as, e.g., GLUT1 or GLUT3.

Insulin

Insulin is the main hormone controlling the glucose metabolism. It is a protein consisting of three peptide parts; an A-, B- and C-chain. In healthy subjects it is produced in the β-cells in the pancreas, whereas IDDM patients depend mostly on injections of artificially produced insulin analogs. Three categories of different types of therapeutic insulins exist; rapid-, intermediate and long-acting insulins. The long-acting insulins are used to cover the basal metabolism, i.e., mainly to support the insulin-dependent tissue in the post-absorptive state. The most recent insulin types of this category, detemir [Levemir™, 2012] and glargine [Lantus™, 2012] type have almost flat pharmacokinetic profiles, i.e., even and constant insulin levels without pronounced peaks. Rapid-acting insulins, such as lispro [Humalog™, 2012], aspart [Novolog™, 2015] and glulisine [Apidra™, 2015] are designed to handle the glucose flux following a meal in the absoptive state. Therefore, these insulins have a short pharmacokinetic profile with a distinct peak after about 60 minutes. Intermediate-acting insulin are a mix of both, and are often used to support in cases when some insulin production is still left, i.e., insulin-dependent T2DM patients or the so-called latent auto-immune diabetes (LADA) patients [Landin-Olsson, 2002].

Insulin is normally injected in the subcutaneous tissue of the torso or legs. Rapid-acting insulin is injected in the abdominal fat layer, whereas long-lasting insulin is usually taken in the upper side of the thigh. From these depots the insulin is transferred to the blood system via the capillaries. The absorption rate depends on a series of factors. One contributing factor is the capillary density. A higher density results in a greater diffusion area between the depots and the capillaries. The abdominal region has the highest capillary density and the thigh the lowest [Home, 1997]. This explains why rapid-acting insulin is preferably infused in the abdominal fat layer and long-lasting in the thigh.

The size of the insulin molecules is a dominant rate limiter. Large molecules will have difficulties passing through the capillary pores. The structure of the insulin molecules are either monomer, dimer or hexamer. Insulin will spontaneously form hexamers if the concentration is sufficiently high. This so-called self-association can be catalyzed by zinc ions. Therefore, zinc is added to the insulin solution in slow-acting insulins, thereby considerably reducing the absorption rate [Home, 1997]. In the rapid-acting insulins, the insulin molecules are mainly monomeric or dimeric. They have been modified so that hexamer formation is completely avoided [Shoelson and Halban, 1994], and are also called monomeric insulins. Another major factor affecting

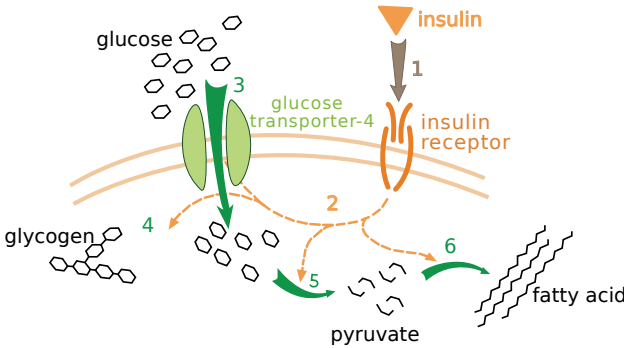

Figure 2.2 Insulin receptor and GLUT4 cycle. 1. Insulin attaches to the insulin receptor, 2. a signal cascade is induced to translocate GLUT4 transporters to the plasma membrane, 3. allowing gluocse to enter into the cell. [Source: Wikipedia]

the absorption rate is the size of the injection dose. A large dose reduces the ratio between the absorption area and the depot volume, thus reducing the absorption. Several studies have been undertaken, all indicating a linear relationship between insulin dose and absorption half-time [Hildebrandt et al., 1984] and [Plank et al., 2005]. These studies have been performed using slow-acting or intermediate-acting insulins. However, studies indicate that the linear relationship is not valid for monomeric insulin [Brange and Vølund, 1999]. Finally, blood flow and temperature of the injected site have a significant contribution to absorption rate. Raised temperature enhances the disassociation of hexameric insulin and accelerates insulin diffusion, and increased blood flow raises absorption rate. Thus, exercise plays a key role for absorption, since it raises both body temperature and blood flow. After the absorption from the depots, the insulin is circulated in the blood system and finally interacts with a insulin receptor at the cell surface.

The insulin receptors are so-called tetramers, consisting of two α- and two β-subunits. The α-subunits are entirely extracellular and serve as a binding site for the insulin molecule [Taniguchi et al., 2006]. When the insulin has attached to the α-subunits, a signal process is initiated via the β-subunits, resulting in increased glucose transporter 4 (GLUT4) activity. The glucose transporters facilitate glucose cell membrane crossing, thereby reducing blood glucose concentration [Wood and Trayhurn, 2003]. The receptor/transporter cycle can be seen in Figure 2.2. There are different types of glucose transporters, but only GLUT4 require insulin to become active. Therefore, the glucose utilization is divided into insulin-dependent and insulin-independent utilization. It is a well-known fact that exercise enhances insulin sensitivity and is therefore one part of common T2DM therapy. However, the underly-

Figure 2.3 Examples of insulin pens. [Source: Private photo]

.

ing mechanism to the increased insulin sensitivity is still not well understood. Studies indicate that the GLUT4 transporter activity is stimulated, resulting in increased insulin-dependent glucose utilization [Kahn, 1997].

Treatment

The most common therapy for IDDM patients is the multiple daily injection (MDI) basal-bolus regime. The patients use insulin pens (see Figure 2.3), or perhaps the new Swedish mini pen—the DailyDose [Daily Dose, 2012]—to administer basal insulin, once or sometimes twice a day, and rapid-acting or regular insulin for each meal, as well as for additional corrections. An alternative therapy is to use continuous subcutaneous insulin infusion (CSII) using an insulin pump, which, loaded with rapid-acting insulin, provides a continuous infusion, corresponding to the basal need and bolus doses accordingly. Doses are based on heuristic rules derived from the patient's understanding of his/her metabolism, assessment of current glucose level from glucose meters and expected future evolution and estimates of carbohydrate content in digested meals. One common measure used in this regard is the carbohydrate-to-insulin ratio, which is an estimate of how many insulin units to administer to match the amount of digested carbohydrates.

In order to avoid acute and long-term complications, the goal is to maintain normoglycemia (blood glucose (G) between 70-180 mg/dl) as far as possible, and especially to avoid insulin-induced hypoglycemia ($G < 70$ mg/dl)

altogether, and to minimize time spent in hyperglycemia ($G > 180$ mg/dl). An extensively used evaluation criterion of the outcome is the glycosylated hemoglobin (HbA1c) blood measure, which provides an assessment of average blood glucose level over a 8-12 week period [Hanas and John, 2010].

2.2 Technology

Glucose Sensors

Blood glucose is generally measured manually by the individual patient using a personal glucose meter. A small blood sample is analysed in a test strip by the meter using enzymatically catalyzed-based electro-chemical or photometric methods [Hönes et al., 2008]. Today, there exist more than 27 different personal glucose meters from 18 different manufacturers [Freckmann et al., 2010]. The accuracy requirements for meters marked with the European CE mark should comply with the DIN EN ISO 15197 standard, specifying that the measurements may not differ more than 15 mg/dl for glucose concentration below 75 mg/dl and less than 20 % for glucose concentration above 75 mg/dl [Freckmann et al., 2010], when evaluated against a laboratory equipment such as a Yellow Springs Instrument Analyzer [Yellow Springs Instrument, 2012]. Other norms and regulations have similar requirements [Tonyushkina and Nichols, 2009].

Self-monitored blood glucose (SMBG, BG or G) thus provides accurate readings, but reveals little about the dynamics, unless sampled frequently enough. Generally, the diabetic populations seem to measure their glucose level far too seldom, considering, e.g., the average HbA1c level [The Swedish National Board of Health and Welfare, 2009b]. Numerous different studies show a definite positive correlation between increased testing frequency and lowered HbA1c [St John et al., 2010].

Frequent automatic glucose measurements have become commercially available over the last ten years. Today, there are three companies with commercial systems, and this number will likely increase in the coming years, e.g., Roche is researching and developing a similar system [Schmelzeisen-Redeker et al., 2013]. These sensor systems are called Continuous Glucose Measurement (CGM) systems and consist of a disposable sensor including a subcutaneous probe, a radio transmitter connected to the external part of the sensor and a receiver device to process, record and display the results. The sensor lasts for six to seven days, depending on system, after which it is replaced. The measurements are made in the interstitial fluid and do not directly correspond to the blood glucose level, due to the first-order diffusion-like relationship between the blood stream and the interstitial compartment, see e.g., [Rebrin and Steil, 2000]. An interesting technical alternative is presented by the upcoming company Senseonics, which is about to launch an

Figure 2.4 Examples of modern insulin pumps. Medtronic Veo 754 system to the left and the Omnipod patch pump to the right. [Source: Private photo]

.

implantable sensor with a 90 day life span, starting in the Scandinavian market in 2015 [Senseonics, 2015]. The use of CGM has been shown to promote improved glycemic control with decreased level of HbA1c [Chetty et al., 2008; Poolsup et al., 2013].

Insulin pumps

The first commercial wearable insulin pumps became available in the late 1970s, but the bulky size limited its spread and use. Advances in technology has allowed for more compact design and modern pumps are of the size of a pager, see Figure 2.4. The basal dose can typically be programmed to change throughout the day, thereby making it possible to better tailor the basal dose to diurnal patterns in insulin requirements. Apart from normal bolus doses, extended bolus doses, where the bolus dose is injected over a predefined time, or combinations of the two may be administered. A few manufacturers have integrated the receiver unit of the CGM system in the pump, allowing the user to monitor the CGM measurements directly on the pump display. Medtronic has taken the integration the furthest with active suspension of the pump at low glucose values in their Veo and recent M640G models [Medtronic, 2012].

Smartphone Applications

The explosion of program applications for smartphones has affected the healthcare market, and specifically the diabetes self-management market, as well. Acceptance among both the public and the medical profession seems high. Surveys suggest that 90% would be fine with a prescription of a mobile app at the next doctor's visit, and a third of the American clinicians have recommended a health app to a patient in the recent year [Huckvale et al., 2015]. However, the risks associated with malfunction or misuse need to be carefully considered. The regulatory framework by the Food and Drug Administration (FDA) is still fairly untested when it comes to mobile health applications, and the agency recently issued guidelines for the industry [FDA, 2015]. The focus of the regulatory oversight will be apps that *'... could pose a risk to a patient's safety if the mobile app were not to function as intended'*. Furthermore, the guidelines also explicitly lists apps that calculate dosage as apps that will be specifically targeted in the oversight. It remains to be clarified which apps that can be exempted from heavier classification and regulation. In Europe, mobile health apps are basically unregulated.

Thus so far, internal quality control assessment of the issuing companies have provided the main safeguard for the end consumer, exemplified in 2012 when Sanofi withdrew their bolus calculating app after having found that it was unreliable [Cortez et al., 2014]. Many of the apps are harmless in this sense, as the content ranges over cookbooks, general health information, diet guidelines, meal diaries and training guides. However, some also claim to offer decision support on bolus dosing. A recent review found a total of 2633 apps for Android and iOS related to diabetes, whereof 46 were identified to offer bolus calculators [Huckvale et al., 2015]. Several serious deficiencies were found, such as lack of input validation (e.g. blood glucose values of zero could be entered), or that the algorithm failed to consider previous doses in the calculation. Only one of the apps fulfilled all quality criteria set forward by the reviewers. However, enforced regulation can hopefully rectify this situation.

2.3 Current Research in Systems Science

Current research is focused on improving insulin therapy along two main directions; closed-loop control and semi-closed loop control by means of decision support systems. In this section, an overview of the modeling and control approaches in these research directions will be presented.

Physiological Models

The development of physiological diabetic glucose modeling started with the simple models of [Bolie, 1961] and [Ackerman et al., 1965], aiming at describ-

ing the relationship between glucose and insulin utilization. External meal and insulin administrations were not considered. Following these efforts, the slightly more complex and well-established minimal model [Bergman and Cobelli, 1980] was suggested as a means to estimate insulin sensitivity from an intravenous glucose tolerance test (IVGTT). Detailed models of the glucose metabolism; separating insulin and non-insulin dependent glucose utilization, incorporating models of hepatic balance, renal clearance, and in some cases pancreatic insulin synthesis and release, have surged since then.

A sparse fourth-order linear model, with physiological interpretation of the state variables, was suggested in [Salzsieder et al., 1985], with six tunable parameters. The original model was validated on data from intravenous experiments involving diabetic dogs. Thereafter, the model has been both reduced, and extended to include exercise load, and to also consider oral hyperglycaemic agents. The model order is still four, but the number of tunable parameters has been reduced to five, and incorporated into a decision support system (DSS) called KADIS [Salzsieder et al., 2011].

In [Lehmann and Deutsch, 1992], a simulation model based on the insulin kinetics from [Berger and Rodbard, 1989], and including hepatic balance (described by a look-up table), peripheral and insulin-independent glucose utilization (Michaelis-Menten like relationship), renal clearance and the meal digestion model from the same paper (described above), was presented. Overall, the model contains only two tunable parameters, the rest are considered patient invariant. Later, the freely downloadable educational simulation software AIDA [Lehmann, 1994] was developed using this model. The system was validated on a set of 24 subjects with parameter convergence achieved in 80% of the cases [Lehmann et al., 1994].

Another simulation model, that has been turned into an advisory system, is the DIAS model [Hejlesen et al., 1997]. Especially noteworthy of this model is the nonlinear model of the hepatic balance [Arleth et al., 2000], fitted to tracer literature data, and the model extension to include the delayed hypoglycemic effect of alcohol intake [Plougmann et al., 2003]. The model was incorporated into a prototype eHealth tool called DiasNet [Jensen et al., 2007], with a central server-based web service, which also communicates over the cellular network with the user's mobile application implemented on a smartphone. The system has been tested in a small field trial, but was mainly evaluated on overall data acquisition, transmission and application usability aspects, and not on results concerning model performance.

A large model with 19 tunable parameters was proposed in the Sorensen thesis [Sorensen, 1985], a model often used as a verification tool to assess different control approaches, e.g., [Eren-Oruklu et al., 2009a]. The web-based educational simulation model GlucoSim [Agar et al., 2005] has been developed based on another thesis [Puckett, 1992]. Generally, these models are difficult to fit to an individual person, and may lack structural identifiability.

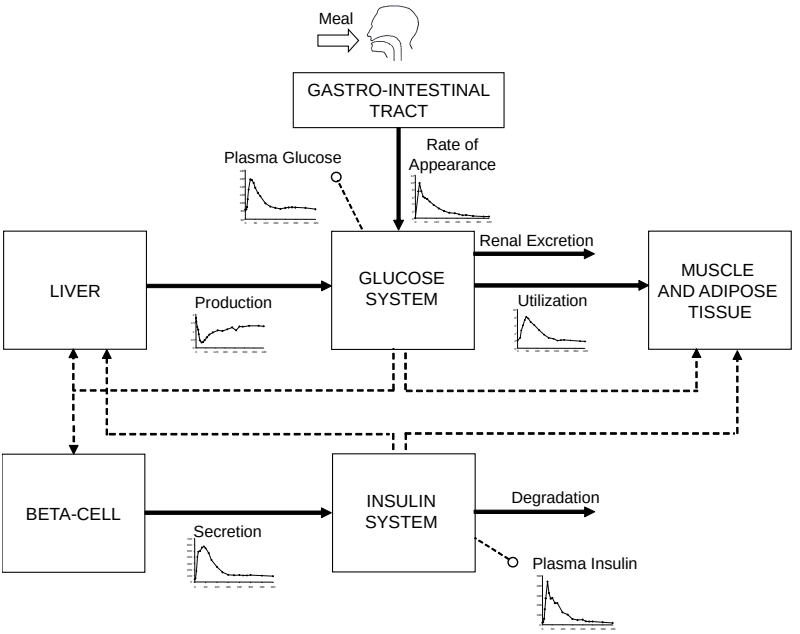

Figure 2.5 Overview of the Padova/UVa simulation model. The solid lines represent flow and the dotted lines indicate effect. [Source: C. DallaMan]

This makes them unsuitable for predictive purposes, but synthetic subjects may be created for simulation studies.

Currently, the most influential simulation model is the University of Virginia and Padova University (UVA/Padova) model described in [Dalla Man et al., 2007b] and [Dalla Man et al., 2007a], which has been accepted by the FDA to be used as a substitute for animal trials in preclinical trials of closed-loop development [Kovatchev et al., 2008]. To this purpose, 300 artificial subjects have been derived from estimated parameters from population studies, and used in, e.g., [Lee et al., 2009]. This model is based upon the classical minimal model [Bergman and Cobelli, 1980], and the glucose rate-of-appearance model in [Dalla Man et al., 2006a]. The population data for estimating the 300 artificial subjects were derived using the triple-tracer protocol described in [Basu et al., 2003]. An outline of the model can be seen in Figure 2.5.

In [Roy and Parker, 2006a], the minimal model was augmented with additional states to include the dynamical interaction between free fatty acids and the insulin and glucose compartments. The model parameters were partly fixed, and partly identified using experimental data, and showed reasonable resemblance to data. In [Roy and Parker, 2006b], the model was used, to-

gether with the gastric emptying function taken from [Lehmann and Deutsch, 1992], to fit the model against data from one mixed meal consumed by normal subjects, with good correspondence.

The limitation of the classical minimal model to provide consistent estimates of insulin sensitivity, when different insulin concentrations arise during an IVGTT, was addressed in [Prigeon et al., 1996]. Modifications to the model were suggested to incorporate the saturation effect of insulin on insulin-dependent glucose utilization [Rizza et al., 1981; Natali et al., 2000], as well as a saturation effect on insulin transport from the plasma to the interstitial compartment. Generally, the saturation effect is not pronounced at insulin infusion levels of most insulin-dependent patients. However, the critically ill patient may often experience reduced insulin sensitivity, and are treated with intensive insulin treatment with abnormal insulin levels to maintain normoglycemia, thereby reducing mortality and morbidity outcome [Van den Berghe et al., 2001]. Thus, for the purpose of improved glycemic control of the critically ill in Intensive Care Units (ICU), this model was picked up in [Lonergan et al., 2006]. Thereafter, the table-based protocol SPRINT, which acts as a decision support in the manual infusion control for the ICU personal, was derived [Chase et al., 2007]. This approach has been successfully validated in a large study covering 371 subjects, achieving a very tight glucose control [Chase et al., 2008].

Another extension of the minimal model was proposed in [Derouich and A.Boutayeb, 2002], by incorporating effects of physical exercise by adding parameters, which increase insulin sensitivity, insulin-independent glucose utilization and insulin clearance during exercise, to the model. The model has not been evaluated empirically. Also the UVA/Padova model has been extended to cover physical activity in [Dalla Man et al., 2009], based on the model in [Breton, 2008]. The model links elevated heart rate to increased insulin sensitivity and insulin-independent glucose utilization. In [Breton, 2008], the model was fitted to data from a hyperinsulemic clamp test, including a 15-minute exercise period (50% VO_{2max}), for 21 T1DM subjects, with a weighted mean square estimation error of 7.7 mg/dl (unclear how the weights were chosen).

Yet another ambitious extension with 19 parameters, whereof 10 are subject to identification, and including modeling of the circadian rhythm was given in [Fabietti et al., 2006]. In [Fabietti et al., 2007], the model was validated by simulation comparisons on two datasets of six and nine T1DM patients with excellent results (RMSE about 1 mmol/L), however, apparently without cross-validation.

Before leaving the minimal model, the work in [Kanderian et al., 2009] needs to be commented. Here, the minimal model, extended with a simple pharmocokinetic compartment model for the insulin kinetics and a compartment meal model of the same type as in [Worthington, 1997], was tested on

closed-loop data from a trial involving ten T1DM subjects. Intraday variations of the model parameters related to the insulin sensitivity, hepatic balance and insulin-independent glucose utilization was allowed over three different sections of the day. Also in this case, the model was validated without cross-validation, but with an impressive average simulation prediction error (RMSE about 16 mg/dl).

A smaller model, with only five tunable parameters, is the Hovorka model [Hovorka et al., 2002], later extended and altered for the critically ill in [Hovorka et al., 2008]. The former model has been validated for predictive capacity on 15 subjects with a RMSE of 3.6 mg/dl for a prediction horizon of 15 minutes [Hovorka et al., 2004]. Parameter estimates were retrieved recursively from a sliding data window using a Bayesian approach. This model is also used extensively for MPC-oriented closed-loop validation in a simulation environment, including a cohort of 18 virtual patients [Wilinska et al., 2010]. Eight out of the eighteen parameter sets have been derived from experimental data, and the rest from so-called informed prior distributions. The model has also been used, e.g., in the evaluation of PID control in [Farmer et al., 2009], which also made use of the Sorensen [Sorensen, 1985] and the minimal model [Bergman and Cobelli, 1980].

The models vary in complexity, but generally, do not explicitly consider other hormonal metabolic effects than insulin and glucagon.

The physiological models are typically based upon balance equations over compartments, where the rate of change of plasma glucose and insulin are made up of the contribution or consumption by different parts of the physiology. For the glucose metabolism, the following sinks and sources are normally considered:

$$\dot{G} = r_{Ra} + r_{EGP} + u_{iid} + u_{id} + u_{RE} \tag{2.1}$$

where r_{Ra} is the rate of glucose appearance following digestion of a meal, r_{EGP} is the total endogenous glucose production rate, u_{iid} is the rate of insulin-independent glucose utilization, u_{id} is the rate of insulin-dependent utilization by muscle and adipose tissue, and finally u_{RE} is the rate of renal excretion. Likewise, the insulin dynamics are also modeled with compartments, where the plasma compartment is accompanied by additional compartments where the insulin has an active effect. Both the pharmacokinetics and the compartment approach to insulin diffusion will be presented in Chapter 4.

Below, the overall modeling approaches to the terms in the glucose dynamics are presented.

Digestion and Gut Absorption, r_{Ra} Several models have been proposed to describe the absorption of glucose from the gut following a meal. An overview will be presented in Chapter 6.

Endogenous Glucose Production, r_{EGP} The Endogenous Glucose Production stems from the liver, the kidneys and intestines, but is dominated by the hepatic glucose output. Generally, this output is considered to have a constant upper limit ($r_{EGP,0}$) from which it can be down-regulated by both insulin and glucose signaling:

$$r_{EGP} = r_{EGP,0} - k_G G - k_I I \tag{2.2}$$

where I may be the plasma insulin, or if more insulin compartments are used, the insulin level in a relevant compartment, e.g., the liver, and k_G and k_I are model parameters.

Insulin-independent Glucose Utilization, u_{iid} The glucose utilization of the central nervous system, the blood cells, but also the gut, is generally considered to be independent of insulin. Normally this term is kept as a constant, but in, e.g., the Hovorka model a Michaelis-Menten relationship (see below) is postulated.

Insulin-dependent Glucose Utilization, u_{id} This term corresponds to the uptake and utilization of glucose in the peripheral tissue, and is often expressed in terms of a Michalis-Menten relationship to the glucose level:

$$u_{id} = \frac{V_{max} G}{K_m + G} \tag{2.3}$$

where V_{max} and K_m are the Michaelis-Menten constants [Keener and Sneyd, 2009].

Renal Excretion, u_{RE} Re-absorption of glucose in the kidneys is limited, and to model the renal excretion, a linear threshold model is often suggested. When the glucose level increases beyond the threshold level G_{RE}, the clearance increases proportionally.

$$u_{RE} = \begin{cases} k_{RE}(G - G_{RE}) & \text{if } G > G_{RE}, \\ 0 & \text{if } G \leq G_{RE} \end{cases} \tag{2.4}$$

Empirical data support that both the threshold G_{RE} and the slope k_{RE} may vary significantly in-between subjects [Johansen et al., 1984; Rave, 2006].

Additionally, glucagon dynamics also play a significant role in the glucose and insulin dynamics, specifically in the counter-regulatory mechanism to raise the glucose level in an hypoglycemic event. In an updated version of the Padova/UVa model, glucagon dynamics have been incorporated [Man et al., 2014], but we omit the details here. Injection of glucagon is in current clinical practice considered as a means to rescue a unresponsive patient from severe hypoglycemia, and many patients with insulin-dependent diabetes have auto-injectors readily available. It has also been suggested as a means of control in

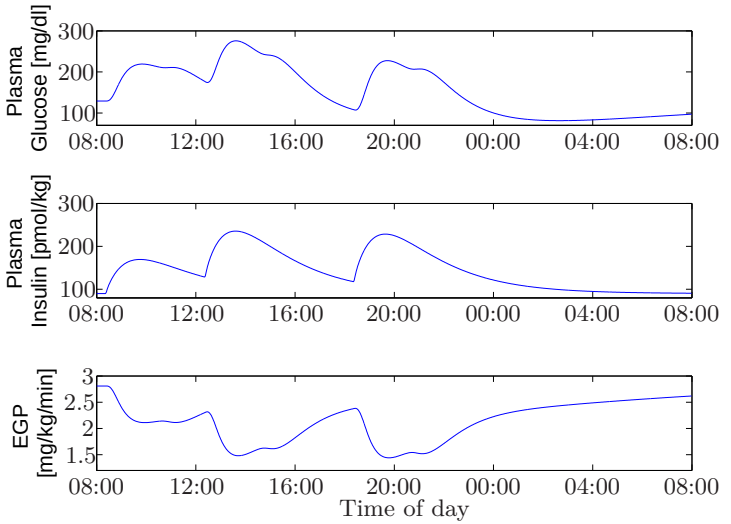

Figure 2.6 Simulated day with three meals (Breakfast 08:30, Lunch 12:30, Dinner 18:30) using the PAdova/UVa model.

.

a bi-hormonal pump, to allow for bilateral control. This has spurred interest in the pharmacokinetics of such injections [Lv et al., 2013].

Example of simulated postprandial data of an insulin-dependent individual generated by the Padova/UVa model can be found in Figure 2.6. From this simulation several model features can be identified, such as the rise in plasma insulin following the bolus injection at the meal start, the postprandial response of the glucose level and the down-regulation of the hepatic output due to increased serum levels of both these variables.

Black Box Models

Data-driven models have been investigated on CGM time-series alone, or by considering inputs as well. The meal absorption models of [Dalla Man et al., 2007a] and [Lehmann and Deutsch, 1992] are sometimes used as input generating components in data-driven models to approximate the glucose flux input from the gut following a meal intake. The modeling focus has been prediction for the purpose of early hypoglycemic detection, e.g., to be used for alarm triggering in CGM devices, or temporary insulin pump shut-off, as well as establishing models suitable for model-based control. In this context, the Clarke Error Grid Analysis (p-CGA) [Clarke et al., 1987] is often considered. It is a metric originally developed for evaluating blood glucose meters, relating the measurement error to clinical implications. This metric

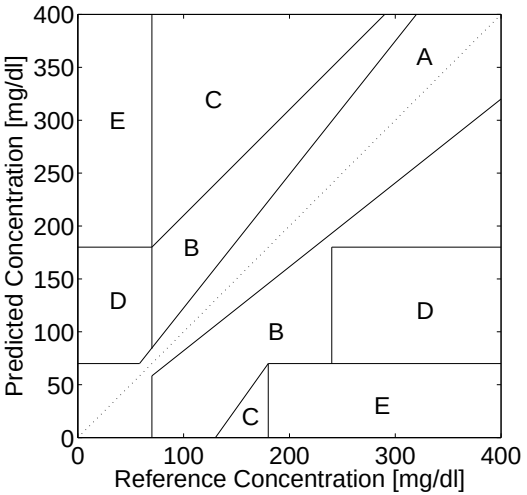

Figure 2.7 The Clarke Error Grid [Clarke et al., 1987] is divided into different zones; the A zone corresponds to errors of little clinical significance, the B zone represent values that deviate more than 20% from the reference, but would lead to benign or no treatment decisions if acted upon, the C zone error could result in overcorrection, the D zone represents failure to detect dangerously low or high glucose values and zone E corresponds to predictions that would lead to erroneous and dangerous treatment decisions (e.g. administrating insulin when already hypoglycemic).

is also often used to rate CGM precision, and recently to assess prediction performance as well. Estimated glucose is plotted against the reference measurements and evaluated according to how the points fall into the different error zones, each with a different clinical interpretation, see Figure 2.7.

Time-series analysis by auto-regressive (AR) models started with [Bremer and Gough, 1999], who evaluated the basic underlying assumptions concerning stationarity and auto-covariance that AR modeling is based upon. The conclusion was that diabetic data in general is non-stationary, but highly auto-correlated, thus recommending the models to be recurrently re-estimated. Following this, AR and ARMA models were developed in [Ståhl, 2003] and [Ståhl and Johansson, 2009] using glucose data from a recently diagnosed T1DM patient. In [Sparacino et al., 2007], first-order recursive AR models were investigated for 28 subjects using a low-pass filtered CGM signal from the GlucoDay CGM system. The results indicate that hypoglycemia can be detected by the model 25 min before the CGM signal passes the same threshold, but with unknown risk of false positives. Another example of recursive AR and ARMA models of third order, incorporating a change

detection feature for more rapid parameter re-estimation when large changes in the dynamics are detected, is found in [Eren-Oruklu et al., 2009b]. The models were evaluated for 30 healthy, 7 glucose-intolerant and 25 T2DM diabetic subjects, with less than 4% mean Relative Average Deviation (RAD) and almost no values in D or E zones of the Clarke Error Grid for the 30-minute predictions in comparison to the CGM Medtronic Gold reference [Medtronic, 2012]. Contrary to the above, the authors of [Gani et al., 2009] claim that a generic patient- and time-invariant AR model of order 30 can be identified from any patient and used for glucose prediction for any other patient. Very promising results were achieved in [Gani et al., 2010], where the model was evaluated for three different datasets, each utilizing a different CGM device, and the patient cohorts included both T1DM and T2DM diabetes. The RMSE prediction error was on average less than 3.6 mg/dl for a 30-minute prediction, with negligible delay, and with 99% of the paired prediction-reference points in the A and B zones of the p-CGA. However, these results were achieved by filtering the CGM signal in both training and test data using a non-causal filter, removing the high frequency components. In [Lu et al., 2011] the causality aspect of the input filtering was addressed. The AR model, here reduced to order eight after model complexity considerations, was reformulated as a linear model with a Kalman filter, and the filter parameters were adjusted to account for the filtering of the CGM signal. For evaluation purposes, the reference was, however, still filtered in the same non-causal way as before. Using this approach on the same dataset as in [Gani et al., 2010], yielded more moderate results with an average prediction error of 16 mg/dl, and a 9 minute lag for the 20-minute prediction.

Algorithms specifically developed for hypoglycemic detection have also been proposed. In [Palerm et al., 2005], a Kalman filter approach was proposed. The filter was used to estimate the states corresponding to the interstitial glucose level, and the first and second time-derivative thereof, i.e., rate of glucose change and acceleration. In [Palerm and Bequette, 2007] this method was evaluated for 13 hypoglycemic clamp datasets. Using a hypoglycemic threshold of 70 mg/dl, the sensitivity and specificity were 90% and 79%, respectively, with unknown alarm time. Combining three different methods for hypoglycemic detection with the ARMA model of [Eren-Oruklu et al., 2009b], data from insulin-induced hypoglycemic tests for 54 T1DM subjects were evaluated in [Eren-Oruklu et al., 2010]. With a hypoglycemic threhold of 60 mg/dl, sensitivity of 89%, 88%, and 89% and specificity of 67%, 74%, and 78% were reported for each method, respectively. Mean values for time to detection were 30, 26, and 28 minutes. In [Dassau et al., 2010], five different algorithms were used together in a voting based detection system called hypoglycemic prediction algorithm (HPA). The system was developed using 21 datasets from a 24-hour Abbott Navigator CGM trial for children with T1DM, and was validated on hypoglycemic induced studies on 22 T1DM

patient records. With a voting scheme of 3-out-of-5, and a hypoglycemic defined as 60 mg/dl, a sensitivity of 91% was achieved, and when 4-out-of-5 positive alarms were required, the sensitivity dropped to 82%.

A shortcoming of the AR models and the algorithms above is the lack of input-output relationship, excluding them from being used in a model-based control framework. A natural extension to the AR concept is to include external inputs, transforming the model to an ARX model. This type of model has been considered in, e.g., [Finan et al., 2009], where both batch-wise and recursively identified patient-specific ARX models have been analysed for 9 patients with a mean 30-minute prediction error RMSE of 26 mg/dl. In [Cescon, 2011] both ARX, ARMAX and state space models were investigated using different identification methods for 30-, 60-, 90- and 120-minute prediction for nine Montpellier patients from the DIAdvisor DAQ trial. The best performance was achieved with the ARX and the ARMAX models. The ARX model gave a standard deviation of the prediction error of 17, 34, 46 and 56 mg/dl on average for the 30-, 60-, 90- and 120-minute prediction, respectively. The corresponding results for the ARMAX model were 16, 30, 39 and 44 mg/dl.

Another type of transfer function model, cast in the continuous-time domain, was approached in [Percival et al., 2010], where it was evaluated for nine T1DM subjects on separated meal and insulin intakes. Model parameters were determined both heuristically and by least-squares estimation. The carbohydrate and insulin impacts of the model, i.e., the steady-state rise and drop of glucose following these intakes, were further compared to the corresponding practically used estimates of these factors. No independent prediction validation was given. This model was later evaluated in a control framework in [Percival et al., 2011], where two datasets were created by the Hovorka (four subjects) and Padova (ten subjects) simulation models. Here, the model could approximate the simulated data very well, with a reported three hour look-ahead prediction error of 26 mg/dl. A very similar model structure was used in [Kirchsteiger et al., 2011], the difference being a time delay changed into a time lag. In this paper, breakfast glucose excursion prediction was addressed for ten Montpellier patients from the DAQ trial. For each patient, model parameters were determined by constrained least-squares estimation for two breakfast meals and validated on a third breakfast, with an average coefficient of determination of 0.42.

Neural network (NN) models have been shown to be a competitive approach in [Daskalaki et al., 2012], where a feed-forward NN model was compared against an AR and an ARX model on a 30 patient dataset, retrieved from the Padova simulation model. Here, the NN clearly outperformed the competing models with an average RMSE of 4.9 mg/dl versus 29 mg/dl (AR) and 26 mg/dl (ARX) for the 45-minute prediction. Apart from meal and insulin information, emotional factors, hypoglycemic/hyperglycemic symptoms

and lifestyle/activities, were collected in an electronic diary and used as inputs in the NN model of [Pappada et al., 2011]. Training was performed on a dataset from 17 patients, and performance was evaluated on ten patient datasets not included in the training set, with a RMSE of 44 mg/dl for the 45-minute prediction.

A fully connected three-layer (5,10,1 neuron per layer) NN, with sigmoidal transfer functions in the first two layers and a linear for the output block was used in [Pérez-Gandía et al., 2010]. No insulin nor meal information were used, but the concurrent and previous CGM values, up to 20 minutes back, acted as inputs. The model was evaluated on two datasets with different CGM devices (Abbott Freestyle and MedTronic Guardian). Three subject datasets were used for training for each patient group and were thereafter excluded from the validation data. For the six Guardian patients and the three Abbott Freestyle patients the performance was 10, 18 and 27 mg/dl for the 15, 30 and 45-minute prediction, with a delay of around 4, 9, and 14 min for upward trends, and 5, 15, and 26 min for downward trends. In [Zecchin et al., 2011], the linear predictor from [Sparacino et al., 2007] worked in a cascade-like configuration with a NN model, which also used both CGM and glucose flux from the meal model of [Dalla Man et al., 2007a] into account as inputs. Training and validation was done using 15 patient records from the seven day free-living conditions set of the DAQ trial. The NN was trained and validated on 25 time series, each one of three days, selected to ensure a wide variety of glycemic dynamics. Nine daily profiles, containing several hypo- and hyperglycemic events, were used to test the NN with an average of 14 mg/dl and a 14 min delay for the 30-minute prediction. For an assessment on 20 simulated subjects using the UVA/Padova model, the corresponding metrics were 9.4 mg/dl and 5 min. Both insulin and carbohydrate digestion were considered by incorporating input-generating sub models in the support vector machine of [Georga et al., 2011]. Additionally, exercise-induced glucose and insulin absorption variations were also considered as inputs by processing a metabolic equivalent (MET) estimate, derived from a SenseWear body monitoring system (BodyMedia Inc.) used in the study, in a model by [Roy and Parker, 2007]. The NN was trained individually for seven T1DM patients with RMSE of 9.5, 16, 25 and 36 mg/dl for the 15, 30, 60 and 120-minute prediction.

Examples of other machine learning approaches that have been considered, include, e.g., support vector regression [Georga et al., 2013] and random forests [Georga et al., 2012]. Both techniques were evaluated on the same dataset of 27 T1DM patient records from free-living conditions collected within the METABO project [Georga et al., 2009]. The recorded insulin injections as well as the meal intakes were fed into compartment models to provide estimated profiles of plasma insulin and glucose rate of appearance. Furthermore, physical activity, estimated from a body monitoring system,

and the time of the day were also added as input variables. The predictive performance of each method was assessed for a 15-, 30-, 60- and 120-minute ahead prediction horizon with impressive results. The reported RMSE of the support vector regression for these predictions horizons was 5.2, 6.0, 7.1 and 7.6 mg/dl, whereas the random forest method managed slighty worse; 6.6, 8.2, 9.3 and 10.8 mg/dl.

Deeper reviews can be found in [Makroglou et al., 2006], [Balakrishnan et al., 2011] and [Georga et al., 2011].

Identifiability

The challenges of structural identifiability in physiologically-based models have been widely recognized [Chis et al., 2011], and specifically for the diabetic glucose dynamics [Docherty et al., 2011]. Optimal experimental design to facilitate parameter estimation has been addressed in [Galvanin et al., 2009; Galvanin et al., 2011]. Empirical black-box identification problems have received less attention, but the problems associated with identification of ARX models of glucose dynamics have been considered in [Finan et al., 2009].

In diabetic real world data, the problem is especially important, since the two main inputs affecting the dynamics, meal and insulin intake, have opposing impact and similar dynamics, and generally act simultaneously. The aspect is further problematic since safety concerns impose constraints on the possibility to excite the system sufficiently (which of course does not apply to simulated data). Thus, from an identification viewpoint, the impact from inputs may be entangled with one another, and it may be impossible to separate the impact of each input without considering constraints to the identification routine, incorporating prior information of the expected qualitative response. In [Percival et al., 2010], this was resolved by applying an experimental protocol, where a small meal and the corresponding bolus dose were separated by a few hours. However, such an approach yields only short datasets and may be infeasible, e.g., if re-estimation recurrently is required due to, e.g., shifting dynamics.

Closed-Loop Control

Closed-loop control, or as it is often referred to in the diabetes context—the artificial pancreas—is most often suggested in the form of a regulator controlling an insulin pump by glucose sensor feedback. The earliest closed-loop system in this sense dates back to the ’60s and ’70s. The first commercial closed-loop system, the bed-side Biostator system, was introduced in 1977, relying on venous insulin infusion and glucose measurement [Fogt et al., 1978]. Today, the prerequisites have changed dramatically with major improvements in pump and sensor technology, and both academic researchers

and biotechnology companies pursue closed-loop control using primarily the subcutaneous route. The first step to implement an autonomous function in a commercial outpatient system has been made in the MedTronic Veo and 640G pumps, which automatically suspend for two hours when a predefined hypoglycemic threshold is passed [Medtronic, 2012]. Reviews of current and historical development and of the challenges ahead can be found in [Cobelli et al., 2011] and [Bequette, 2012].

Closed-loop control is in many aspects a promising technology, but some concerns need to be considered when evaluating the prospects of this technology to resolve glucose control for a larger part of the IDDM population. Firstly, using a closed autonomous system calls for a robust safe design. This aspect needs to be considered throughout the system design, and identified hurdles, concerning, e.g., sensor accuracy and reliability, modeling and parameter estimation errors, disturbance detection and rejection and programming and software errors, still remain to be resolved. The second aspect is the cost aspect, as such a system relies on many expensive components. Thirdly, and this relates to the first aspect, regulatory and liability considerations need to be worked out. Considering these obstacles, it is unlikely that an artificial pancreas system will be the default therapy for a majority of the IDDM population in the near future.

2.4 Decision Support and Defence-In-Depth

An alternative technology to closed-loop control is to provide the patient with decision support, which sports some advantages in comparison to the artificial pancreas approach. It is more flexible in underlying therapy format, as it is not locked to the pump technology. Since no injections are made automatically, an opportunity to detect wrongful and potentially dangerous actions is provided. Finally, the total cost is lower, implying possible better cost effectiveness. On the other hand, the dependency on user interaction makes it more vulnerable in many aspects. Unless user confidence to the system is achieved, poor compliance to the suggested decisions may prove the system useless. Furthermore, in situations where the user is unable to respond, no action can be taken. Also, the potential risk reduction, associated with capturing dangerous actions, relies on an independent basic insight to the glucose dynamics of the user, and a sound non-authoritarian attitude to the system. Of course, to the extent possible, self-monitoring and evaluation need to be implemented at a system level, to catch such errors before actions are suggested to the user. This calls for a hybrid safety systems where some decisions are autonomous whereas others require active participation and decision making by the user. In this context, the concept of defence-in-depth is useful to develop and assess the safety of the system. The concept originates

from military defence tactics, but has become popularized in safety critical engineering applications, such as nuclear engineering [IAEA, 1996], fire prevention [U.S. NRC Fire Protection, 2015] and information security [National Security Agency, 2015], even though with somewhat different interpretations and practices. Multiple layers of administrative and technical barriers work together to reduce the risk of unsafe events. Each layer should reduce the possibility of an unsafe event occurring, or if it has already happened, to reduce the consequences thereof. If one barrier fails, the next in line should step in. The principle is often accompanied by supporting safety design principles and analysis tools as single failure analysis, diversification and deterministic [IAEA, 2009] and probabilistic safety analysis [IAEA, 2010]. A typical defence-in-depth approach utilizes the following barriers:

1. Prevention of abnormal operation and failures. Covers administrative rules, regulations, guidelines, code of conduct, safety principles. By following and enforcing behavioural aspects of the management of the safety critical system and how it interacts with the environment, unwanted and potentially dangerous events may be avoided or mitigated before they progress further.

2. Systems for automatic detection and notification of warnings. This technical barrier covers systems for monitoring safety critical parameters and to issue alarms when predefined thresholds are broken.

3. Systems for activation of safety features to mitigate an adverse event. These systems may be automatically or manually activated and should forcefully reduce the risk of damage to the safety critical system due to the adverse event.

$\geq$4. Systems and procedures aiming at reducing the damages, and consequences thereof, to the safety critical objective and the environment if all previous barriers have failed and a damaging event could not be avoided.

Applying the concept to diabetes glucose self-management would mean to develop barriers and supporting principles to reduce the frequency and consequences of adverse glycemic events such as severe hypo- and hyperglycemia, e.g.:

1. Risk-mitigating self-care strategies that reduce the frequency of hypo- and hyperglycemia. This barrier involves activities and knowledge such as; frequent glucose testing, basic understanding of the personal glucose dynamics, familiarity with personal health care equipment, and training and use of best practices to determine the basal and bolus doses, and mainly involves the patient but also requires support of the healthcare

team. Clinical guidelines can be regarded as the underlying framework for this barrier.

2. Continuous glucose monitoring. The recent developments in continuous glucose monitoring have allowed for keeping constant track of the glucose level. Current systems allow for alarms to be raised when predefined hypo- and hyperglycemic thresholds are surpassed.

3. Active safety systems. The pump suspension feature of the Medtronic insulin pumps is an example of an active safety system that autonomously intervenes to reduce the impact of an expected adverse event (hypoglycemia).

In this thesis, models and methods that could contribute to some of the building blocks in such a concept will be developed, investigated and scrutinized.

3

Data and Data Characteristics

This chapter introduces the data used in this thesis and some analysis of fundamental glucose data characteristics.

The DIAdvisor project [DIAdvisor, 2012] was an EU FP7 Integrated Project (IP) running between 2008 and 2012. The aim of the project was to develop a personal decision support system for IDDM patients using user-provided input, minimally invasive sensors and individualized models of glucose dynamics, in order to provide the user with short-term predictions of glucose evolution, together with insulin therapy decision support.

3.1 The DIAdvisor Project

A mobile research system, incorporating these aspects, was developed and successfully evaluated under clinical conditions at three clinical sites covering 50 patients, with a significant reduction of time spent in hypoglycemia, and increase in time in normoglycemia [The DIAdvisor Consortium, 2012]. The reduction of time in hyperglycemia was not statistically significant. Using an Ultra Mobile PC (UMPC), the user could follow his/her glucose curve together with an estimate of the near-time (2 hours) ahead projection, see Fig. 3.1. The same information was concurrently provided to the clinician's laptop application by a wireless network according to the network layout in Figure 3.2.

The project consortium consisted in total of 14 partners, both academic institutions and commercial companies—each providing expertise in areas relevant for the development of the system. Especially noteworthy for the coming chapters are the three clinical partners where the data were collected; Montpellier University Hospital, Department of Clinical and Experimental Medicine (Montpellier), University of Padova, UNIPD (Padova) and the Institute for Clinical and Experimental Medicine, IKEM (Prague).

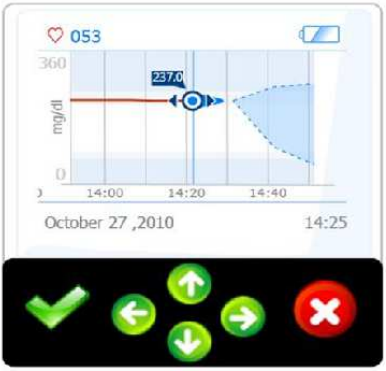

Figure 3.1 User Interface of the DIAdvisor system patient application implemented on the UMPC. On the screen, the user can follow the present and recent glucose values together with a projected future trajectory within specified uncertainty limits. Other vital signs, such as heart rate (see upper left screen corner), may also be possible to follow. User inputs, regarding, e.g., insulin and meal intake, are provided by a menu system controlled by the buttons at the bottom of the screen. Reproduced from [The DIAdvisor Consortium, 2012].

3.2 The DIAdvisor Data

The clinical part of the DIAdvisor project consisted of three clinical studies; the data acquisition (DAQ) trial (2009), the DIAdvisor I (2010) and DIAdvisor II (2011-2012) trials. The purpose of the first trial was to collect data in order to facilitate model and algorithmic development of the individual modules of the DIAdvisor system. The two following trials were set up for testing and validating the entire system in clinical settings. The results presented in this thesis are based on retrospective analysis of the data collected in the DAQ and DIAdvisor I trials.

A total of 90 patients participated (29 Montpellier, 31 Padova, 30 Prague) in the DAQ trial, including users of both MDI and subcutaneous pump therapy. For this thesis, the data were assessed for data completeness and data consistency. Exclusion criteria were missing bolus doses and missing meal data in the diary, missing continuous glucose measurement (CGM) data and large discrepancies between the CGM and the reference glucose meter data. Data segments not fulfilling the criteria were rejected, and only data records containing at least 48 hours of consecutive qualitative data were included in the study. In all, 47 out of the 90 patient data records reached the quality standards of inclusion (17 Montpellier, 19 Padova, 11 Prague). A summary of collected population statistics can be found in Table 3.1.

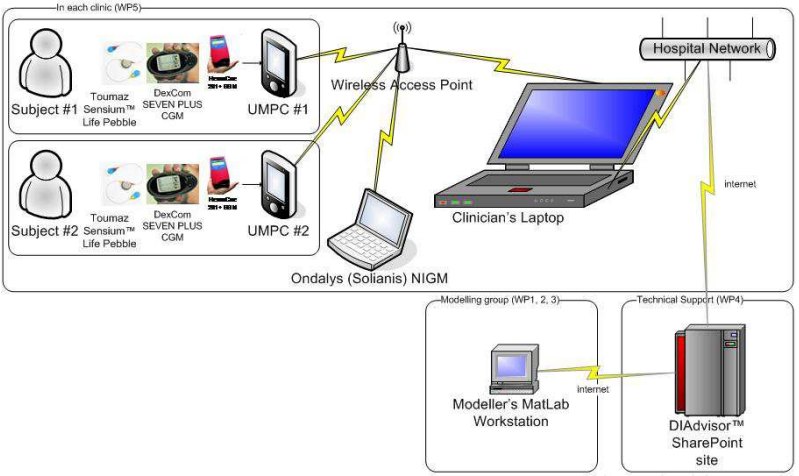

Figure 3.2 DIAdvisor system network. The UMPC communicated with the sensors attached to the patient, and transmitted the information to the clinician's laptop through a wireless network. After each visit the clinical team uploaded the data to a common FTP-server. Reproduced from [The DIAdvisor Consortium, 2012].

The DAQ trial was divided into two main parts; a three day hospitalized study and an ambulatory second part, where the patients were allowed to bring the system home under normal living conditions. In this thesis, data from the hospitalized part of the trial were used in Chapters 8 and 9.

In the second trial, the first configuration of the DIAdvisor system was tested for some of the patients that participated in the DAQ trial, as well as for some new patients. The trial was divided into six different sub-trials, DIAdvisor I A-F—each with a specific evaluation purpose. Trial A was a data collection study in order to validate that the system could retrieve data from the external sensors as expected, the B and C trials had identical protocols but with different purposes. The intention of trial B was to test the predictive performance, whereas trial C aimed at an assessment of the therapeutic advices provided by the system. In trial D, the patients underwent two different exercise tests, and in trial E, free meals, not regulated by the standardized procedure, were allowed. In the final F trial, periods of hypo- and hyperglycemia were induced. Trials A, B, D were conducted at the Montpellier hospital, trial E at the Padova site and trial F in Prague. Trial C was evaluated at all three sites. Data from the B and C trials were used in Chapter 9. The third trial, DIAdvisor II, was set up to validate the final performance against the project endpoints using an updated version of the

Table 3.1 Population Statistics of the DAQ trial. Body Mass Index (BMI), Total Daily Dose (TDD). Mean values and [min-max].

Parameter	Montpellier	Padova	Prague
Male/Female	13/4	10/9	6/5
Pump/MDI	9/8	10/9	8/3
Rapid Insulin	11 Aspart	15 Aspart	4 Aspart
	1 Glulisine	4 Lispro	7 Lispro
	5 Lispro		
Age	44 [22-68]	42 [25-67]	33 [19-65]
BMI [kg/m^2]	24.2 [19.7-30.1]	24.5 [18.7-33.2]	25.0 [16.8-35.9]
HbA1c [mmol/mol]	7.7 [5.6-9.1]	8.0 [6.0-9.3]	7.8 [6.4-9.7]
TDD [IU]	47 [18-82]	44 [22-74]	22 [6-54]
Antibodies [% binding]	15.6 [0-62.1]	20.4 [0-75]	12.9 [0-53]

DIAdvisor system. Data from this trial has not been analysed in this thesis.

3.3 Equipment

During the trials, the patients were equipped with sensor devices in order to collect vital signs of potential interest in metabolic modeling.

Glucose Sensors

The HemoCue Glucose 201+ Analyzer (Figure 3.3, [HemoCue Glucose 201+ Analyzer, 2012]) is a high-quality glucose meter of laboratory precision [Stork et al., 2005]. This device was used as blood glucose reference in both trials.

In the DAQ trial, the patients were equipped with the Freestyle CGM system (Figure 3.4) from Abbott [Abbott Freestyle Navigator, 2015]. The system provided a CGM reading every 10 minutes, but the raw current signal from the sensor was also collected on a one-minute basis at the Montpellier and Padova sites. The sensors require initialisation during 10 hours and have a life time of five days, after which they need to be replaced. In the DIAdvisor I trial, the CGM system Seven Plus (Figure 3.4) from Dexcom was used [Dexcom Seven Plus, 2012]. This sensor has an initial calibration time of 2 hours and is replaced after seven days. Both systems need to be recalibrated every 12 hours.

3.4 Vital Signs Sensors

During the DAQ trial the patients wore the Clinical LifeShirt (Figure 3.5) from VivoMetrics [VivoMetrics, 2012], which is specially designed for clinical

Figure 3.3 The HemoCue 201+ Analyzer, [HemoCue Glucose 201+ Analyzer, 2012].

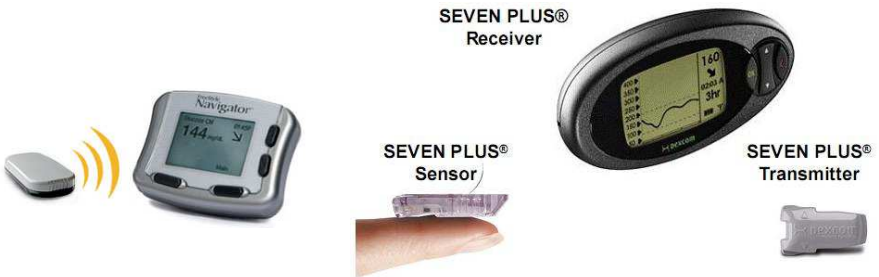

Figure 3.4 CGM systems used in the DIAdvisor project; the Abbott Freestyle CGM system, [Abbott Freestyle Navigator, 2015] (left), and the Dexcom Seven Plus CGM system [Dexcom Seven Plus, 2012] (right).

trials. This non-invasive monitoring system continuously collects, records and analyses several vital signs. To measure respiratory function, sensors are woven into the shirt around the wearer's chest and abdomen. A single-channel ECG measures heart rate, a three-axis accelerometer records posture and activity level, and a thermometer measures the skin temperature.

In the DIAdvisor trial, the LifeShirt was replaced by the Sensium Life Pebble sensors (Figure 3.5) developed by Toumaz [Toumaz, 2012]. These continuously monitor ECG, heart rate, physical activity (3-axis accelerometer) and skin temperature, and stream the data using a wireless datalink over a short range (5 m).

Figure 3.5 Vital signs sensor systems used in the DIAdvisor project; the VivoMetrics' LifeShirt system [VivoMetrics, 2012] (left), and the Sensium Life Pebble sensors by Toumaz [Toumaz, 2012] (right).

3.5 Experimental Protocols and Conditions

The DAQ and the DIAdvisor I trials followed the same basic protocol. Standardized meals were served for breakfast (08:00), lunch (13:00) and dinner (19:00), according to the protocol. The amount of carbohydrates included in each meal was about 40 (45 in DAQ), 70 and 70 grams, respectively. Additional snacks, in some cases related to counter-act hypoglycemia, were also digested. No specific intervention on the usual diabetes treatment was undertaken during the studies, since a truthful picture of normal blood glucose fluctuation and insulin-glucose interaction was pursued. Meal and insulin administration were noted in a logbook, glucose was monitored by the Continuous Glucose Measurement system and by frequent blood glucose measurements in the DAQ trial (37 measurements daily according to the protocol). On average, the outcome was that 39, 37 and 7 measurements (Montpellier, Padova and Prague) were made every day. In the DIAdvisor B and C trials, even more reference measurements were collected, making the average 43 measurements a day.

3.6 Graphical Data Evaluation Tool

The trial data was continuously uploaded into an Oracle database on a common FTP-server, from which the model developers could download data as they became available. In order to facilitate data overview and management, a stand-alone Graphical User Interface (GUI), see Figure 3.6, was developed in Matlab code [MathWorks, 2012]. Using this GUI, different data channels and time periods could be selected for any individual patient in order to evaluate the data for completeness and correctness, before extracting and

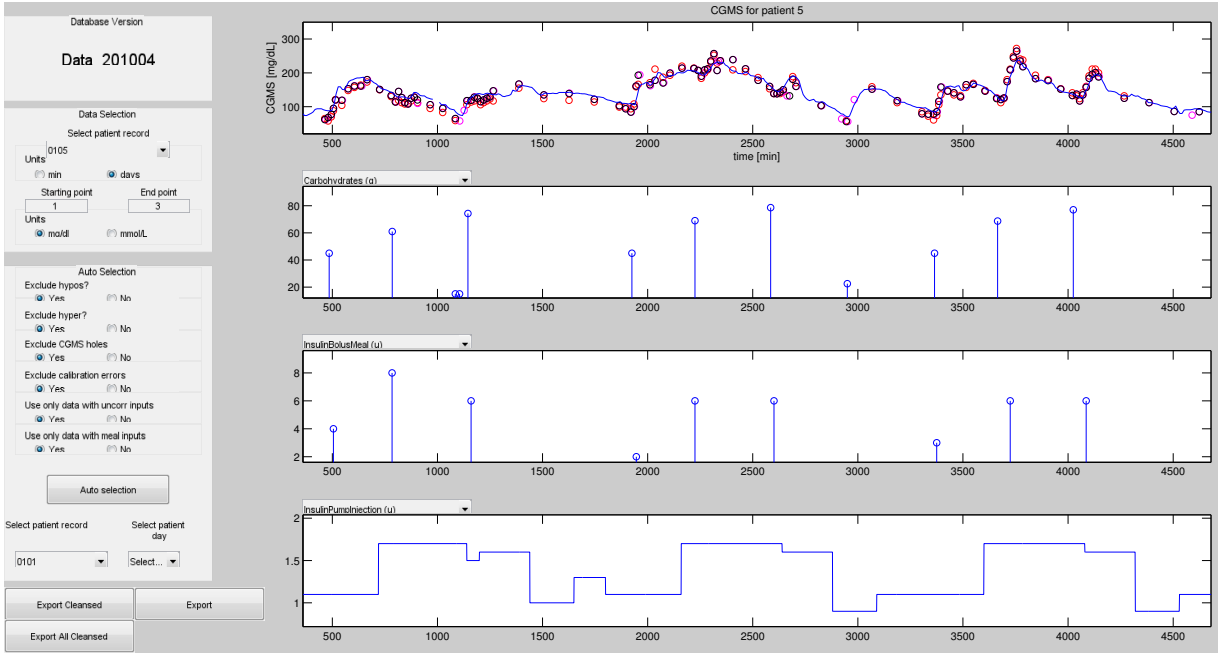

Figure 3.6 The Graphical User Interface (GUI) to manage the DAQ data. Different data sections from both the clinical and the home-monitored part of the DAQ trial can be analysed. The upper plot always shows the linearly interpolated CGM (blue curve) and the HemoCue reference measurements (circles). The lower windows can be used to display any of the recorded signals. In this example, the three days data from the clinical part of the trial has been selected. The second plot from the top shows timing and amount of ingested carbohydrates, the third plot depicts bolus and correction insulin doses, and in the bottom window the pump basal curve has been chosen for investigation.

Table 3.2 Summary of statistics for the patients that finalized the study. [min–max]

Parameter	Animas/Dexcom	Medtronic
Number of patients	15	14
Gender	6F/9M	8F/6M
Age	32[23-53]	37[19–68]
Years since diagnosis	15[6–30]	22[10–55]
BMI [kg/m^2]	26[21.6–46.7]	25[19.6–29.1]
HbA1c before the study [mmol/mol]	63[45–84]	62[42–89]
Pump	Animas Vibe	Medtronic Veo
CGM Sensor	Dexcom G4	Medtronic Sof (6) and Enlite (8)
Nr of days in study	39 [11–43]	33 [25–39]
Nr of days in study	109 [0–290]	236 [51–433]
Nr of CGM measurements	10477 [3154–11919]	10477 [3154–11919]
Nr of meals reported	157 [30–268]	147 [22–255]

exporting them into a single Matlab data file. The evaluation described in Section 3.2 was performed using this tool.

3.7 The Lund University (ULund) Trial

The study was a non-randomized trial conducted under free-living conditions. After review and approval of the study protocol by the [Regional Ethical Review Board in Lund, 2014], Sweden, 32 T1DM patients on Continuous Subcutaneous Insulin Infusion therapy (CSII), enrolled at the Endocrinology Department, were recruited. The patients used two different insulin pump systems and were divided into two groups based on this. The Animas Vibe pump ([Animas Vibe, 2015]) was used by 15 patients and 17 patients used the Medtronic Veo pump ([Medtronic, 2012]). In total, 29 of the patients finished the study (15 from the Animas and 14 from the Medtronic cohort). Exclusion criteria were manifested retinopathy, nephropathy, neuropathy or hypertonia and cognitive difficulties. The total study duration was 42 days for the Animas Vibe patients and 36 days for the Medtronic patients. Weight and height were recorded and blood samples for HbA1c analysis were drawn at the start-up visit at the clinic. The baseline characteristics of the patients that completed the study are found in Table 3.2.

The patients were provided information about the study and instructed on the use of the Continuous Glucose Measurement system (CGM), and written consent of participation was collected. Specifically, the patient received

information about the delayed glucose readings of the CGM in comparison to venous blood samples. The Animas Vibe patients were equipped with a Dexcom G4 CGM sensor and a total of four sensors for the entire study period. Each sensor was supposed to be used for two weeks, i.e., one week more than the nominal lifespan of this sensor type. Thereby, the fourth sensor was to be considered as a back-up in case any of the previous sensors failed. The Medtronic patients were randomly equipped with two sensor types; Enlite (eight patients) and Sof sensor (six patients). Each patient received a total of six sensors, each to be used for six days. The Medtronic patients were provided with a Bayer Contour Link glucose meter which automatically and wirelessly transfers the glucose reading to the pump. The Animas patient used their own glucose meters. Calibration was to be conducted at least as often as prescribed by the CGM manufacturer, and to be performed when the glucose level was stable in order to reduce the risk of calibration errors related to the sensor delay. The patients were asked to carefully register all meals, including alcohol intake, and physical exercise using a web service provided by the company Linkura [Linkura AB, 2015], see Figure 3.7. This logbook enabled the users to predefine recipes, such that entry of a meal instance of a recipe that had been noted at a previous occasion was simplified. Finally, the patients were instructed to treat their bolus doses at their own discretion. Data from this trial were used in Chapters 4-7.

3.8 Glucose Data Characteristics

Before digging into modeling and prediction of glucose dynamics, some interesting features of the glucose data are worthwhile to explore a little more in-depth.

Optimal sampling frequency

An interesting question is how often sampling is needed in order to reconstruct the most important features of the glucose signal, and thus how important CGM measurements may be, and whether interpolation of frequent BG measurements can be used to reconstruct the glucose curve. According to [Worthington, 1990], at least 8 samples per day are needed to get the lowest essential dynamics of the system, namely the rise and fall of the blood glucose level due to the carbohydrate intake and the associated insulin injections. This is a rigid assumption, relying on that the meal-related period is about 6 hours, and that the subject follows a strict schedule. In reality, people tend to have more irregular routines. This is generally overcome by non-equidistant sampling, collecting data on an event-driven basis, rather than a time-scheduled ditto.

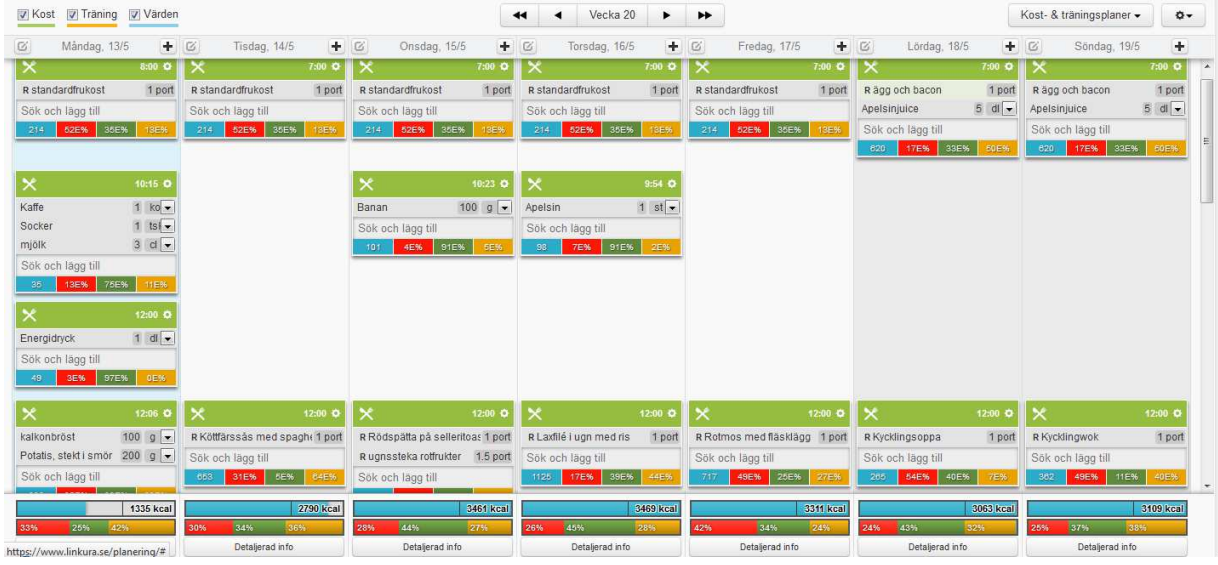

Figure 3.7 Example of the week overview in the Linkura web service GUI. Each green box corresponds to a meal instance where the user can fill in the timing of the meal intake and the content of what has been consumed from personal predefined recipes.

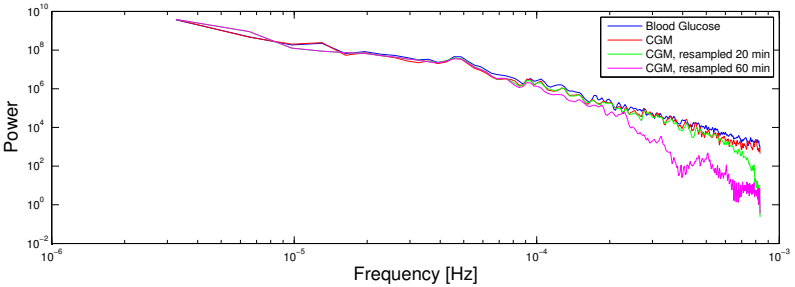

Figure 3.8 Periodogram of the SMBG, the original and the down-sampled CGM signals. Average for the Montpellier patients.

Method In order to evaluate how much information is lost as the sampling rate decreases, the CGM data collected at the Montpellier hospital 3-day visit of the DAQ trial were used. The data were down-sampled to a sampling period of 20, 40, 60 min and then interpolated by piecewise splining (pchip in Matlab [MathWorks, 2012]). Likewise, the frequent BG measurements were also interpolated by the same method. Error analysis of the down-sampled signals in comparison to the original signal was done by frequency domain analysis, see [Johansson, 2009], and statistical analysis of the time-domain data.

Results Obviously, the frequency content diminished with increased sampling period, as seen in Figure 3.8, where the periodogram of the original signal and the interpolated signals can be seen.

The spectrum of the blood glucose signal is very similar to that of the CGM signal. For the down-sampled CGM signals, the energy decreases for the higher frequencies as expected. However, frequency assessment does not easily translate to clinically relevant information. Turning to the time-domain, the difference between the signals deteriorates as depicted in Table 3.3. Already at a reduced sampling period of 60 min, the maximum average error amounts to more than 30 mg/dl. This is not surprising, as the glucose rise/drop over

Table 3.3 Comparison between the original and the resampled CGM signals in terms of Root Mean Square Error (RMSE) and maximum error. Average over the DAQ population.

Criteria	**Sampling period [min]**				
	20	40	60	80	100
RMSE [mg/dl]	1.4	4.0	7.0	10.4	12.7
maximum error [mg/dl]	8	18	30	45	51

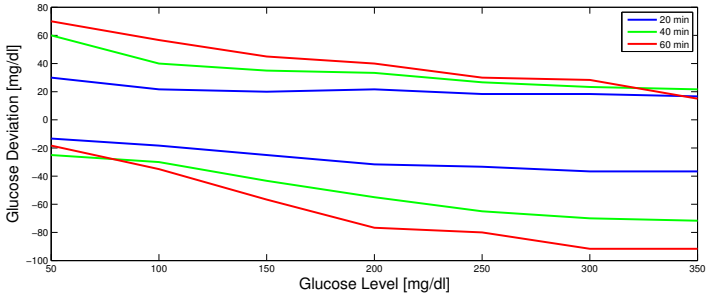

Figure 3.9 95 % confidence bounds of the deviation distribution over different time horizons. Average for all three clinical sites.

an hour can be in the magnitude of -35 mg/dl to +60 mg/dl (95 % conf. bound) at glucose levels of 100 mg/dl, and with an even wider spread for higher glucose levels, see Figure 3.9.

Discussion It should be borne in mind that these values are under-estimated considering the low-pass character of the relationship between interstitial and blood glucose value (see discussion about the sensor lag later on in this chapter). This aspect also inhibits the possibility for direct comparison between these signals. However, the frequency response shows that the interpolated BG curve incorporates the same frequency content as the original CGM signal and should thus be a reasonable approximation of the true blood glucose evolution. Thus, even though only 37 samples were collected a day, making the average sample period about 40 min, the applied sampling schedule made it possible to capture the dynamical changes. In general, glucose self-monitoring does not follow a strict sampling schedule. Rapid changes in the blood glucose can be recognized by persons with normal hypoglycemic sensitivity as hypoglycemia, changes into hypoglycemia or hyperglycemia are often detected, and these circumstances call for unscheduled measurement to establish glycemic status. Therefore, the high and low peaks are, for many instances, represented in home-monitored data, but as the hypoglycemic sensitivity decreases over the years since diagnosis, the risk of undetected hypoglycemia increases [Mokan et al., 1994].

Distribution

In order to investigate the range of excitation in the data in terms of glucose level, and to determine if there are any systematic differences in this aspect between the different sites, the distribution of the CGM data was analysed.

Method The distribution of the CGM data from the DAQ trial was assessed by standard statistical methods for all three clinical sites.

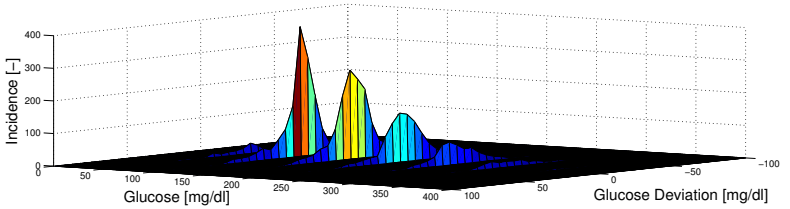

Figure 3.10 Total distribution of glucose level $G(t)$ and the 20 minute glucose deviation, $G(t+20) - G(t)$. Montpellier patients, the DIAdvisor DAQ trial.

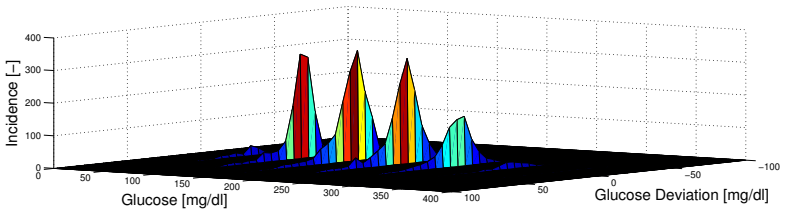

Figure 3.11 Total distribution of glucose level $G(t)$ and the 20 minute glucose deviation, $G(t+20) - G(t)$. Padova patients, the DIAdvisor DAQ trial.

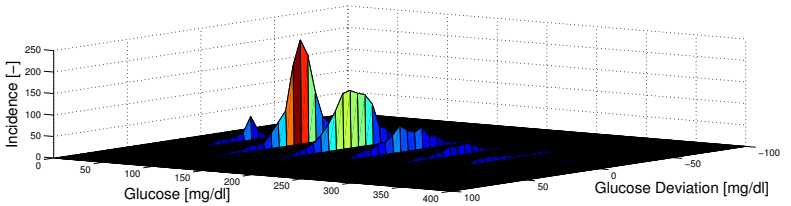

Figure 3.12 Total distribution of glucose level $G(t)$ and the 20 minute glucose deviation, $G(t+20) - G(t)$. Prague patients, the DIAdvisor DAQ trial.

Table 3.4 Likelihood of each glycemic zone [%], and average mean glucose [mg/dl] for the patient data from each clinical site.

Glycemic Zone	Zone Limits [mg/dl]	Montpellier	Padova	Prague
Severe Hypoglycemia	$G \leq 50$	0	0	0
Hypoglycemia	$50 < G \leq 75$	3	2	4
Lower Euglycemia	$75 < G \leq 125$	32	23	37
Upper Euglycemia	$125 < G \leq 175$	31	30	34
Lower Hyperglycemia	$175 < G \leq 225$	20	27	15
Hyperglycemia	$225 < G \leq 275$	14	18	10
Upper Hyperglycemia	$G > 275$	0	0	0
Mean Glucose [mg/dl]	-	153	169	142

Results The dynamical total distribution of glucose level $G(t)$ and glucose deviations over 20 minutes, $G(t+20)-G(t)$ can be seen in Figures 3.10, 3.11 and 3.12. There is a clear difference in distribution between the clinical sites. The glucose range can be divided into 7 different zones of different clinical importance, and the likelihoods of each zone are found in Table 3.4.

The glucose data are clearly non-Gaussian, as seen from Figure 3.13, depicting the total distribution of the accumulated CGM readings collected at all three site. The samples fluctuate around an average of about 160 mg/dl, but the deviations are not normally scattered around this mean. This phenomenon has been noted in [Kovatchev et al., 1997] as well, where the following data transformation was suggested to transform the data into a Gaussian distributed variable with zero mean.

$$f(G, \alpha, \beta) = (\log G)^{\alpha} - \beta \tag{3.1}$$

The parameters α and β should be 1.084 and 5.381 when using the

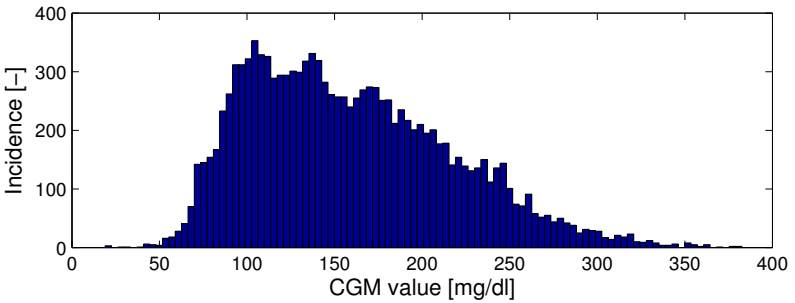

Figure 3.13 Total distribution of CGM glucose level. All DAQ patients.

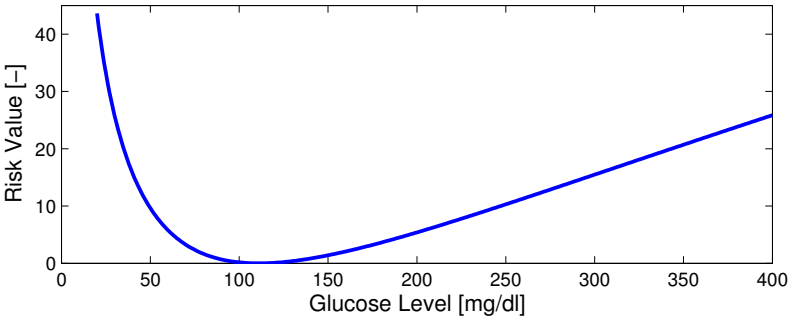

Figure 3.14 Risk function using Kovatchev's transformation.

milligram-per-dl scale. The accumulated data from each site was transformed in this manner and the distributions can be seen in Figures 3.15, 3.16 and 3.17. The data from Padova do not fit the normal distribution very well, but the data from the other sites show better resemblance. However, the normal hypothesis was rejected in every case using the Kolmogorov-Smirnov test [Johansson, 2009], contrary to the results in [Kovatchev et al., 1997]. From Figures 3.15, 3.16 and 3.17 it can be seen that the upper tail of the normal distribution is missing or deformed, which is due to the low incidence of hyperglycemia, see Table 3.4.

Discussion The Prague patients have the most aggressive glucose control, with fewer high values and more time spent in hypoglycemia. The Padova patients have more hyperglycemic events, but also half as much time spent in hypoglycemia compared to the Prague patients. This is also reflected in the average mean glucose values, which are statistically significantly different from each other ($p<0.01$ for all possible comparisons).

The total distribution was found to be non-Gaussian, but the log-normal like distribution suggested by [Kovatchev et al., 1997] could not be confirmed. Under free-living conditions, the hyperglycemia tendency is generally higher than for the DIAdvisor DAQ data evaluated here, which may explain why [Kovatchev et al., 1997] found that 203 out of 205 transformed home-monitored SMBG datasets confirmed the normal hypothesis.

The data transformation stems from an intention to create a risk value describing the increased clinical risk associated with hypoglycemia and hyperglycemia. By taking the square of the transformated glucose level and multiplying by 10, the risk function of [Kovatchev et al., 2000] is retrieved, see Figure 3.14. This function forms the basis for the cost function used in Chapter 9.

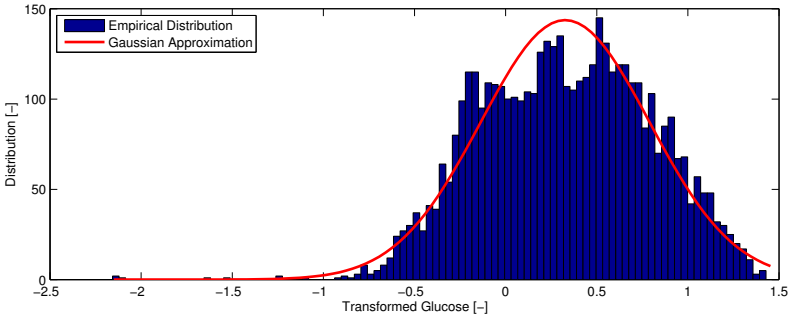

Figure 3.15 Empirical and Approximated Distribution of transformed CGM data. Montpellier patients.

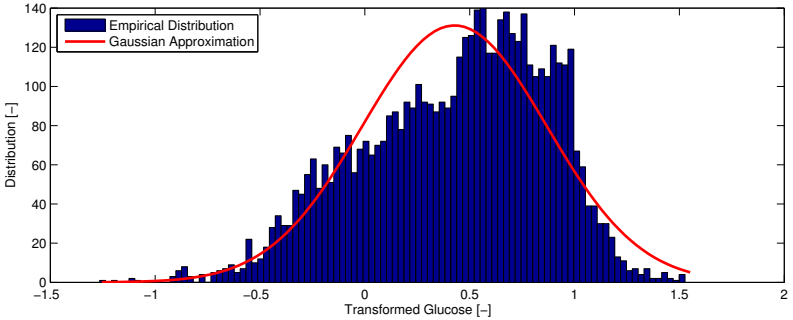

Figure 3.16 Empirical and Approximated Distribution of transformed CGM data. Padova patients.

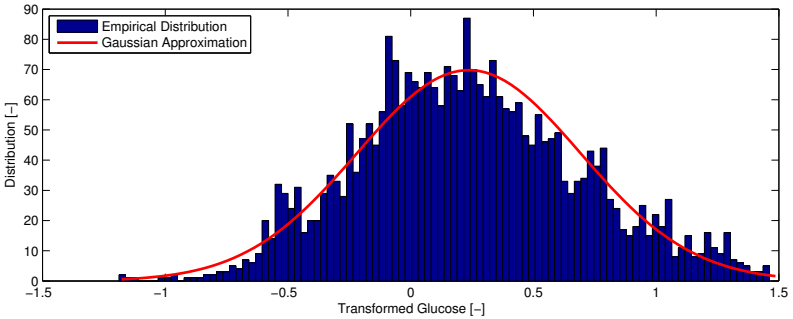

Figure 3.17 Empirical and Approximated Distribution of transformed CGM data. Prague patients.

Time-variability

Another important aspect of diabetic glucose data is the question of time-variability. The circadian rhythm may have a significant impact on insulin sensitivity over the course of the day [Van Cauter et al., 1997], especially in the early morning, when counter-regulatory hormones (primarily growth hormone, cortisol and adrenalin) are released—triggering increased hepatic production [Perriello et al., 1991].

Variability over longer time horizons has not been thoroughly investigated in the literature, which may be explained by the scarcity and difficulty of obtaining qualitative longer data records. Very few longitudinal datasets longer than a few days, or weeks at best, seem to be available for T1DM in the research community. The dataset used in [Ståhl and Johansson, 2009] is thus quite unique in this aspect. This dataset was collected during the first months of a newly diagnosed T1DM patient (the author). This period of time is generally referred to as the 'honey-moon period', during which the pancreatic β-cells recover somewhat, resulting in temporary remission with considerably varying insulin doses and glycemic response [Abdul-Rasoul et al., 2006]. Mathematically, this translates into time-varying model parameters.

Method The honey-moon data were analysed. In order to estimate and validate different models, data segments with constant parameter values are needed. To find such segments, the data were investigated using the Adaptive Forgetting Multiple Model change detection algorithm (AFMM), implemented in the Matlab command "SEGMENT" [MathWorks, 2012].

Results In Figure 3.18, the variations of the estimated ARMAX parameter over the time period can be seen.

Discussion The model parameters shifted a number of times during the honey-moon period, giving an indication of both more stable and unstable data sections, and this behavoir is expected during this remission phase. The last stable parameter section is more than a month in length, signalling the end of the honey-moon period. It may also be noted that the parameter values end up close to the original values, which may be another indication that the temporary β-cell recovery has ended. Longer time-variability in non-newly-diagnosed patients is generally less dramatic, but should not be overlooked, especially for the so-called 'brittle' patients [Voulgari et al., 2012]. Time-variability will be further investigated in Chapter 4.

Blood-to-Interstitial Glucose Lag

The diffusion-like relationship between the blood and interstitial compartments implies a low-pass character in the response to glucose changes, which means lagging glucose levels in the CGM sensor in comparison to the reference SMBG.

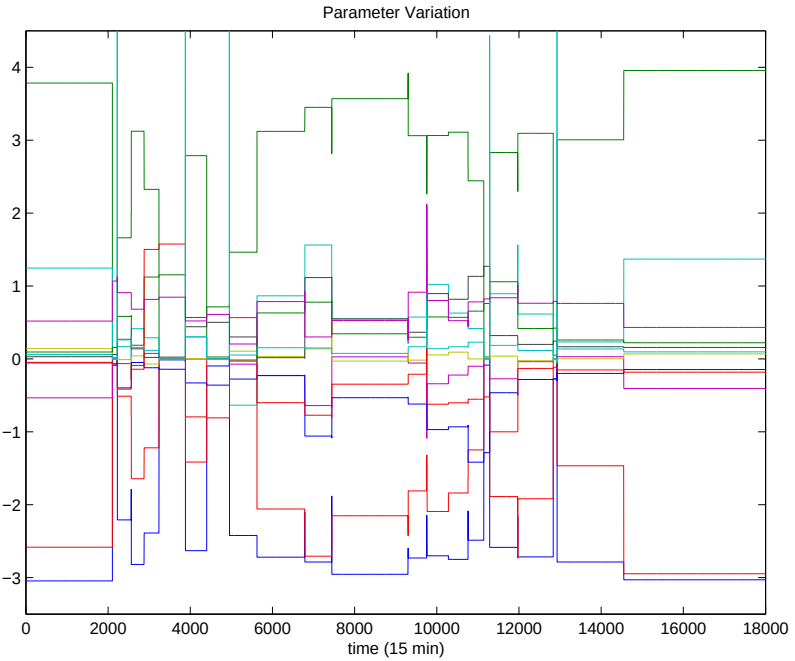

Figure 3.18 Data segmentation using the Matlab command SEGMENT. Variability of the parameters of the recursive ARMAX model over approximately 200 days.

Methods The CGM signal and the blood glucose reference measurements from the DAQ trial were analysed as follows. To retrieve an initial non-parametric estimate of the magnitude of the lagging between the blood glucose reference $BG(t)$ and the CGM signal, the lag was approximated to a delay, and was found by finding the delay Δ which minimized the Root Mean Square Error (RMSE) between the blood glucose measurements $BG(t_{BG})$ and the corresponding backward-translated CGM measurements $CGM(t_{BG} + \Delta)$ for the time point t_{BG}, corresponding to time points when the blood glucose reference measurements were sampled. The measurement error was also assessed by RMSE between the untranslated CGM signal and the blood glucose reference, and a possible correlation between sensor delay and Body Mass Index (BMI) was investigated.

Results In Tables 3.5, 3.6 and 3.7 the estimated delay and RMSE between the CGM signal $CGM(t)$ and the HemoCue reference $G(t)$ is given for every included patient. The BG-CGM delay was statistically larger for the Prague patients than for the Montpellier patients ($p<0.05$) and for the Padova pa-

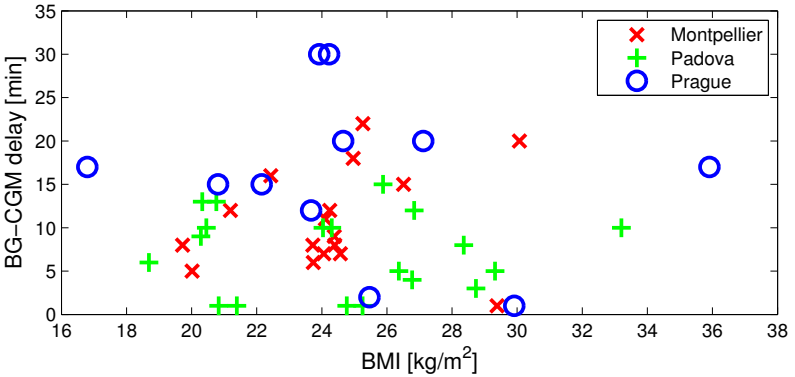

Figure 3.19 Delay between blood glucose reference measurement and the corresponding CGM measurement vs. BMI for the DAQ data from the three clinical sites.

tients ($p<0.001$), and the BG-CGM delay of the Montpellier patients was larger than that of the Padova patients ($p<0.02$). In terms of BG-CGM measurement error, the Prague patients had a significantly larger BG-CGM RMSE than the Padova patients ($p<0.002$) and the Montpellier patients ($p<0.003$). No correlation between BMI and BG-CGM delay was found, see Figure 3.19.

Discussion The differences between the Prague data and the other sites could be explained by the significantly lower number of reference measurements at the Prague site (7 measurements) compared to the Padova (37 measurements) and the Montpellier (39 measurements) patients, and the simplified assumption of estimating the delay and not the lag. The low number of samples, mainly collected during periods of substantial glucose changes, where the low-pass filter relationship causes long delays and mismatches, result in that the delay estimate is biased. Thus, the estimates for the Prague patients should be disregarded.

Intuitively, a correlation was expected between high BMI, often indicating a thicker abdominal layer, and longer BG-CGM time delay, as a possible explanation for the large interpersonal differences. However, the diffusion may be more dependent on other factors than mere amount of abdominal fat, such as capillary density and blood turn-over rate.

A model of the interstitial lag and how it can be used to compensate to get more timely estimates of the capillary glucose value will be presented in Chapter 8.

Table 3.5 Glucose Data Statistics Montpellier.

Patient ID	BG-CGM Delay [min]	BG-CGM RMSE [mg/dl]
102	15	19.8
103	6	11.8
104	5	22.1
105	7	14.7
106	12	27.7
107	22	28.1
108	8	15.3
111	9	19.6
112	18	23.9
115	8	15.4
117	20	27.6
118	11	23.7
120	16	24.9
122	7	17.9
126	12	21.5
127	8	14.4
130	1	34.3
Mean (std)	**10.9**(**5.7**)	**21.3**(**6.0**)

Table 3.6 Glucose Data Statistics Padova.

Patient ID	BG-CGM Delay [min]	BG-CGM RMSE [mg/dl]
201	1	22.8
202	10	14.5
203	5	27.2
205	10	30.1
209	1	21.5
211	12	24.6
212	6	21.9
213	10	20.6
214	1	16.2
215	5	15.6
216	3	24.0
217	8	14.8
219	13	25.6
220	13	19.8
221	15	23.3
222	4	30.0
226	10	28.4
227	9	24.2
231	1	18.3
Mean (std)	**7.2**(**4.6**)	**22.3**(**4.9**)

Table 3.7 Glucose Data Statistics Prague.

Patient ID	BG-CGM Delay [min]	BG-CGM RMSE [mg/dl]
301	20	30.7
310	20	22.0
313	15	41.0
316	17	36.2
317	30	50.3
318	17	16.8
322	12	34.5
324	15	28.9
325	1	17.7
326	30	44.5
328	2	23.3
Mean (std)	**16.3(9.2)**	**31.4(11.6)**

4

Modeling Insulin Action

4.1 Introduction

Understanding how insulin affects the glucose level is perhaps the most fundamental part of modeling and identifying glucose dynamics. In insulin-dependent diabetes, external administered insulin is constantly required to control the balance between hepatic output and peripheral glucose utilization and clearance. As described in Chapter 2, several different insulin types exist, used in different combinations to achieve proper glucose control. In this thesis, focus will be on rapid-acting insulin used in insulin pump therapy and as bolus insulin in multiple daily injection therapy.

Pharmacokinetics and Pharmacodynamics

Empirical methods The golden standard of estimating the glucose-lowering effect of insulin is the intravenous euglycaemic glucose clamp technique [DeFronzo et al., 1979]. Following an overnight fast, the test subject is given a bolus shot of insulin and subjected to a continuous intravenous infusion of glucose, which is varied during the test period to keep the frequently monitored glucose level constant. At such a glucose steady state, the glucose infusion profile matches the net clearance of glucose, and is thus used as a description of the glucose-lowering effect of the investigated insulin. This test is normally performed on healthy subjects, which may lead to overestimation of the insulin action due to insufficient suppression of endogenous insulin release. The test is non-physiological with an artificially maintained euglycemia. Thus, any heterogeneous effects on insulin effectiveness over the glucose range cannot be evaluated. The protocol further stipulates that the test is to be performed in the morning following a fast, implying that possible diurnal patterns in insulin action cannot be discovered and thus may have been missed.

Physiological Models The transport of rapid-acting insulin from the subcutaneous injection site to the blood stream has been described in quite a few

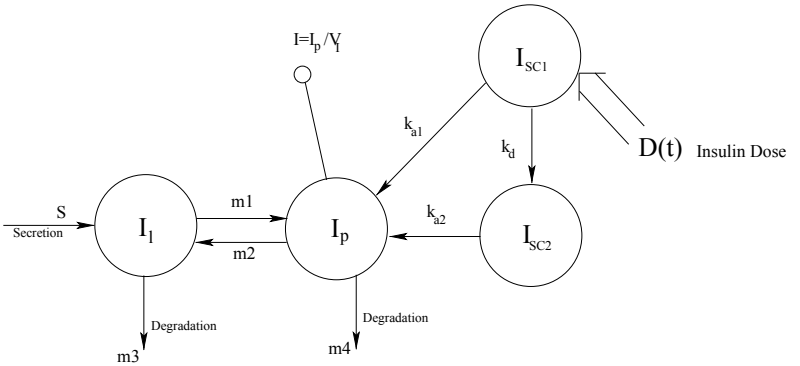

Figure 4.1 The compartment model of [Dalla Man et al., 2007b] and [Dalla Man et al., 2007a].

models of insulin pharmacokinetics. Most of these are linear compartment models, and reviews can be found in [Nucci and Cobelli, 2000] and [Wilinska et al., 2005]. This phenomenon has generally been considered independent to the metabolic interaction, and thus separated as a stand-alone model. In [Wilinska et al., 2005], eleven different models (ten compartment models and the model from [Berger and Rodbard, 1989] were fitted to empirical meal test data from seven T1DM patients using rapid-acting bolus insulin. A third-order compartment model, with local degradation of insulin at the injection site (modeled as a Michaelis-Menten relationship), turned out to be the best choice, according to the Akaike criterion [Johansson, 2009]. A similar model, the compartment model in [Dalla Man et al., 2007b] and [Dalla Man et al., 2007a] (see Fig. 4.1), has been selected as a representative example of the modeling approaches in this field. The model equations are:

$$\begin{aligned}
\dot{I}_{sc1}(t) &= -(k_{a1} + k_d) \cdot I_{sc1}(t) + D(t) \\
\dot{I}_{sc2}(t) &= k_d \cdot I_{sc1}(t) - k_{a2} \cdot I_{sc2}(t) \\
\dot{I}_p(t) &= k_{a1} \cdot I_{sc1}(t) + k_{a2} \cdot I_{sc2}(t) - (m_2 + m_4) \cdot I_p(t) + m_1 \cdot I_l(t) \\
\dot{I}_l(t) &= m_2 \cdot I_p(t) - (m_1 + m_3) \cdot I_l(t)
\end{aligned} \tag{4.1}$$

Following the notation in [Dalla Man et al., 2007b] and [Dalla Man et al., 2007a], I_{sc1} is the amount of non-monomeric insulin in the subcutaneous space, I_{sc2} is the amount of monomeric insulin in the subcutaneous space, k_d is the rate constant of insulin dissociation, k_{a1} and k_{a2} are the rate constants of non-monomeric and monomeric insulin absorption, respectively, $D(t)$ is the insulin infusion rate, I_p is the level of plasma insulin, I_l the level of insulin in the liver, m_3 is the rate of hepatic clearance, and m_1, m_2, m_4 are rate parameters. The relationships defining rate parameters $m_1 - m_3$ are based

on reasoning on the hepatic insulin clearance, see [Dalla Man et al., 2007c] for further details.

Current Decision Support—Bolus Guides

Many modern insulin pumps, as well as some glucose meters, offer decision support systems (DSS) for insulin therapy to the user in the form of so-called bolus guides. Several studies have shown the usefulness of these bolus guides in terms of reducing postprandial excursions for both CSII, see e.g. [Zisser et al., 2008; Shashaj et al., 2008], and MDI therapy, see e.g. [Ziegler et al., 2013] and reduced incidence of hypoglycemia in a pediatric cohort in [Ramotowska and Szypowska, 2014], or see [Schmidt and Nørgaard, 2014] for a comprehensive review. These systems rely on assumptions on the glucose-lowering effect of insulin—insulin action—and the dynamics thereof. The duration of the insulin action may usually be selected by the user from anywhere in-between 2 and 8 hours. The shape of the insulin action profile is sometimes linear, i.e., the glucose-lowering effect is considered constant over the active period, and in some cases nonlinear curves are used to better reflect the pharmacokinetic shape, see [Zisser et al., 2008].

In terms of how to determine the total glucose-lowering effect—the insulin sensitivity factor (ISF)—different formulas exist. The most widely used is the so-called 100-rule (or 1800-rule if the mg/dl scale is used). This rule suggests that the ISF can be calculated by dividing 100 by the amount of the total daily insulin dose (TDD). Recently these rules were revised by the originators in [Walsh et al., 2010; Davidson et al., 2008] with slight adjustments to the 100-rule (one author suggests using 109 and the other to use 95). Additionally, many patients complement this rule by estimating the ISF from personal experience, e.g., from occasional correction boluses. Determining the duration and the shape of the insulin action is more difficult, and in our experience the patients most often resort to the default values for insulin action duration given by the DSS. The underlying assumption of the 100-rule is that there is a static and generic relationship between the amount of daily insulin and the glucose-lowering effect of insulin. While this may be true in a population sense, adopting it to a specific individual may produce poor estimates. Likewise, personal heuristic estimates may give very poor estimates, as confounding aspects such as meals and the duration of the current and previous bolus doses are not fully appreciated or understood. In addition, the generic estimates of the profile of the insulin action also contribute to a large uncertainty in the assessment of the insulin action. These factors may lead to poor glycemic control related to insulin stacking from one meal to the next (due to the true insulin action duration being longer than what the generic assumption indicates), over/underbolusing (due to the effect of the insulin being less/more rapid than the generic profile) and unexpected

hypo/hyperglycemia as pointed out by [Walsh et al., 2014].

Identification of the glucose dynamics

Approaches to estimation of input-output models of the glucose dynamics, including the insulin action, span, e.g., ARX families [Finan et al., 2009], continuous-time transfer functions [Kirchsteiger et al., 2011], state-space models [Ståhl, 2012] or [Cescon, 2013], and Volterra kernel networks [Mitsis and Marmerelis, 2014].

However, these approaches do not explicitly consider potential heterogeneous effects of the insulin action across the glucose range, i.e., higher or lower glucose-lowering effect depending on the current glucose level, as indicated in [Chan et al., 2010], and may be poor approximations to nonlinear dynamics. Furthermore, we believe it is important to recognize the day-to-day variability in glucose metabolism and insulin action. Whereas, this variability may partly be due to pharmacokinetic and pharmacodynamic properties of the insulin [Heinemann, 2002], time variability in insulin sensitivity may also be an important factor.

To address the aspect of nonlinear glucose dynamics and time-variability, we suggest individualized estimates of the insulin action using a kernel-based approach, which may incorporate heterogeneous effects across the glucose level as well as a nonlinear temporal response.

4.2 Data and Methods

Data selection

In this chapter data from the ULund trial has been used. To perform the analysis, data records where insulin intake alone affected the glucose level were needed. To this purpose, CGM glucose traces for the overnight periods (from midnight until breakfast) together with the corresponding insulin dosage data were extracted from the data material for each patient. These datasets were thereafter assessed for completeness and relevance. Data containing reports of meals were discarded, as were data periods where the glucose trace showed clear indications of digested meals (sudden spontaneous and dramatic rises in glucose shortly after bolus doses) but where this information was missing in the meal data record. To reduce the effect of previously digested meals, the data records were truncated, when necessary, to allow for at least three hours in-between the last evening meal intake and the beginning of the data period. Furthermore, data where the CGM showed large deviations to the reference glucose meter were also discarded as unreliable. Finally, in the event of a hypoglycemic event, the data record was truncated after the point where the glucose dropped into the hypoglycemic region. The reason for this was

to avoid interference from the counter-regulatory response following such an event. On average, data from 65% of the nights could be used.

Model

There is reason to believe that the insulin action is nonlinear across the glucose range. That chronic or temporary hyperglycemia reduces insulin sensitivity is well-known and affects both T1DM and T2DM [Yki-Järvinen, 1990]. Also hypoglycemia may affect the insulin sensitivity by increasing the metabolic effect of insulin [Chan et al., 2010]. To estimate the dynamical glucose-lowering effect of rapid-acting insulin and the nonlinear effects described above, a nonlinear black-box Finite Impulse Response (FIR) model was considered to describe the insulin action. However, the fasting glucose dynamics depends on internal dynamics related to the hepatic glucose production and fasting metabolism as well as the externally provided insulin. In this approach, this was summarized into a total net basal endogenous glucose balance G_b in fasting state. In total, the glucose dynamics during fasting at time point t_k after may then be described as

$$y(t_k)^{(j)} = y(t_{k-1})^{(j)} + \sum_{i=0}^{n} a_i(y(t_k)^{(j)})I(t_{k-i}) + G_b^{(j)}(t_k) + v(t_k), \quad t_k \in T_j \tag{4.2}$$

where $I(t_k)$ represents the insulin infusion and $y(t_k)$ is the glucose level at time sample t_k and $v(t_k) \sim N(0, \sigma_v)$ corresponds to a process noise perturbation, with variance σ_v^2. Each dataset j covers the time instances T_j, and the impulse-response model parameters $\mathbf{a} = [a_1, a_2 \dots a_n]$ have a glucose dependence.The sampling time is equivalent to the measurement frequency (5 min).

The net basal endogenous glucose balance (EGB) $G_b(t_k)$ changes both in-between datasets, and over the course of each overnight dataset. The diurnal pattern of the short-term changes occurring over each dataset is assumed to be the same in every dataset. The G_b corresponds to a basal insulin requirement I_b convolved with the insulin action. In stationarity, with fixed $I(t_k) = I_b$ and $y = y_b$, this implies that:

$$\sum_{i=1}^{n} a_i(y_b) \cdot I_b = K_{ISR}(y_b)I_b = -G_b \tag{4.3}$$

where $K_{ISR}(y_b)$ is the Insulin Sensitivity Ratio, i.e., the total glucose-lowering effect of one unit of insulin, at glucose level y_b.

To estimate the model, a number of different steps are required as outlined in the text box on the next page. These steps will be described in more details in the following sections.

Summary of the Estimation Process

1. Determine the prior G^0 of the EGB. Here, the pump settings of each patient were used. The average overnight basal rate was multiplied with the insulin sensitivity factor setting in the insulin pump bolus guide to get G^0 (see Eq. (4.3)).
2. The next step is to estimate the duration of the insulin action. Run Eq. (4.4) assuming $G_b^{(j)}$ to be constant in each dataset j (i.e. without diurnal pattern) and with n set to a large value (here we choose 8 hours). The resulting maximum length of non-zero a parameters determines the length n to use for this variable.
3. Thereafter, Eq. (4.4) is rerun with the updated n, and without 1-norm regularization of $\mathbf{a}$. Hereby, an estimate of the insulin action $\mathbf{a}$, as well as the mean endogenous glucose balance over each dataset $G_{b,0}^{(j)}$, is retrieved.
4. Finally, find the overnight pattern of the G_b by running Eq. (4.7) with the estimated parameters from step 3.

Kernel-based Estimation Method

To estimate the model, locally-weighted least-squares estimation, see e.g. [Hastie and Tibshirani, 1990], using a quadratic Epaneichnikov kernel ([Epanechnikov, 1969]) was employed. In order to keep the estimate smooth, second-order regularization was also considered, and we utilized a Gaussian prior for G_b. To reduce the model size, the parameters were regularized by the 1-norm. To fulfil the physiological requirements of glucose-lowering response to insulin, the parameters were constrained to non-positive numbers, and the start and end of the insulin action were enforced to zero. For each glucose level G of interest, the following optimization problem was solved to retrieve the parameter estimates; $\mathbf{a} = [a_0, \dots a_n]$ and $\mathbf{G_b} = [G_b^{(1)}, \dots, G_b^{(N)}]$ using N nights of data, where the glucose index of $\mathbf{a}$ has been dropped for notational convenience.

$$\{\mathbf{a}(G), \mathbf{G_b}\} = \underset{\mathbf{a},\mathbf{G_b}}{\arg\min} \sum_{j=1}^{N} \|\mathbf{y}^{(j)} - \hat{\mathbf{y}}^{(j)}\|_{\mathbf{W}^G} + \|\frac{\mathbf{G_b}}{G_b^0}\|_\Gamma + \alpha\|\mathbf{a}\|_\mathbf{R} + \|\mathbf{a}\|_1 \tag{4.4}$$

subject to $a_0 = 0, a_i \leq 0, i = [1 \dots n-1]$ and $a_n = 0$, and where the second-order regularization matrix $\mathbf{R}$ is populated as follows:

$$\mathbf{R}(j, j-1:j+1) = \begin{bmatrix} 1 & -2 & 1 \end{bmatrix}, \quad j = [1, \dots, n] \tag{4.5}$$

and

$$\|\mathbf{x}\|_{\Gamma_{k,\theta}} = (k-1)\sum_{i=1}^{N} \ln x_i - \frac{1}{\theta}\sum_{i=1}^{N} x_i \tag{4.6}$$

corresponds to the data-dependent terms in the likelihood function of a gamma distribution with shape parameter k (set to 3) and scale parameter θ (set to 0.5). A gamma distribution was chosen as prior for the normalized EGB because it guarantees positive values. The quadratic kernel matrix $\mathbf{W}^G$ defines the weight of each glucose measurement according to the euclidean distance to the glucose level G, G_b^0 is the prior expected value estimate of G_b, and α determines the smoothness of $\mathbf{a}$. The problem can be considered as a maximum-likelihood estimation if the kernel weight and the smoothness criteria are given adequate probabilistic interpretations. The optimization was solved using the CVX toolbox in Matlab, see [Grant and Boyd, 2014]. The duration of the insulin action may be different from patient to patient. To determine the number of parameters n to use, an initial run was conducted, from which the number of non-zero parameters could be assessed thanks to the 1-norm term. Thereafter, the optimization was updated with the new n for the final estimation run.

Finding the overnight G_b pattern

So far, we have assumed that the G_b stays fixed throughout the night. However, this may be a too limiting constraint for some patients. Changes in basal requirement may occur, e.g., in transition between the active awake state and the passive sleep state. Furthermore, some patients also have a pronounced dawn phenomenon in the morning hours. To capture these effects, we investigate the possibility to improve the predictive capacity by considering the following. Let $\mathbf{a}$ and $\mathbf{G_b}$ be fixed to the estimates retrieved from (4.4). Define a multiplier vector ρ of length n_ρ, where each entry corresponds to a different multiplier value for each half hour in the overnight period. Find these multipliers by

$$\rho = \arg\min_{\rho} \sum_{j=1}^{N} (\|\mathbf{y}^{(j)} - \hat{\mathbf{y}}^{(j)}\| + \|\rho - \mathbf{1}_{n_\rho}\| \tag{4.7}$$

where $\hat{\mathbf{y}}^{(j)} = \{\hat{y}^{(j)}(t_k) : t_k \in T_j\}$, $\mathbf{1}_{n_\rho}$ is a vector of ones of the same size as ρ, and

$$\hat{y}^{(j)}(t_k) = \hat{y}^{(j)}(t_{k-1}) + \sum_{i=0}^{n} a_i I(t_{k-i}) + \rho(\Pi(t_{k-i}))G_b^{(j)} \tag{4.8}$$

where $\Pi(t)$ is a function determining which half hour the time t belongs to.

4.3 Results

The insulin action was successfully estimated for all patients for a glucose range between 4 and 16 mmol/l with a 0.5 mmol/l increment. The patients demonstrated a large variability in both shape and magnitude of the insulin action dynamics as indicated in Figure 4.2 where the insulin action estimated at the 10 mmol/L glucose level is depicted. The default shape and duration found in the Animas pump setting are also included in the figure.

The individualized action profiles had an average glucose-lowering effect of 2.4 mmol/(L·IU) [1.1-3.7] and half of the effect was achieved after 135 minutes [105-165]. It is noteworthy that all estimated profiles have a slower onset and a longer time to peak than the profile suggested by the pump (half effect after 100 min). The total duration was also longer; 90% of the insulin action took effect after 250 min [200-350] in comparison to the 195 min suggested by the Animas pump. There were no observed differences between the two insulin types used, in line with previous clamp studies in [Plank et al., 2002].

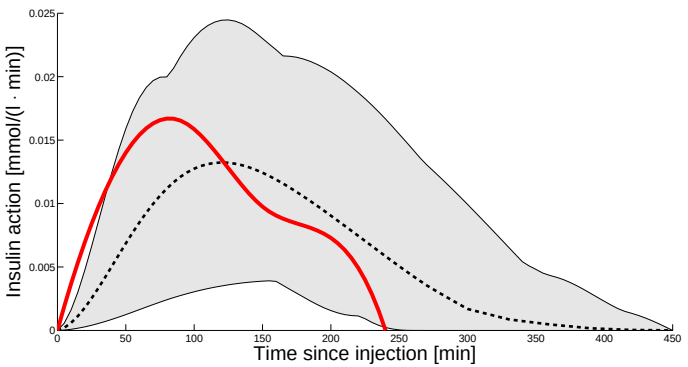

Figure 4.2 The insulin action profile used in the Animas pump (red curve) plotted together with the variability of insulin action estimates when $G =$ 10mmol/l (the grey area). The dotted black line represents the estimated mean population insulin action.

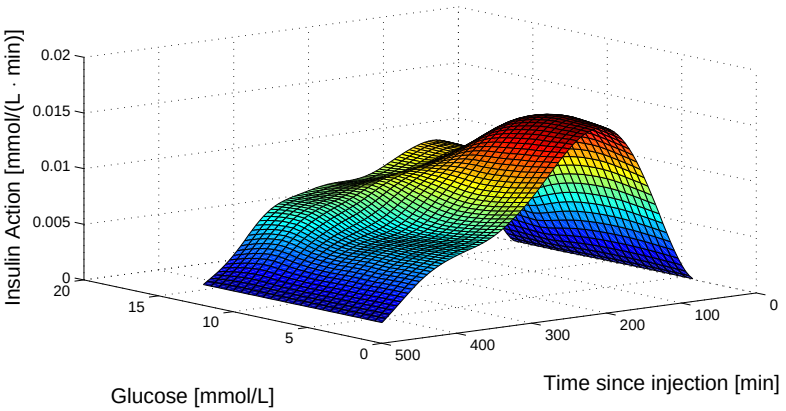

Figure 4.3 Example of the insulin action across the glucose range. Patient nr 1 from the Dexcom cohort.

Another important aspect of insulin action, which may have severe implications for glucose control, is whether the glucose-lowering effect is invariant to the present glucose value, i.e., whether an insulin injection produces the same response regardless of the glucose level. Our model estimates suggest that there are differences in insulin action depending on the glucose level. Generally, the peak was somewhat delayed and the total glucose-lowering effect diminished for higher glucose levels, see Figure 4.3 for an example. The latter aspect was significant and exhibited a sigmoidal or Hill shaped ([Keener and Sneyd, 2009]) type of relationship to the glucose level, see Figure 4.4. The relative gain is statistically different ($p < 0.05$) for all glucose values at least 4 mmol/l apart.

The EGB estimate changes over the night for most patients. Typically it drops quite a lot the first hours of the night, after which it stabilises. In the morning, normally around 6 a.m., the EGB rises again—the dawn phenomenon. The normalized EGB can be seen in Figure 4.5. The mean estimated EGB in the early morning hours (4-7 a.m.) is significantly higher than the mean night EGB (2-4 a.m.) for the entire population ($p < 10^{-10}$).

To validate the insulin action models, cross-validation of the predictive performance of overnight glucose traces was assessed. Using the insulin data from the pump together with information about the basal insulin requirement estimate and model parameters estimated from data not present in the validation data, glucose traces from bedtime until morning were simulated and compared to the reference CGM. Corresponding traces were simulated using a third-order continuous-time transfer function $M(s)$ with an integrat-

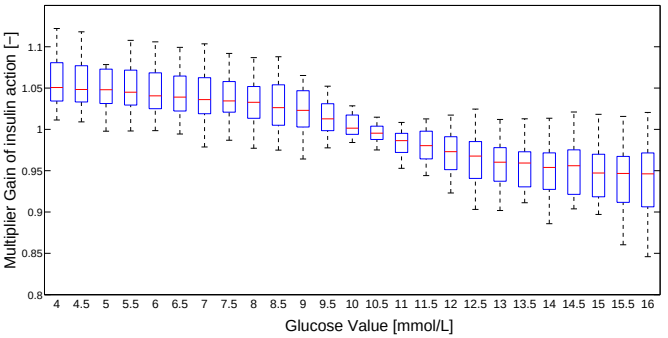

Figure 4.4 The relative total glucose-lowering effect of insulin over the glucose range. The glucose-lowering effect is elevated at low glucose values and reduced at glucose values above 10 mmol/L.

ing pole as outlined in [Kirchsteiger et al., 2011]:

$$M(s) = \frac{K}{s(T_1 s + 1)(T_2 s + 1)} \tag{4.9}$$

subject to

$$0 \leq K \leq 5 \tag{4.10}$$

$$0 \leq T_i \leq 100 \tag{4.11}$$

which fulfils the physiological requirement of persistent glucose-lowering effect (K [mmol/(L· IU)] corresponds to K_{ISR}), and where the dynamics are governed by time constants T_1 and T_2 ([min]). The model was estimated using the System Identification Toolbox in Matlab. The prediction error in terms of RMSE can be found in Table 4.1. Our proposed model has an overall better predictive performance, which is pronounced in the low and high glucose ranges. The low interpersonal variability in prediction results also indicates that the method is robust across the population.

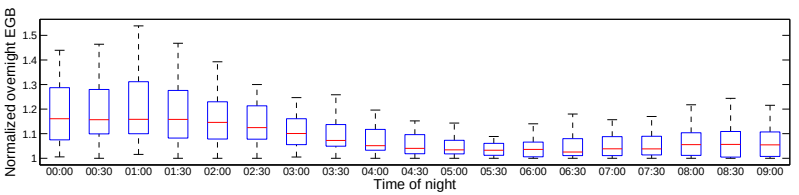

Figure 4.5 Changing EGB throughout the night. Normalized by the minimum value during the night.

Table 4.1 Prediction evaluation in terms of root mean square error (RMSE) for the kernel and transfer function models evaluated over different glucose (G) ranges.

	RMSE (%)		
Model	**G < 5**	**G > 10**	**All G**
TF model	47	12.2	22.2
Kernel model	18	7.4	11.6

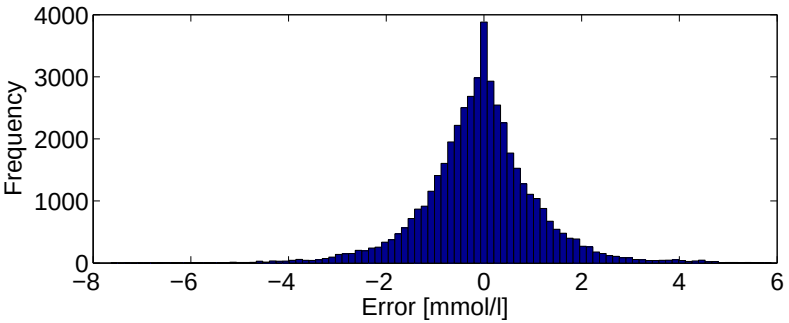

Figure 4.6 The total distribution of the prediction error.

There was a difference ($p = 0.067$) in predictive performance between the Animas/Dexcom (10.1%) and Medtronic (13.2%) groups, which may be explained by that the Medtronic sensors had a significantly larger deviation to the glucose reference (13.8 vs 10.7% MARD, $p < 0.05$), which may also imply higher noise for these sensor types. Finally, the standard deviation for the prediction results in the same subject averages around 8% and this suggests that the intrapersonal variability in insulin action is manageable, and in line with previous estimates in [Heinemann et al., 1998]. The error is symmetrically distributed around a small positive bias (0.07 mmol/l), see Figure 4.6. Despite the correction factor to reflect the temporal changes in EGB, the bias increases somewhat over the night (Figure 4.7). In Figure 4.8 the Clarke Error Grid is given, with 87% of the values are in zone A, 12% in zone B and 1% in zone D, indicating the clinical usefulness of the results.

4.4 Discussion

Insulin pump settings

Insulin action duration, or as it is generally referred to—Insulin On Board (IOB)—is a very important, but also difficult, aspect of insulin therapy for

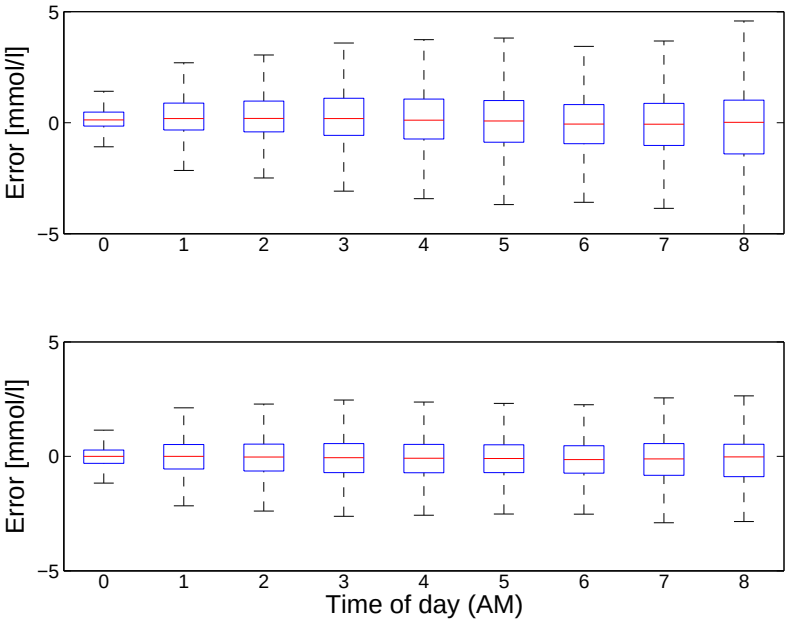

Figure 4.7 The distribution of the prediction error over the night period. In the upper plot the distribution of errors of the model without the temporal correction factors ρ is given, and in the lower plot the errors of the full model can be seen.

the patient to determine. Relying on poor estimates of the duration of the insulin action is potentially very misleading and dangerous. However, there are no clear guidelines for how to determine this parameter. For patients who look for guidance in online material provided by healthcare professional organizations often encounter quite short suggested duration of the insulin action. This stand in contrast to numerous clamp studies that suggest that the duration may be up to 8 hours, see e.g. [Mudaliar et al., 1999; Morrow et al., 2013; Rave et al., 2005].

The American Diabetes Association (ADA) online patient information advices that the rapid acting insulins peak in about an hour and that the total duration is 2-4 hours [American Diabetes Association. Living with diabetes., 2014]. National Institutes of Health (NIH) suggests a peak somewhere between 30 and 90 minutes and a total duration of 3 to 5 hours [NIH online, 2015]. Group HealthCare, a non-profit member-owned healthcare organization based in Seattle, claims that the peak is at 90 minutes and a total duration of 3 hours [GroupHealth, 2015]. Joslin Diabetes Center informs about a 30 min - 3 hour peak and a total duration of 3-5 hours [Joslin Diabetes Cen-

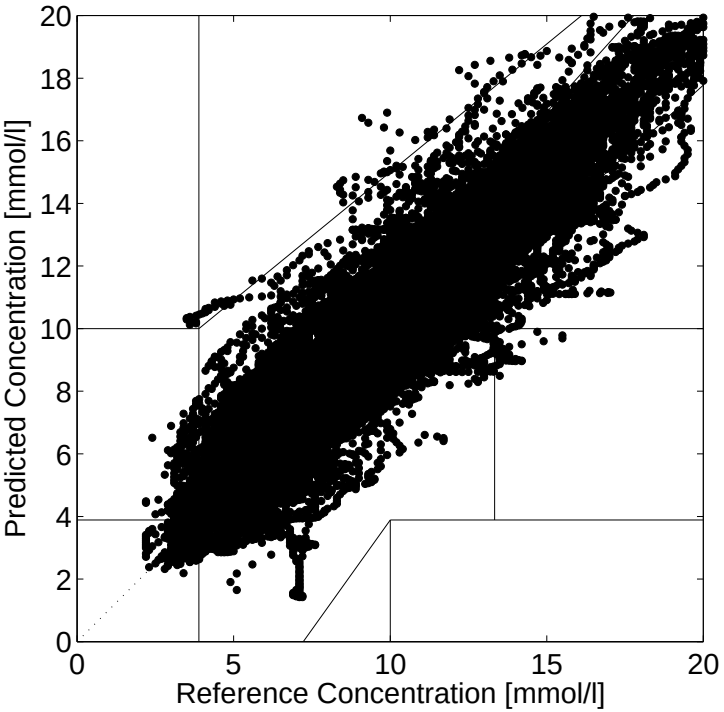

Figure 4.8 The Clarke error grid.

ter, 2015]. Similar information is provided by NovoNordisk; maximum effect in-between 1 and 3 hours and a total duration of 3-5 hours [Novo Nordisk, 2014]. The suggestions have been summarized in Table 4.2.

Based on this, the 4 hour default duration in the Animas pump bolus guide may seem reasonable. However, looking at our population results and

Table 4.2 Suggestions on insulin action characteristics by different international organisations.

Organisation	Peak	Duration
ADA	60 min	2–4 h
NIH	30–90 min	3–5 h
GroupHealth	90 min	3 h
Joslin	30–180 min	3–5 h
NovoNordisk	60–180 min	3–5 h

the estimated insulin action profiles, and summarizing the remaining estimated glucose-lowering effect left after 4 hours show that on average 10% of the total effect remain. For a few patients with long durations (7 hours or more) as much as 25% is left. This may seem as small amounts, but for large meal bolus doses the unexpended remainder may be quite potent. Underestimating the duration has many detrimental effects, especially at bedtime. A too short duration implies that the effect of previous bolus doses, e.g. late meal bolus doses, are underestimated or even disregarded, which may lead to early-night nocturnal hypoglycemia or to overcompensation by heavily reduced basal doses, which in turn may lead to rising glucose levels in the early morning similar to the effect of hormonally induced dawn phenomenon and poor morning control. Likewise, the slower onset and the longer time to peak of the profile in comparison to what is suggested by the pump may also imply several potential dangerous situations, such as overdosing due to that the patient take additional correction doses since the short-term insulin effect is lower than expected from the pump curve.

Almost all of the patients had a IOB duration setting of 4 hours, see the histogram in Figure 4.9. A few of the Medtronic patients had a duration setting of 6 hours, which is the default for that pump. For the Animas pump, 4 hours is the default. The corresponding distribution of the duration for the estimated models is a bit more diverse. The clustering of the IOB settings seem to indicate that the patients feel uncertain about this variable.

The model has shifting insulin sensitivity factors depending on the glucose level. However, to allow comparison to the pump setting as well as the factor retrieved using the 100 rule, we use the average $\bar{K}_{ISR}$. In Figure 4.10, $\bar{K}_{ISR}$ can be seen together with the 100 rule estimate and the patients' pump settings. Also for this setting, some patients resort to the default provided by the pump. Among the Dexcom/Animas patients, six had the default setting

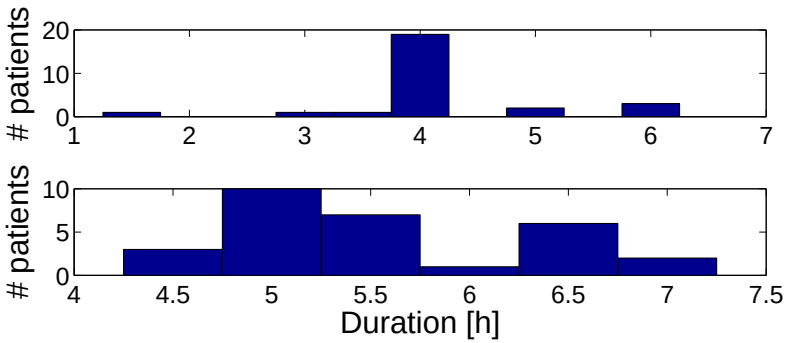

Figure 4.9 Upper plot: Distribution of the IOB duration setting in the patients' pumps. Lower plot: Distribution of the IOB duration estimates.

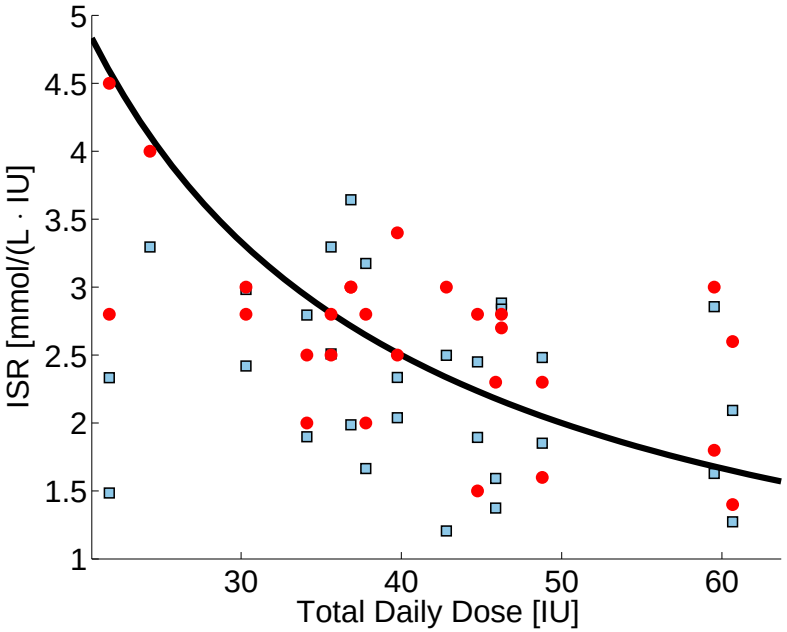

Figure 4.10 Insulin sensitivity factor (ISF) plotted against total daily dose (TDD). The black line represents ISF according to the 100 rule, the red dots are the patients' pump settings, and the squares correspond to the model estimates.

of 2.8 mmol/l, and two of the Medtronic patients did not have any setting for this parameter at all. Similar clustering of pump settings to specific values have been noted in [Walsh et al., 2010]. Generally, our estimates are somewhat lower than the user setting ($-10 \pm 40\%$), whereas the 100 rule was slightly higher ($2 \pm 26\%$). Comparing patients where the model estimate was higher than the setting (14 patients) to the patients where the opposite was true (13 patients), show that time in severe hypoglycemia was significantly higher ($p < 0.006$). The corresponding test on time in hypoglycemia was almost significant ($p = 0.07$). This indicates that the patients underestimate the potency of the glucose-lowering effect with higher incidence of hypoglycemia as result.

Heterogeneous Insulin Action

The heterogeneous response across the glucose range may have multiple and different root causes. In normal healthy subjects an elevation of the glucose level rapidly decreases the hepatic output. In T2DM, this autoregulation may be impaired and contributes to insulin resistance. Also in T1DM the apparent

reduced effect of insulin at elevated glucose levels may be due to disturbances related to hepatic down-regulation. In T1DM, the lack of pancreatic insulin release implies lower portal vein insulin concentrations and loss of first-pass insulin release to the liver. Thereby, the operating point of the dose response curve for hepatic regulation is shifted and the hepatic regulation may also be disturbed with reduced response to elevated glucose levels as result. This nonlinear effect has a destabilizing effect on glucose control, especially when combined with a long duration of insulin action. For individuals with an exaggerated multiplier effect of insulin action across the glucose range and long insulin action, a correction dose to come out of a temporary hyperglycemia may well result in a subsequent hypoglycemia. Further studies are needed to see if high glucose variability is associated with this phenotype.

Confounding factors

There are a number of potential confounding factors that need to be considered.

The models are estimated only from overnight data. There may exist reoccurring hormonal and other metabolic temporal patterns, specific to the sleep state or night period, which systematically bias the results. Further studies where the models are tested and validated on day time data are needed to clarify this aspect.

Another aspect is that the models rely on CGM data, and errors in these measurements may thus also bias the estimate. Such errors are related to sensor drift, calibration bias, sensor noise and the plasma-to-interstitial delay, see e.g. [Vaddiraju et al., 2010] for in-depth information about these sensor types. Of these, the last one clearly contributes with a bias in terms of a delay in the insulin action estimate. Due to the low-pass filter character of this physiological delay, the bias is most exaggerated for the steepest changes in the insulin action, which occur around the peak. It is therefore likely that our model has overestimated the timing of the peak somewhat (in the magnitude of 5-15 minutes), whereas the estimate of the total duration of the insulin action probably is correct.

Potential nonlinear effects related to the bolus size have not been addressed. Previous studies in [Becker et al., 2007] have indicated that larger bolus doses may imply longer insulin action. Such an effect has not been possible to investigate in this data material, as most of the insulin doses are small and of similar size—in general basal doses and some occasional small correction bolus doses. Also this aspect needs to be further investigated, with, e.g., dedicated study protocols stipulating large bolus doses.

The data was collected under free-living conditions, and external factors such as unregistered meals, physical activity and alcohol intake may play a significant role. Here, the size of the data material together with safe-guard

measures such as the data quality assessment reduces the risk of systematic errors from these disturbances.

Finally, the necessity of sufficient excitation in the data is also an important aspect that may contribute to poor results. Consider especially the case with a static basal dose I_0 and no bolus doses giving rise to a static change of glucose Δ_G. Given the model, all combination of $G_b + K_{ISR}I_0 = \Delta_G$ are now equally plausible. Thankfully, the datasets do contain information on bolus doses as well as changes in the basal regime, giving rise to dynamic responses in the measured output.

Comparison to Physiological Models

In the physiological models, the pharmacokinetics and the pharmacodynamics are normally modeled separately. Typically a linear pharmacokinetic model provides a basis for the dynamic effect, and the pharmacodynamics thereafter adds lags, nonlinear effects and the magnitude. In the model suggested here, these effects have been lumped together, and it is not possible to get an estimate of the plasma insulin level. Another important difference is how the insulin-glucose interaction is modeled. In the physiological models, the insulin action, defined as $dG/du_I = \partial G/\partial I_p \cdot \partial I_p/\partial u_I$ (where u_I is the insulin dose and I_p is the plasma insulin level), normally increases as the glucose level increase in a Michaelis-Menten like relationship, due to modeling of the the regulation of the hepatic output and the insulin-dependent glucose utilization. To capture interaction between the insulin action and the glucose level, the model described here allows for different insulin action across the glucose range, however without stipulating the character of this relationship. The parameters of the impulse response are merely coupled by smoothness constraints. The net endogenous balance is made out of several contribution factors in the physiological models. Apart from the hepatic output and the glucose utilization, renal excretion has an important contribution in hyperglycemic range. This is not captured in the presented model. In order to limit model and identification complexity, G_b was not allowed to vary with the glucose level. Finally, whereas the physiological models have clear physiological interpretations and the different effects of meal and insulin intake may be followed throughout the different modeled compartments of the body, the proposed model does not. However, the clinical interpretation of insulin action and net endogenous glucose balance are meaningful and useful to both the clinician and the patient.

Comparison to other Black Box Approaches

In comparison to alternative black box modeling approaches, the method outlined here incorporates several key properties, see Table 4.3. The nonparametric approach allows for better tailoring to the nonlinear dynamics.

Table 4.3 Comparison of model features

Model	Nonlinear Temp. Dyn.	Guar. Physiol. Correct Resp.	Heter. Dynamics
ARX	✘	✘	✘
State-space	✘	✘	✘
Transfer function	✘	✔	✘
Volterra Kernel	✔	✘	✘
Kernel-based	✔	✔	✔

Obviously none of the linear models can exhibit this. Whereas a nonlinear response may be possible for the interesting Volterra kernel model, it lacks guarantees of a qualitatively correct static gain and is therefore not able to accurately represent the long-term effect of insulin bolusing. The novel feature of considering heterogenic dynamics across the glucose range seems to capture significant physiological characteristics and to improve the predictive performance in the important hypoglycemic range as well as in the hyperglycemic region. Apart from improving the predictive capacity, the recognition and quantification of this interesting physiological aspect may potentially shed light on why some subjects exhibit high glucose variability and more difficulties in glucose control. On the other hand, the number of parameters is quite large in this model. However, the high degree of smoothing (see Figure 4.3) reduces the number of effective parameters and the cross-validation indicates that there is no apparent risk of overfitting.

The impact of EGB variability

Quite a few of the patients have a substantial day-to-day variability in the EGB estimate. A large variability in insulin requirement could spill over into difficulties in maintaining a sound glucose control, and could be reflected in increased glucose variability. Indeed, when investigating the data, we found a positive relationship between the variance of the EGB estimate and the variance of the CGM glucose ($p < 0.036$), and also to time-in-range (4-12 mmol/l) ($p < 0.046$). The correlation analysis further showed that the estimated EGB was significantly lower than the average for dates where nocturnal hypoglycemia occurred ($p < 0.001$). The hypothesis that variability in the glucose metabolism may play a key role in developing hypoglycemia was supported by a study where severe hypoglycemia could be linked to glucose variability in the 24 hour period prior to the episode ([Kovatchev et al., 2000]). Mean glucose may also be affected—correlation to mean CGM was close to significant ($p < 0.066$)—but perhaps with an indirect causality. Patients experiencing high variability may deliberately target a more elevated glucose level to avoid the risk of hypoglycemia. In the next chapter we will see

how the model can be exploited to reduce the risk associated with nocturnal hypoglycemia.

4.5 Conclusions

Improved understanding of insulin action and the associated variability is vital to reducing the risk of adverse glucose events. In this chapter individualized finite impulse response models of insulin action have been identified for 29 patients on CSII therapy using overnight CGM and CSII data in a six week home-monitored study. The model is individualized, implying that patient-specific results can be achieved and not only population parameters of limited value to the individual. Apart for the insulin pump and the continuous monitoring devices no extra equipment is required. There is no intervention in the therapy and no requirement for hospitalization, and the data collection may be conducted under free-living conditions. Overall, the results show that there is a large variability in the shape of the insulin action in-between subjects which cannot be handled by generic estimates. Furthermore, the estimates imply that the duration of action often is longer than the 3-5 hours frequently suggested, and in some cases may be up to 7 or 8 hours. The model also incorporates the possibility of heterogeneous action across the glucose range. Our results indicate that the metabolic effect is improved at lower glucose levels and diminishes somewhat at glucose levels above 10 mmol/L. These findings are in line with results from a human clamp study specifically designed to investigate this matter. To validate the models the overnight glucose traces were compared to simulated traces retrieved when using the models using leave-one-out cross-validation. The results were compared to the corresponding predictions received using a linear transfer function model. The model clearly outperformed the alternative approach, with good performance across the population, and with manageable intrapersonal variability. The results indicate that individualized insulin action models can be estimated from a limited dataset with useful accuracy.

Current decision support systems for bolus dosing could be potentially better tailored to each individual using the personalized insulin action model, thereby increasing the clinical benefit. These systems rely on generic insulin action curves, whose shape and duration are altered by two parameter values, K_{ISR} and IOB, selected by the user. Both the duration of the insulin action and the total glucose-lowering effect are difficult to determine. The patients seem especially confounded regarding the duration, where most resort to the default value provided by the pump bolus guide decision support. With the suggested method these parameters can be estimated individually from overnight data records. However, further improvements would be achieved if the decision support incorporated the entire model. Apart from personalized

shape and duration of the insulin action, the description of the heterogeneous insulin action across the glucose range and the estimate of the insulin requirement would thereby also contribute to improved glycemic control. Furthermore, the insulin action model is a critical component in other potential building blocks of a defence in depth concept for glucose management, as will be described in the following chapters.

5

Nocturnal Hypoglycemia Prediction

5.1 Introduction

Hypoglycemia is one of the major barriers to successful intensive insulin therapy. The DCCT trial found that the incidence of severe hypoglycemia was inversely correlated to the HbA1c [DCCT Group, 1997]. The same study also indicated that a majority of these events occur during the night [DCCT Group, 1991]. The overall incidence of nocturnal hypoglycemia ranges from 13% to 56% of the nights in insulin-dependent diabetes in reported studies [Yale, 2004]. Among children and adolescents, the frequency is even greater, with increased risk at lower age. In [Beregszaszg et al., 1997], an overnight study conducted on 150 children and adolescents (age 2 to 15), an inverse relationship between the age and the frequency of nocturnal hypoglycemia was found. Overall, nocturnal hypoglycemia occurred in 47% of the nights. In a large study [Davis E, 1997], covering 657 children and adolescents, 75% of the severe hypoglycemic episodes, defined as an event leading to seizures or coma, occurred during the night. Many of these episodes are asymptomatic due to impaired hypoglycemic awareness. The counter-regulatory response to hypoglycemia may be blunted during sleep [Jones et al., 1998]. Furthermore, recurrent hypoglycemia induces hypoglycemic unawareness [Veneman et al., 1993], leading to a vicious circle. Apart from the acute risks of seizures, coma, and in very severe cases, death, reoccurring hypoglycemia may have implications for cognitive functionality [Warren and Frier, 2005]. These aspects are especially worrisome for the developing brain in children and adolescents. The fear of (nocturnal) hypoglycemia is in itself an important aspect to consider in terms of its contribution to reduced quality of life, but may also result in patients reducing the insulin dosage in order to reduce the hypoglycemic risk [Edelman and Blose, 2014].

Current technology

Some of the current CGM systems allow for predictive threshold alarms based on extrapolating the current glucose trend by numerical differentiation [Vashist, 2013]. Generally, the use of real-time CGM and the hypoglycemic alarms have implied reduced incidence and time spent in hypoglycemia [Bode et al., 2008; Davey et al., 2010; New et al., 2015]. In 2008, Medtronic introduced the Medtronic Veo insulin pump in Europe, which coupled with their CGM system, featured automatic insulin delivery suspension for two hours if a predefined low glucose level was reached. Studies show that the system could further reduce the duration and frequency of nocturnal hypoglycemia [Bergenstal et al., 2013]. Despite these encouraging results, the predictive capacity is still low and the incidence of (nocturnal) hypoglycemia is still unacceptably high. Several algorithms have been suggested in recent years to improve the predictive capability. In [Palerm et al., 2005], a Kalman filter approach was proposed, estimating the interstitial glucose level, and the first and second time-derivative thereof, i.e., the rate of glucose change and acceleration. Combining three different methods for hypoglycemic detection with the ARMA model has also been suggested [Eren-Oruklu et al., 2009b]. In [Dassau et al., 2010], five different algorithms were used together in a voting-based detection system called hypoglycemic prediction algorithm (HPA). An overview of these and related methods can be found in [Bequette, 2014].

The approaches above rely on time-series analysis and lack input-to-output relationship and thereby do not fully exploit the data available from the insulin pump. Approaches to estimation of input-output models of the glucose dynamics, including the insulin action, span, e.g., ARX families see e.g. [Finan et al., 2009], continuous-time transfer functions, see e.g. [Kirchsteiger et al., 2011], state-space models, see e.g. [Ståhl, 2012; Cescon, 2013; Turksoy et al., 2013], and Volterra kernel networks, in [Mitsis and Marmerelis, 2014]. However, these approaches do not explicitly consider any potential heterogeneous effects of the insulin action across the glucose range, i.e., higher or lower glucose-lowering effect depending on the current glucose level, as indicated in [Chan et al., 2010], and may be poor approximations of the nonlinear dynamics. Furthermore, we believe it is important to recognize the day-to-day variability in glucose metabolism and insulin action. Whereas, this variability may partly be due to pharmacokinetic and pharmacodynamic properties of the insulin [Heinemann, 2002], time variability in insulin sensitivity may also be an important factor. To address the aspect of nonlinear glucose dynamics and time-variability, we suggest individualized estimates of the insulin action using the model developed in Chapter 4. Utilizing this model, the possibility to predict nocturnal hypoglycemic events in advance is investigated for data records from 29 patients on sensor-augmented insulin pump therapy.

5.2 Data and Methods

Data selection

To perform the analysis, data records where insulin intake alone affected the glucose level were needed. To this purpose, CGM glucose traces for the overnight periods (from midnight until breakfast) together with the corresponding insulin dosage data were extracted from the ULund trial data material for each patient. Thereafter, these datasets were assessed for completeness and relevance. Data containing reports of meals were discarded, as were data periods where the glucose trace showed clear indications of digested meals (sudden spontaneous and dramatic rises in glucose shortly after bolus doses) but where this information was missing in the meal data record. To reduce the effect of previously digested meals, the data records were truncated, when necessary, to allow for at least three hours in-between the last evening meal intake and the beginning of the data period. Furthermore, data where the CGM showed large deviations to the reference glucose meter were also discarded as unreliable. Finally, in the event of a hypoglycemic event, the data record was truncated after the point where the glucose dropped into the hypoglycemic region. The reason for this was to avoid interference from the counter-regulatory response following such an event. The truncation leads to short data records in some cases. A minimum of three hours duration was therefore also considered as a necessary criterion. On average, data from 65% of the nights could be used. The distribution of hypoglycemic events was quite even over the night period, see Figure 5.1.

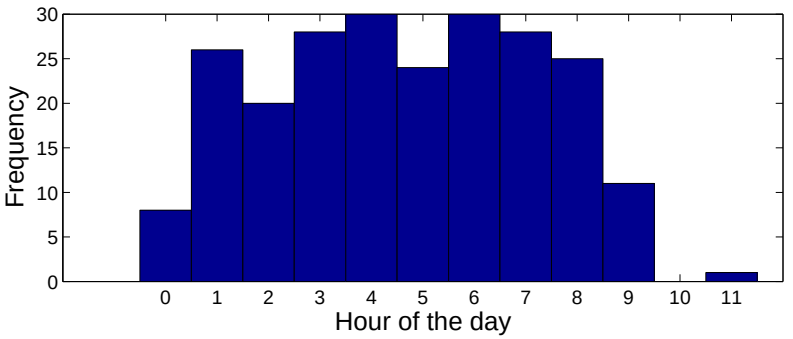

Figure 5.1 Distribution of the hypoglycemic episodes ($G < 4$ mmol/l) over the night/morning period.

Predicting the nocturnal glucose level

The prediction was based on the model developed in Chapter 4. To predict the nocturnal glucose level p minutes ahead at time t_k, a one-dimensional Kalman filter with filter constant α was used with measurement update using the CGM reading y_{t_k}

$$\hat{y}_{t_k|t_k} = (1-\alpha)\hat{y}_{t_k|t_{k-1}} + \alpha y_{t_k} \tag{5.1}$$

and time update

$$\hat{y}_{t_{k+1}|t_k} = \hat{y}_{t_k|t_k} + \sum_{i=0}^{n} a_i(y(t_k))I(t_{k-i}) + \hat{G}_{b,t_k} \tag{5.2}$$

and prediction

$$\begin{aligned}\hat{y}_{t_{k+j+1}|t_{k+j}} = \hat{y}_{t_{k+j}|t_{k+j-1}} + \sum_{i=0}^{n} a_i(\hat{y}_{t_{k+j}|t_{k+j-1}})I(t_{k+j-i}) \\ + \frac{\rho(\Pi(t_{k+j+1}))}{\rho(\Pi(t_k))}\hat{G}_{b,t_k}, \quad 1 \le j \le p\end{aligned} \tag{5.3}$$

and where $\hat{G}_{b,t_k}$ is the recursive estimate of the endogenous glucose production for this night at time t_k. The overnight basal multiplier ρ was evaluated both at the time of prediction and at the future time point, using $\Pi(t)$ to determine which half hour the time t belongs to. The day index has been dropped for notational convenience. Using the collected data $Y_{t_k} = [y_0, \ldots, y_{t_k}]$ up to this time point, the posterior estimate of $\hat{G}_{b,t_k}$ is given by the locally weighted (quadratic kernel) maximum likelihood estimate given a prior distribution p_0 of the EGB.

Pump suspension simulation

As a second line of defence, this method could also prove useful for the insulin pump low glucose suspension feature. The longer warning times will allow for even earlier intervention in the basal delivery, thereby further reducing the time spent in hypoglycemia. To investigate this aspect, simulations of pump shutoff, similar to the current pump suspension feature of the Medtronic Veo pump, were carried out for the collected data. When the 60 minute ahead prediction passed the hypoglycemic trigger level (3.8 mmol/l), the insulin delivery was turned off for two hours. Applying the reduced insulin delivery, a new prediction was calculated and compared to the true outcome.

5.3 Results

The individual model estimates from Chapter 4 were used together with a prior p_0 for the EGB to make predictions of the nocturnal glucose values.

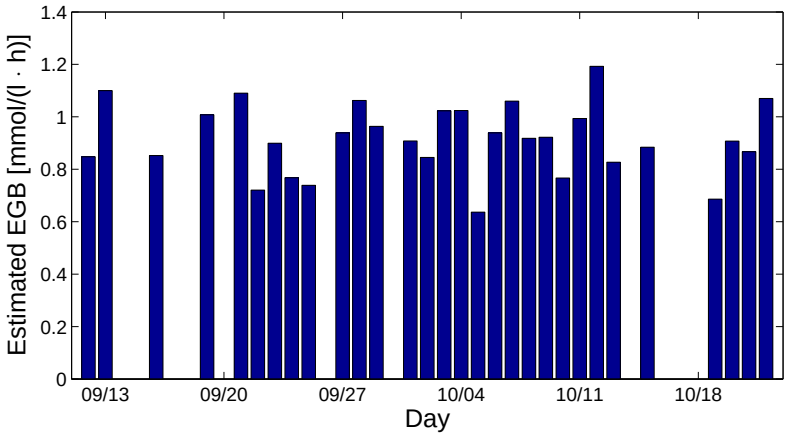

Figure 5.2 Example of the day-to-day variability in estimated EGB. Patient nr 6 from the Dexcom cohort.

To find a suitable prior, an attempt to find a dynamic model explaining the day-to-day shifts in EGB was made using an ARMA model. Due to the data quality constraints, missing estimates of G_b can be expected for some days. In Figure 5.2, an example of the variation for one of the Dexcom patients can be seen. To identify the model under these conditions, the missing data were considered as latent variables and co-estimated together with the model parameters using the expectation-maximization algorithm [Bishop, 2006]. The ARMA model was rewritten in innovation state-space form and a Kalman smoother was used to estimate the states in the estimation step. Using the updated state estimates, including the missing data points, the joint negative log-likelihood, of both the states and the output, was maximized to find new parameter estimates in the expectation maximization step. The procedure is outlined in [Shumway and Stoffer, 1982]. However, the limited length of the data records constrained the model size and no model of sufficient explanatory value could be retrieved. Instead, a Gaussian prior was based upon the statistics of the estimated EGB values for each patient.

In total, 721 nights, whereof 219 (7.6/patient) with nocturnal hypoglycemic episodes were assessed. Since the definition of hypoglycemia differs somewhat across the academic field, we tested two different settings: hypoglycemia defined as glucose values below 4.0 mmol/l, and the alarm threshold set to 4.2 mmol/l, and a lower hypoglycemic limit (3.3 mmol/l) and corresponding threshold (3.8 mmol/l). In total, 129 of the hypoglycemic events also covered this lower limit. Both settings were evaluated with different prediction horizons (PH), see Table 5.1. An alarm was considered true positive (TP) if it managed to flag an event before it occurred. Many users of CGM

Table 5.1 Summary of prediction results using different prediction horizons and simulation (S) when the hypo level is 3.3 (4.0) mmol/l. Prediction Horizon (PH), Warning Time (WT), Sensitivity (SE), False Alarm Rate (FAR).

PH (min)	WT (min)	SE (%)	FAR (%)
30	32 (24)	96 (95)	12 (4)
60	51 (44)	96 (94)	16 (8)
90	77 (72)	83 (75)	19 (11)
120	108 (101)	74 (65)	21 (12)
S	N/A	65 (64)	19 (14)

sleep through the hypoglycemic alarms, as indicated in [Buckingham et al., 2005; Revital and Moshe, 2014]. For this reason, we also tested the potential to predict the risk of hypoglycemia before bedtime (assumed to be at midnight). The data records were extended to start two hour prior to this time point, considering the same data selection criteria as before. Using these data, the estimation filter was allowed to make an estimate of the basal requirement, and after that the rest of the night was simulated using this value. If the simulated value dropped below the hypoglycemic threshold, hypoglycemia was considered to have taken place. Thus, in the case a hypoglycemic episode did take place any time during the night and the simulated trace also fell below the hypoglycemic threshold, a true positive was scored regardless of the timing of the alarm and the real event.

The larger false alarm rate for the 3.3/3.8 mmol/l setting is due to that many of the events with a minimum value below 4.0 mmol/l also fall below 3.3 mmol/l in the prediction. These event are thus classified as hypoglycemia, which is also reflected in the average glucose value for the misclassified events (3.7-4.2 mmol/l for all prediction horizons).

The pump suspension simulations indicate that up to 46% of the hypoglycemic events (3.3 mmol/l) could be avoided all together and for the hypoglycemic episodes that still occurred, the time spent in the hypoglycemia was reduced by 68%. No subsequent hyperglycemia was noted. A demonstrating example can be found in Figure 5.3.

5.4 Discussion

To evaluate the performance in terms of predictive capacity it is relevant to compare our results to those of previous publications also conducted in a retrospective manner. In [Palerm and Bequette, 2007], a Kalman filter based approach was evaluated for 13 hypoglycemic clamp datasets. Using a hypoglycemic threshold of 70 mg/dl (4 mmol/l), the sensitivity and speci-

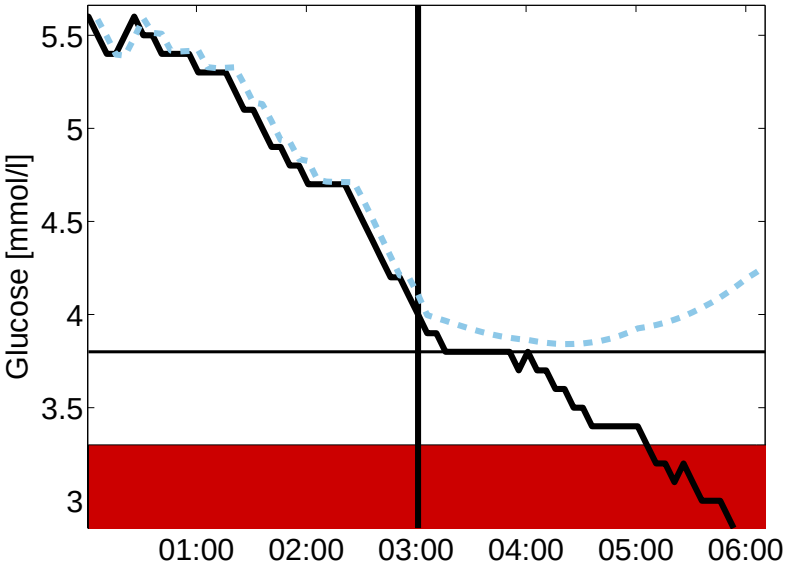

Figure 5.3 Example of the effect of full two-hour pump suspension at predicted hypoglycemia 60 minutes ahead. The black solid line represents the CGM reference, the dotted blue line the prediction considering the pump suspension and the solid vertical black line marks the time point when the hypoglycemic alarm was triggered and the pump was turned off.

ficity were 90 and 79%, respectively, with a 30 minutes alarm time. Three different algorithms, based on a recursive ARMA model, were suggested in [Eren-Oruklu et al., 2010], and evaluated on data from insulin-induced hypoglycemic tests from 54 T1DM subjects. With a hypoglycemic threshold of 60 mg/dl (3.3 mmol/l), sensitivity of 89, 88, and 89% and specificity of 67, 74, and 78% were reported for each method, respectively. Mean values for time to detection were 30, 26, and 28 minutes. A combined approach merging up to five different models was used in [Dassau et al., 2010]. The system was developed using 21 datasets from a 24-hour Abbott Navigator CGM trial for children with T1DM, and was validated on hypoglycemic induced studies on 22 T1DM patient records. With a voting scheme of 3-out-of-5, and a hypoglycemic level defined as below 60 mg/dl (3.3 mmol/l) and a prediction horizon of 35 minutes, a sensitivity of 91% was achieved, and when 4 out of 5 positive alarms were required, the sensitivity dropped to 82%.

Finally, the last method we benchmarked against is also a recursive model. In [Turksoy et al., 2013], a recursive state-space model incorporating the ef-

Table 5.2 Summary of results from previous studies. Prediction Horizon (PH), Warning Time (WT), Sensitivity (SE), False Alarm Rate (FAR) and Hypoglycemic Threshold (HT).

Study	PH [min]	WT [min]	SE [%]	FAR [%]	HT [mmol/l]
26	30	30	90	21	4.0
27	30	30	89	33	3.3
27	30	26	88	26	3.3
27	30	28	89	22	3.3
11	35	35	91	9	3.3
11	55	55	82	N/A	3.3
17	30	29	81	34	4.0
17	60	38	96	48	4.0

fect of insulin was used for retrospective analysis of 14 datasets, covering in total 201 hypoglycemic (70 mg/dl, 4 mmol/l) episodes. The authors report many different prediction horizons, and here we extract the 6 and 12 step ahead predictions. With these settings, the 6-step prediction had a sensitivity of 81% with a false alarm rate of 34 % and an average warning time of 29 minutes. All competing methods are summarized in Table 5.2. In comparison to the presented methods, our approach, with the preferred setting of a hypoglycemic trigger level at 4.2 mmol/l and a 60 minute prediction horizon, allows for longer warning times while maintaining a high sensitivity (94%) and keeping the false alarm rate at an acceptable level (8%).

From the results of the estimated EGB we could see that the level changed from day to day. Unfortunately, the data records were too short to allow for an ARMA model to be estimated. A dynamic model of the EGB, providing improved priors, could potentially vastly improve the predictive performance, especially in the early time of the night where the recursive update still has not contributed very much to the estimate. The day-to-day variability may be due to normal variations in the insulin sensitivity, but external factors such as glycemic loading and physical activity may also play significant parts. Further studies are required to investigate the mechanisms to glucose variability in this regard.

The evaluation shows that the model is capable of predicting almost two out of three nocturnal hypoglycemic episodes even before bedtime. About every sixth time, it will be a false alarm. For persons suffering from reoccurring nocturnal hypoglycemia, this may be an acceptable shortcoming.

Outpatient validation of prediction-based pump suspension of an algorithm based upon the Kalman filter approach of [Palerm et al., 2005] was conducted for both children [Buckingham et al., 2015] (82 individuals) and adults/adolescents [Maahs et al., 2014] (45 individuals). In both studies, the

pump was shut off when the glucose was predicted to go below 80 mg/dl in the coming 30 minutes. The pump studies had somewhat different primary outcomes. For the adult study, the number of nights with a glucose reading below 60 mg/dl was reduced by about 36%, and for the children the authors reported that the time spent below 70 mg/dl was reduced by 54% (children 11-14 years old) and 50% (children 4-10 years old), both in comparison to the control nights with the suspension system deactivated. For both our simulation study and the outpatient experiments, the results indicate that not all hypoglycemic episodes may be avoided by pump suspension. As pointed out by the authors of [Buckingham et al., 2015], this may be due to too heavy bolus doses previous in the night, from which a mere reduction of subsequent insulin delivery is insufficient to avoid hypoglycemia. On the other hand, in cases where the glucose-lowering amount of insulin on-board is low, full pump shut-off may even be unnecessary, and the long warning time provided by our method may allow for more flexible down-regulation of the insulin pump. This is beneficial, since a smoother insulin delivery reduces the risk of unwanted subsequent hyperglycemic episodes following a hypoglycemic prevention action.

5.5 Conclusions

Prediction, detection and prevention of nocturnal hypoglycemia are major challenges in insulin-based therapy. Recent advances in sensor and pump technology and algorithmic development have provided tools for reducing the detrimental effects of this potentially very dangerous aspect of living with diabetes.

In this chapter, a novel method for prediction has been presented based on a non-parametric model of the insulin action and by considering day-to-day time-variability in the glucose metabolism. The suggested approach was successfully tested on 29 patients on sensor augmented insulin pump therapy, covering in total 223 nocturnal episodes. The results show that the method has a useful sensitivity and acceptable false alarm rate and that the warning time is sufficiently long for adjustments of the insulin delivery to be undertaken to reduce time spent in hypoglycemia. The method may be employed to all three layers of the defence in depth. The first barrier, avoiding adverse events, is addressed by simulating the overnight period before going to bed. The results indicate that 64% of the nocturnal hypoglycemic episodes may be detected in such a simulation. This allows for the user to instigate countermeasures to avoid the event, such as digesting a small snack or temporarily reducing the basal delivery. However, the implications of the false alarm rate (14%) have to be investigated. An analysis of suitable actions to take in the event of an alarm have to be analysed and the consequences highlighted for

both the true positive as the false positive case. The second line of defence is to allow for alarms to be set off when a hypoglycemic event is imminent. Different prediction horizons were investigated with diminishing sensitivity and increasing false alarm rate as the prediction horizon increases. The optimal setting is probably given by personal preferences regarding sensitivity to hypoglycemia and acceptance for false alarms. However, even the shortest prediction horizons seem to be able to give the user sufficient amount of time for a snack to be digested in order to avoid the event. Finally, also the third function level of active safety systems may be relevant. Autonomous suspension of the insulin pump based on an algorithm relying on trend extrapolating prediction is already a reality. With the improved prediction horizon offered by the suggested method, more efficient, and with lower risk of subsequent hyperglycemia, means to reduce the insulin suspension may be possible.

6

Meal Impact Identification

6.1 Introduction

Several external factors affect the glucose dynamics, but no disturbance has a more profound effect than meal intake. Characterization of this disturbance, combined with an insulin action model, would allow for better tailoring of meal boluses to achieve a sound postprandial glucose level. Carbohydrates have generally been considered as the main driver of postprandial hyperglycemia, and carbohydrate content is often used as the sole explanatory variable of expected total glucose elevating impact [Gillespie et al., 1998]. However, meals are heterogeneous in many dimensions, e.g., in terms of carbohydrate complexity, macro-nutrient composition, fibre content and food preparation techniques, all contributing to the digestion and absorption kinetics [Wolpert et al., 2013; García-López et al., 2013], and possible also to the degree of postprandial hepatic down-regulation [Lam et al., 2003]. Furthermore, specific ingredients, such as cinnamon, which cannot be identified by merely looking at the nutritional composition, may significantly delay gastric emptying [Hlebowicz et al., 2007]. For these reasons, carbohydrate counting alone will not suffice. The glycemic index (GI) is a measure used to characterize the effect on blood glucose following a meal intake [Jenkins et al., 1981]. A standardized portion size, to the equivalent of 50 grams of carbohydrates content, is digested and the postprandial response (PPG) is recorded. By summarizing the area under the curve (AUC) of the PPG, subtracting the initial glucose level, a measure is obtained. This is compared to the corresponding value from a reference meal, usually white bread or glucose, eaten by the same individual. The ratio between the AUC of the reference and the AUC of the digested meal makes out the GI. Determination of GI has been conducted in both healthy, NIDDM and IDDM individuals with similar results [Brouns et al., 2005]. However, while providing a means to get an approximate ranking of the total glucose impact of different meals, neither the dynamic properties nor the absolute magnitude of the PPG are

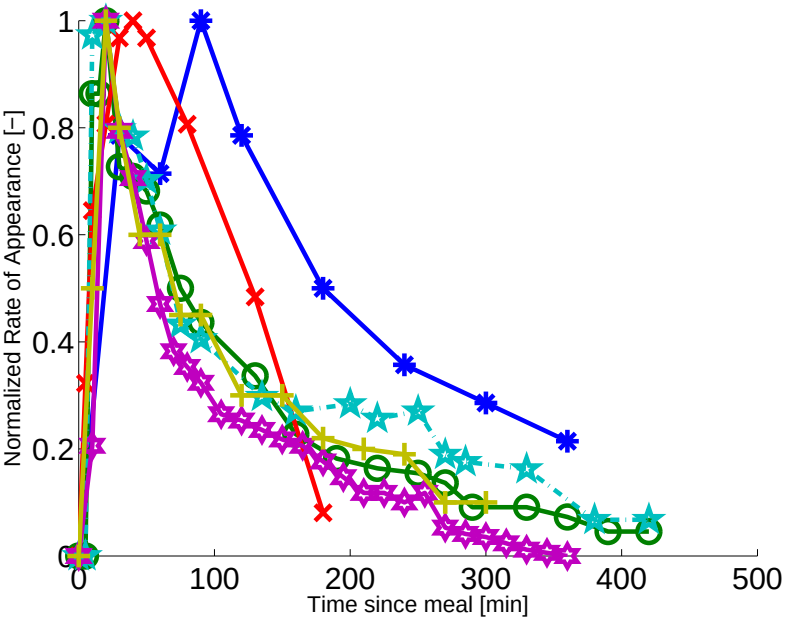

Figure 6.1 Rate of appearance retrieved from tracer experiments. Blue line with stars: Glucose [Dinneen et al., 1995], Green line with circles: 45% Carbohydrates, 15% Protein, 40% Fat [Dalla Man et al., 2006b], Red line with crosses: Glucose, Light blue line with pentagrams: 55% Carbohydrates, 15% Protein, 30% Fat [Livesey et al., 1998], Violet line with hexagrams: High glycemic index meal 65% Carbohydrates, 19% Protein, 16% Fat [Basu et al., 2006], Brown line with plus signs: 60% Carbohydrates, 19% Protein, 21% Fat [Vella et al., 2007].

characterized. In this chapter, a finite impulse response model approach is used to describe the postprandial response of different meal types.

6.2 Current Research

Experimental methods

Tracer experiments are used to estimate the rate of appearance of glucose and endogenous glucose production in the postprandial phase following a meal intake. The methodology has later been revised, e.g., with a use of a triple tracer protocol [Basu et al., 2003]. Estimates of the rate of glucose appearance from the gut from some different studies can be seen in Fig. 6.1.

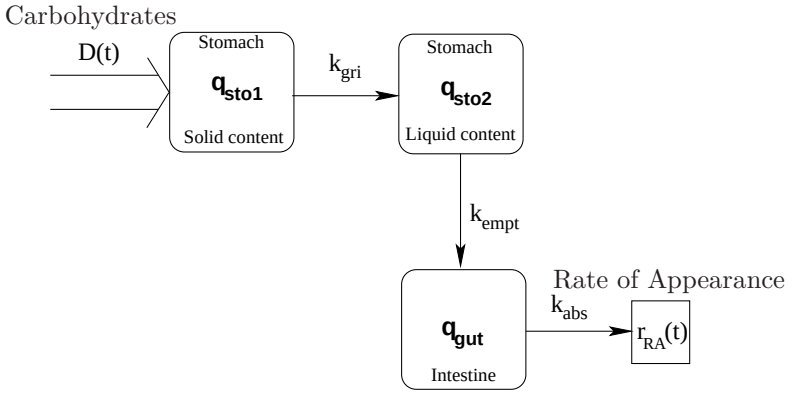

Figure 6.2 The gastric compartment model by Dalla Man describing the digestion and rate of appearance, R_a following a meal.

Physiological models

Several models have been developed to describe the initial stages of glucose metabolism, covering the digestive process and the flux of glucose from the intestines. There is evidence that gastric emptying, to some extent, is dependent on current glucose level, see, e.g., [Schvarcz et al., 1997], but this relationship has not been incorporated in any model so far. Thus, the digestive process is also considered as a stand-alone model, without dependencies to the glucose metabolism. Two models have been widely used; the models by [Lehmann and Deutsch, 1992] and [Dalla Man et al., 2007a]. In [Lehmann and Deutsch, 1992], the model consists of a single compartment with fixed limited gastric emptying rate constant, and with a duration dependent on the meal size. Earlier work on models of glucose rate of appearance during an oral glucoe tolerance test (OGTT) [Dalla Man et al., 2002] and mixed meal test [Dalla Man et al., 2006a] formed the basis for the model in [Dalla Man et al., 2007a]. Here, a third-order nonlinear compartment model was used, and also in this case, the gastric emptying rate was limited dependent upon the amount of ingested carbohydrates. This model, see Fig. 6.2, is described below.

$$\begin{aligned} q_{sto}(t) &= q_{sto1}(t) + q_{sto2}(t) \\ \dot{q}_{sto1}(t) &= -k_{gri} \cdot q_{sto1}(t) + D(t) \\ \dot{q}_{sto2}(t) &= k_{gri} \cdot q_{sto1}(t) - k_{empt}(q_{sto}(t)) \cdot q_{sto2}(t) \\ \dot{q}_{gut}(t) &= -k_{abs} \cdot q_{gut}(t) + k_{empt}(q_{sto}(t)) \cdot q_{sto2}(t) \\ R_a(t) &= \frac{f \cdot k_{abs} \cdot q_{gut}(t)}{M_{BW}} \end{aligned} \tag{6.1}$$

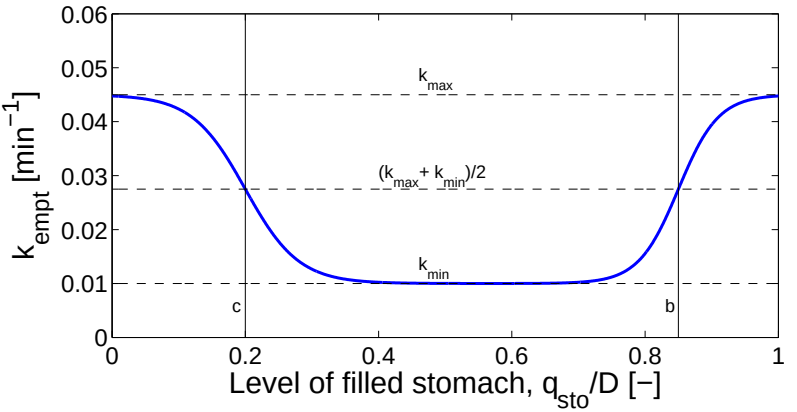

Figure 6.3 The dependence of gastric emptying k_{empt} on the amount of food in the stomach left from the digested amount D.

Following the notation in [Dalla Man et al., 2006a], q_{sto} is the amount of glucose in the stomach (q_{sto1} solid, and q_{sto2} liquid phase) and q_{gut} is the glucose mass in the intestine. The rate parameters determine the flux between the compartments. Here, k_{gri} is the rate of grinding, k_{empt} is the rate constant of gastric emptying and k_{abs} is the rate constant of intestinal absorption. The fraction of intestinal absorption f is a measure of the absorption efficiency and determines the fraction of glucose that actually appears in the blood stream. The rate of appearance of glucose in the blood $R_a(t)$ from the amount of ingested carbohydrates $D(t)$ is normalized by the body weight M_{BW}. The parameter k_{empt} is a non-linear function of q_{sto} and $D(t)$:

$$k_{empt}(q_{sto}) = k_{min} + k \cdot \{\tanh[\alpha(q_{sto} - b \cdot G(t))] - \tanh[\beta(q_{sto} - d \cdot G(t))] + 2\} \quad (6.2)$$

with $k = (k_{max} - k_{min})/2$, $\alpha = 5/2D(1-b)$, $\beta = 5/2D$, with parameters k_{max}, k_{min}, b, and d. The gastric emptying is biphasic with a maximum rate k_{max} when the stomach is full or empty and reduced to a minimum k_{min} in-between, see Fig. 6.3. An example of rate of appearance using this model can be seen in Figure 6.4. Notice the second peak due to the increased gastric emptying rate as the stomach compartment begins to empty.

Data-driven approaches

Based on fixing all parameters but the insulin sensitivity in the minimal model (see Chapter 2), an approach to estimating the rate of appearance based on measurements of plasma glucose and insulin was presented in [Herrero et al., 2012]. The concept was successfully validated on data from both

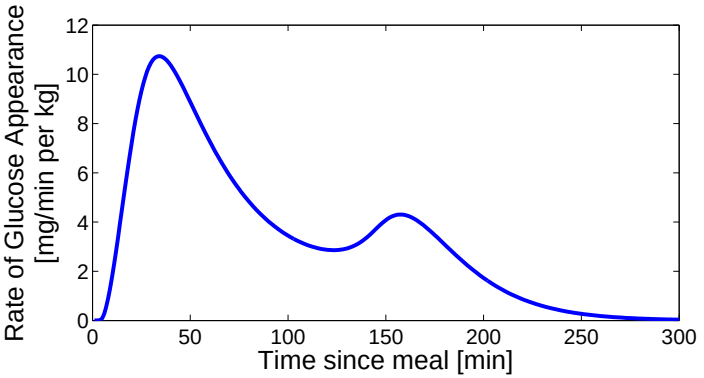

Figure 6.4 Example of rate of appearance using the simulation model from [Dalla Man et al., 2006a].

simulation and empirical trials. However, the need for insulin assays limits its use.

Several of the blackbox models described in Chapter 2 utilized meal information when present in the data. Meal intake has been considered as input in, e.g., ARMAX [Cescon, 2013], state-space models [Ståhl, 2012], support vector machines [Georga et al., 2011] and continuous-time transfer function models [Cescon, 2013; Kirchsteiger et al., 2014]. In both [Cescon, 2013] and [Kirchsteiger et al., 2014], the continuous-time models were applied to breakfast meals. It was recognized that applied to another meal type with an alternative composition of macro-nutrients, different meal parameters may result. However, none of the models above explicitly discriminate between different recipes, and all rely on the assumption that the postprandial response can be described by the carbohydrate content alone. Additionally, the linearity assumption may prove restrictive in order to characterize the temporal response of the meal impact. To resolve these issues, a finite impulse response model is employed with parameters sets uniquely identified for each meal type considered.

6.3 Data

To estimate the meal impact, data from the ULund trial were used. During this trial the patients were living at home as usual, following their normal eating patterns. Meals were registered in an electronic logbook as described in Chapter 3. Even though several features of the logbook simplified meal logging, for many of the patients the number of reported meals dropped as the study progressed, see Figure 6.5. In total, 2112 recipes and 5312 meal

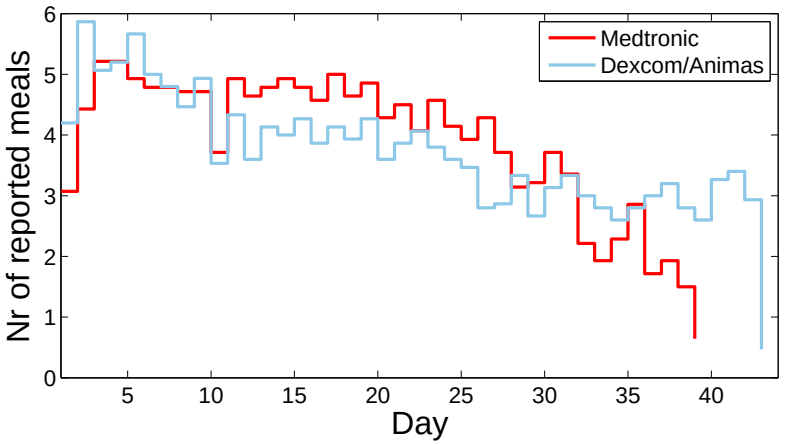

Figure 6.5 Number of reported meal instances over the trial period.

instances were included, averaging about five meals a day. The estimation was based on individual data records from each meal instance. The nominal time length of each record was 4.5 hours. This length was chosen with the maximum expected length of postprandial response in mind, based on the tracer experiments presented above. Practical concerns in home-monitored data, related to the duration between meals, also set a hard constraint on the length of the data record.

In order to circumvent interference in the estimation process from other sources than the intended meal, the following data inclusion criteria were enforced. No previous meal was allowed within two hours of the meal start. To avoid the effects associated with the counter-regulatory response, hypoglycemia was not allowed during this time window nor during the rest of the data. Extreme hyperglycemia (>25 mmol/l) was not accepted. datasets where the CGM showed large deviations (> 15%) to the glucose meter reference were also discarded as unreliable. If these conditions were violated, the data record was prematurely terminated. Furthermore, an assessment was made regarding the time stamp of the meal. Data with obvious errors in timing (e.g., where the glucose level started rising before the meal, despite a simultaneous bolus dose) and meal content (e.g., energy content>10.000 kcal) were discarded. Finally, at least five meal instances of the same recipe was required for estimation to be pursued.

6.4 Variability in Endogenous Glucose Balance and Insulin Action

Before describing the full model we need to revisit the aspect of variability in EGB. So far, the day-to-day variability in insulin demand has been explained solely by the endogenous balance. However, there is reason to believe that not only the EGB varies, but also the peripheral sensitivity to the metabolic effect of insulin is subject to variations. To investigate this possibility, a insulin action multiplier $\lambda = [\lambda_1, \dots \lambda_N]$ was introduced into the model. The revised model becomes

$$y(t_k)^{(j)} = y(t_{k-1})^{(j)} + \lambda_j \sum_{i=0}^{n} a_i (y(t_k)^{(j)}) I(t_{k-i}) + G_b^{(j)} + v(t_k), \quad t_k \in T_j \tag{6.3}$$

with the same notation as in Chapter 4. Using this model, estimates of λ and re-estimates of $\mathbf{G_b}$ and $\mathbf{a}$ can be retrieved. Assuming a marginal gamma distribution for both the insulin multiplier and the EGB, these variables can be estimated given the current insulin action by maximum likelihood (ML). The choice of the gamma distribution is motivated by that it only has positive support, just as these variables. The ML estimate is

$$\{\lambda, \mathbf{G_b}\} = \arg\min_{\lambda, \mathbf{G_b}} \|\mathbf{Y} - \hat{\mathbf{Y}}\|_2^2 + (k-1) \sum_{i=1}^{N} (\ln \lambda_i + \ln G_b^{(i)}) - \frac{1}{\theta} \sum_{j=1}^{N} (\lambda_j + G_b^{(j)}) \tag{6.4}$$

where $\mathbf{Y} = [\mathbf{y_1} \dots \mathbf{y_N}]^T, \mathbf{y_j} = [y_1^j \dots y_{n_j}^j]^T, j = [1 \dots N]$ is the concatenated glucose reference for all days in the data, and $\hat{\mathbf{Y}}$ is the corresponding estimate retrieved from using Eq. 6.3 using the current impulse-response model parameters $\mathbf{a}$, and k and θ are the shape and scale parameters of the gamma distribution. In order to get updated estimates of the insulin action as well, this variable can be considered as a latent variable in the estimation, which thereby would constitute the maximization step in the expectation-maximization (EM) algorithm. The expectation step would mean to take the expected value of the the entire $\mathbf{a}$ matrix. This could be done using, e.g., a Gibbs sampler [Bishop, 2006]. However, the total size of the $\mathbf{a}$ variable makes this impractical. Instead, the following approach is considered. Using the new estimates of λ and $\mathbf{G_b}$, the insulin action $\mathbf{a}(G)$ for each glucose level G was re-estimated from

$$\mathbf{a}(\mathbf{G}) = \arg\min_{\mathbf{a}} \|\mathbf{Y} - \hat{\mathbf{Y}}\|_{\mathbf{W}^G} + \alpha \|\mathbf{a}\|_{\mathbf{R}} \tag{6.5}$$

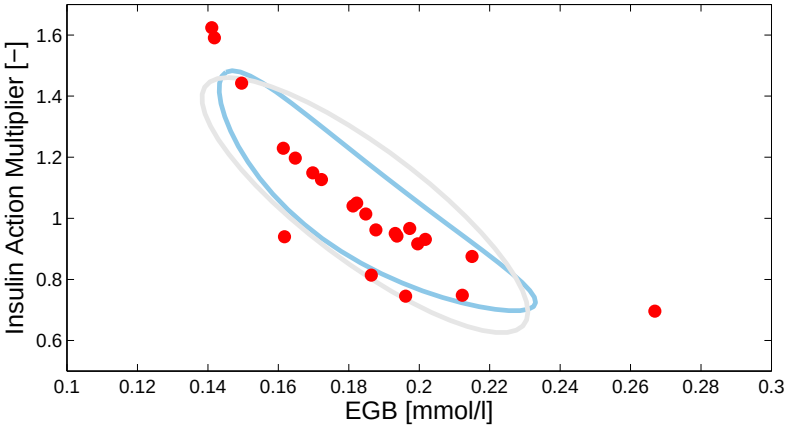

Figure 6.6 Example of the distribution of EGB/insulin multiplier estimates. Patient M1. The blue curve is a level curve for the corresponding log-normal distribution and the grey curve is a Gaussian approximation.

which is recognized from Chapter 4, Eq. 4.4, but without the regularization of the EGB since this is considered fixed in this step. The two steps (Eqs. (6.4) and (6.5)) were iterated until the relative norm $\|\mathbf{a}_{k+1} - \mathbf{a}_k\|/\|\mathbf{a}_k\|$ of two subsequent insulin action estimates ($\mathbf{a}_k$ and $\mathbf{a}_{k+1}$) was less than a given threshold (0.05).

As it turns out, running the estimation results in that the estimated EGB E_{GB} and insulin multiplier λ exhibit a relationship similar to

$$E_{GB} = \frac{C}{\lambda^{\alpha}} \tag{6.6}$$

where C and α are constants, as can be seen from the example plot in Figure 6.6, effectively coupling the peripheral and hepatic insulin sensitivity. Log-transforming both variables results in a joint Gaussian distribution.

6.5 Meal Impact Model

To represent the pharmacokinetics/pharmacodynamics of insulin, the same principle insulin action model was used as outlined in Chapter 4. This model was extended with another finite impulse response model, which represents the glucose flux into the blood stream following a meal. Incorporating the insulin gain λ as described above, the glucose dynamics at time point t_k,

during meal instance j, may then be described as

$$y(t_k)^{(j)} = y(t_{k-1})^{(j)} + \lambda_j \sum_{i=0}^{n} a_i(y(t_k)^{(j)})I(t_{k-i}) + \sum_{r=1}^{R}\sum_{i=0}^{m} b_i^r M_r^{(j)}(t_{k-i}) + G_b^{(j)} + v(t_k), \quad t_k \in T_j \tag{6.7}$$

where notation as in Chapter 4, except $M_r(t_k)$, which is the meal intake in grams of carbohydrates in recipe r, and the meal impact parameters $\mathbf{b}_r = [b_{r,1}, b_{r,2} \dots b_{r,m}]$, which are fixed for each recipe. A recipe is a unique combination of ingredients, and may denote a single ingredient. Also note that the recipes are specific to an individual (i.e., two persons eating a banana constitutes two different recipes). During estimation, only one recipe is allowed at a time ($R = 1$). The order m of the meal impact model was chosen to correspond to 270 minutes. The net basal endogenous glucose production G_b and the insulin multipliers are allowed to vary between different meal instances to capture variations in insulin sensitivity. To estimate $\mathbf{b}^r$, $\mathbf{G_b} = [G_b^{(1)} \dots G_b^{(N)}]$ and $\lambda = [\lambda^{(1)} \dots \lambda^{(N)}]$ for N number of meal instances, a maximum-likelihood approach is considered. The total likelihood for the entire dataset from all the meal instances is

$$p(\mathbf{Y}, \mathbf{I}, \mathbf{M}_r, \mathbf{G_b}, \lambda, \mathbf{b}) \propto p(\mathbf{Y}|\mathbf{G_b}, \lambda, \mathbf{b}) \cdot p(\mathbf{G_b}, \lambda) \cdot p(\mathbf{b}) \tag{6.8}$$

where $\mathbf{Y} = [y_1^{(1)} \dots y_n^{(1)} y_1^{(N)} \dots y_n^{(N)}]$ is the concatenated glucose reference for all meal instances. We would like to maximize this in order to retrieve our parameter estimates. Unfortunately, the joint lognormal distribution $p(\mathbf{G_b}, \lambda)$ makes the problem non-convex. A possible work-around is to use a Gibbs sampler where samples are drawn in an iterative scheme from the conditional distributions [Bishop, 2006]:

$$\begin{aligned} (\mathbf{G_b}, \lambda)^{(k)} &\sim p(\mathbf{G_b}, \lambda|\mathbf{Y}, \mathbf{b}^{(k-1)}) \\ b_i^{(k)} &\sim p(b_i|\mathbf{Y}, \mathbf{b}_{\neg i}^{(k)}, (\mathbf{G_b}, \lambda)^{(k)}), \quad \forall b_i \in \mathbf{b} \end{aligned} \tag{6.9}$$

where k is the sampling index and $\mathbf{b}_{\neg i}^{(k)}$ is the meal impact vector without term b_i. When a sufficient number of samples have been collected the expected values can be retrieved. A suitable number of iterations is 5000 [Raftery and Lewis, 1992]. The samples were restricted to positive numbers to fulfil the physiological constraints.

EGB and insulin gain variability revisited

The variability in insulin requirement, divided into variability in both EGB and peripheral insulin sensitivity was investigated for the overnight data

above. However, the EGB/insulin gain range experienced during night time is only a limited frame of the total variability that may occur over an entire day. Patient basal programs where the minimum to maximum basal dose ratio is larger than 1.5-2 are not uncommon. The lowest basal dose is typically found during the night (compare with the results in Chapter 4 indicating that the minimum EGB occurred around 4-6 a.m.). Therefore, the prior provided by the overnight data may prove insufficient, with too limited support. In order to make the concept work for meals digested during every possible time throughout the day, we need to extrapolate the EGB-to-insulin gain relationship beyond the values found in the night data. A first pass is made assuming marginal gamma distributions for both the insulin gain and the EGB for all meals and all meal instances for each patient. These parameters are estimated together with the meal impact parameters. The set of EGB and insulin gain points ($\{\mathbf{G_b}^0, \lambda^0\}$) retrieved are then used together with the night data to form a new joint posterior distribution for $\mathbf{G_b}$ and λ. Together with the initial estimate of the meal impact $\mathbf{b}_{r,0}$, they are used as a starting point for the Gibbs sampler. The following optimization problem is solved.

$$\{\mathbf{b}_{r,0}, \mathbf{G_b}, \mathbf{0}, \lambda_0\} = \underset{\mathbf{b}_r, \mathbf{G_b}, \lambda}{\arg\min} \sum_{j=1}^{N} (\|\mathbf{y}^{(j)} - \hat{\mathbf{y}}^{(j)}\| + \|\mathbf{G_b}\|_{\Gamma_{k,\theta}} + \|\lambda\|_{\Gamma_{k,\theta}} + \|\mathbf{b}\|_{\mathbf{R}} \tag{6.10}$$

subject to $b_k \geq 0, \quad k = [1, \ldots, n-1]$, and where the estimated glucose excursion $\hat{\mathbf{y}}^{(j)}$ is calculated using (6.7). The different steps of the estimation procedure have been summarized in the text box on the next page.

6.6 Meal Impact Diversity Analysis

As described above, it is common in the literature to treat all meals as having the same kind of meal impact. To investigate the amount of diversity between the estimated glucose impacts (one for each recipe) retrieved using the outlined method, the following approach was considered. Principal component analysis is a statistical method used to extract the subspace of main variability in a multi-dimensional dataset [Bishop, 2006]. In this context, we will employ the method to the collected meal impact parameter set derived from the estimation procedure described above. Thereby, a minimum set of principal meal parameters can be retrieved, from which all meal impacts can be formed by linear combination. All the meal impacts are collected in a common matrix, where each row correspond to a meal impact vector. The principal components are simply the eigenvectors of the covariance of this matrix.

Summary of the Estimation Process

1. We need a prior for the EGB-insulin multiplier distribution. Starting with the overnight data, we retrieve an estimated dataset $\{\lambda, \mathbf{G_b}\}$ using (6.4).
2. Re-estimate the insulin action parameters $\mathbf{a}$ using Eq. (6.5) and the estimated values from Step 1.
3. Re-iterate between Steps 1 and 2 until the difference between two subsequent insulin action parameter sets ($\mathbf{a}_k$ and $\mathbf{a}_{k+1}$) is less than a given threshold (0.05).
4. Complement the estimates from Step 1 with estimates from the meal data records, using (6.10). An initial estimate of the meal impact $\mathbf{b}$ is also retrieved.
5. Run the Gibbs sampler (6.9) to get the final posterior estimates of the meal impact and the EGB and insulin multipliers. Initial values for the iterative process are given by step 4.

Having reduced the dimension of complexity, the next step is to determine whether the meal impact are grouped together in this subspace. Here, Gaussian Mixture Modeling (GMM) may be employed [Bishop, 2006]. The underlying assumption in GMM is that the data cloud is grouped together in separate Gaussian distributions. The gmm library in the Matlab Statistics and Machine Learning Toolbox was used [MathWorks, 2012], which utilizes the EM algorithm. The method does not guarantee a global minimum, and the number of clusters is often chosen in a heuristic manner. To resolve these issues, the algorithm was run multiple times and with different number of clusters.

6.7 Results

All in all, 56 different recipes fulfilled the inclusion criteria and were estimated for meal impact, see Appendix 6.9. Most patients had some recipe that could be estimated, but for a few patients none could be found, the reason being too few meal instance and in some cases due to recurrent timing issues in the meal reporting.

In Figure 6.7, the estimated glucose elevating effect of two different recipes are depicted. Generally, the meal impacts were less than 3 hours long with a

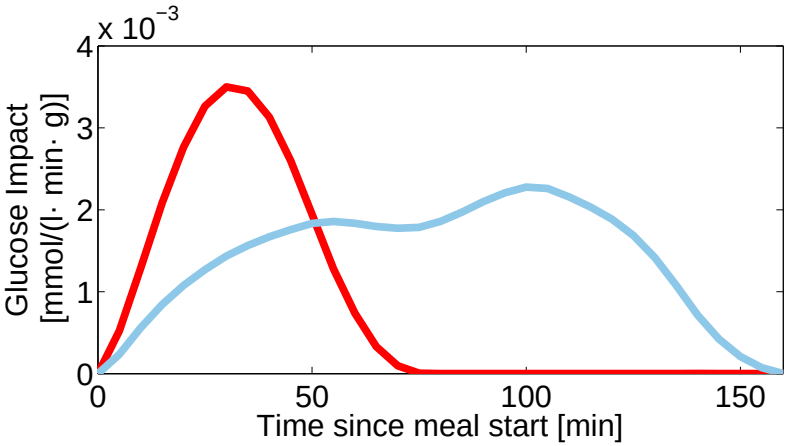

Figure 6.7 Example of meal impact using carbohydrates as input. Blue curve: Breakfast, Patient M1. Red curve: Banana. Patient D3.

peak around 30-40 minutes after the meal started, similar to the impact of the banana seen in the figure (red curve). However, some recipes had double peaks, with a very delayed major peak. Without tracer experiments, or other means to get a fuller picture of the digestion and absorption processes, it is difficult to know the mechanism behind such a behavior. However, double peaks are supported by tracer experiments, and this has been modeled in the Padova digestion model, see above.

A vast majority of the meal impact peak around 35-40 minutes, see Figure 6.8. This is well in accordance with the rate of appearance estimates retrieved using the tracer experiments. The distribution of the duration is more spread out (180 ± 63 min), with a local minor peak at 270 minutes. This represents the meal instances where the duration was longer than the maximum length of the meal impact vector. The Glucose Elevating Magnitude (GEM) of the meal impact is the area under the curve of a meal with 10 grams of carbohydrates. This parameter changes a lot between the different recipes (2 ± 0.67 mmol/l after removing the high outliers).

The possibility to reproduce the reference glucose traces was tested by leave-one-out cross-validation where the impulse-response parameters were fixed for the validation data, according to the values estimated from the training data. Prediction performance was assessed using MARD, and was calculated using the data record from the time of digestion up to one to four hours afterwards. The mean values of these metrics were only calculated when at least four meal instances were available. The mean prediction MARD results were 7.7%, 11.5%, 13.8% and 13.2% for the evaluated time

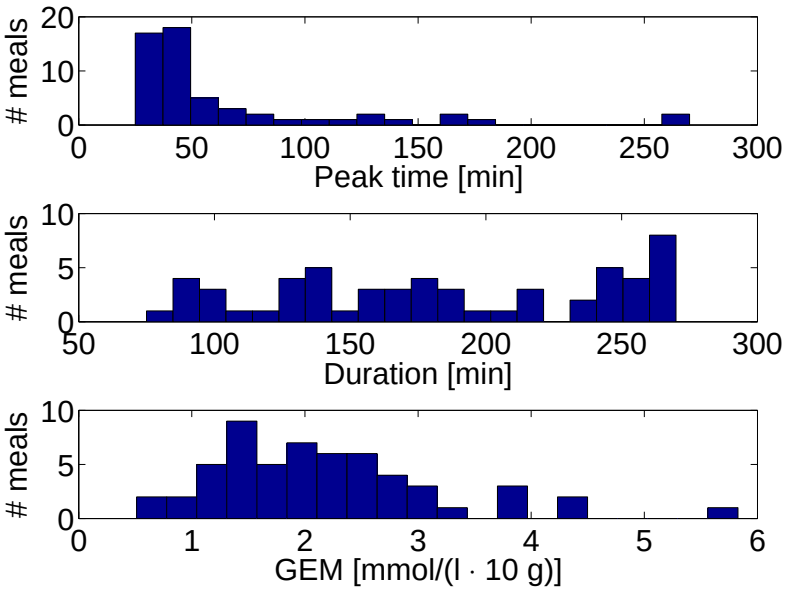

Figure 6.8 Distribution of estimated peak, duration and Glucose Elevating Magnitude (GEM) of the meal impacts. For recipes with a duration estimated to be longer than 270 min were marked as having a duration of 270 min in this diagram.

horizons. Summarized meal data and estimation parameter characteristics can be found in Appendix A. A prediction example can be seen in Figure 6.9. For comparative purposes, validation was also conducted using a Gaussian approximation of the EGB/insulin multiplier distribution, allowing for a convex direct solution of maximum likelihood, but with reduced predictive performance.

The principal components of the normalized meal impacts were derived. The top five components explain 91% of the variability among the meal impacts, see Figure 6.10. The cluster analysis successfully identified three main clusters (I, II, III) of the carbohydrate models, corresponding to 67% (30%, 19% and 18%) of the meal parameter sets. The recipes belonging to each of the three clusters are found in Table 6.1.

The meal impacts ($\mathbf{b_I}, \mathbf{b_{II}}$ and $\mathbf{b_{III}}$) calculated from the cluster centers represent the mean meal impact within each cluster, see Figure 6.11. Cluster I represent the fastest meals with an early peak and short duration. Recipes with a somewhat slower, and a more prolonged duration, belongs to cluster III. Cluster II can be characterized as meals with a less pronounced peak and long duration.

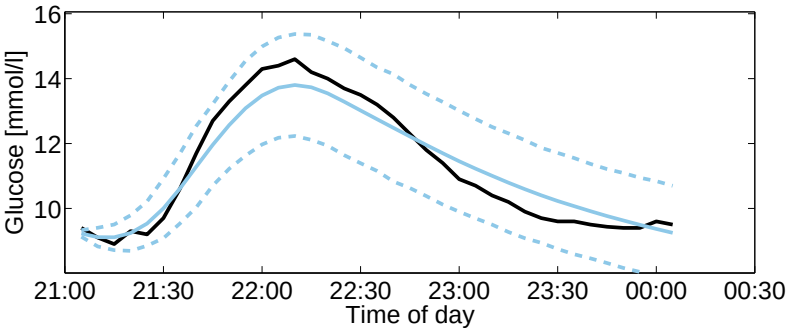

Figure 6.9 Example of validation of meal impact. CGM reference (black line) and prediction (solid light blue line), including standard error interval (dotted light blue lines). Recipe number 8 (Modifast, Patient D3).

Table 6.1 Recipes with similar normalized glucose impacts. Recipe numbers according to Appendix A.

Cluster	Fraction	Recipes
I	30%	1,4,6,7,8,10,17,19,26,31,32,43,44,45,46,53,55
II	19%	5,11,12,18,22,23,25,30,36,40,52
III	18%	2,9,15,16,20,28,35,41,42,50

To determine how well these match the individual meal impacts, the cumulative glucose response $\Sigma_r(k)$ was used

$$\Sigma_r(k) = \sum_{i=1}^{k} b_i \tag{6.11}$$

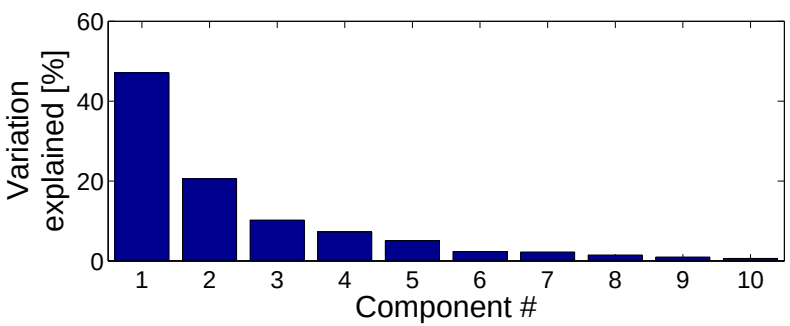

Figure 6.10 The variance explained by each principal component.

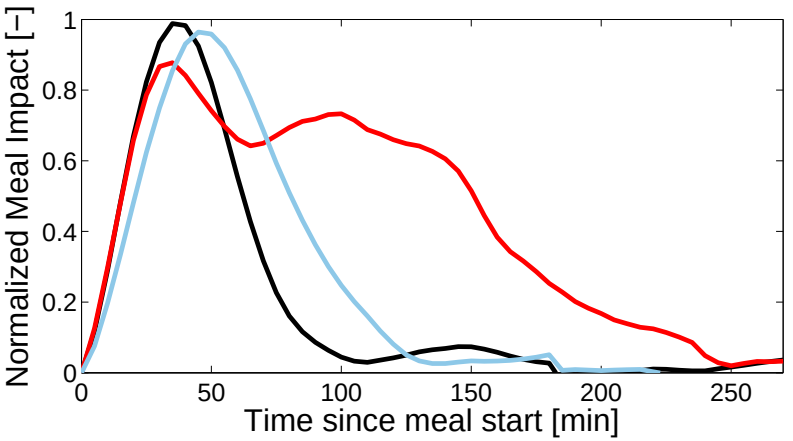

Figure 6.11 The normalized cluster center models. Cluster I (black curve), II (red curve) and III (light blue curve)

which describes the gradual glucose elevating impact of the meal, see Figure 6.12. Comparing the relative euclidean norm between the cumulative glucose response of the cluster means to the corresponding cumulative responses of each member (e.g. $\|\mathbf{\Sigma}_r - \mathbf{\Sigma}_I\|/\|\mathbf{\Sigma}_r\|$) showed that the differences were small ($11 \pm 9\%$, $14 \pm 6\%$ and $10 \pm 8\%$). This indicates that up to 67% of the recipes can be represented by the cluster means scaled with an individual factor to

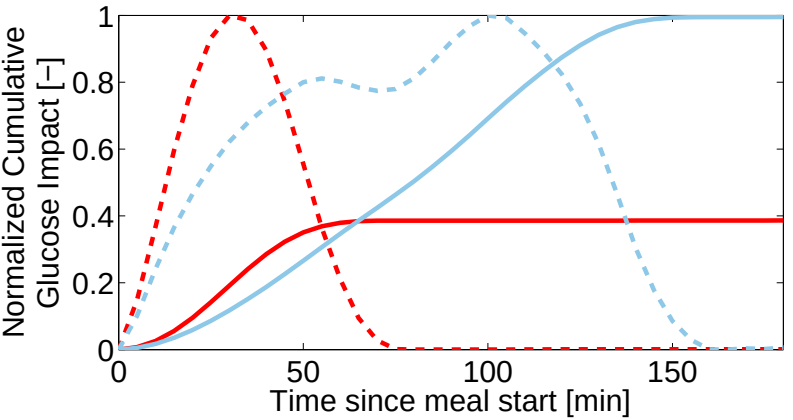

Figure 6.12 Example of normalized cumulative meal impacts(solid lines) and meal impacts (dashed lines). Blue curves: Breakfast, Patient M1. Red curves: Banana. Patient D3.

Table 6.2 Macro-nutrient composition in the clusters [mean±std].

Cluster	Protein [%]	Carbohydrates [%]	Fat [%]
I	15 ± 11	70 ± 22	15 ± 15
II	23 ± 9	53 ± 13	24 ± 10
III	20 ± 15	65 ± 22	15 ± 11

capture the absolute magnitude of the impact. The magnitude of the meal impact changes significantly within each cluster (CV 46%, 45%, 47%). Running the scaled cluster mean models for the three clusters on the data, yielded very similar prediction performance as retrieved from the individual models belonging to each cluster (MARD increased by 1%). The meal composition in terms of macro-nutrients (see Table 6.2) was significantly different between clusters I and II in all three macro-nutrients. The fat percentage was also significantly different between cluster II and III.

Finally, when comparing the predictive performance of the clusters, cluster I was significantly better than the two others, as well as the unclustered models.

6.8 Discussion

Predictive quality

The predictive performance was generally good in terms RMSE for the evaluated prediction horizons in the cross-validation. However, to determine the clinical value, a specific purpose of the prediction has to be considered. Two possible applications would be hypoglycemia detection and meal bolus optimization. Since the data were cleansed from hypoglycemic episodes for identification purposes, the possibility to utilize the models for hypoglycemic prediction cannot be assessed. However, the possibility of determining meal boluses using this model will be investigated in Chapter 9.

There is a negative bias in the prediction, which grows to 0.7 mmol/l around two hour into the postprandial phase, and then gradually reduces again, see Figure 6.13. The variance is also largest at this point with a maximum of 2.0 mmol/l. This peak in variance may be the cause of natural variability in the digestion process, shifting the absorption rate and efficiency somewhat in-between the different meal instances, but a sensor induced error cannot be ruled out, see discussions in Chapters 3 and 4 about CGM sensor errors. This may have different implications for the use of the model when determining meal bolus doses. On one hand, the undershoot of the peak means that the hyperglycemic peak may be underestimated. On the other hand, the more accurate description of the tail of the postprandial response, where

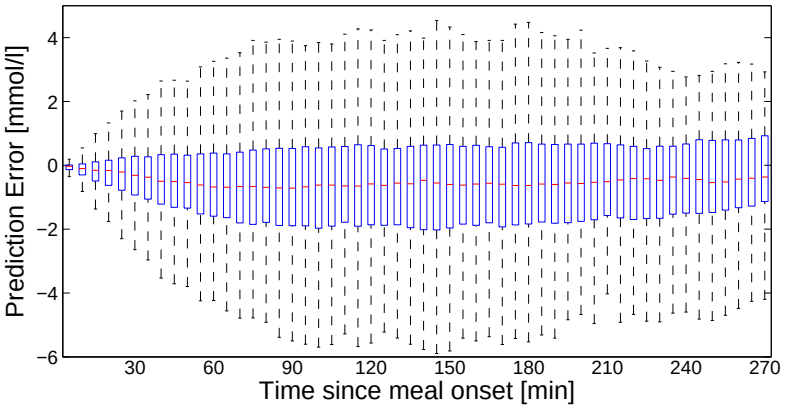

Figure 6.13 Distribution of the prediction error over the postprandial time period. Mean (Red line), 25%–75% quartiles (blue area), maximum and minimum values (whiskers).

hyoglycemia is more likely to occur, means that this aspect is well covered. The longer time horizon is generally of more interest when determining the bolus dose to achieve a stable glucose value within the normoglycemic region after the meal.

Other possible sources to variability include errors in meal reporting and estimation of meal sizes. A few studies describe the accuracy (bias) and precision of carbohydrate counting and meal size estimation, and the results differ somewhat. One study on 15 IDDM subjects reported in [Kildegaard et al., 2007], found the intrapersonal variation in carbohydrate counting to be 30%. Another study, covering 102 children and adolescents and 110 caregivers, found a majority of the estimates to be within a 10 gram error and less than 7% of the participants to have an error larger than 30% [Smart et al., 2010]. Less promising results were achieved in [Bishop et al., 2009], where only eleven of the 48 adolescent participants managed to estimate the carbohydrate content to within 10 grams. Also in [Shapira et al., 2010], where 60 patients estimated the carbohydrate content of different meals, the coefficient of variation was high (range 28%–45% for the different meals). However, in the data used here, several factors contribute to keeping the variability down. The high degree of repeatability for the reported meals also implies low variability in meal size. Thus, bias in the estimate may exist, but variability is probably low. Furthermore, the fact that the aggregated total meal size was calculated by the Linkura web service, and that the ingredients were collected from the digital database, also contribute to reducing both variability and bias.

The scarcity of repetitive data has been an issue, and the prediction re-

sults for an individual recipe with a low number of meal instances should be considered with caution. While individual estimates may be poor, the total amount of data analysed offers credibility to the main results. In total, 56 recipes and 475 number of meal instances were included. However, compared to the total number of recipes and meal instances this highlights the difficulties in finding qualitative postprandial data, sufficiently set apart, in free-living data records.

Glucose Elevating Magnitude (GEM) and the 500 rule

Similar to the 100 rule used for determining the insulin sensitivity ratio, the 500 rule is commonly used to determine the so called Carbohydrate-to-Insulin Ratio (CIR), see e.g. [BD Patient Information, 2015]. This generic rule teaches that every unit of rapid-acting insulin covers $500/T_{DD}$ grams of digested carbohydrates, where T_{DD} is the total daily dose. In practice, it is common that the patients and treating physician alter this parameter based on assessment of empirical data, and many bolus wizards allow for different parameter settings throughout the day. In comparison to what can be expected from this rule, the total glucose elevating magnitude (GEM) fitted well on average. Values close to 2.0 was expected considering the 500 rule and the 100 rule combined, and this is actually the mean of the estimated GEM. However, looking at the distribution, curios values are found both in the low and high ranges. Especially strange is the outlier with an estimated impact larger than 5 mmol/l. The recipe affected, coffee and milk (nr 34), has quite a low amount of carbohydrates. Apart from the risk of missed meal entries in the diary as a possible explanation, coffee alone has previously been shown to have a glucose elevating effect in diabetes [Lane et al., 2008]. At the other end of the range, the low GEM values could be caused by a mix up in the identification between the meal impact and the combined insulin gain/EGB estimate. All three terms contribute to changes in the glucose level, though the insulin gain does so through the insulin dynamics and the EGB is considered constant. To ensure that the mix up effect is negligible, the low magnitude meals were re-estimated incorporating one hour of data prior to the meal. Thereby, data unaffected by the meal was added, putting more emphasis on forcing the EGB/insulin gain to be able to predict the glucose level even when no meal is present. However, no significant differences in the parameter estimates were noticed.

Recipe clustering

The low number of principal components seems promising regarding the total variability in meal impact, and the clustering analysis indicates that a majority of recipes can be described by scaled versions of as few as three basic meal impact models. Furthermore, the analysis also point to that the

postprandial response of the fast meals with early peak and short duration, represented by cluster I, can be more accurately predicted by the model than slower meals belonging to the other clusters. Several studies have indicated that both protein and fat may contribute to the postprandial response [Bell et al., 2015; García-López et al., 2013; Wolpert et al., 2013], and fat is known to delay gastric emptying, see e.g. [Gentilcore et al., 2006]. Both clusters I and III have significantly lower relative fat content than the slower cluster II, and also the protein content is different between clusters I and II. Looking at the recipe list of each cluster also gives some hint to what kind of meals that can be expected in each group. Clusters I and II are similar, containing mainly fruits and sandwiches. In cluster III, yoghurt-based meals seem to belong. However, even though the results are encouraging, it important to consider that the diversity in meal complexity in the evaluated dataset is quite low. Many of the recipes are variants of breakfast or snack meals such as fruits. Unfortunately, few dinner recipes could be included. This was due to a combined effect of few meal instances of each recipe in this category and difficulties in obtaining sufficiently clean data records for this meal type without interference from other meals. It remains to see whether more principal components will be revealed if a larger and more diverse recipe dataset is analysed, and if the number of significant clusters will increase.

Comparison to physiological models

In the physiological models, a complex interaction between the rate of appearance of glucose from the gut, hepatic down-regulation due to increased insulin and glucose levels, and peripheral glucose utilization form the postprandial response, see Figure 2.6 in Chapter 2. All these dynamic effects are lumped together in the impact parameters of the insulin action and the meal impact models. As noted in Chapter 4, this does not allow for a estimation of the glucose or insulin concentrations in different compartments of the body, but delivers a input-output characteristic with intuitive parameters. The gastric model described previously exhibits an interesting property of nonlinear gastric emptying, which is partly supported by tracer experiments. This property may be more exaggerated for larger meals, thus making the duration of the rate of appearance a function of the meal size. Generally the meal sizes in the trial was quite small (mean 317 kCal), and with moderate variability (CV 30%), with a few recipes (breakfast meals) repeating the same meal size for all meal instances, see Figure 6.14. A more systematic approach to ensure larger meal sizes, as well as larger variability, may be needed to investigate whether this effect is of clinical significance.

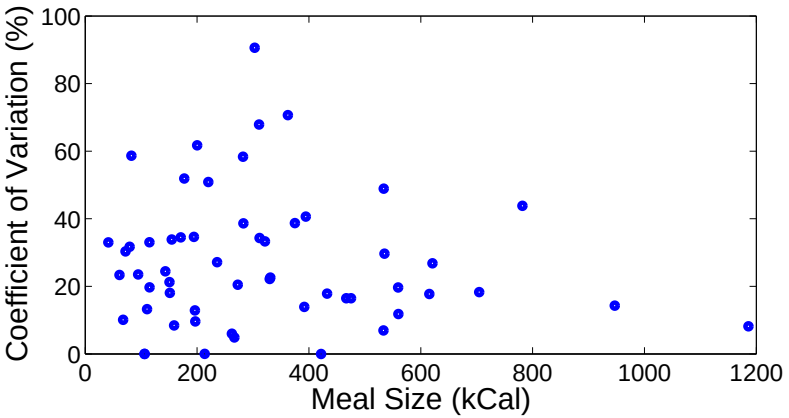

Figure 6.14 Average meal size and variation.

6.9 Conclusions

The understanding of how different meals affect the glucose level is yet at an early stage. Numerous studies have been conducted to establish the glycemic index of meals in healthy individuals and in NIDDM diabetes. In contrast, very few studies have systematically investigated the dynamic response of different meals in IDDM patients. Due to the lack of descriptive research in this area, and the shortage of better means, the concept of carbohydrate counting, and the underlying assumption of carbohydrates as the sole driver of glucose excursions, prevails. This is reflected in the bolus guides available in many insulin pumps, where carbohydrate to insulin ratios (CIR) may be used to calculate bolus doses. While different settings may be used at different times of the day, no discrimination is made between different meal types. However, interest in the matter grows, and several recent studies have indicated that the meal composition has a profound effect on the postprandial response, and that both fat and protein needs to be considered when determining bolus doses.

In this chapter, models of the glucose elevating impact of different meal recipes have been developed. The amount of carbohydrates in the meal is still used as an input, but since the effect is allowed to be different in-between recipes, no fixed CIR exists. Cross-validation shows that the models are able to reproduce the postprandial response with acceptable accuracy. The diversity in impact was sufficiently low for a low number of principal components to be identified, and clustering of the meal impacts showed that a majority of the recipes could be represented by as few as three clusters. While this may be an artefact of the low number of recipes investigated, the result

is encouraging as the impact of previously unseen recipes thereby could be reproduced from these components. More data, covering more recipes, are needed to investigate these interesting properties.

The outlined framework may be used in several ways to support the different layers of defence in depth in glucose management. The meal impacts can be used to rank different meals in terms of the extracted parameters of peak, duration and GEM, which may be useful in meal planning for both IDDM and NIDDM. Closed-loop systems, effectively covering all three layers, may benefit from the concept both in terms of meal models to incorporate into the algorithm, but also in a simulation environment. Here, new recipes may be created from the principal components, forming a test bed to test the closed-loop system disturbance rejection performance. Simulation may also prove useful as a educational tool for both clinicians and patients to help them better understand how different meals may effect the glucose level, and how different bolus schemes can be used to cover the impact. It may also be applied in a decision support for meal bolus dosing, allowing for the user to simulate the expected effect of a meal intake, and to receive suggestions on adequate bolus doses to reach, or maintain, normoglycemia in the postprandial phase. This aspect will be investigated in the next chapter.

6.A Summary of Estimated Meal Impact Data

Table 6.3 Summary of meal identification results. Recipe number (R#), Patient number (P#), Carbohydrates (C) [%], Protein (P) [%], Fat (F) [%], Calories (C) [kCal] Number of instances (NOI), Average record length (ARL), Peak Time (PT)[min], Duration (DT) [min], Glucose Elevating Magnitude (GEM) [mmol/(l·10 g)], Mean Absolute Relative Deviation, n hours (γ_{nh}) [%], Medtronic (M) and Dexcom (D).

R#	Recipe Name	P#	P	C	F	Cal	NOI	ARL	PT	DT	GEM	γ_{1h}	γ_{2h}	γ_{3h}	γ_{4h}
1	Breakfast	D1	19	55	26	422	5	184	40	125	1.7	9.5	9.4	N/A	N/A
2	Bread with pastry	D2	20	54	25	312	16	195	35	130	2.7	11.0	13.2	15.2	N/A
3	Candy	D2	3	93	4	362	8	133	170	> 270	2.3	12.4	11.9	N/A	N/A
4	Chocolate	D2	10	52	38	303	5	238	40	110	3.9	9.7	12.0	17.8	N/A
5	Wheat bread	D2	21	61	18	273	8	204	35	150	2.0	11.9	16.1	22.2	N/A
6	Pretzels	D2	12	80	7	159	5	225	40	235	2.0	9.1	12.6	11.1	N/A
7	Banana	D3	4	94	2	111	5	173	30	75	1.4	11.9	N/A	N/A	N/A
8	Modifast	D3	29	60	11	214	52	232	40	85	2.8	7.0	8.9	11.3	11.0
9	Cottage Cheese and fruit	D4	44	53	2	115	8	179	45	180	2.9	8.5	14.3	N/A	N/A
10	Milk	D4	37	51	12	72	5	215	40	125	3.4	14.9	18.1	N/A	N/A
11	Breakfast 1	D5	27	49	24	615	5	231	135	245	2.2	13.8	21.3	21.6	N/A
12	Breakfast 2	D5	29	47	24	560	13	246	35	185	2.6	8.2	14.7	18.7	26.7
13	Sandwich	D6	14	82	4	151	7	272	65	240	2.1	10.1	10.1	12.1	12.9
14	Pasta Bolognese	D7	27	58	15	621	5	180	45	85	0.5	5.5	N/A	N/A	N/A
15	Apple	D7	1	98	1	61	5	194	50	135	2.9	11.7	13.6	N/A	N/A
16	Banana	D7	4	94	2	95	6	159	50	130	2.2	12.1	15.1	N/A	N/A
17	Beer	D7	16	82	15	171	5	165	40	95	1.4	6.1	7.1	N/A	N/A
18	Coffee and chocolate	D11	15	51	33	143	6	205	40	195	3.9	10.5	15.8	N/A	N/A

Table 6.3 (continued)

R#	Recipe Name	P#	P	C	F	Cal	NOI	ARL	PT	DT	GEM	γ_{1h}	γ_{2h}	γ_{3h}	γ_{4h}
19	Nougat paste	D11	6	52	42	200	7	165	40	190	2.3	12.2	15.7	N/A	N/A
20	Sandwich	D11	30	38	31	196	6	163	40	165	3.8	4.5	6.8	N/A	N/A
21	Yoghurt and fruit	D11	19	43	38	321	18	162	40	250	2.4	7.4	12.3	12.3	11.8
22	Yoghurt, Fruit and sandwich	D11	28	33	39	535	7	195	85	215	4.3	11.1	12.1	12.9	N/A
23	Chocolate	D12	6	67	27	177	7	225	30	220	2.2	9.7	12.2	11.7	13.7
24	Yoghurt and Granula	D12	20	65	15	467	5	159	270	>270	2.5	6.6	14.8	N/A	N/A
25	Breakfast	M1	43	29	28	392	13	257	100	220	2.4	10.2	16.1	16.5	16.6
26	Banana	M2	4	94	2	106	5	252	35	140	2.7	14.4	13.9	14.8	17.7
27	Breakfast	M2	20	48	31	534	7	248	130	260	2.0	10.2	15.6	20.1	25.6
28	Cottage Cheese and Fruit	M2	41	38	21	197	5	250	45	135	3.0	12.0	18.3	22.0	30.7
29	Oatmeal Porridge	M2	11	83	6	262	10	171	40	180	1.9	11.6	15.3	N/A	N/A
30	Sandwich and milk	M3	30	57	13	395	11	201	35	>270	1.1	8.8	15.8	15.7	12.7
31	Omelette	M4	32	27	41	533	14	254	35	155	2.4	5.7	9.7	13.2	15.8
32	Breakfast	M4	24	42	34	267	11	264	30	185	2.0	7.3	10.6	14.4	16.6
33	Yoghurt and almonds	M4	27	29	44	947	5	275	75	245	1.9	8.4	13.0	14.1	14.5
34	Coffee with milk	M5	38	50	13	41	10	159	65	160	5.8	10.1	14.6	18.3	N/A
35	Sandwich	M5	26	58	17	236	9	168	55	170	1.4	14.1	21.1	N/A	N/A
36	Yoghurt and Granula	M5	21	72	7	330	5	263	25	250	1.5	16.1	19.1	19.2	16.4
37	Lentil Peanut Stew	M6	23	39	38	1186	5	197	175	>270	1.3	8.4	N/A	N/A	N/A
38	Oatmeal porridge and sandwich	M6	21	58	20	475	5	234	65	255	1.7	9.9	16.9	22.7	N/A

Table 6.3 (continued)

R#	Recipe Name	P#	P	C	F	Cal	NOI	ARL	PT	DT	GEM	γ_{1h}	γ_{2h}	γ_{3h}	γ_{4h}
39	Pasta and soy based sauce	M6	20	54	25	782	5	215	145	250	1.1	11.9	14.6	18.3	N/A
40	Sandwich	M6	15	52	33	282	5	211	115	255	2.9	11.5	16.9	N/A	N/A
41	Twix chocolate bar	M6	6	71	23	194	8	142	50	160	1.4	11.2	9.2	N/A	N/A
42	Sandwich	M7	27	52	21	311	16	209	50	140	2.0	8.0	11.6	13.9	18.4
43	Apple	M8	2	97	1	68	6	117	35	165	1.3	7.5	N/A	N/A	N/A
44	Oatmeal porridge	M8	15	77	8	151	8	195	35	90	1.8	13.0	16.5	16.1	N/A
45	Sandwich	M8	30	45	25	155	5	212	40	100	1.7	5.5	8.1	8.3	N/A
46	Candy	M9	4	93	3	220	5	208	35	180	1.2	13.0	16.5	15.8	N/A
47	Clementine	M9	6	92	2	82	9	242	40	210	2.5	15.1	24.2	27.4	N/A
48	Breakfast and Cortisone	M12	22	53	25	432	11	198	270	>270	1.2	7.1	12.6	14.8	N/A
49	Crisp bread	M13	28	24	48	560	6	223	95	>270	4.3	6.1	10.0	N/A	N/A
50	Banana	M13	4	94	2	106	5	140	45	135	1.8	8.7	N/A	N/A	N/A
51	Rye Bread	M13	24	58	18	331	6	227	40	180	0.8	9.6	11.0	12.9	N/A
52	Pasta with Tuna Sauce	M14	21	67	12	704	5	267	35	265	0.6	9.2	15.7	18.1	18.6
53	Apple	M14	1	98	1	79	10	221	35	85	1.3	7.1	9.0	9.1	10.3
54	Crisp bread	M14	6	85	9	375	7	237	35	> 270	0.9	15.3	18.0	24.8	25.5
55	Orange	M14	7	92	1	115	7	179	35	115	1.3	11.7	13.8	N/A	N/A
56	Sunflower bread	M14	17	58	24	283	17	213	170	255	1.6	6.9	11.3	14.7	15.4

7

Meal Bolus Optimization

7.1 Introduction

Every time a person with diabetes eats a meal, he/she is faced with the challenge of how much insulin to bolus. Meal bolusing is notoriously difficult, due to the complexity in assessing the contributing factors which may influence the postprandial response. Recognizing the effect of the meal at hand and determining the amount of food on the plate is just the beginning. While the postprandial response to the largest extent is determined by the glucose-elevating impact of the meal, the choice of basal and bolus insulin settings also contribute significantly to the ability to shape the glucose excursion. Additionally, changes in insulin efficacy and insulin basal requirement, together with recent basal, bolus and meal history have to be taken into account when determining an appropriate meal dose. Several studies have indicated the significant contribution of postprandial excursions to HbA1c and long-term complications [IDF, 2011]. This emphasizes the need to reduce any postprandial hyperglycemia, which is reflected in several of the postprandial recommendations found in the clinical guidelines. However, too strenuous efforts in this regard may prove counter-productive. Excessive limitations on postprandial hyperglycemia may result in overbolusing, which is a gateway to post-absorptive hypoglycemia, with subsequent hyperglycemia due to the counter-regulatory rebound response, and high glucose variability. Considering the above, in this chapter we address two questions;

1. What is the optimal combination of meal bolus and basal settings to counter the postprandial excursion produced by meal intake of a specific recipe?

2. Are the postprandial glucose targets, provided in recommendations by the leading diabetes organizations and medical associations, always achievable?

7.2 Current Technology and Research

Insulin Pumps and bolus alternatives

In most insulin pumps, the usual bolus dose is supplemented with dosing alternatives which involve temporary changes to the basal level as well. Temporary elevated basal level for a predefined period of time may be used instead (called square wave bolus or extended bolus), or together (dual wave, combo bolus), with a instantaneous bolus injection.

Bolus guides

The bolus guides available in many modern insulin pumps, glucose meters and smart-phone apps provide meal dose suggestions based on variants of the following calculation

$$D = \frac{G - G_R}{K_{ISR}} + \frac{M_C}{K_{CIR}} \tag{7.1}$$

where D is the suggested amount of insulin, G is the current glucose level, G_R is the target glucose level and M_C is the amount of carbohydrates in the meal. The Insulin Sensitivity Ratio K_{ISR} is recognized from Chapter 4, and the Carbohydrate-to-Insulin Ratio K_{CIR} describes how many grams of carbohydrates each unit of insulin is expected to cover, and was introduced in Chapter 6. So, the first term in Eq. (7.1) represents the correction boluses needed to correct an offset glucose level, and the second term the insulin required to cover the postprandial response of the meal. This is the simplest version, but sometimes the amount of remaining insulin from previous doses is subtracted before providing the suggested dose. The 100 rule, often used to determine K_{ISR}, has already been described in Chapter 4, and the corresponding 500 rule for K_{CIR} in Chapter 6. Usually, no distinction is made between different meal compositions, and the same K_{CIR} is used for all meal types, but sometimes different parameter settings are used in different time blocks of the day. No suggestions on changes to the basal level are provided. The clinical usefulness of bolus guides was reviewed in Chapter 4.

Research on optimal meal bolus dosing

Some clinical studies have investigated what type of bolus that is optimal to use for different meal types. In [Chase et al., 2002], a small study was conducted where participants on CSSI therapy digested a meal rich in carbohydrates, fat and calories (pizza, tiramisu and cola, 11% protein, 53% carbohydrates, 36% fat, 829 kCal) at four separate occasions. At each occasion, the same amount of insulin was administered, but using different methods; a single bolus, two separate bolus doses of equal size (the second after 90 minutes), an extended two hour bolus, or as a combination bolus (70% as

a bolus, 30% over two hours). The result favoured the combination bolus, which yielded significantly lower postprandial glucose values in comparison to the other bolus alternatives. Combination bolus (50% as bolus, 50% over two hours) was also successfully used for meals with low glycemic index in [O'Connell and Gilbertson, 2008]. Both the area under the glucose curve of the postprandial response and the risk of developing hypoglycemia were significantly lower when compared to normal bolus doses.

Few experimental studies can be found on open-loop bolus dosing using novel algorithms. Attempts to provide bolus suggestions based on a computer algorithm have been validated in [Rossetti et al., 2012], using a concept previously tested in simulation using the UVa/Padova simulator, see [Revert et al., 2011]. The study included 12 subjects on CSSI, who underwent four meal test over a period of six weeks. The algorithm is based on an interval method which can suggest different combinations of bolus doses and basal adjustments. A model with ten tunable parameters, put together by combining elements from different physiological models, was fitted to each patient [Laguna et al., 2010]. The parameters were re-estimated after half of the tests using three days of data. Compared to determining the bolus doses using fixed CIR, no significant improvement could be found. The Diabetes Insulin Guidance System (DIGS), using an non-disclosed heuristic algorithm, was shown to be able to significantly reduce mean glucose level in a trial with 38 patient with both T1DM and T2DM over a time period of 12 weeks [Bergenstal et al., 2012].

A scheme based on run-to-run control, was suggested in Owens and was later refined in [Palerm et al., 2007]. The concept is based on the assumption that the same meal type is digested every day and that conditions affecting, e.g., insulin sensitivity, remain unchanged or change gradually. The CIR is iteratively updated each day based on a performance metric derived from two postprandial SMBG measurements. In [Zisser et al., 2009], nine T1DM followed the protocol for six weeks, and after convergence of the meal doses, the one hour postprandial glucose value was significantly lower than before the trial. Data on increased or decreased incidence of hypoglycemia were not reported. While the assumption on static meal plans from day to day seem unrealistic, it may prove relevant to the breakfast meal for some people.

Previous simulation studies to investigate optimal open-loop meal bolus dosing have been conducted in [Roy and Parker, 2006c] and [Srinivasan et al., 2014]. In [Roy and Parker, 2006c], the extended minimal model incorporating free fatty acids dynamics from [Roy and Parker, 2006a], was used together with two variants of a rate of appearance model. Two artificial subjects were simulated, each eating a mixed meal (70 g carbohydrates, 18 g protein and 20 g fat). Each subject represented one of the two gastric models. Using a closed-loop MPC controller, optimal dosing was determined with insulin delivery profiles very similar to extended boluses with about 50 minutes

duration. Based on published data on glucose rate of appearance for different meals in healthy subjects, a library of parameters sets for the gastric model in [Dalla Man et al., 2006a] was identified in [Herrero et al., 2008]. This library was used in [Dassau et al., 2008], where it was combined with the full UVA/Padova simulation model to investigate different closed-loop set-ups in a small simulation study. The same modeling approach was used in [Srinivasan et al., 2014], where both closed- and open-loop bolus dosing were optimized for high, medium and low fat meals for an in-silico trial of ten adult subject. Each meal type was digested in three different quantities (equivalent to 50, 75 and 100 g of carbohydrates). For the open-loop dosing, which is of interest here, the following conclusions were drawn. For the small and medium sized low fat meals, a normal bolus administered 30 minutes before the meal is optimal. For the largest meal (100 g), an extended bolus for 15 minutes was the best choice. For the medium fat meals, a two hour extended bolus worked best for the small meal, whereas a divided dosing was suggested for the larger meals. Here, a combined bolus is dosed at the meal start with a short duration (10-30 min), and later another combined bolus is administered after 30-45 minutes. The same concept, with even a third combination bolus, was the suggested dosing strategy for high fat meals. Obviously, for practical concerns, such delivery patterns would have to be incorporated as possible dosing choices in a insulin pump to be practically feasible.

Pre- and postprandial glucose targets

To assist both clinicians and the patients directly, several non-governmental (NGO) and governmental organizations have issued guidelines on suitable targets for glycemic control. Here, we will specifically look at the targets for pre- and postmeal glucose. Mainly the large international organisations will be considered. However, national and local guidelines are probably more important when treatment targets are implemented. For this reason, some national and local guidelines were also considered in the review.

The International Diabetes Federation (IDF) states that the postprandial glucose level should seldom rise above 7.8 mmol/l (140 mg/dl). The recommendation is based on evidence that healthy individuals rarely have a postmeal glucose level above this limit. However, the guideline recognizes that this limit may be too low for insulin-treated diabetes due to the hypoglycemic risk. Based on this, a suitable upper limit was defined as 9 mmol/l (160 mg/dl), to be assessed by SMBG 1-2 hours after the meal [IDF, 2011].

The American Diabetes Association (ADA), suggests preprandial glucose levels between 3.9-7.2 mmol/l (70-130 mg/dl) and postprandial levels below 10 mmol/l (180 mg/dl)[American Diabetes Association, 2013]. (For pregnant women with T1DM the boundaries are extremely tight; preprandial 3.3-5-4 mmol/l (60-99 mg/dl) and postprandial 5.4-7.1 mmol/l (100-129 mg/dl).

Table 7.1 Premeal (PreM) and Postprandial (PPG) targets from different guidelines. Time since meal intake (Δ_T).

Organization	PreM target [mmol/l]	PPG target [mmol/l]	Δ_T
ADA	3.9-7.2	10	N/A
IDF	N/A	9	1-2 h
AACE	6.1	7.8	2 h
NICE	4-7	5-9	>1.5 h
SKL	4-6	6-8	2 h

(Pregnancy is a very specific condition, where extra-ordinary measures need to be taken, and will not be considered further in this thesis.) The guideline states that these goals may have to be altered on an individual basis depending on duration of diabetes, age/life expectancy, co-morbid conditions, known cardiovascular complications, hypoglycemic unawareness and other personal considerations.

The American Association of Clinical Endocrinologists (AACE) defines the premeal goal to 6.1 mmol/l (110 mg/dl) and the two hour postprandial level to below 7.8 mmol/l (140 mg/dl) [Handelsman et al., 2015].

In England, the National Institute for Health and Care Excellence (NICE) provides national guidance and advice to improve healthcare. In the guideline regarding blood glucose targets, the advises are a premeal level of 4-7 mmol/l (72-126 mg/dl), and a >90 min postprandial glucose level between 5-9 mmol/l [NICE guideline, 2015]. In Sweden, the Swedish Association of Local Authorities and Regions, a membership organization of the municipalities and county councils, have issued principals of care for T1DM [Nationella Programrådet Diabetes, 2014]. The pre- and postmeal targets are 4-6 mmol/l (72-108 mg/dl) and 6-8 mmol/l (108-145 mg/dl).

As can be seen from this review, there is somewhat of disparity among the recommendations, see Table 7.1, in terms of both pre- and postprandial levels, as well as when the upper postprandial limit should be enforced. While ADA has the highest level, no slack is given for any early but short hyperglycemic episodes. At the other end, the regional recommendations have the lowest target levels, but just like IDF and AACE, are more flexible during the first and second hour of the postprandial response. In the following, the PPG limits put forward by the ADA, IDF and AACE will be used as representatives of the various levels of conservatism in the recommendations. For the analysis, a strict interpretation of the boundary conditions according to Table 7.2 were employed and the premeal glucose level was set to 6 mmol/l. Additionally, an interpretation of that the premeal target should be fulfilled in the long run was also included. The function $T_{G_{th},t_{th}}(t)$ defines a gradually decreasing upper threshold after two hours to ensure that the glucose level

Table 7.2 Boundary conditions $\Omega_{(\cdot)}(G(t))$ used in the analysis of the PPG recommendations. Glucose level at time t ($G(t)$) [mmol/l], meal time (t_0) [hours].

Organization	PPG target
ADA	$\Omega_{ADA}(G(t)): \quad 4 < G(t) < T_{10,0}(t), \quad t > t_0$
IDF	$\Omega_{IDF}(G(t)): \begin{cases} G(t) > 4, & t < t_0 + 1, \\ 4 < G(t) < T_{9,1}(t), & t \geq t_0 + 1 \end{cases}$
AACE	$\Omega_{AACE}(G(t)): \begin{cases} G(t) > 4, & t < t_0 + 2, \\ 4 < G(t) < T_{8.7,2}(t), & t \geq t_0 + 2 \end{cases}$

stabilizes at an acceptable level no later than six hours after the meal start:

$$T_{G_{th},t_{th}}(t) = \begin{cases} G_{th}, & t_0 + 1 \leq t < t_0 + 2 \\ G_{th} - (G_{th} - 7) \cdot (t - t_0 - 2)/4, & t_0 + 2 \leq t \leq t_0 + 6 \\ 7, & t \geq t_0 + 6 \end{cases} \tag{7.2}$$

where G_{th} is the upper threshold given at t_{th} by each organisation.

7.3 PPG Constraint Analysis

To investigate the feasibility of the postprandial constraints, the following procedure was used. For every recipe listed in Appendix 6.9, the limiting meal size that could be digested without violating the constraints, using an optimized bolus dose, was calculated. The procedure to calculate the doses is described below.

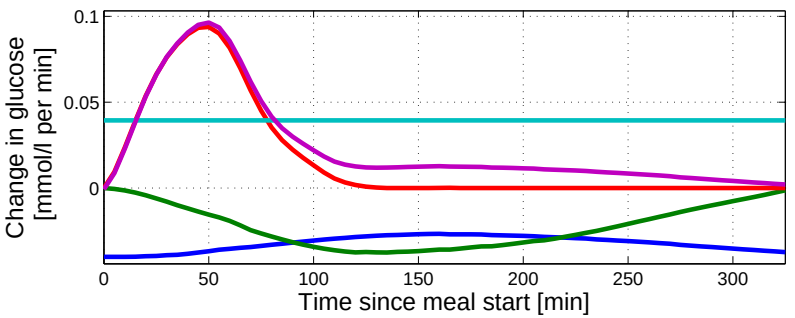

Figure 7.1 The effect of a superbolus. The reduced basal dose increases the glucose elevating effect that the bolus dose has to counter after the meal impact peak. Effect of bolus dose (green line), basal dose (blue line), EGB (turquoise line), meal impact (red line), combined effect of meal impact + EGB - basal dose (purple line).

In [Goodwin et al., 2015], an analysis of the limitations in fulfilling output constraints in linear positive systems, where the effect of both the disturbance and the control signal are modeled as finite impulse response model, is given. Specifically, modeling of glucose dynamics and the question of suitable meal bolus doses to achieve postprandial excursions within predefined boundaries is presented as a possible application. However, the insulin model suggested here has glucose-dependent impulse parameters, thereby violating the necessary prerequisites for the results to be applicable. Instead, a constraint analysis was conducted using optimization, with constraint on $G(t)$ according to Table 7.2. Premeal glucose was assumed to be 6 mmol/l. A lower premeal value can neither be considered realistic nor desirable. Having a premeal value close, or even on the border, to hypoglycemia, puts the patient at unnecessary risk. The bolus is administered at the meal time using a combined bolus. A combined bolus consists of a meal bolus given at the meal start, and a temporary constantly elevated or reduced basal dose for a predefined time period. This concept includes the extended bolus and the superbolus as two extreme cases, and the normal bolus as the nominal case (keeping the basal level as is). The extended bolus is a combined bolus where the meal bolus has been eliminated, but with a temporary elevated basal dose for a predefined time period, starting at the time of the meal. This is useful for meals with a very prolonged and peakless meal impact. Contrary, the superbolus idea is to shut off the basal dose at the same time as the bolus dose is given [Walsh and Roberts, 2012]. The basal is thereafter kept off for a predefined period of time. The superbolus effectively adds bulk to the meal impact, with maximum contribution some time after the basal dose is restarted. Most meal impacts have a peak much earlier (around 40 minutes, see Chapter 6) than the insulin action (around 110 minutes, see Chapter 4). The added glucose elevating effect of the absent basal dose has softening effect on post-peak glucose drop, when the insulin action dominates the meal impact, and reduces the tendency to hypoglycemia, see Figure 7.1. Thereby, larger bolus doses may be administered to trim the peak of the response. Three different time periods will be investigated (one, two and three hours). The endogenous balance EGB was set to the average value retrieved from the estimation in Chapter 6 and the basal level was selected to match this in stationarity.

The doses and meal size are given by the following optimization problem where the maximum meal size (and associated insulin dosage) is sought that will generate a postprandial response during the next T_{dur} hours that will not violate predefined constraints:

$$\{I_B, I_L\} = \arg\min_{I_B, I_L} -M_r \tag{7.3}$$

subject to

$$\begin{aligned} -I_B &\leq 0 \\ -I_L &\leq 0 \\ \Omega_{(\cdot)}(G(t)), &\quad t \geq t_0 \end{aligned} \tag{7.4}$$

where I_B is the meal bolus dose, $I_{L,T}$ is the temporary basal dose for T hours, and M_r is the meal size of recipe r digested at time t_0, and where the postprandial response of $G(t)$ is given by

$$\begin{aligned} G(t_k) = G(t_{k-1}) + \sum_{i=0}^{n} a_i (y(t_k) I(t_{k-i}) \\ + \sum_{i=0}^{m} b^r_{k-i+1} M_r + G_b, \quad G(t_0) = 6.0, \quad t_0 \leq t_k \leq t_0 + T_{dur} \end{aligned} \tag{7.5}$$

which is recognized from Eq. (6.7) in Chapter 6, but with the insulin action multiplier fixed to 1. The problem is non-convex due to the glucose dependence of the insulin action parameters. However, a convex solution may be obtained by using the average insulin action parameters. This solution can thereafter be used as a starting point in the above optimization. Results where $I_{L,T}$ is practically zero will be reported as superboluses.

The possibility to achieve a good postprandial response thus depends on three factors; the shape of the meal impact, the shape of the insulin action and the EGB level that the basal insulin needs to cover. The better the meal impact and the insulin action curves matches, the flatter the postprandial response. A large EGB, requiring a high level of basal dose, implies increased possibility to 'shape' the meal impact of rapid meals in a favourable manner to better correspond to the insulin impact. In the analysis above, the combinations of these effects depends on what recipes each patient has been eating. However, from the results in Chapter 6, we learnt that the base meals defined by the cluster centres corresponds to more than 67% of the recipes, and covers both fast and more slowly digested meals. Therefore, to get a fuller picture, the limiting meal size for the cluster mean meals was also calculated for each patient assuming a glucose elevating magnitude of 2 mmol/l per 10 grams of carbohydrates.

7.4 Results

The three sets of postprandial constraints were evaluated for every recipe listed in Appendix 6.9 using one, two and three hours time period for temporarily manipulated basal dose. The three hour duration gave the best results and is reported below.

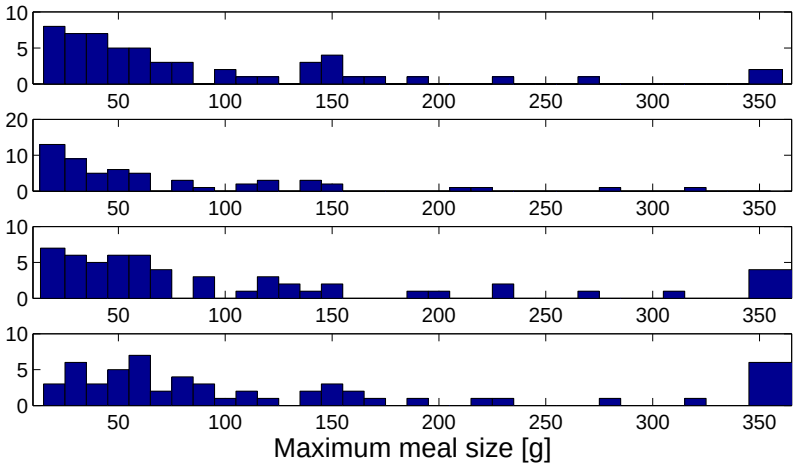

Figure 7.2 Distribution of maximum meal sizes for the recipes from Appendix 6.A enforcing the different sets of constraints. First plot: ADA, Second plot: IDF, Third plot: AACE, Fourth plot: ADA/AACE. Number of recipes on the y-axis.

The maximum meal size allowed without violating the boundaries differed a lot between the different recipes, see Figure 7.2. The different constraint sets also produced somewhat different outcomes, with the IDF requirements being the strictest (medians: Ω_{ADA} 57 g, Ω_{IDF} 46 g and Ω_{AACE} 62 g). For almost all recipes, the optimization resulted in superboluses, with a few exception for recipes which have extremely long durations. Most of these had about half the dose in the form of an elevated basal level, but noteworthy is number 39 (Pasta and soy-based sauce) with a combination dose almost equivalent to a normal bolus dose with untouched basal dose. All the investigated requirements resulted in extremely low meal sizes for some recipes, due to the very low acceptance for even the slightest hyperglycemia in the strict interpretation of the constraints.

Combining the ADA guideline setpoint of 10 mmol/l and the two hour mark of the AACE guideline, a somewhat more realistic hyperglycemic constraint set (ADA/AACE) can be defined. Rerunning the optimization with these constraints yielded somewhat more moderate results (median 78 g), see bottom plot in Figure 7.2, but still with low meal sizes for rapidly absorbed meals (see Figure 7.3 for an example). The base meal impact models retrieved from the cluster analysis in Chapter 6 were tested on every patient against this new set of constraints. The two fastest base meal impacts ($\mathbf{b_I}$ and $\mathbf{b_{III}}$) gave very similar results, and only results for $\mathbf{b_I}$ will be presented (see Figure 7.4). Also here, the spread in results was large, due to the inter-personal

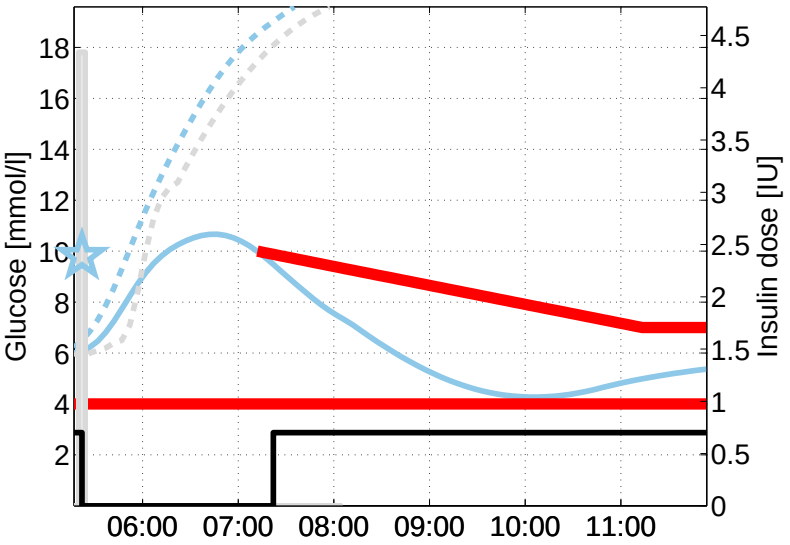

Figure 7.3 Example of the effect of an optimized bolus dose. The postprandial response of the true dose (grey dashed line) chosen by the patient clearly violates the upper threshold for this meal instance. The model is able to reproduce the outcome with a slight bias (light blue dashed line). With the optimized dose, the modified ADA/AACE thresholds (red lines) are barely cleared at the two and five hour marks (light blue solid line). The meal size is slightly lower than the estimated maximum. The star indicates the meal time, the grey bar the bolus dose and the solid black line the basal level. Recipe nr 2, Patient D2.

differences in the shape of the insulin action. Unfortunately, the number of patients is too low for clustering analysis, but results for representative slow, medium and fast insulin action are found in Table 7.3.

Table 7.3 Maximum meal size (gram) possible to digest without violating the relaxed ADA/AACE postprandial recommendations.

Type of Insulin Action	Fast Meal (b_I)	Slow Meal (b_{II})
Fast	80	200
Medium	60	140
Slow	40	70

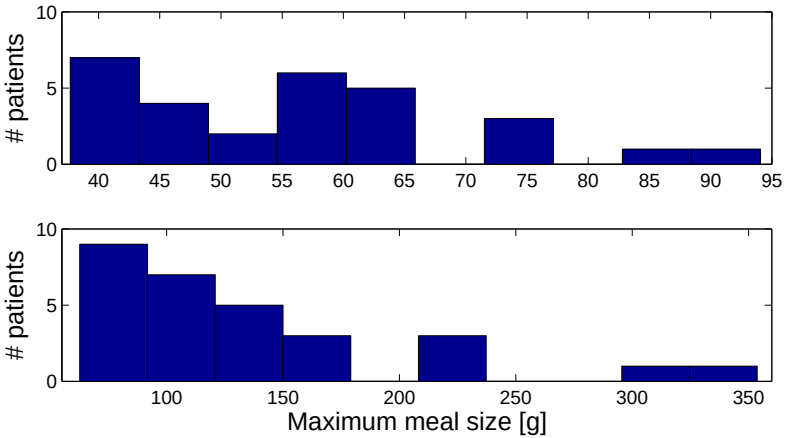

Figure 7.4 Distribution of maximum meal sizes for the fast base meal b_I (upper plot), and the slow base meal b_{II} (lower plot).

7.5 Discussion

For almost all recipes investigated, including the base recipes, the superbolus was most successful in maximizing the meal size without breaking any of the constraints. For a few recipes, a combination bolus was a better choice. These recipes did not belong to any of the identified clusters, which stresses that more meal data, with a wider selection of recipes, are required to get a fuller picture of the diversity in meal impact. Comparing the calculated maximum meal sizes to the actual meal sizes shows that many estimated maximum meal sizes lie very close to the actual meal sizes. Indeed, this is supported by the fact that most meal instance do not fulfil the postprandial constraints (less than 19%, 13%, 14% and 23% for the ADA, IDF, AACE and the ADA/AACE constraints). However, for four recipes, the actual meal size, that still fulfilled the constraints, was larger than the estimated maximum. It is relevant to consider that the records were truncated after at most 4.5 hours, and thus that hypoglycemic threshold may have been breached beyond this time point. Additionally, residual insulin from earlier meal or correction may have contributed to reducing the peak of the postprandial response, and differences in basal dose and EGB may contribute. Furthermore, the identification of the meal impacts in Chapter 6 revealed that the variability in postprandial response was large close to the two hour mark, which may also explain why some meal instances managed to slip under the threshold. Bearing this in mind, the estimated meal sizes should not be regarded as absolute bounds, but rather as indicators of the magnitude. Still, it is clear that these constraints are too conservative for many rapidly absorbed

meals. This is especially exaggerated when the insulin action is slower than normal, as the analysis of the base meal impacts on the entire patient cohort confirmed.

While these results are interesting in terms of what kind of postprandial response that may be achieved in an ideal setting, it is important to remember that real-world meal bolusing is more complex. Here, remaining insulin from previous doses or shifts in the basal dose level often have to be considered. Additionally, remaining meal impact from previous meals, as well as the need for correction doses to adjust for hyperglycemia or even delayed bolus dosing due to an impeding hypoglycemia must also be factored in. As noted above, some of these conditions may contribute in a positive manner to the postprandial glycemia, whereas others do not. However, it should also be recognized that most meals are more densely spaced than for the entire postprandial and post-absorptive states to be fully realized without a new meal impact. Thereby, bolus doses that would otherwise lead to late hypoglycemia may be countered by the new meal. This implies that larger bolus doses may be applicable, at least for breakfast and lunches, when subsequent meals can be expected. For dinner meals it may be more important to consider the entire response though.

Sometimes it is suggested that the bolus dose should be given 15-30 minutes before the meal [Cobry et al., 2010; Luijf et al., 2010; Srinivasan et al., 2014]. This may be an aggressive strategy to deal with rapid meal types, but carries a hypoglyceimc risk in the event of delayed or altogether absent meal intake due to unforeseen circumstances, that should not be underestimated.

The results indicate that over-stressing the hyperglycemic peak may be counter-productive for some patients, and possibly instigate large correction boluses as the patient aims at achieving an unreachable target. This generates a lot of late downward pressure and may produce a hypoglycemic event many hours later. This is especially worrisome for the dinner boluses, with the subsequent risk of nocturnal hypoglycemia. As noted in Chapter 6, few recipes belonged to the dinner category. More data is thus needed to understand the implications for dinner recipes.

Considering the above, it may also be appropriate to define different recommendations for the breakfast, lunch and dinner meals. However, in the end, the fundamental limitation boils down to the mismatch between the meal and insulin impact dynamics. Novel ultra-fast insulins under development may hopefully resolve this issue [Heinemann and Muchmore, 2012].

7.6 Conclusions

In this chapter, the postprandial recommendations set forward by the ADA, IDF and AACE were investigated, using the meal impact models and the base

meal impact models estimated in Chapter 6. The maximum possible meal size allowed without violating the postprandial constraints derived from the recommendations were calculated. The results show that these recommendations may be unrealistic for meal with rapid meal impacts, especially for persons with slower insulin action. This makes it apparent that not all individuals can reach the postprandial goals on any diet, regardless of how optimal their bolus doses are. For patients with delayed insulin action, the current postprandial recommendations may prove counter-productive and harmful. In these cases, attention to how rapid the onset of the glucose elevating response is for different meals is probably more important. These meal types may need to be consumed in smaller quantities, or over a longer time span, to avoid excessive hyperglycemia. Even though the results on the feasibility of the postprandial constraints are based on simulations, these results could be an interesting starting point for a discussion among clinicians regarding reasonable postprandial recommendations. The results also give an indication on what type of bolus dose is most favourable for different types of meals, which may be used in a bolus decision support system. Both these aspects may thereby support the fist level of a defence in depth strategy. Further studies, allowing for intervention with calculated bolus doses, need to be undertaken to confirm these results.

7.A Summary of Postprandial Constraint Analysis

Table 7.4 Results from the postprandial constraint analysis for all the recipes where a meal impact has been identified. Actual meal size (mean±std) M_{act} in the meal instances for this recipe, maximum meal size allowed for the ADA, IDF, AACE and combined ADA/AACE requirements M_{ADA}, M_{IDF}, M_{AACE} and $M_{ADA/AACE}$, all in grams of carbohydrates. A star next to the meal size indicates that a combination bolus was used, otherwise a superbolus was employed.

Recipe #	M_{act}	M_{ADA}	M_{IDF}	M_{AACE}	$M_{ADA/AACE}$
1	44 ± 0	37	29	40	49
2	32 ± 23	27	21	24	31
3	80 ± 56	100	76	187	219
4	27 ± 24	17	13	19	24
5	33 ± 1	41	32	35	45
6	28 ± 2	43	34	46	59
7	24 ± 3	38	30	55	73
8	28 ± 0	21	16	28	36
9	14 ± 5	24	19	26	33
10	8 ± 2	18	14	18	24
11	57 ± 9	167	139	1064*	1156*
12	50 ± 9	105	83	154	186
13	28 ± 6	80	64	68	87
14	67 ± 30	106	83	122	165
15	14 ± 3	24	19	22	31
16	21 ± 5	28	22	28	37
17	13 ± 8	40	32	46	62
18	13 ± 3	47	34	41	51
19	17 ± 11	43	34	52	64
20	13 ± 3	29	23	28	35
21	23 ± 11	71	55	112*	140*
22	29 ± 8	58	48	47	60
23	22 ± 12	76	62	94	115
24	63 ± 8	73*	60*	62*	78*
25	19 ± 11	59	49	47	58
26	23 ± 0	21	16	24	31
27	46 ± 23	228	209	197	228
28	15 ± 4	22	18	21	27
29	48 ± 4	46	36	74	95
30	35 ± 5	191	148	267	317
31	24 ± 5	28	22	34	44

Table 7.4 (continued)

Recipe #	M_{act}	M_{ADA}	M_{IDF}	M_{AACE}	$M_{ADA/AACE}$
32	20 ± 3	34	26	48	61
33	43 ± 7	141	124	119	141
34	4 ± 2	16	13	14	17
35	28 ± 8	56	45	58	74
36	54 ± 13	146	120	121	146
37	76 ± 14	151*	139*	135*	151*
38	53 ± 5	137	110	133	173
39	80 ± 33	351*	321*	312*	351*
40	26 ± 16	143	114	229	600
41	27 ± 9	65	53	74	94
42	32 ± 10	48	38	43	56
43	15 ± 2	48	37	64	79
44	25 ± 7	32	25	38	48
45	13 ± 3	34	27	40	50
46	48 ± 25	76	60	94	118
47	17 ± 10	63	50	89	106
48	44 ± 9	152*	139*	135*	152*
49	20 ± 5	164*	154*	151*	164*
50	23 ± 0	60	49	73	90
51	39 ± 6	118	94	350	427
52	100 ± 25	361	283	404	490
53	18 ± 6	43	34	62	78
54	71 ± 27	148	118	226*	279*
55	24 ± 8	50	39	60	76
56	31 ± 17	272	225	497	532*

8

Sensor Lag Compensation

Predicting the glucose level in a real-time setting means relying on CGM data. In previous chapters, the delay between the blood glucose and the measured interstitial glucose level was ignored, and the CGM signal was used as a proxy for blood glucose. This is the most common way of glucose modeling and prediction, and applies to all the models listed in Chapter 2. However, in many cases there is a significant lag between the interstitial glucose and the blood glucose due to physiological and sensor dynamics [Keenan et al., 2009]. Ignoring this delay in the modeling implies corresponding delays in the prediction, an aspect of special importance during falling glucose levels and impending hypoglycemia, when an hypoglycemic alarm, based on the prediction, could warn the patient and instigate corrective actions. For an assessment of the delay between these signals in the data at hand, see Chapter 3.

The capillary and sensor characteristics of the finger-stick measurement sensors are, in this context negligible, and are generally disregarded (and the delay is indicated to be small [Dye et al., 2010]). In this chapter, the GIIM, M_1 in Figure 8.1, and the interstitial and sensor dynamics (here treated as one model M_2, see [Boyne et al., 2003] for a brief discussion on the contribution of each term to the delay) are identified separately, and thereafter merged together into one single grey-box model. Using an observer, the blood glucose evolution is predicted ahead, based on the raw sensor output.

The interstitial and CGM sensor dynamics have been investigated assuming a first-order diffusion model in [Kovatchev et al., 2006] and [Facchinetti et al., 2007]. In [Facchinetti et al., 2007], the blood glucose level was recovered from the CGM signal using deconvolution, and in [Bequette, 2004] an early attempt at observer-based estimation was presented. In [Leal et al., 2010] a third order Box-Jenkins model was used to estimate the glucose level from the raw sensor signal. However, so far (to the best of the author's knowledge) no attempts have been made on merging modesl of glucose-insulin interaction and sensor dynamics together for the purpose of blood glucose prediction.

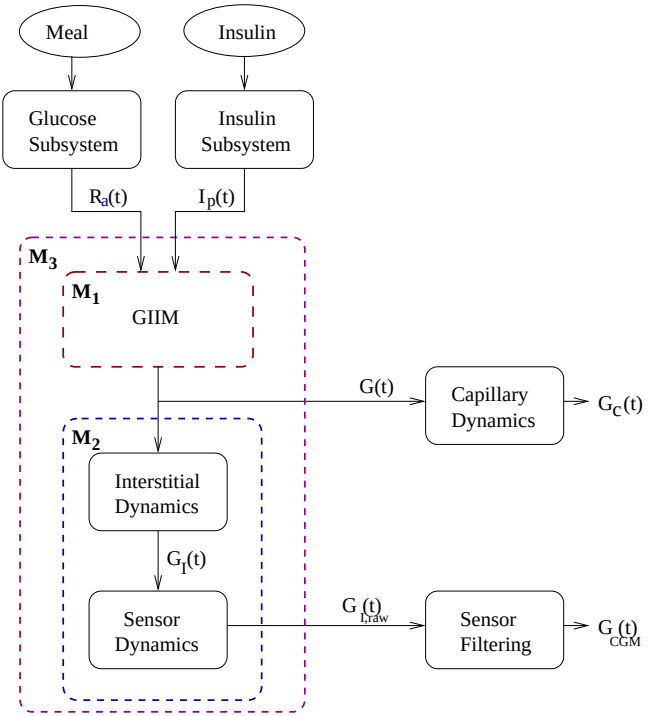

Figure 8.1 Overview of the modeling approach. Notation: Plasma Insulin $I_p(t)$, Rate of glucose appearance following a meal $R_a(t)$, Blood glucose $G(t)$, Capillary glucose $G_C(t)$, Interstitial Glucose $G_I(t)$, CGM raw current signal $G_{I,raw}(t)$ and CGM signal $G_{CGM}(t)$. M_1 represent the model describing the glucose-insulin interaction in the blood and inner organs (GIIM), the M_2 model represents the diffusion-like relationship between blood and interstitial glucose and the CGM sensor dynamics, and M_3 is the joint model of M_1 and M_2.

8.1 Data and Methods

Data

Based on the assessment of blood-to-interstitial delay in Chapter 3 and data completeness, one patient was chosen from the hospitalized part of the DAQ dataset. The dataset covers three consecutive days. In order to show significant results, a patient with large lag was chosen (patient 107 from Montpellier). The HemoCue measurements were interpolated using a shape preserving spline interpolation method (pchip in Matlab [MathWorks, 2012]) to retrieve an equidistant sampled signal $G(t)$ with sampling period 5 minutes.

Apart from the $G_{CGM}(t)$ signal (10 min sampling rate), an intermediate

signal $G_{I,raw}(t)$ from the glucose sensor was collected (1 min sample rate). The signal, corresponding to the electrical current measured by the sensor, was normalized to the same amplitude as the blood glucose data and resampled to a 5-minute basis, and was used in the identification instead of the CGM signal $G_{CGM}(t)$.

Insulin and Glucose Sub Models

The Insulin Sub Model (ISM) was based on the compartment model in [Dalla Man et al., 2007b] and [Dalla Man et al., 2007a], see Chapter 4. The parameters m_2, m_3, m_4 are determined based on steady-state assumptions—relating them to the constants in Table 8.1 and the body weight M_{BW}. Only rapid-acting insulins were considered. This means that the dynamics of the basal doses of the MDI patients were not included in the insulin signal. To represent the glucose flux following digestion, the compartment model in [Dalla Man et al., 2006a], described in Chapter 6, was used. The model equations are reproduced here for convenience. Please see Chapters 4 and 6 for notation and descriptions.

$$\begin{aligned}
\dot{I}_{sc1}(t) &= -(k_{a1} + k_d) \cdot I_{sc1}(t) + D(t) \\
\dot{I}_{sc2}(t) &= k_d \cdot I_{sc1}(t) - k_{a2} \cdot I_{sc2}(t) \\
\dot{I}_p(t) &= k_{a1} \cdot I_{sc1}(t) + k_{a2} \cdot I_{sc2}(t) - (m_2 + m_4) \cdot I_p(t) + m_1 \cdot I_l(t) \\
q_{sto}(t) &= q_{sto1}(t) + q_{sto2}(t) \\
\dot{q}_{sto1}(t) &= -k_{gri} \cdot q_{sto1}(t) + C(t) \\
\dot{q}_{sto2}(t) &= k_{gri} \cdot q_{sto1}(t) - k_{empt}(q_{sto}(t)) \cdot q_{sto2}(t) \\
\dot{q}_{gut}(t) &= -k_{abs} \cdot q_{gut}(t) + k_{empt}(q_{sto}(t)) \cdot q_{sto2}(t) \\
R_a(t) &= \frac{f \cdot k_{abs} \cdot q_{gut}(t)}{M_{BW}}
\end{aligned} \tag{8.1}$$

Both models were evaluated using generic population parameter values according to Table 8.1.

GIIM modeling - M1

Denoting the blood glucose $G(t_k)$, at sampling time t_k, with $y(k)$, and the raw CGM signal $G_{I,raw}(t_k)$ with $z(k)$:

$$\gamma(k) = \begin{bmatrix} y(k) \\ z(k) \end{bmatrix} = \begin{bmatrix} G(t_k) \\ G_{I,raw}(t_k) \end{bmatrix} \tag{8.2}$$

and the filtered inputs $u_k = [I_p(k) \quad R_a(k)]^T$ from the insulin and glucose sub models, the GIIM is modeled with a discrete-time state space model $\mathbf{M_1}$.

$$\begin{aligned}
x(k+1) &= A_1 x(k) + B_1 u(k) + \omega(k) \\
y(k) &= C_1 x(k) + \upsilon(k)
\end{aligned} \tag{8.3}$$

Table 8.1 Generic parameter values used for the GSM and ISM.

Parameter	Value	Unit
$\mathbf{k_{gri}}$	0.0558	[min^{-1}]
$\mathbf{k_{max}}$	0.0558	[min^{-1}]
$\mathbf{k_{min}}$	0.008	[min^{-1}]
$\mathbf{k_{abs}}$	0.0568	[min^{-1}]
$\mathbf{b}$	0.82	[-]
$\mathbf{d}$	0.01	[-]
$\mathbf{f}$	0.9	[-]

Parameter	Value	Unit
$\mathbf{k_{a1}}$	0.004	[min^{-1}]
$\mathbf{k_{a2}}$	0.0182	[min^{-1}]
$\mathbf{k_d}$	0.0164	[min^{-1}]
$\mathbf{k_d}$	0.0164	[min^{-1}]
$\mathbf{m_1}$	0.1766	[min^{-1}]
$\mathbf{V_i}$	0.05	[L/kg]
$\mathbf{C_L}$	1.1069	[L/min]

where $x(k) \in \mathbb{R}^n$ is the state vector and ω is process noise and υ is the finger-stick measurements noise with covariances:

$$E\Big\{ \begin{pmatrix} \omega \\ \upsilon \end{pmatrix} \begin{pmatrix} \omega \\ \upsilon \end{pmatrix}^T \Big\} = \begin{bmatrix} Q_1 & 0 \\ 0 & R_1 \end{bmatrix} \tag{8.4}$$

The model order was determined using the Akaike criterion [Johansson, 2009].

Interstitial and sensor model - M2

The dynamics between blood glucose y and interstitial glucose z, as measured by the sensor, was modeled as an ARX process.

$$A(z) \cdot z(k) = B(z) \cdot y(k-d) + e(k) \tag{8.5}$$

where A, B are polynomials of the zero-order-hold operator z, d is a delay, and $e(k)$ is the CGM measurement noise, with evaluated model orders $n_A = [1-2]$, $n_B = [1-2]$ and $d = [1-4]$ determined using the MDL criterion [Johansson, 2009]. The choice of evaluated model orders covers the compartment model suggested in [Rebrin and Steil, 2000].

Model merging - M3

Converting the sensor ARX model into a state-space model $\mathbf{M_2}$: $\{A_2, B_2, C_2\}$ with process and measurement noises Q_2 and R_2, the GIIM and sensor models are merged into one model $\mathbf{M_3}$: $\{A_3, B_3, C_3\}$, with the

augmented state vector ξ and the output γ.

$$
\begin{aligned}
A_3 &= \begin{bmatrix} A_1 & 0_{[n_{A_1} \times n_{A_2}]} \\ B_2 \cdot C_1 & A_2 \end{bmatrix}, \quad B_3 = \begin{bmatrix} B_1 \\ 0_{[n_{A_2} \times 2]} \end{bmatrix} \\
C_3 &= \begin{bmatrix} C_{31} \\ C_{32} \end{bmatrix} = \begin{bmatrix} C_1 & 0_{[1 \times n_{C_2}]} \\ 0_{[1 \times n_{C_1}]} & C_2 \end{bmatrix} \\
Q_3 &= \begin{bmatrix} Q_1 & 0_{[n_{Q_1} \times n_{Q_2}]} \\ 0_{[n_{Q_2} \times n_{Q_1}]} & Q_2 \end{bmatrix} \\
R_3 &= \begin{bmatrix} R_1 & 0_{[n_{R_1} \times n_{R_2}]} \\ 0_{[n_{R_2} \times n_{R_1}]} & R_2 \end{bmatrix}
\end{aligned}
\tag{8.6}
$$

State estimation and sensor fusion

Data is available at different rates from the two measurement devices, and at least from the finger-stick measurements, in a non-equidistant manner. Thus, combinatorially there are 3 (4) possibilities; (1) data from both, (2) Data from HemoCue and (3) Data from the CGM sensor, ((4) No data). This calls for a time-varying system of switched dynamics. The boolean variables δ_1 and δ_2 are used to keep track of which signal is present in the feedback, and the new system becomes:

$$
\begin{aligned}
\hat{\xi}(k+1) &= A_3\hat{\xi}(k) + K(\gamma(k) - C_3\hat{\xi}(k)) \\
\hat{\gamma}(k) &= \begin{bmatrix} \delta_1 & 0 \\ 0 & \delta_2 \end{bmatrix} C_3\hat{\xi}(k)
\end{aligned}
\tag{8.7}
$$

where the time-varying Kalman gain K depends on the unknown covariance of the process noise Q and measurement noises R_1 and R_2. The accuracy of the finger-stick HemoCue glucose monitor [HemoCue Glucose 201+ Analyzer, 2012] has been studied in [Stork et al., 2005], which indicated a standard deviation in the area of 10-15 mg/dl when compared to a state of the art laboratory device (Yellow Spring Instrument [Yellow Springs Instrument, 2012]). The study indicates a linear relationship between noise and glucose level, which is common for glucose meters. No information on the measurement noise of the relatively new Abbott CGM system [Abbott Freestyle Navigator, 2015] has been found, but a standard deviation of 20 mg/dl is not an unrealistic assumption (compare to the BG-CGM deviation in Chapter 3). Also for CGM systems, a proportional increase in noise level to the glucose level is found. Current evaluation methods to assess the performance of CGM systems are based on comparing the CGM signal to a blood glucose reference. As the previous discussion shows, the signal-to-reference deviation incorporates deviation due to the time lag between the signals and does not accurately capture the stochastic variation in the CGM signal. Recent developments in CGM error assessment aim to quantify these

error dynamics, but do not address the estimate of CGM variation per se [Clarke and Kovatchev, 2009]. In this thesis, the initial guess for noise level standard deviation was chosen to correspond to 15 mg/dl for the HemoCue device and 20 mg/dl for Abbott CGM. The measurement errors were considered to be uncorrelated. Given the initial guesses $\hat{Q}_0$ and $\hat{R}_0$, Q and R can be iteratively estimated by first calculating the state estimation sequence $\hat{\Xi}_N = [\hat{\xi}_1 \dots \hat{\xi}_N]$ and the estimation error sequence $\hat{W}_N = [\hat{w}_1 \dots \hat{w}_N]$ from the estimation data $\{Y_N, U_N, \hat{\Xi}_0\}$ [Johansson, 2009].

$$\begin{aligned} \hat{\Xi}_{N+1} &= A\,\hat{\Xi}_N + B\,U_N + K(Y_N - C\,\hat{\Xi}_N) \\ \hat{W}_N &= C\,\hat{\Xi}_N - Y_N \end{aligned} \tag{8.8}$$

Thereafter the covariance estimates

$$S = E\{(\hat{\xi} - \xi)\,(\hat{\xi} - \xi)^T\}, \quad R = E\{\hat{w}\hat{w}^T\} \tag{8.9}$$

are determined. Given that the sequence is stationary, we get:

$$\lim_{N\to\infty} S_N = S \tag{8.10}$$

and

$$\lim_{N\to\infty} R_N = R \tag{8.11}$$

Now $\{A, B, C\}$ may be re-estimated by recognizing that

$$\begin{aligned} \hat{\xi}_{k+1} &= (A - KC)\hat{\xi}_k + [B \quad K][u_k^T \quad \gamma_k^T] \\ \hat{w}_k - \gamma_k &= -C\hat{\xi}_k \end{aligned} \tag{8.12}$$

Finally,

$$\begin{aligned} \hat{Q} &= S_N - A\,S_N\,A^T - K\,R_N\,K^T \\ \hat{R} &= C\,S_N\,C^T - R_N \end{aligned} \tag{8.13}$$

Note that this computation may result in sign-indefinite solutions [Johansson, 2009].

Estimation and validation

The overnight data between the first and the second day were used together with breakfast meal data from the second day for estimation. It was decided to use overnight data together with meal data, in order to have a dataset with sufficient excitation. Using meal data alone is problematic, since both inputs act simultaneously during these circumstances. An assessment of the importance of input excitation to identification using simulated diabetic datasets was made in [Finan et al., 2009]. The first and third days' breakfasts were used

for cross-validation. Additionally, to challenge the predictor, all HemoCue measurements were removed from the validation datasets. To evaluate the predictive performance of the model, 20, 40 and 60 minute predictions were considered. The correspondence to the reference HemoCue measurements were assessed using the Clarke Pointwise Error Grid Analysis (p-CGA), see Chapter 3, RMSE and maximum absolute error. The performance was compared to the CGM signal's ability to reproduce the blood glucose.

8.2 Results

First, the GIIM M_1 was identified. Using the interpolated HemoCue data and the meal and insulin sub models to retrieve the filtered inputs, a second-order state-space model was identified using the N4SID command of the System Identification Toolbox in Matlab [MathWorks, 2012]. The model was stable and responded qualitatively correctly to input (not shown). The interstitial mode M_2 was thereafter identified from the interpolated blood glucose data G and the raw CGM signal $G_{I,raw}$. The model order chosen according to the MDL criteria was $n_A = 2$, $n_B = 1$ and $d = 1$. Converting the M_2 model to state space format, the merged model M_3 was retrieved.

Since only CGM data were available in the validation data ($\delta_1 = 0$), the system became time-invariant and a stationary Kalman filter was designed.

Using the initial guess for Q and R produced noisy predictions. The attempt to estimate the noise characteristics from the estimation data broke down into non-positive definite covariance matrices. Instead, Q and R were heuristically chosen as user parameters to strike a sound balance between signal smoothness and responsiveness to model-to-feedback mismatch.

In Figure 8.2, the 20, 40 and 60 minutes predictions together with normalized $G_{I,raw}$ signal and the G_{CGM} signal can be seen, and in Figure 8.3 an example of p-CGA is given.

All performance metrics have been summarized in Table 8.2.

Table 8.2 Performance evaluation for the M_3 predictor and the G_{CGM} in comparison to the blood glucose reference G on validation data.

Prediction Horizon	**p-CGA[%]**			**RMSE**	**max | e |**
	A	**B**	**CDE**	**[mg/dl]**	**[mg/dl]**
20	84.2	15.8	0	19	42
40	84.9	15.1	0	20	46
60	83.7	16.3	0	21	45
G_{CGM}	45.9	51.6	2.5	47	90

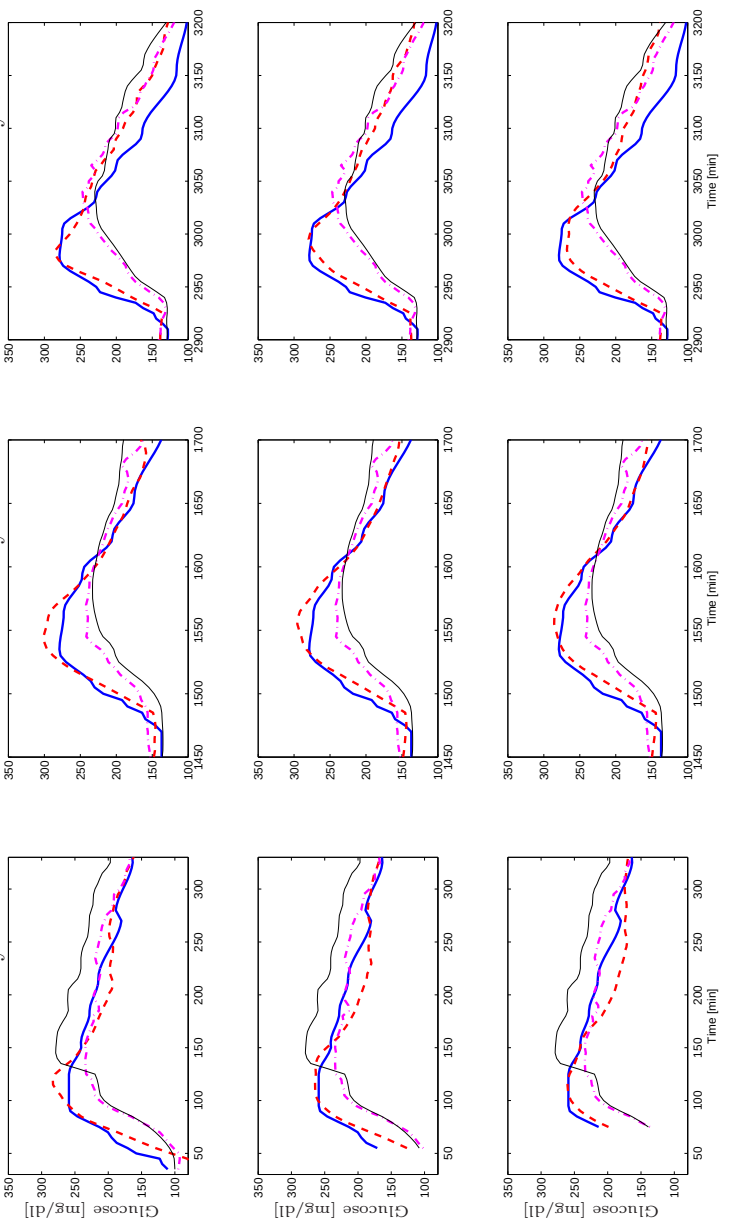

Figure 8.2 Plasma glucose predictions. Interpolated HemoCue measurements (thick solid blue), G_{CGM} (solid black), $G_{I,raw}$ (dash dotted magenta) and $M3$ predictions (dashed red) for estimation data (middle plot) and validation data (left and right plots). Upper plots: 20 min prediction, Middle plots: 40 min prediction, Lower plots: 60 min prediction.

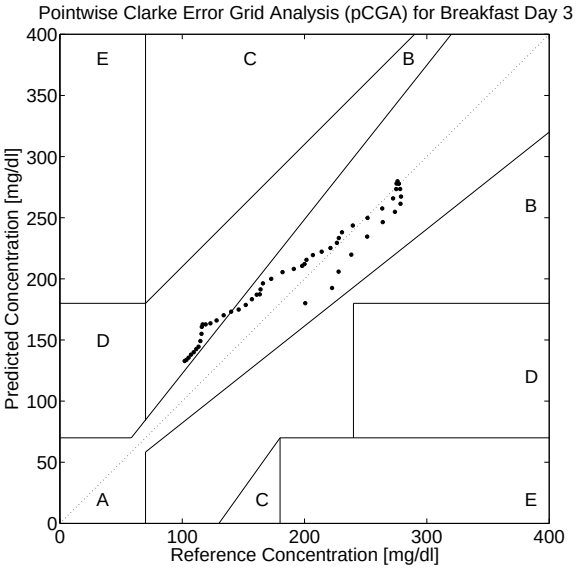

Figure 8.3 Example of Clarke Error Grid Diagram, 40 min prediction Day 3. Prediction versus the interpolated HemoCue blood glucose reference.

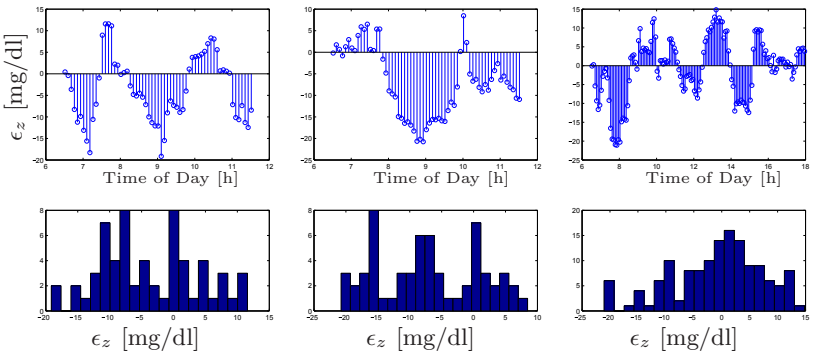

Figure 8.4 Upper plots: Simulation error ϵ_z of the simulated raw CGM signal $\hat{z}(k)$ given blood glucose $y(k)$ using the sensor model M_2. Lower plots: Distribution of the error. Estimation data (middle plot) and validation data (left and right plots).

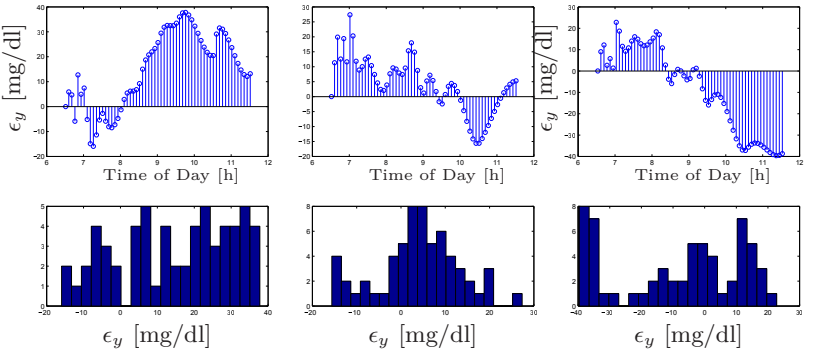

Figure 8.5 Upper plots: Simulation error ϵ_y of blood glucose $y(k)$ given inputs $u(k)$ using M_1. Lower plots: Distribution of the error. Estimation data (middle plot) and validation data (left and right plots).

8.3 Discussion

Error Analysis

To determine the source of the prediction error, the simulation errors of the sensor model,

$$\epsilon_z = z - \hat{z} \tag{8.14}$$

and of the GIIM model

$$\epsilon_y = y - \hat{y} \tag{8.15}$$

were investigated separately. In Figure 8.4, the simulation error between the simulated raw CGM signal $\hat{G}_{I,raw}$ and the true signal can be seen. The error distribution is clearly non-Gaussian. This could be explained by time-varying dynamics, and in [Sparacino et al., 2007] a recursive sensor model is used to handle such occurences. However, the evaluated time periods are short, and applying the model over the entire data record gives a more even distribution (Figure 8.6). Given a tolerance interval of ±20 mg/dl, corresponding to the p-CGA A zone for a 100 mg/dl blood glucose value, the model error can be considered acceptable.

The simulation error of the GIIM can be seen in Figure 8.5. The contribution is significantly larger. For breakfast day one, the model underestimates the glucose drop after the peak. On day three on the other hand, the model overestimates the same drop. Given that these are infinite-horizon prediction without any measurement feedback, a maximum error in the magnitude of 40 mg/dl should be considered to be a very good result. In fact, the error is almost within the p-CGA A zone at all times.

Looking at the predictions in Figure 8.2, the behavior of the prediction error can be understood from the error contribution from the sensor model,

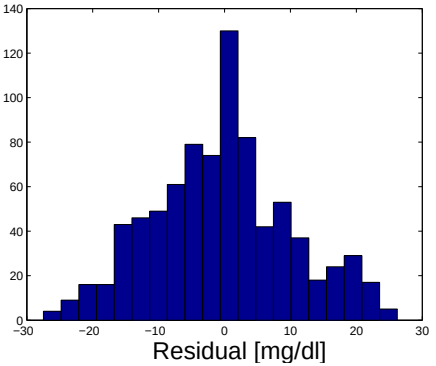

Figure 8.6 Distribution of the simulation error of the sensor model over the entire data record.

sensor errors and the GIIM. As the prediction horizon increases, the GIIM error becomes more and more dominant.

The corresponding prediction error for the model without the sensor model and with CGM as feedback signal, in terms of RMSE, can be found in Table 8.3. Compared to the results in Table 8.2, an improvement can be seen for every evaluated prediction horizon, with a relatively larger improvement as the prediction horizon increases, when the full model is utilized.

Table 8.3 Prediction error assessment for the model without incorporated sensor model in terms of RMSE.

Prediction	**RMSE [mg/dl]**	
Horizon [min]	vs G_{CGM}	vs G
20	8.0	25.0
40	16.3	31.4
60	24.4	37.6

Glucose and Insulin Sub Models

Major sources of uncertainty are the intermediate inputs R_a and I_p and the assumptions made to retrieve them. Unfortunately, these obstacles are hard to overcome in the applied modeling framework. Neither the rate of glucose appearance following a meal nor the plasma insulin level are normally available for measurement. Estimates of R_a have been made in [Dalla Man et al., 2006a] and require a tracer based experiment. I_p can be obtained from lab assays of blood samples. Obviously, such arrangements cannot be expected in

a normal day setting. Further work to assess the intra- and inter-individual variations of these processes, and on mitigations to handle these principle obstacles, is needed.

Plasma-to-Interstitial Dynamics

These dynamics were assumed to be time invariant, and homogeneous in direction and magnitude of glucose change and glucose level. The assumption of independence of the sign of the glucose change has been shown to be questionable, see [Kovatchev et al., 2009], where statistically significant differences in response time, depending on the direction of glucose change, are presented. However, in this study no such differences could be observed.

8.4 Conclusions

In this chapter a method for sensor-delay compensation was presented. Comparison of the merged prediction to the interpolated SMBG reference clearly showed that the augmented model manages to significantly reduce the delay, that otherwise is present when only relying on the CGM signal to estimate the blood glucose. Furthermore, the results indicate that the underlying GIIM model seems to, with acceptable accuracy, describe the combined impact of a breakfast and the subsequent insulin injection. Further research is needed to evaluate the concept on more patient data to investigate whether generic sensor models can be utilized. In terms of defence in depth, the concept is especially useful in the second layer, since timely measurements are extra important when monitoring for alarm purposes.

9

Ensemble Prediction

9.1 Introduction

Diabetic glucose dynamics are known to be subject to time-shifting dynamics, as indicated in Chapters 3 and 4. Considering this, and the vast number of models developed in the literature, as described in Chapter 2, it is unclear if a single model can be determined to be optimal under every possible situation. Such different circumstances may be, e.g., physical activity versus resting, periods with differences in insulin sensitivity or meal intake resulting in different postprandial responses, see Chapter 6. This raises the question whether it is more useful to use one of the models solely, or if it is possible to gain additional prediction accuracy by combining their outcomes. Accuracy may be gained from merging, due to mismodeling or to changing dynamics in the underlying data creating process, where a single model capturing the system behavior may be infeasible, e.g., for practical identification concerns. Thus, by an ensemble approach, robustness and performance may be improved. In this chapter, a novel merging approach—combining elements from both switching and averaging techniques, forming a 'soft' switcher in a Bayesian framework—is presented for the glucose prediction application.

9.2 Related Research

Merging models for the purpose of prediction has been developed in different research communities. In the meteorological and econometric communities, regression-oriented ensemble prediction has been a vivid research area since the late '60s, see, e.g., [Raftery et al., 2005] and [Elliott et al., 2006].

Also in the machine learning community, the question of how different predictors or classifiers can be used together for increased performance has been investigated, and different algorithms have been developed, such as the bagging, boosting [Breiman, 1996] and weighted majority [Littlestone and

Warmuth, 1994] algorithms, and online versions of these [Oza, 2005; Kolter and Maloof, 2003].

In most approaches the merged prediction $\hat{y}_k^e$ at time k is formed by a linear weighted average of m individual predictors $\hat{\mathbf{y}}_k = [\hat{y}_1 \dots \hat{y}_m]$.

$$\hat{y}_k^e = \mathbf{w}_k^{\mathbf{T}} \hat{\mathbf{y}}_k \tag{9.1}$$

It is also common to restrict the weights $\mathbf{w}_k$ to $[0, 1]$. The possible reasons for this are several, where the interpretation of the weights as probabilities, or rather Bayesian beliefs, is the dominating. Such restrictions are however not always applicable, e.g. in the related optimal portfolio selection problem, where negative weight (short selling) can reduce the portfolio risk [Elton et al., 1976].

A special case, considering distinct switches between different linear system dynamics, has been studied mainly in the control community. The data stream and the underlying dynamic system are modelled by pure switching between different filters derived from these models, i.e., the weights w_k can only take value 1 or 0. A lot of attention has been given to reconstructing the switching sequence, see, e.g., [Gustafsson, 2000; Ohlsson et al., 2010]. From a prediction viewpoint, the current dynamic mode is of primary interest, and it may suffice to reconstruct the dynamic mode for a limited section of the most recent time points in a receding horizon fashion [Alessandri et al., 2005].

Combinations of specifically adaptive filters has also stirred some interest in the signal processing community. Typically, filters with different update pace are merged, to benefit from each filter's specific change responsiveness, respectively steady state behaviour [Arenas-Garcia et al., 2006].

Finally, in fuzzy modeling, soft switching between multiple models is offered using fuzzy membership rules in the Takagi-Sugeno systems [Takagi and Sugeno, 1985].

Merging of predictions in the glucose prediction context have previously been investigated in terms of hypo- or hyperglycemic warning systems. In [Daskalaki et al., 2013], the glucose prediction from a so-called output corrected ARX predictor (see the reference for method details) was linearly combined with the prediction from an adaptive recurrent neural network model. The balancing factor for the linear combination was determined offline by optimizing a trade-off between hypo- and hyperglycemic sensitivity, effective prediction horizon and the false alarm rate. This factor was determined individually for each patient and the balance may be different for hypo- and hyperglycemia. A different mechanism was used in [Dassau et al., 2010]. Here, five different predictors were running simultaneously, and the hypoglycemic alarm was based upon a voting scheme between the individual predictors. If a number of the five predictors exceeded the predefined hypoglycemic threshold value an alarm was raised. Both studies indicated an improvement in alarm sensitivity compared to the individual predictors.

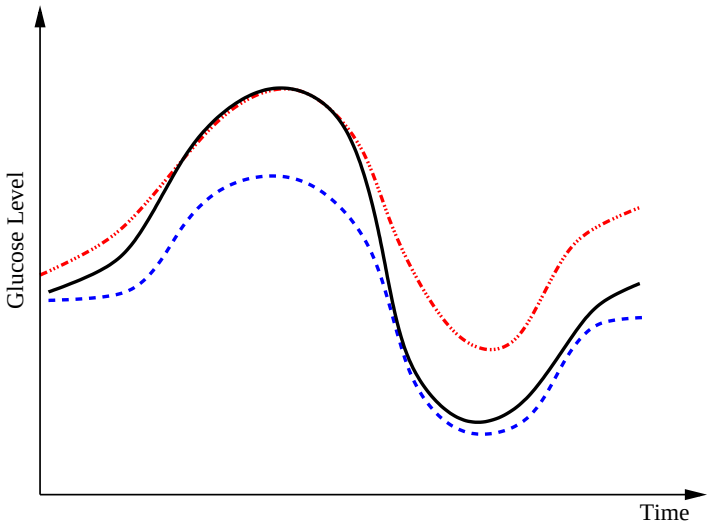

Figure 9.1 Example of when merging between different predictors may be beneficial. Initially the model corresponding to the red dash-dotted prediction resembles the true reference (black solid curve) best, but as the conditions change the prediction given by the other prediction model (blue dashed curve) gradually takes the lead.

9.3 Problem Formulation

As seen from the review above, many different approaches to glucose modeling and predicting have been established. These methods may each be more suitable to specific conditions for the glucose dynamics, and improvements in robustness and prediction performance may be achieved by combining their outcomes, as indicated from the studies from the hypo-/hyperglycemic alarm systems. Such a situation is depicted in Figure 9.1, where two prediction models try to capture the true glucose level. In different situations, each predictor is clearly outperforming the other and is capable of providing good estimates of the true glucose level. However, as the conditions change the performance deteriorates, and instead the other predictor is more suitable to rely upon. Given this informal background, a more formal problem formulation is now outlined.

A non-stationary data stream $z_k : \{y_k, u_k\}$ arrives with a fixed sample rate, set to 1 for notational convenience, at time $t_k \in \{1, 2, ...\}$. The data stream contains a variable of primary interest called $y_k \in \mathbb{R}$ and additional variables u_k. The data stream can be divided into different episodes T_{S_i} of similar dynamics $S_i \in S = [1...n]$, and where $s_k \in S$ indicates the current dynamic mode at time t_k. The system changes between these different modes

according to some unknown dynamics.

Given m number of expert q-steps-ahead predictions, $\hat{y}^j_{k+q|k}, j \in \{1, ..m\}$ of the variable of interest at time t_k, each utilizing different methods, and/or different training sets; how is an optimal q-steps-ahead prediction $\hat{y}^e_{k+q|k}$ of the primary variable, using a predefined norm and under time-varying conditions, determined?

9.4 Sliding Window Bayesian Model Averaging

Apart from conceptual differences between the different approaches to ensemble prediction, the most important difference is how the weights are determined. Numerous different methods exist, ranging from heuristic algorithms [Takagi and Sugeno, 1985; Arenas-Garcia et al., 2006] to theory-based approaches, e.g., [Hoeting et al., 1999]. Specifically, in a Bayesian Model Averaging framework [Hoeting et al., 1999], which will be adopted in this chapter, the weights are interpreted as partial beliefs in each predictor M_i, and the merging is formulated as:

$$p(y_{k+q}|D_k) = \sum_i p(y_{k+q}|M_i, D_k)p(M_i|D_k) \tag{9.2}$$

where $p(y_{k+q}|D_k)$ is the conditional probability of y at time t_{k+q} given the data, $D_k : \{z_{1:k}\}$ received up until time k. If only point-estimates are available, one can, e.g., use:

$$\begin{aligned} \hat{y}^e_{k+q|k} &= \mathbb{E}(y_{k+q}|D_k) = \sum_i \mathbb{E}(M_i|D_k)\mathbb{E}(y_{k+q}|M_i, D_k) = \bar{\mathbf{w}}_k^T \hat{\mathbf{y}}_k \\ \bar{\mathbf{w}}_k^{(i)} &= \mathbb{E}(M_i|D_k) \\ p(\mathbf{w}_k^{(i)}) &= p(M_i|D_k) \end{aligned} \tag{9.3}$$

where $\hat{y}^e_{k+q}$ is the combined prediction of y_{k+q} using information available at time k, and $\mathbf{w}_k^{(i)}$ indicates position i in the weight vector. The conditional probability of predictor M_i can be further expanded by introducing the latent variable $\theta_k \in \Theta = [1...p]$.

$$p(M_i|D_k) = \sum_j p(M_i|\theta_k = j, D_k)p(\theta_k = j|D_k) \tag{9.4}$$

or in matrix notation

$$\mathbf{p}(\mathbf{w}_k) = \left[\mathbf{p}(\mathbf{w}_k|\theta_k = 1) \dots \mathbf{p}(\mathbf{w}_k|\theta_k = p)\right] \left[p(\theta_k = 1|D_k) \dots p(\theta_k = p|D_k)\right]^T \tag{9.5}$$

Here, Θ represents a *predictor mode* in a similar sense to the dynamic mode S, and likewise θ_k represents the prediction mode at time k. $\mathbf{p}(\mathbf{w}_k|\theta_k = j)$ is a column vector of the joint prior distribution of the conditional weights of each predictor model given the predictor mode $\theta_k = j$. Generally, there is a one-to-one relationship between the predictor modes and the corresponding dynamic modes, i.e., $p = n$.

Data for estimating the distribution for $\mathbf{p}(\mathbf{w}_k|\theta_k = i)$ is given based upon using a constrained optimization on the training data. In cases of labelled training datasets, the following applies:

$$\{\mathbf{w}_{k|\theta_k=i}\}_{T_{S_i}} = \arg\min \sum_{m=k-N/2}^{k+N/2} \mathscr{L}(y(t_m), \mathbf{w}^T_{k|\theta_k=i}\hat{\mathbf{y}}_\mathbf{i}), \quad k \in T_{S_i} \tag{9.6}$$

subject to $\sum_j \mathbf{w}^{(j)}_{k|\theta_k=i} = 1$, and where T_{S_i} represents the time points corresponding to dynamic mode S_i, the tunable parameter N determines the size of the evaluation window and $\mathscr{L}(y, \hat{y})$ is a cost function. From these datasets, the prior distributions can be estimated by the Parzen window method [Bishop, 2006], giving mean $\mathbf{w}_{0|\theta_k=i}$ and covariance matrix $\mathbf{R}_{\theta_k=i}$. An alternative to the Parzen approximation is of course to estimate a more parsimoniously parametrized probability density function (pdf) (e.g., Gaussian) for the extracted data points. For unlabelled training data, with time points T, the corresponding datasets $\{\mathbf{w}_k|\theta_k = i\}_T$ are found by cluster analysis, e.g., using the k-means algorithm or a Gaussian Mixture Model (GMM) [Bishop, 2006]. A conceptual visualisation is given in Figure 9.2. Now, in each time step k, the $\mathbf{w}_k|\theta_{k-1}$ is determined from the sliding window optimization below, using the current active mode θ_{k-1}. For reasons soon explained, only $\mathbf{w}_k|\theta_{k-1}$ is thus calculated:

$$\begin{aligned}\mathbf{w}_{k|\theta_{k-1}} = \arg\min \sum_{j=k-N}^{k-1} \mu^{k-j}\mathscr{L}(y_j, \mathbf{w}^T_{k|\theta_{k-1}}\hat{\mathbf{y}}_j) \\ + (\mathbf{w}_{k|\theta_{k-1}} - \mathbf{w}_{0|\theta_{k-1}})\Lambda_{\theta_{k-1}}(\mathbf{w}_{k|\theta_{k-1}} - \mathbf{w}_{0|\theta_{k-1}})^T\end{aligned} \tag{9.7}$$

subject to $\sum_j \mathbf{w}^{(j)}_{k|\theta_{k-1}} = 1$. Here, μ_j is a forgetting factor, and $\Lambda_{\theta_k=i}$ is a regularization matrix. To infer the posterior $\mathbf{p}(\theta_k|D_k)$ in (9.5), it would normally be natural to set this probability function equal to the corresponding posterior pdf for the dynamic mode $\mathbf{p}(S|D_k)$. However, problems arise if $\mathbf{p}(S|D_k)$ is not directly possible to estimate from the dataset D_k. This is circumvented by using the information provided by the $\mathbf{p}(\mathbf{w}_{k|\theta_k})$ estimated from the data retrieved from equation (9.6) above. The $\mathbf{p}(\mathbf{w}_{k|\theta_k})$ prior density functions can be seen as defining the region of validity for each predictor mode. If the $\mathbf{w}_{k|\theta_{k-1}}$ estimate leaves the current active mode region θ_{k-1} (in a sense that

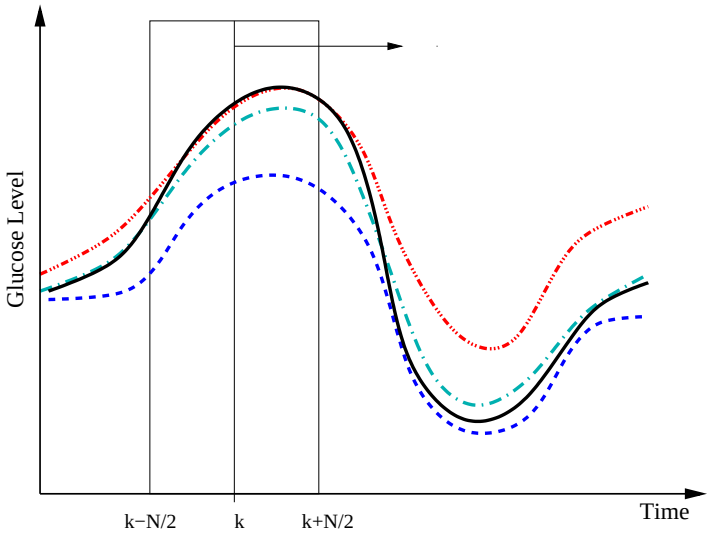

Figure 9.2 Principle of finding the predictor modes for unlabelled data over the training dataset time period T. For every time point $t_k \in T$, the optimal $\mathbf{w}_k$ is determined by Eq. (9.6), where the optimal prediction $\mathbf{w}_k\hat{\mathbf{y}}$ (light green dash-dotted curve) formed from the individual predictions $\hat{\mathbf{y}}$ (the blue dashed and the red dash-triple-dotted curves) is evaluating against the reference (black solid curve) using the cost function $\mathscr{L}$ over a sliding data window between $t = k - N/2$ and $t = k + N/2$. The aggregated set $\{\mathbf{w}_k\}_T$ is thereafter subjected to clustering to find the different mode centers $\mathbf{w}_{0|\theta=i}, i = [1..p]$.

$\mathbf{p}(\mathbf{w}_{k|\theta_{k-1}})$ is very low), it can thus be seen as an indication of that a mode switch has taken place. A logical test is used to determine if a mode switch has occurred. The predictor mode is switched to mode $\theta_k = i$, if:

$$p(\theta_k = i|\mathbf{w}_k, D_k) > \lambda \tag{9.8}$$

where

$$p(\theta_k = i|\mathbf{w}_k, D_k) = \frac{p(\mathbf{w}_k|\theta_k = i, D_k)p(\theta_k = i|D_k)}{\sum_j p(\mathbf{w}_k|\theta_k = j, D_k)p(\theta_k = j|D_k)} \tag{9.9}$$

A λ somewhat larger than 0.5 gives a hysteresis effect to avoid chattering between modes. Unless otherwise estimated from data, the conditional probability of each prediction mode $p(\theta_k = i|D_k)$ is set equal for all possible modes, and thus cancels in (9.9). The logical test is evaluated using the priors received from the pdf estimate and the $\mathbf{w}_{\mathbf{k}|\theta_\mathbf{k}}$ received from (9.7). If a mode switch is considered to have occurred, (9.7) is rerun using the new predictor mode.

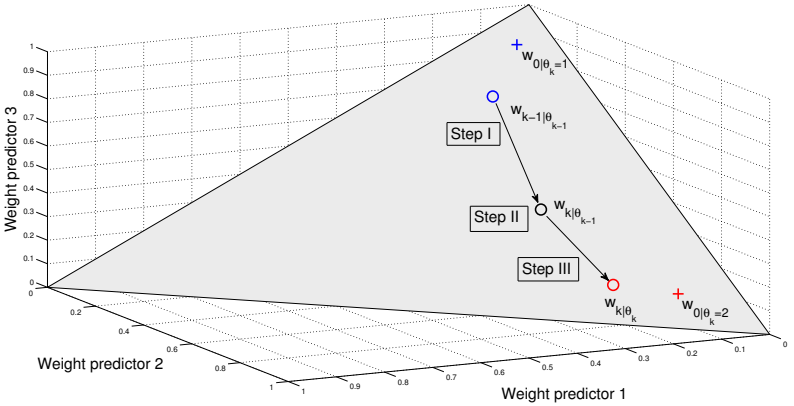

Figure 9.3 Predictor mode switching for an example with three individual predictor models. Step I: At time instance t_k the new $w_{k|\theta_{k-1}}$ is determined from Eq. (9.7) In this case, the data forces the optimal weight away from the active prediction mode center. Step II: The likelihood values $p(w_k|\theta_k = i), i = [1..p]$ are calculated and if the condition according to Eq. (9.8) is fulfilled, a predictor mode switch occurs. Step III: Based on the new predictor mode, Eq. (9.7) is rerun and the weight vector now gravitates towards the new mode center.

Now, since only one prediction mode θ_k is active; (9.5) reduces to $\mathbf{p}(\mathbf{w}_k) = \mathbf{p}(\mathbf{w}_{k|\theta_k})$. The predictor mode switching concept is visualised in Figure 9.3.

Parameter choice

The length N of the evaluation period is, together with the forgetting factor μ, a crucial parameter determining how fast the ensemble prediction reacts to sudden changes in dynamics. A small forgetting factor will put much emphasis on recent data, making it more agile to sudden changes. However, the drawback is of course that the noise sensitivity increases.

The quantity $\Lambda_{\theta_k=i}$ should also be chosen, such that a sound balance between flexibility and robustness is found, i.e., a too small $||\Lambda_{\theta_k=i}||_2$ may result in over-switching, whereas a too large $||\Lambda_{\theta_k=i}||_2$ will give an inflexible predictor. Furthermore, $\Lambda_{\theta_k=i}$ should force the weights to move within the perimeter defined by $p(\mathbf{w}|\theta_k = i)$. This is approximately accomplished by setting $\Lambda_{\theta_k=i}$ equal to the inverse of the covariance matrix $\mathbf{R}_{\theta_k=i}$, thus representing the pdf as a Gaussian distribution in the regularization.

Optimal values for N and μ can be found by evaluating different choices for some test data. However, from our experience we have seen that $N = 10 - 20$ and $\mu = 0.8$ are suitable choices for this application.

Summary of algorithm

1. Estimate m numbers of predictors according to best practice.
2. Run the predictors and the constrained estimation (9.6) on labelled training data and retrieve the sequence of $\{\mathbf{w}_{k|\Theta=i}\}_{T_{S_i}}, \forall i \in \{1, .., n\}$.
3. Classify different predictor modes, and determine density functions $\mathbf{p}(\mathbf{w}_{k|\Theta=i})$ for each mode $\Theta = i$ from the training results by supervised learning. If possible; estimate $p(\Theta = i|D)$.
4. Initialize mode to the nominal mode.
5. For each time step; calculate $\mathbf{w_k}$ according to (9.7).
6. Test if switching should take place by evaluating (9.8) and (9.9), and switch predictor mode if necessary and recalculate new $\mathbf{w}_k$ according to (9.7).
7. Go to 5.

Nominal mode

Apart from the estimated prediction mode centres, an additional predictor mode can be added, corresponding to a heuristic fall-back mode. In the case of sensor failure, or other situations where loss of confidence in the estimated predictor modes arises, each predictor may seem equally valid. In this case, a fall-back mode to resort to may be the equal weighting. This is also a natural start for the algorithm. For these reasons, a nominal mode $\theta_k = 0 : p(\mathbf{w_k}|\theta_\mathbf{k} = \mathbf{0}) \in N(\mathbf{1/m}, \mathbf{\Sigma})$ is added to the set of predictor modes (where $\mathbf{\Sigma}$) is a predefined covariance matrix, e.g., the identity matrix of size m). The outlined ensemble engine (see text box above for a summary) will hereafter be referred to as Sliding Window Bayesian Model Averaging (SW-BMA) Predictor.

9.5 Choice of Cost Function $\mathscr{L}$

The cost function $\mathscr{L}$ should be chosen with the specific application in mind. A natural choice for interpolation is the 2-norm, but in certain situations asymmetric cost functions are more appropriate. For the glucose prediction application, a suitable candidate for determining appropriate weights should

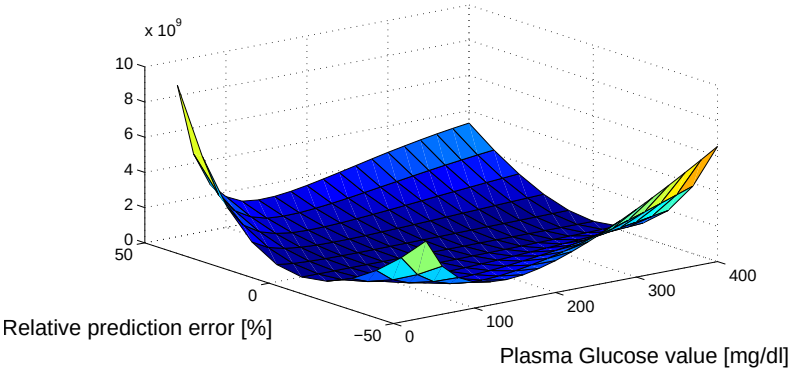

Figure 9.4 Cost function of relative prediction error.

take into account that the consequences of acting on too high glucose predictions in the lower blood glucose (G) region (<90 mg/dl) could possibly be life threatening. The margins to low blood glucose levels, that may result in coma and death, are small, and blood glucose levels may fall rapidly. Hence, emphasis should be put on securing small positive predictive errors and sufficient time margins for alarms to be raised in due time in this region. In the normoglycemic region (here defined as 90-200 mg/dl), the predictive quality is of less importance. This is the glucose range that healthy subjects normally experience, and thus can be considered, from a clinical viewpoint in regards to possible complications, a safe region. However, due to the possibility of rapid fluctuation of the glucose into unsafe regions, some considerations of predictive quality should be maintained.

Based on the cost function in [Kovatchev et al., 2000], the selected function incorporates these features; asymmetrically increasing cost of the prediction error depending on the absolute glucose value and the sign of the prediction error.

In Figure 9.4 the cost function can be seen, plotted against relative prediction error and absolute blood glucose value.

Correspondence to the Clarke Error Grid Plot

A de facto accepted standardized metric of measuring the performance of CGM signals in relation to reference measurements, and often used to evaluate glucose predictors, is the Clarke Grid Plot [Clarke et al., 1987]. This metric meets the minimum criteria raised earlier. However, other aspects makes it less suitable; no distinction between prediction errors within error zones is made, switches in evaluation score are instantaneous, etc.

In Figure 9.5, the isometric contours of the chosen function for different prediction errors at different G values has been plotted together with the

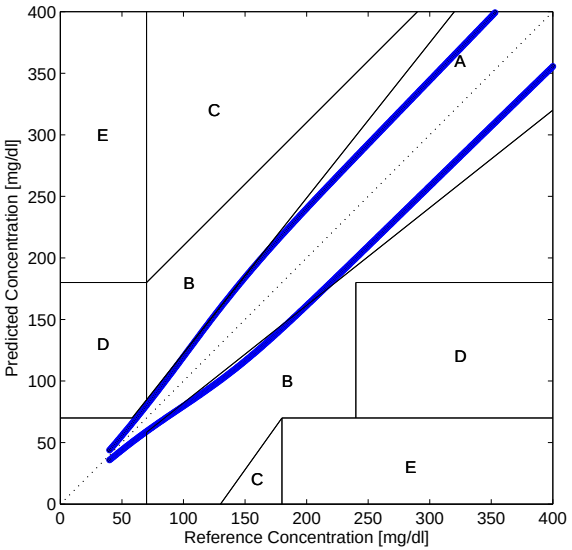

Figure 9.5 Isometric cost in comparison to the Clarke Grid.

Clarke Grid Plot. The boundaries of the A/B/C/D/E areas of the Clarke Grid can be regarded as lines of isometric cost according to the Clarke metric. In the figure, the isometric value of the cost function has been chosen to correspond to the lower edge, defined by the intersection of the A and B Clarke areas at 70 mg/dl. Thus, the area enveloped by the isometric border can be regarded as the corresponding A area of this cost function. Apparently, much tougher demands are imposed both in the lower and upper glucose regions in comparison to the Clarke Plot.

9.6 Example I: The UVA/Padova Simulation Model

Data

Data were generated using the non-linear metabolic simulation model, jointly developed by the University of Padova, Italy and University of Virginia, U.S. (UVa) and described in [Dalla Man et al., 2007a], with parameter values obtained from the authors. The model consists of three parts that can be separated from each other. Two submodels are related the influx of insulin following an insulin injection and the rate of appearance of glucose from the gastro-intestinal tract following meal intake, respectively, and have been described in Chapters 4 and 6. Both models were evaluated using generic population parameter values according to Table 8.1 in Chapter 8.

Table 9.1 Meal amount and timing randomization. Standard deviation in parenthesis.

Meal	Time	Amount carbohydrates (g)
Breakfast	08:00 (30 min)	45 (5)
Lunch	12:30 (30 min)	70 (10)
Dinner	19:00 (30 min)	80 (10)

The final part of the total model is concerned with the interaction of glucose and insulin in the blood stream, organs and tissue, including renal extraction, endogenous glucose production and insulin and non-insulin dependent glucose utilization. The model equations are partly nonlinear and are found in [Dalla Man et al., 2007a].

Using a parameter set corresponding to a subject with T1DM, twenty datasets, each eight days long, were generated. The timing and size of meals were randomized for each dataset, according to Table 9.1. The amount of insulin administered for each meal was based on a fixed carbohydrate-to-insulin ratio, perturbed by normally distributed noise, with a 20% standard deviation.

Process noise was added by perturbing some crucial model parameters p_i in each simulation step; $p_i(t) = (1 + \delta(t))p_i^0$, where p_i^0 represent nominal value and $\delta(t) \in N(0, 0.2)$. The affected parameters were (again following the notation in [Dalla Man et al., 2007a])) $k_1, k_2, p_{2u}, k_i, m_1, m_{30}, m_2, k_{sc}$, and represent natural intra-personal variability in the underlying physiological processes.

Two dynamic modes A and B were simulated by, after 4 days, changing four model parameters (following the notation in [Dalla Man et al., 2007a]) k_1, k_i, k_{p3} and p_{2u}, related to the endogenous glucose production and insulin and glucose utilization. This represents an example of shift in the underlying patient dynamics, which may occur due to, e.g., sudden changes in physical or mental stress levels.

A section of four days of a dataset, including the period when the dynamic change took place, can be seen in Figure 9.6. One of the twenty datasets was used for training and the others were considered test data.

Predictors

For prediction modeling purposes, the system was considered to consist of three main parts in a similar sense as the simulation model was constructed. The absorption models of glucose and insulin were adopted and considered known. The outputs $I_p(t_k)$ and $R_a(t_k)$ from these models were fed into a linear state-space model of the Glucose-Insulin Interaction (GIIM), with system matrices A, B and C, generating the final output, i.e., the blood glucose

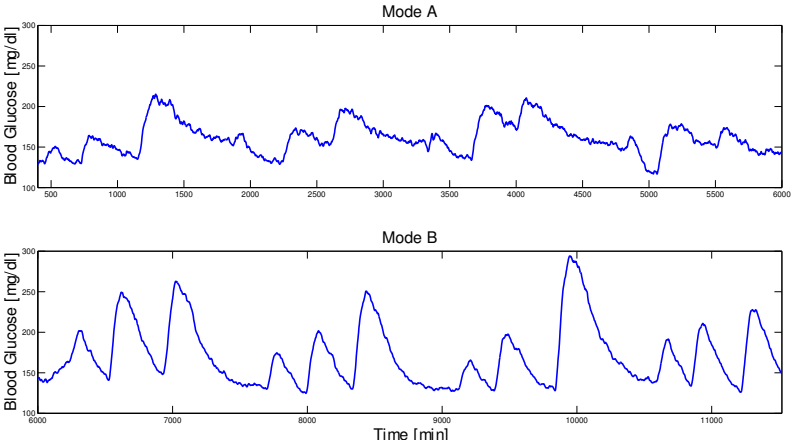

Figure 9.6 The training dataset. The upper plot represents four days of dynamic mode A data and the lower plot the corresponding last four days of dynamic mode B, where four model parameters have been modified. Example I: UVA/Padova Model.

$G(k)$ at time $t_k \in (5, 10, \ldots)$ min. Short-term predictions, p steps ahead, were evaluated using the Kalman filter with gain K:

$$\begin{aligned} \hat{x}(k+1) &= A\hat{x}(k) + Bu(k) + K(y(k) - C\hat{x}(k)) \\ \hat{x}(k+p) &= A\hat{x}(k+p-1) + Bu(k+p-1) \\ \hat{G}(k+p) &= C\hat{x}(k+p) \end{aligned} \tag{9.10}$$

where meal and insulin announcements were assumed at least T_{PH} minutes ahead, implying that $u(k+l)$ was known for all $0 \leq l \leq p$.

Three models were identified using the subspace-based technique with the N4SID algorithm of the Matlab System Identification Toolbox. The model order $[2-4]$ was determined by the Akaike information criterion [Johansson, 2009]. The first model I was estimated using data from dynamic mode A in the training data, and the second II from the mode B data, and the final model III from the entire training dataset. Thus, model I and II are each specialized, whereas III is an average of the two dynamic modes. Evaluation was performed for a prediction horizon of 60 min.

Results

Training the Mode Switcher The three predictors were used to create three sets of 60-minute-ahead predictions for the training data. Using (9.6) with $N = 10$, the weights $\mathbf{w}_k$ were determined. The mode centers were found by k-means clustering, and the corresponding probability distribution for each

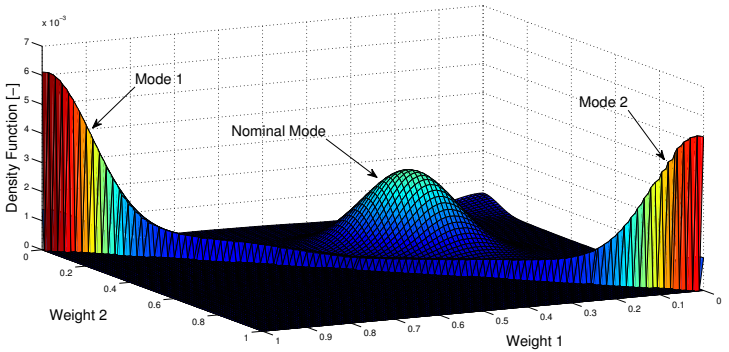

Figure 9.7 Estimated probability density functions for the weights in the training data, including nominal mode. Example I: UVA/Padova model.

mode, projected onto the (w_1, w_2)-plane, was thereafter estimated by Parzen window technique [Bishop, 2006]. The densities are well concentrated to the corners $[1, 0, 0]$ and $[0, 0, 1]$, with means $\mathbf{w_{0|1}} = [0.96, 0.03, 0.01]$ and $\mathbf{w_{0|2}} = [0.03, 0.96, 0.01]$ defining the expected weights for each predictor mode. The nominal mode probability density function was set to $N(\frac{\mathbf{1}}{\mathbf{3}}\frac{\mathbf{1}}{\mathbf{3}}\frac{\mathbf{1}}{\mathbf{3}}, \mathbf{0.1I})$ where I is the identity matrix. In Figure 9.7 all density functions, including the nominal mode, projected onto the (w_1, w_2)-plane, can be seen together.

Ensemble Prediction vs. Individual Predictions Using the estimated probability density functions and the expected weights $\mathbf{w}$ of the identified predictor modes, the ensemble machine was run on the test data. An example of the distribution of the weights for the two dynamic modes A and B can be seen in Figure 9.8. An example of how switching between the different modes occurs over the test period can be found in Fig 9.9.

For evaluation purposes, all predictors were run individually. In Table 9.2, a comparative summary of the predictive performance of the different approaches over the test batches, in terms of mean RMSE, is given. It was also noted that the merged prediction did not introduce any extra prediction delay in comparison to the best individual prediction (not shown).

9.7 Example II: The DIAdvisor Data

Data

Data from the clinical part of the DAQ trial and the DIAdvisor I B and C trials, conducted within the DIAdvisor project [DIAdvisor, 2012], were used. A number of patients participated in all three trials. Based on data complete-

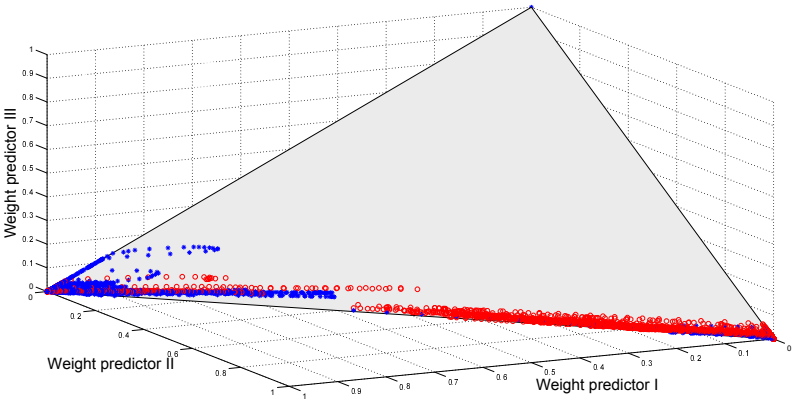

Figure 9.8 Example of the distribution of weights in the test data using the estimated pdf:s and expected weights. Blue dots: Dynamic Mode A (days 1-4). Red dots: Dynamic Model B (days 5-8). Example I: UVA/Padova model.

Table 9.2 Performance evaluation by RMSE for the 60 minute predictors using different approaches.

	RMSE [mg/dl]		
Predictor Type	**Section A**	**Section B**	**A+B**
Predictor I	8.0	16.1	12.6
Predictor II	15.3	7.2	12.1
Predictor III	9.8	9.9	9.9
Merged prediction	8.4	7.6	8.1

ness, six of these (namely patients 3, 7, 8, 18, 25 and 30 from the Montpellier clinic) were selected for this study with population characteristics according to Table 9.3. Each trial ran over three days. The patients received standardized meals where the amount of carbohydrates included in each meal was

Table 9.3 Population Statistics of data. Mean values and [min-max].

Parameter	**Value**
Gender	3 Men /3 Women
Therapy	3 Pump / 3 Multi-Dose Injection
Age	54 [32-68]
HbA1c	7.9 [5.7-9.1]
BMI	25.8 [23.7-29.4]

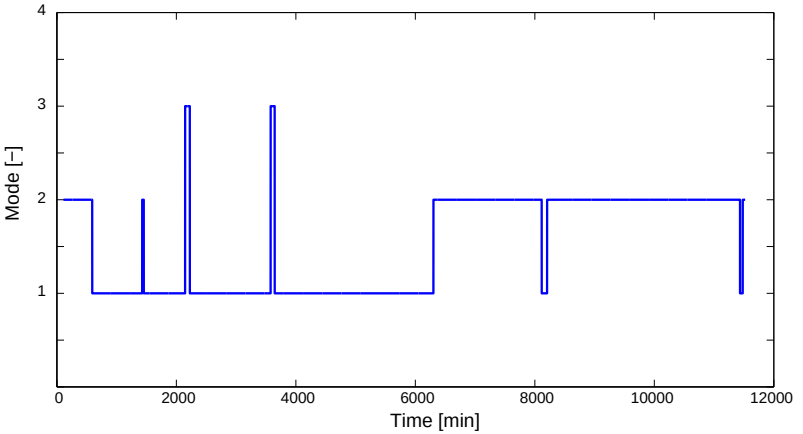

Figure 9.9 Example of switching between different predictor modes in the test data. The transition from dynamic mode B to mode A takes place at 6000 min (c:a 4 days). Mode 3 represents the nominal mode. The late switch to predictor mode 2 in comparison to when the dynamic mode switch takes place is due to that the excitation for the first hours of the fifth day is low until the breakfast meal takes place, i.e., there is little incitament to switch predictor mode before that point. Example I: UVA/Padova model.

about 40 (45 in DAQ), 70 and 70 grams, respectively. Additional snacks, in some cases related to counter-act hypoglycemia, were also digested. Further details of the trials can be found in Chapter 3.

The first trial data (DAQ) were used to train the individual predictor models. The second and third trial data (DIAdvisor I.B and C) were used to train and cross-validate the SW-BMA, i.e., the SW-BMA was trained on B data and validated on C data, and vice versa.

Predictors

Three different predictors of different structure were developed within the DIAdvisor project, and used in this study; a state-space-based model (SS) [Ståhl, 2012], a recursive ARX model [Estrada et al., 2010] and a kernel-based predictor [Naumova et al., 2012]. For all three models, the CGM signal $G_{CGM}(t)$ was considered a proxy for the blood glucose $G(t)$, i.e., the lag between the interstitial glucose and the blood glucose, described in e.g. [Rebrin and Steil, 2000], was ignored.

The state-space model and the ARX model used the modeling approach described in Chapter 8, with insulin and glucose sub models according to (8.1), and without interstitial and sensor dynamics modeling (M_2). The state-

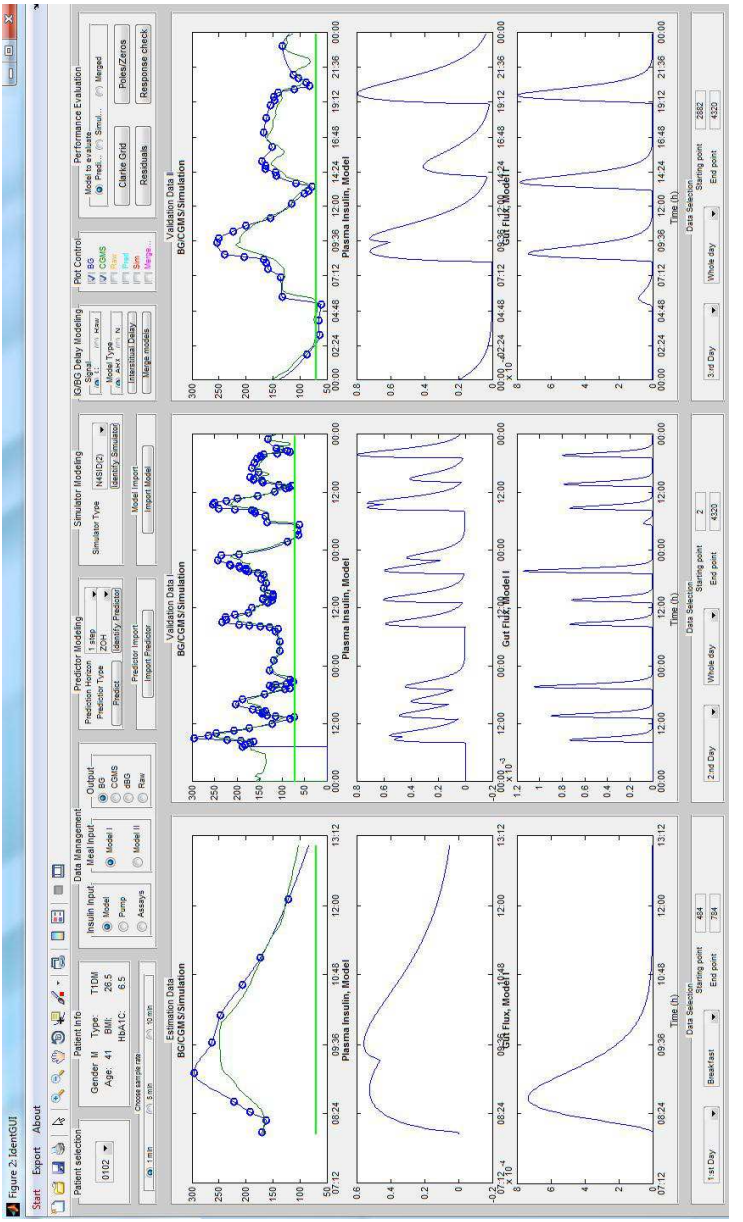

Figure 9.10 A Graphical User Interface (GUI) developed in order to facilitate manual model identification. Patient specific data can be loaded from each of the DIAdvisor trials and displayed in three different columns of data windows. The top windows depict glucose data, where the blue circles correspond to blood glucose reference values, the blue line represents the splined interpolation of these values (G) and the dark green line is the interpolated Continuous Glucose Measurements (G_{CGM}). The light green bar corresponds the hypoglycemic threshold, 4 mmol/l (72 mg/dl). The middle plots show the plasma insulin level I_p, given by the Insulin Sub Model (ISM), derived from basal and bolus doses. The lower plots describe the corresponding results from the Glucose Sub Model (GSM), yielding the rate of appearance of glucose R_a following meal intakes. Different types of models can be evaluated by changing in the scroll-down menu in the header of the GUI, and previous developed models can also be imported for comparative purposes. Model evaluation plots can be requested using the push buttons in the upper right corner of the GUI header.

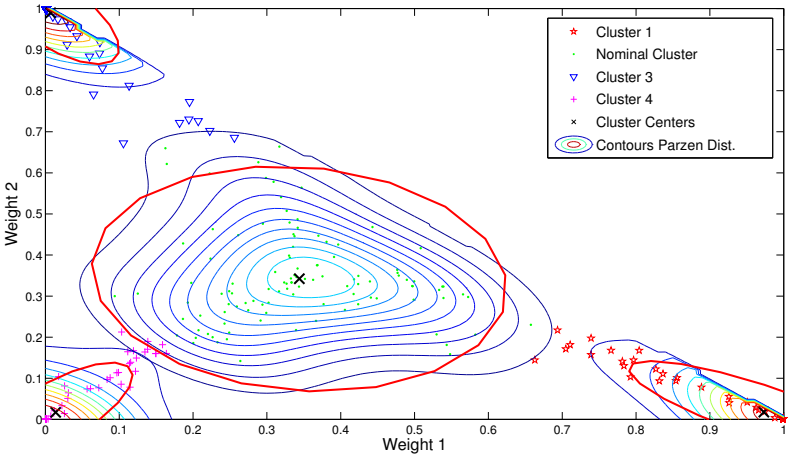

Figure 9.11 Example of distribution of weights in the training data by (9.6) and clusters given by the k-means algorithm. The red ellipses represent the fitted Gaussian covariances of each cluster (patient 0103, Trial B). Example II: DIAdvisor Data.

space model equations are found in Eq. (9.10). The ARX predictor was recursively updated at each time step with an adaptive update gain dependent upon the glucose level according to [Estrada et al., 2010]. The state-space model was identified using the graphical user interface in Figure 9.10.

The kernel-based predictor did not directly utilize the insulin or meal data channels. Instead, the linear trend and offset parameters given by linear regression of recent CGM data were used as meta features to switch between different predefined kernel-based prediction functions, see [Naumova et al., 2012] for a full explanation. Furthermore, this predictor was only trained on one patient dataset and was thus considered patient invariant.

Evaluation Criteria

The prediction results were compared to the interpolated blood glucose G in terms of Clarke Grid Analysis [Clarke et al., 1987] and the complementary Root Mean Square Error (RMSE).

Results

Training the Mode Switcher

Cluster Analysis - Finding the Modes The three predictors were used to create 40 minute ahead predictions for both training datasets $D_{T_{B(C)}}$. Using (9.6) with $N = 20$, the weights $\{\mathbf{w}_k\}_{T_{B(C)}}$ were obtained; example depicted in the (w_1, w_2) plane in Figure 9.11. The weights received from the training

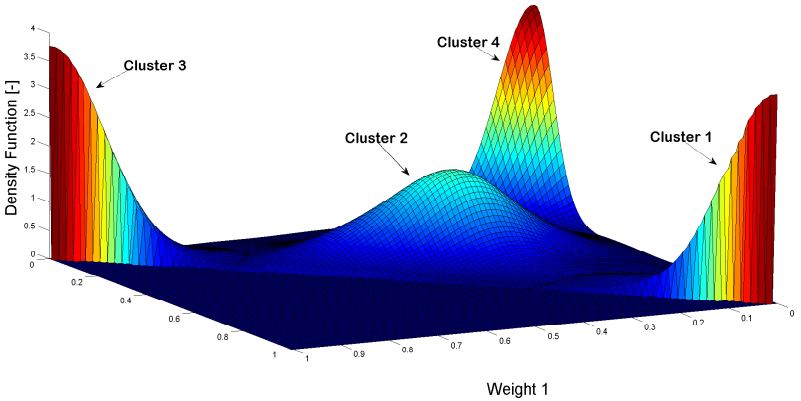

Figure 9.12 Example of estimated probability density functions for the different predictor mode clusters in the training data (patient 103, Trial B). Example II: DIAdvisor Data.

are easily visually recognized as belonging to different groups (true for all patients, not shown). Attempts were made to find clusters using a Gaussian Mixture Model (GMM) by the EM algorithm, but without viable outcome. This is not totally surprising, considering, e.g., the constraints $0 \geq w_i \geq 1$ and $\sum w = 1$. A more suitable distribution, often used as a prior for the weights in a GMM, is the Dirichlet distribution, but instead the simpler k-means algorithm was applied using four clusters (number of clusters given by visual inspection of the distribution of $\{\mathbf{w}_k\}_{T_{B(C)}}$), providing the cluster centers $\mathbf{w}_{0|\Theta_i}$.

The corresponding probability distribution for each mode $p(\mathbf{w}|\Theta_i)$, projected onto the (w_1, w_2)-plane, was estimated by Parzen window technique, and an example can be seen in Figure 9.12. Gaussian distributions were fitted to give the covariance matrices $\mathbf{R}_{\Theta_i}$ used in (9.7).

Feature Selection The posterior mode probability $p(\theta_k|D_k)$ is likely not dependent on the entire data D_k, but only a few relevant data features, possible to extract from D_k. Features related to the performance of a glucose predictor may include meal information, insulin administration, level of physical activity, measures of the glucose dynamics, etc. By plotting the training CGM data, colored according to the best mode at the prediction horizon retrieved by the training, interesting correlations become apparent (Figure 9.13). The binary features in Table 9.4 were selected. When extracting the features, meal timing and content were considered to be known 30 minutes before the meal.

From the training data, the posterior mode probabilities $p(\theta_k = i|f_j)$,

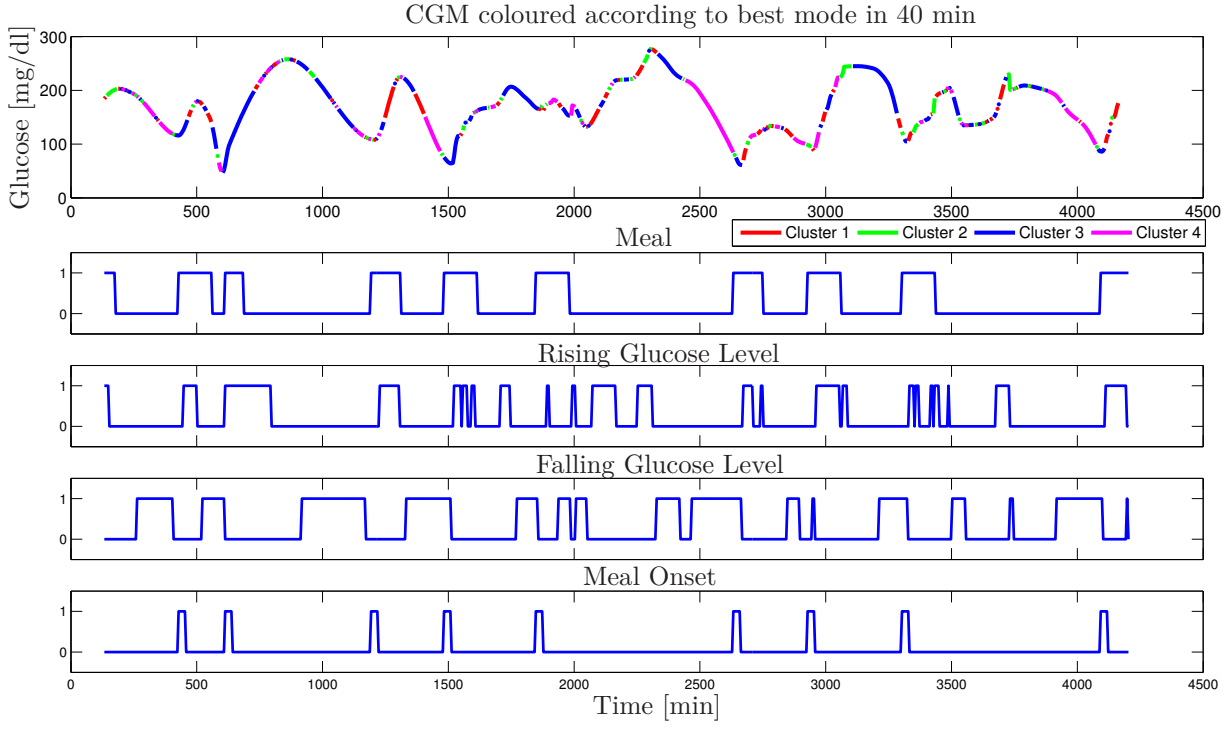

Figure 9.13 Example of CGM coloured according to best predictor mode 40 minutes ahead, together with active features at the moment the prediction was made (patient 0103, Trial B). Example II: DIAdvisor Data.

given each feature f_j, were determined by the ratio of active time for each mode over the time periods when each feature was present. Additionally, the overall prior $p(\theta_k = i)$ was determined by the total ratio of active time per cluster over the entire test period.

The different features are overlapping, and the combinations thereof could be regarded as features by themselves. However, the data support for each such new feature would be small and could potentially disrupt, rather than improve, the switching performance. To resolve this issue, the features were not combined (apart from concurrent rising glucose and meal intake, which formed a new feature), and each feature was given different priority—only allowing the feature of highest priority, f_k^* to be present at each time step t_k. The priority rank was chosen to allow the more specific features to take presidence over the more general features. At each cycle, $p(\theta_k = i|D_k) = p(\theta_k = i|f_k^*)$ was determined, and if no feature was active, $p(\theta_k = i|D_k)$ was approximated by the $p(\theta_k = i)$ estimate.

Prediction Performance on Test Data

Using the estimated mode clusters $\{w_{0|i}, R_{0|i}\}, i = [1 \dots M]$, and the estimated posteriors $p(\Theta_i|f^*)$ from Trial B (C), the ensemble machine was run on the Trial C (B) data. The parameter μ was set to 0.8 and N to 20 minutes. An example of the distribution of the weights $\mathbf{w}_k$ for the three predictors can be seen in Figure 9.14. Table 9.5 summarizes a comparison of predictive performance over the different patient test datasets for the RMSE evaluation criteria, and in Table 9.6 the evaluation in terms of Clarke Grid Analysis is given. The optimal switching approach, here defined as using the non-causal fitting by Eq. (9.6), is used as a measure of optimal performance of a linear

Table 9.4 Selected features. Here, ϵ corresponds to the maximum amplitude of glucose rate-of-appearance, R_a after digesting 10 g CHO, and $\Delta G = G_k - G_{k-5}$.

Feature	Threshold	Priority
Meal	$\max(Ra_k, .., Ra_{k+30}) > \epsilon$	1
Rising G	mean $(\Delta G_{k-10}, \dots, \Delta G_k)$ > 30 mg/(dl· h)	2
Falling G	mean $(\Delta G_{k-10}, \dots, \Delta G_k)$ < -18 mg/(dl· h)	3
Meal and rising G	See above.	4
Meal Onset	$\max Ra(k-30, ..., k) < \epsilon$ and $\max Ra(k, ..., k+30) > \epsilon$	5

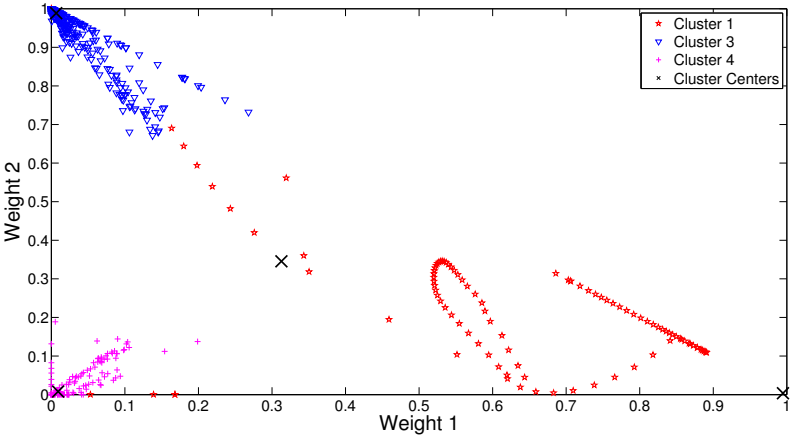

Figure 9.14 Example of the distribution of weights in the test data using the estimated clusters and feature correlations (patient 0108, Trial B). Example II: DIAdvisor Data.

combination of the different predictors.

Table 9.5 Performance evaluation for the 40 minute SW-BMA prediction compared to the optimal switching and the individual predictors. The metric is the Root Mean Square Error (RMSE), normalized against the best individual predictor $M_1 - M_3$ for each patient.

Merging Strategy	median RMSE/RMSE$_{\text{best}}$ [min-max] Trial B	Trial C
SW-BMA	1.03 [0.75-1.04]	1.03 [0.94-1.05]
Optimal switching	0.97 [0.54-1.0]	0.94 [0.73-1.0]
2:nd best individual pred.	1.16 [1.09-1.27]	1.21 [1.04-1.37]
Worst individual pred.	1.44 [1.25-1.73]	1.45 [1.18-1.83]

9.8 Discussion

Example I outlined how the technique may be applied to the specific example of diabetes glucose prediction under sudden changes in the underlying physiological dynamics. In this example, the merged prediction turned out to be the best choice. In Example II, applying the algorithm to real-world data, the SW-BMA has, for most patients, the same RMSE and Clarke Grid performance as the best individual predictor. In one case, the merged prediction clearly outperformed also the best predictor (RMSE/RMSE$_{\text{best}} = 0.75$).

Table 9.6 Performance evaluation for the 40 minute SW-BMA prediction compared to the optimal switching and the best individual predictor by the amount of data (%) in the acceptable A/B zones vs. the dangerous D and E zones.

Merging Strategy	Trial B			Trial C		
	A/B	D	E	A/B	D	E
SW-BMA	95.5	2.2	0	95.3	3.0	0.1
Optimal switching	96.2	1.7	0	96.9	1.3	0
Best individual pred.	94.8	2.6	0	95.0	3.4	0

However, comparison to the optimal switcher indicates that there is still further room for improvement. To fill this gap, timely switching is most important.

The prediction models in Example II were not specifically designed for specialisation, but are diversified in terms of modeling and parameter identification methods in relation to each other. The state-space model is patient-specific, with fixed parameter values after traning—making it agile to interpersonal differences but more sensititive to time-variability. The model is invariant to the absolute glucose level. The ARX model, on the other hand, is recursively updated to capture time-variability, but the approach may be vulnerable to fluctuating system excitation conditions. Both models utilize the insulin and meal data inputs. The kernel-based predictor is generic over the patient cohort, and considers the dynamics to be related to the glucose level rather than directly to the inputs' effects. Overall, the three models thereby complement each other in these aspects. The posterior mode probabilities, conditioned on each selected feature, show that some specialisation exists. For example, when feature 5 (meal onset) was active, cluster 3, dominated by the SS predictor, was clearly favoured an average (61 %). Exploiting these correlations may enhance timely switching, and further specialisation and diversification amongst the prediction models can thus be expected to improve the added value of prediction merging additionally.

The evaluation indicates that the proposed algorithm is robust to sudden changes and in reducing the impact of modeling errors. Apart from that, in many applications, transition between different dynamic modes is a gradual process rather than an abrupt switch, making the pure switching assumption inappropriate. The proposed algorithm can handle such smooth transitions by slowly sliding along a trajectory in the weight plane of the different predictors, perhaps with a weaker Λ if such properties are expected. Furthermore, any type of predictor may be used, not restricting the user to a priori assumptions of the underlying process structure.

The Tagaki-Sugeno (TS) system also gives soft switching. The underlying assumption is that the switching dynamics can be observed directly from the

data. This assumption has been relaxed for the proposed algorithm, extending the applicability beyond that of TS systems.

In [Raftery et al., 2010], another interesting approach to online Bayesian Model Averaging is suggested for changing dynamics. In this approach, the assumed transition dynamics between the different modes are based on a Markov chain. However, in our approach no such assumptions on the underlying switching dynamics are postulated. Instead, switching is based on recent performance in regards to the applicable norm, and possibly on estimated correlations between predictor modes and features of the data stream $P(\theta_k = i|D_k)$, see Eq. (9.9).

9.9 Conclusions

In this chapter, a novel merging mechanism for multiple glucose predictors has been proposed for time-varying and uncertain conditions. The approach was evaluated on both artificial and real-world datasets, incorporating modeling errors in the individual predictors and time-shifting dynamics.

The results show that the merged prediction has a predictive performance in comparison with the best individual predictor in each case, and indicates that the concept may prove useful when dealing with several individual (glucose) predictors of uncertain reliability—reducing the risk associated with definite a priori model selection—or as a means to improve predictive quality if the predictions are diverse enough.

Further research will be undertaken to investigate how interesting features correlated to expected predictor mode changes should be extracted, and in regards to the possibility of making the algorithm unsupervised.

The concept can support several prediction-based features at different levels of a defence in depth concept, such as level 2 hypo- and hyperglycemic alarms or level 3 autonomous pump suspension, where the improved robustness may reduce false-alarm rates and improper safety function activation.

10

Conclusions and Future Research

10.1 Conclusions

This thesis has investigated means to improve self-care in insulin-dependent diabetes. The focus has primarily been CSSI therapy for IDDM patients. The underlying philosophy in the modeling approach has been that the models should be possible to identify from input-output data, preferably from home-monitored data, and that it should reflect real-world situations, i.e., to avoid cumbersome and expensive protocols with, e.g., tracers requiring hospitalization and non-physiological conditions.

A cornerstone in successful insulin therapy is understanding the insulin action, i.e., the magnitude and dynamics of the glucose-lowering effect of insulin. This was investigated in Chapter 4 using overnight data from data collected at home from 29 patients during six weeks. The overnight period was chosen to avoid interference from glucose changes due to meal intake, thereby allowing the insulin action to be studied in isolation. Using a Bayesian procedure, finite impulse response models of the insulin action could be estimated. Interesting properties, previously reported from tracer experiments, of glucose dependence of the insulin action, were reconfirmed and quantified. The models were personalized with individual estimates of the insulin action, showing that large interpersonal differences in both magnitude and peak and duration exist. The analysis also revealed time-variability in insulin requirements, in between days, as well as diurnal patterns. These models were used in Chapter 5 to predict the glucose level in order to assess the risk of nocturnal hypoglycemia. The analysis indicate that these events can be predicted with good accuracy and acceptable false alarm rate, well in advance for counter-measures to be undertaken. One possible application is to use the approach in an insulin pump, where the insulin delivery is suspended at impeding hypoglycemia. Such a feature is already available in one commer-

cial insulin pump, where the concept has been successfully proven. With the suggested method here, further improved performance can be expected. Another possible scenario is to use the model to warn for suspected nocturnal hypoglycemia already at bedtime. Combining these two approaches could drastically reduce the risk of nocturnal hypoglycemia, which is one of the major hurdles in diabetes glucose management.

Next to understanding the effect of insulin, getting to grips with how different meals affect the glucose is fundamental in diabetes management. Using data from the same trial as were used to establish the insulin response, postprandial data records were extracted for 56 different recipes covering 475 meal instances in total. Again, a finite impulse response model was chosen, allowing the glucose elevating impact of the different recipes to be estimated. Cluster analysis demonstrated that many recipes indeed had very similar shape of their glucose elevating impact, and that a majority of the recipes could be assigned to just three groups. The macro nutrient composition was significantly different between these clusters, confirming, e.g., that relatively increased fat content delays the glucose excursion. The cross-validation showed that the models may be of sufficient quality to be used for calculation of meal boluses.

Thereafter, the issue of how to determine such bolus doses was addressed, together with the related question whether the postprandial recommendations issued by the leading professional medical associations are realistic and achievable for all patients and for all types of meals. Modern insulin pumps allow for immediate bolus doses as well as manipulation of the basal level to temporarily adjust the level up or down. Thereby, different combination effects can be created, ranging from the superbolus (a bolus dose followed by complete shutoff of the basal delivery for a predefined time) to extended boluses (no bolus dose but elevated basal dose for a predefined time). In chapter 7, an optimization routine was used to evaluate what type of bolus is most suitable for the different recipes estimated previously, in order to contain the postprandial constraints. These constraints were based on interpretations of the postprandial recommendations. The analysis showed that for almost all recipes, the superbolus with three hours basal elimination was the best option. However, for a few recipes with meal impacts with long durations and delayed peaks, a combination bolus with about 50%/50% division between the instantaneous bolus and the three hours elevated basal dose was the preferred choice. Another important finding was that for some patients with longer than normal insulin action, the postprandial recommendations can only be upheld for small meals (less than about 40 grams of carbohydrates).

Diabetes glucose dynamics is known to comprise both short- and more long-term time-variability, as the analysis of the insulin action demonstrated. Merging different diversified models may prove to be a successful approach, as a means to improve performance and robustness under such conditions. In Chapter 9, a novel merging algorithm based in a Bayesian setting was

developed. The suggested method admits for soft switching and interpolation between the different models based on an evaluation of the different predictors' recent performance, using a sliding data window, and by looking for data feature identified to be correlated to switching. Different aspects of the merging approach were investigated, using a simulated dataset, and the concept was thereafter successfully validated using 12 datasets from the DI-Advisor project, showing improved robustness to the prediction performance in comparison to relying on the individual prediction models.

Another problematic aspect to glucose dynamic modeling and identification was tackled in Chapter 8. The glucose measurements that can be retrieved in a frequent and automatic fashion, i.e., the CGM measurements, are sampled in the interstitial compartment—a tissue that has a diffusion-like relationship to the compartment of primary interest—the circulatory blood system. This aspect is often overlooked in glucose modeling, but significant lagging of the glucose prediction of those models may result, as indicated by the evaluation of the lagging between the CGM signal and the corresponding reference blood glucose measurements in Chapter 3. This is unacceptable, as hypoglycaemia may quickly arise due to rapid glucose drops (see Chapter 3), and these models will, unless perfectly matched, in many cases be unable to capture these potentially dangerous situations. To overcome this deficiency, a modeling approach where a subspace identified state-space model was augmented, to incorporate the dynamics responsible for the sensor delay, was developed. To prove the concept, an individual dataset with significant sensor lag was used for validation, and short-term postprandial prediction was evaluated. The results show that the lag of the glucose estimate and prediction were successfully reduced.

The results listed above are encouraging, but have been developed from small datasets with limited diversity. Larger and more diverse studies are needed to scrutinize and validate these ideas. Some directions for future research are listed below. Regardless, as more knowledge is gathered, better models and algorithms will emerge. Together with the recent advances in sensor technology, insulin formulations, insulin pumps and information technology, more and stronger building blocks are added for development of the different layers in a defence in depth concept. Such a concept would potentially allow for reduced risks of short- and long-term complications, increased patient empowerment, and in the end, improved quality of life for persons with (insulin-dependent) diabetes.

10.2 Future Research

Below some directions for future research are outlined.

Finite impulse response model simplification It would be possible to parametrize the finite impulse response models by splines. Such an approach may prove beneficial in terms of making it more easy to find common dynamics among different patients.

Interpersonal variability in insulin action Larger studies are needed to characterize the variability of duration and magnitude of the insulin action. Can the patient group be stratified by cluster analysis?

Glucose-dependent insulin action The results regarding the heterogeneous aspects of insulin action across the glucose range needs to be further investigated, validated and characterized. Trials specifically designed to collect data in the critical hyperglycemic and hypoglycemic regions are needed to get a fuller picture of this effect.

Intra-personal variability in insulin requirements This important property needs to be investigated thoroughly both in terms of diurnal patterns but also over longer time horizons. Specifically interesting is how this affect glucose variability, as indicated by the results in Chapter 4. Can patterns be identified, and linked to e.g. physical activity?

Meal impact models The recipes investigated had low diversity. Larger studies covering a broader class of meals and macro nutritional composition are needed. Will more meal impact clusters be revealed?

Meal Bolusing Intervention studies where patients are given recommendation on meal bolus doses, calculated using the described models, would be of interest to validate the clinical usefulness of such a bolus advising system.

Population Stratification The diabetic population may be possible to stratify into smaller patient cohorts. Finding such classifications could potentially simplify parametrization of previously unmodelled patients, if model behavior could be linked to directly available, or easily measured, biomarkers. Deeper classification analysis of identified models may indicate such relationships.

Ensemble Predictor In order to detect the optimal switching point as soon as possible, the feature monitoring of the SW-BMA ensemble engine is an interesting functionality. However, finding and extracting relevant features was non-trivial and no systematic approach is utilized.

Sensor delay The concept of augmenting the model with a sensor model, describing the sensor lag, needs to be further validated by more data examples. Additionally, alternative, more complex models of the sensor dynamics, e.g., incorporating sensor drift, should be addressed.

Bibliography

Abbott Freestyle Navigator (2015). http://www.abbottdiabetescare.co.uk/your-products/freestyle-navigator. Accessed Nov 9, 2015.

Abdul-Rasoul, M., H. Habib, and M. Al-Khouly (2006). "'The honeymoon phase' in children with type 1 diabetes mellitus: frequency, duration, and influential factors." *Pediatr Diabetes* **7**:2, pp. 101–7. ISSN: 1399-543X. DOI: 10.1111/j.1399-543X.2006.00155.x.

Ackerman, E, L. C. Gatewood, J. W. Rosevear, and G. D. Molnar (1965). "Model studies of blood-glucose regulation". *B Math Biophys* **27**:Special Issue, pp. 21–37.

Agar, B., M. Eren, and A. Cinar (2005). "Glucosim: educational software for virtual experiments with patients with type 1 diabetes". In: *Proc. IEEE EMBS 27th Annual Int. Conf. (EMBC2005)*. Shanghai, pp. 845 –848.

Alessandri, A., M. Baglietto, and G. Battistelli (2005). "Receding-horizon estimation for switching discrete-time linear systems". *IEEE Trans Autom Control* **50**:11, pp. 1736 –1748. ISSN: 0018-9286. DOI: 10.1109/TAC.2005.858684.

American Diabetes Association (2013). "Standards of medical care in diabetes–2013." *Diabetes care* **36 Suppl 1**:October 2012, S11–66. ISSN: 1935-5548. DOI: 10.2337/dc13-S011.

American Diabetes Association. Living with diabetes. (2014). http://www.diabetes.org/living-with-diabetes/treatment-and-care/medication/insulin/insulin-basics.html. Accessed Oct 13, 2015.

Animas Vibe (2015). http://www.animas.com/.

Apidra™ (2015). http://www.apidra.com/. Accessed Nov 9, 2015.

Arenas-Garcia, J., M. Martinez-Ramòn, A. Navia-Vazquez, and A. R. Figueiras-Vidal (2006). "Plant identification via adaptive combination of transversal filters". *Signal Process* **86**:9. Special Section: Signal Processing in UWB Communications, pp. 2430 –2438. ISSN: 0165-1684. DOI: DOI:10.1016/j.sigpro.2005.11.008.

Arleth, T, S Andreasson, M. O. Federici, and M. M. Benedetti (2000). "A model of the endogenous glucose balance incorparating the characteristics of glucose transporters". *Comp Meth Prog Biomed* **62**, pp. 219–234.

Balakrishnan, N. P., G. P. Rangaiah, and L. Samavedham (2011). "Review and Analysis of Blood Glucose (BG) Models for Type 1 Diabetic Patients". *Ind Eng Chem Res* **50**:21, pp. 12041–12066. ISSN: 0888-5885. DOI: 10.1021/ie2004779.

Basu, R, B Di Camillo, G Toffolo, A Basu, P Shah, A Vella, R Rizza, and C Cobelli (2003). "Use of a novel triple-tracer approach to assess postprandial glucose metabolism". *Am. J. Physiol*, E55–E69.

Basu, R., C. D. Man, M. Campioni, A. Basu, G. Klee, G. Toffolo, C. Cobelli, and R. A. Rizza (2006). "Effects of Age and Sex on Postprandial Glucose Metabolism Differences in Glucose Turnover, Insulin Secretion, Insulin Action, and Hepatic Insulin Extraction". *Diabetes* **55**:July, pp. 2001–2014. DOI: 10.2337/db05-1692.

BD Patient Information (2015). *How to calculate an insulin to carb ratio*. http://www.bd.com/us/diabetes/page.aspx?cat=7001&id=7303. Accessed Sept. 2015.

Becker, R. H., A. D. Frick, L. Nosek, L. Heinemann, and K. Rave (2007). "Dose-Response Relationship of Insulin Glulisine in Subjects With Type 1 Diabetes". *Diabetes Care* **30**:10, pp. 2506–2507. DOI: 10.2337/dc06-2114.Clinical.

Bell, K. J., C. E. Smart, G. M. Steil, J. C. Brand-Miller, B. King, and H. a. Wolpert (2015). "Impact of Fat, Protein, and Glycemic Index on Postprandial Glucose Control in Type 1 Diabetes: Implications for Intensive Diabetes Management in the Continuous Glucose Monitoring Era". *Diabetes Care* **38**:6, pp. 1008–1015. ISSN: 0149-5992. DOI: 10.2337/dc15-0100.

Bequette, B. W. (2004). "Optimal estimation applications to continuous glucose monitoring". In: *Proc. 2004 American Control Conf. (ACC2004)*. Vol. 1. Boston, MA, pp. 958–962.

Bequette, B. W. (2012). "Challenges and recent progress in the development of a closed-loop artificial pancreas". *Annu Rev Control*. ISSN: 13675788. DOI: 10.1016/j.arcontrol.2012.09.007.

Bequette, B. (2014). "Data-driven modeling for diagnosis and treatment of diabetes". In: Marmarelis, V. et al. (Eds.). Lecture Notes in Bioengineering. Springer-Verlag Berlin Heidelberg. Chap. 3. Hypoglycemia Prevention Using Low Glucose Suspension Systems. Pp. 73–89.

Beregszaszg, M., N. Tubiana-Rafi, K. B. D, M. Noa, J. Bloch, and P. Czernichow (1997). "Nocturnal hypoglycemia in children and adolescents with insulin-dependent diabetes mellitus : Prevalence and risk factors". *J Pediatrics* **131**:1, pp. 27–33.

Bergenstal, R. M., E. Bashan, M. McShane, M. Johnson, and I. Hodish (2012). "Can a tool that automates insulin titration be a key to diabetes management?" *Diabetes Technol Ther* **14**:8, pp. 675–82. ISSN: 1557-8593. DOI: 10.1089/dia.2011.0303.

Bergenstal, R. M., D. C. Klonoff, S. K. Garg, B. W. Bode, M. Meredith, R. H. Slover, A. J. Ahmann, J. B. Welsh, S. W. Lee, and F. R. Kaufman (2013). "Threshold-based insulin-pump interruption for reduction of hypoglycemia." *N Engl J Med* **369**:3, pp. 224–32. ISSN: 1533-4406. DOI: 10.1056/NEJMoa1303576.

Berger, M and D Rodbard (1989). "Computer simulation of plasma insulin and glucose dynamics after subcutaneous insulin injection". *Diabetes Care* **12**:10, pp. 725–736.

Bergman, R. N. and C Cobelli (1980). "Minimal modeling, partition analysis, and the estimation of insulin sensitivity". *Fed Proc* **39**:1, pp. 110–115.

Bishop, C. M. (2006). *Pattern Recognition and Machine Learning*. Springer, Secaucus, NJ, USA.

Bishop, F., D. Maahs, G. Spiegel, D. Owen, G. Klingensmit, A. Bortsov, J. Thomas, and E. J. Mayer-Davis (2009). "The Carbohyrdate Counting in Adolescents With Type 1 Diabetes Study". *Diabetes Spectrum* **22**:1.

Bode, B., M. Silver, R. Weiss, and K. Martin (2008). "Evaluation of a continuous glucose monitoring system for home-use conditions". *Manag Care* **17**:8, pp. 40–45. ISSN: 1062-3388.

Bolie, V. W. (1961). "Coefficients of normal blood glucose regulation". *J Appl Phys* **16**:5, pp. 783–788.

Bolin, K., C. Gip, A.-C. Mörk, and B. Lindgren (2009). "Diabetes, healthcare cost and loss of productivity in Sweden 1987 and 2005–a register-based approach." *Diabet Med* **26**:9, pp. 928–34. ISSN: 1464-5491. DOI: 10.1111/j.1464-5491.2009.02786.x.

Boyne, M. S., D. M. Silver, J. Kaplan, and C. D. Saudek (2003). "Timing of changes in interstitial and venous blood glucose measured with a continuous subcutaneous glucose sensor". *Diabetes* **52**, pp. 2790–2794.

Brange, J and A Vølund (1999). "Insulin analogs with improved pharmocokinetic profiles". *Adv Drug Deliv Rev* **35**, pp. 307–335.

Breiman, L. (1996). "Bagging predictors". *Mach Learn* **24**:2, pp. 123–140.

Bremer, T and D. A. Gough (1999). "Is Blood Glucose Predictable From Previous Values? A Solicitation for Data". *Diabetes* **48**, pp. 445–451.

Breton, M. D. (2008). "Physical activity—the major unaccounted impediment to closed loop control". *J Diab Sci Technol* **2**:1, pp. 169–174.

Brouns, F., I. Bjorck, K. N. Frayn, A. L. Gibbs, V. Lang, G. Slama, and T. M. S. Wolever (2005). "Glycaemic index methodology". *Nutr Res Rev* **18**:01, p. 145. ISSN: 0954-4224. DOI: 10.1079/NRR2005100.

Buckingham, B., J. Block, J. Burdick, and et al (2005). "Response to nocturnal alarms using a real-time glucose sensor." *Diabetes Technol Ther* **7**:3, pp. 440–7. ISSN: 1520-9156. DOI: 10.1089/dia.2005.7.440.

Buckingham, B. A., D. Raghinaru, F. Cameron, B. W. Bequette, H. P. Chase, D. M. Maahs, R. Slover, R. P. Wadwa, D. M. Wilson, T. Ly, T. Aye, I. Hramiak, C. Clarson, R. Stein, P. H. Gallego, J. Lum, J. Sibayan, C. Kollman, and R. W. Beck (2015). "Predictive Low-Glucose Insulin Suspension Reduces Duration of Nocturnal Hypoglycemia in Children Without Increasing Ketosis". *Diabetes Care* **38**:7, pp. 1197–1204. ISSN: 0149-5992. DOI: 10.2337/dc14-3053.

Cescon, M. (2011). *Linear Modeling and Prediction in Diabetes Physiology*. Licentiate Thesis TFRT--3250--SE. Department of Automatic Control, Lund University, Sweden.

Cescon, M. (2013). *Modeling and Prediction in Diabetes Physiology*. Ph.D. Thesis TFRT--1099--SE. Department of Automatic Control, Lund University, Sweden.

Chan, A., L. Heinemann, and S. Anderson (2010). "Nonlinear Metabolic Effect of Insulin across the Blood Glucose Range in Patients with Type 1 Diabetes Mellitus". *J Diabetes Sci Technol* **4**:4, pp. 873–881.

Chase, H. P., S. Z. Saib, T MacKenzie, M. M. Hansen, and S. K. Garg (2002). "Post-prandial glucose excursions following four methods of bolus insulin administration in subjects with type 1 diabetes." *Diabetic Medicine* **19**:4, pp. 317–21. ISSN: 0742-3071. DOI: 10.1046/j.1464-5491.2002.00685.x.

Chase, J. G., G. M. Shaw, T. Lotz, A. LeCompte, J. Wong, J. Lin, T. Lonergan, M. Willacy, and C. E. Hann (2007). "Model-based Insulin and Nutrition Administration for Tight Glycaemic Control in Critical Care". *Curr Drug Deliv* **4**:4, pp. 283–296.

Chase, J. G., G. Shaw, A. Le Compte, T. Lonergan, M. Willacy, X.-W. Wong, J. Lin, T. Lotz, D. Lee, and C. Hann (2008). "Implementation and evaluation of the SPRINT protocol for tight glycaemic control in critically ill patients: a clinical practice change." *Crit Care Med* **12**:2, R49. ISSN: 1466-609X. DOI: 10.1186/cc6868.

Chetty, V. T., A Almulla, A Odueyungbo, and L Thabane (2008). "The effect of continuous subcutaneous glucose monitoring (CGMS) versus intermittent whole blood finger-stick glucose monitoring (SBGM) on hemoglobin A1c (HBA1c) levels in Type I diabetic patients: a systematic review."

Diabetes Res Clin Pract **81**:1, pp. 79–87. ISSN: 1872-8227. DOI: 10.1016/j.diabres.2008.02.014.

Chis, O.-T., J. R. Banga, and E. Balsa-Canto (2011). "Structural Identifiability of Systems Biology Models : A Critical Comparison of Methods". *PLoS ONE* **6**:11. DOI: 10.1371/journal.pone.0027755.

Christen, U., C. Bender, and M. G. von Herrath (2012). "Infection as a cause of type 1 diabetes?" *Curr Opin Rheumatol* **24**:4, pp. 417–23. ISSN: 1531-6963. DOI: 10.1097/BOR.0b013e3283533719.

Clarke, W. and B. Kovatchev (2009). "Statistical tools to analyze continuous glucose monitor data". *Diabetes Technol Ther* **11**:1, S45–S54.

Clarke, W. L., D. Cox, L. A. Gonder-Frederick, W. Carter, and S. L. Pohl (1987). "Evaluating clinical accuracy of systems for self-monitoring of blood glucose". *Diabetes Care* **10**, pp. 622–628.

Cobelli, C., E. Renard, and B. Kovatchev (2011). "Artificial Pancreas: Past, Present, Future". *Diabetes* **60**:11, pp. 2672–2682. ISSN: 0012-1797. DOI: 10.2337/db11-0654.

Cobry, E., K. McFann, L. Messer, V. Gage, B. VanderWel, L. Horton, and H. P. Chase (2010). "Timing of meal insulin boluses to achieve optimal postprandial glycemic control in patients with type 1 diabetes." *Diabetes Technol Ther* **12**:3, pp. 173–177. ISSN: 1520-9156. DOI: 10.1089/dia.2009.0112.

Cortez, N. G., I. G. Cohen, and A. S. Kesselheim (2014). "FDA regulation of mobile health technologies". *N Eng J Med* **371**:4, pp. 372–379. ISSN: 0028-4793. DOI: 10.1056/NEJMhle1403384. URL: 10.1056/NEJMhle1403384$\backslash$n25054722.

Daily Dose (2012). http://www.insulution.com/sv/insulution/.

Dalla Man, C, A Caumo, and C Cobelli (2002). "The Oral Glucose Minimal Model: Estimation of Insulin Sensitivity From a Meal Test". *IEEE Trans Biomed Eng* **49**:5, pp. 419–429.

Dalla Man, C., M. Camilleri, and C. Cobelli (2006a). "A system model of oral glucose absorption: validation on gold standard data". *IEEE Trans Biomed Eng* **53**:12, pp. 2472–2478.

Dalla Man, C., R. A. Rizza, and C. Cobelli (2007a). "Meal simulation model of the glucose-insulin system". *IEEE Trans Biomed Eng* **54**:10, pp. 1740–1749.

Dalla Man, C., G. Toffolo, R. Basu, R. a. Rizza, and C. Cobelli (2006b). "A model of glucose production during a meal". In: *Proc. IEEE EMBS 28th Annual Int. Conf. (EMBC2006)*. New York, pp. 5647–5650. ISBN: 1424400325. DOI: 10.1109/IEMBS.2006.260809.

Dalla Man, C., D. M. Raimondo, R. A. Rizza, and C. Cobelli (2007b). "GIM, Simulation Software of Meal Glucose – Insulin Model". *J Diabetes Sci Technol* **1**:3, pp. 1–8.

Dalla Man, C., R. A. Rizza, and C. Cobelli (2007c). "Meal Simulation Model of the Glucose-Insulin System". *IEEE Trans Biomed Eng* **54**:10, pp. 1740–1749. ISSN: 0018-9294. DOI: 10.1109/TBME.2007.893506.

Dalla Man, C., M. D. Breton, and C. Cobelli (2009). "Physical Activity into the Meal Glucose-Insulin Model of Type 1 Diabetes: In Silico Studies". *J. Diab Sci Technol* **3**:1, pp. 56–67.

Daskalaki, E., A. Prountzou, P. Diem, and S. G. Mougiakakou (2012). "Real-time adaptive models for the personalized prediction of glycemic profile in type 1 diabetes patients." *Diabetes Technol Ther* **14**:2, pp. 168–74.

Daskalaki, E., K. Norgaard, T. Zueger, A. Prountzou, P. Diem, and S. Mougiakakou (2013). "An Early Warning System for Hypoglycemic/Hyperglycemic Events Based on Fusion of Adaptive Prediction Models". *J Diabetes Sci Technol* **7**:3, pp. 689–698.

Dassau, E., P. Herrero, H. Zisser, B. a. Buckingham, L. Jovanovič, C. D. Man, C. Cobelli, J. Vehí, and F. J. Doyle III (2008). "Implications of Meal Library & Meal Detection to Glycemic Control of Type 1 Diabetes Mellitus through MPC Control". *Proc. 17th IFAC World Congress*, pp. 4228–4233. ISSN: 14746670. DOI: 10.3182/20080706-5-KR-1001.2057.

Dassau, E., F. Cameron, B. W. Bequette, H. Zisser, L. Jovanovič, H. P. Chase, D. M. Wilson, B. A. Buckingham, and F. J. Doyle (2010). "Real-Time Hypoglycemia Prediction Suite Using Continuous Glucose Monitoring". *Diabetes Care* **33**:6, pp. 1249–1254. DOI: 10.2337/dc09-1487.

Davey, R. J., T. W. Jones, and P. A. Fournier (2010). "Effect of short-term use of a continuous glucose monitoring system with a real-time glucose display and a low glucose alarm on incidence and duration of hypoglycemia in a home setting in type 1 diabetes mellitus." *J Diabetes Sci Technol* **4**:6, pp. 1457–1464. ISSN: 1932-2968.

Davidson, P. C., H. R. Hebblewhite, R. D. Steed, and B. W. Bode (2008). "Analysis of guidelines for basal-bolus insulin dosing: Basal insulin, correction factor, and carbohydrate-to-insulin ratio". *Endocr Pract* **14**:9, pp. 1095–1101.

Davis E, K. B. (1997). "Hypoglycemia : Incidence and Clinical Predictors in a Large Population-Based". *Diabetes care* **20**:I, pp. 22–25.

DCCT Group (1991). "Epidemiology of Severe Hypoglycemia in the Diabetes Control and Complications Trial". *Medicine* **90**:April.

DCCT Group (1993). "The Effect of Intensive Treatment of Diabetes on the Development and Progression of Long-Term Complications in Insulin-Dependent Diabetes Mellitus". *N Engl J Med* **329**:14, pp. 977–986. DOI: 10.1056/NEJM199309303291401.

DCCT Group (1997). "Hypoglycemia in the Diabetes Control and Complications Trial". *Diabetes* **46**:February, pp. 271–286. ISSN: 0012-1797.

DCCT/EDIC Group (2005). "Intensive Diabetes Treatment and Cardiovascular Disease in Patients with Type 1 Diabetes". *N Engl J Med* **353**:25, pp. 2643–2653.

DeFronzo, R. A., J. D. Tobin, and R Andres (1979). "Glucose clamp technique : a method insulin secretion and resistance for quantifying insulin secretion and resistance". *Am J Physiol* **237**:3, E214–E223.

Derouich, M and A.Boutayeb (2002). "The effect of physical exercise on the dynamics of glucose and insulin". *J Biomech* **35**, pp. 911–917.

Dexcom Seven Plus (2012). http://www.dexcom.com/seven-plus.

DIAdvisor (2012). http://www.diadvisor.eu.

Dinneen, S, a Alzaid, D Turk, and R Rizza (1995). "Failure of glucagon suppression contributes to postprandial hyperglycaemia in IDDM." *Diabetologia* **38**:3, pp. 337–43. ISSN: 0012-186X. DOI: 10.1007/BF00400639.

Docherty, P. D., J. G. Chase, T. F. Lotz, and T. Desaive (2011). "A graphical method for practical and informative identifiability analyses of physiological models: a case study of insulin kinetics and sensitivity." *Biomed Eng Online* **10**:1, p. 39. ISSN: 1475-925X. DOI: 10.1186/1475-925X-10-39.

Dye, L., M. Mansfield, N. Laisikiewicz, L. Mahawish, R. Schnell, D. Talbot, H. Chauhan, F. Croden, and C. Lawton (2010). "Correspondance of continuous interstitial glucose measurement against arterialised and capillary glucose following an oral glucose tolerance test in healthy voulenteers". *British J Nutr* **103**, pp. 134–140.

Edelman, S. V. and J. S. Blose (2014). "The Impact of Nocturnal Hypoglycemia on Clinical and Cost-Related Issues in Patients With Type 1 and Type 2 Diabetes." *Diabetes Educ* **40**:3, pp. 269–279. ISSN: 1554-6063. DOI: 10.1177/0145721714529608.

"Handbook of Economic Forecasting" (2006). In: Elliott, G. et al. (Eds.). Elsevier. Chap. 10. Forecast Combinations.

Elton, E. J., M. J. Gruber, and M. W. Padberg (1976). "Simple criteria for optimal portfolio selection". *J. Finance* **31**:5, pp. 1341–1357.

Epanechnikov, V. A. (1969). "Non-parametric estimation of a multivariate probability density". *Theory Probab Appl* **14**:1, pp. 153–158.

Eren-Oruklu, M., A. Cinar, L. Quinn, and D. Smith (2009a). "Adaptive control strategy for regulation of blood glucose levels in patients with type 1 diabetes". *J Proc Control* **19**:8, pp. 1333–1346. ISSN: 09591524. DOI: 10.1016/j.jprocont.2009.04.004.

Eren-Oruklu, M., A. Cinar, L. Quinn, and D. Smith (2009b). "Estimation of future glucose concentrations with subject-specific recursive linear models." *Diabetes Technol Ther* **11**:4, pp. 243–53. ISSN: 1520-9156. DOI: 10.1089/dia.2008.0065.

Eren-Oruklu, M., A. Cinar, and L. Quinn (2010). "Hypoglycemia prediction with subject-specific recursive time-series models." *J Diabetes Sci Technol* **4**:1, pp. 25–33. ISSN: 1932-2968.

Estrada, G., H. Kirchsteiger, L. Del Re, and E. Renard (2010). "Innovative approach for online prediction of blood glucose profile in type 1 diabetes patients". In: *American Control Conf. (ACC2010), 2010*, pp. 2015–2020.

Fabietti, P. G., V. Canonico, M. O. Federici, M. M. Benedetti, and E. Sarti (2006). "Control oriented model of insulin and glucose dynamics in type 1 diabetics." *Med Biol Eng Comput* **44**:1-2, pp. 69–78. ISSN: 0140-0118. DOI: 10.1007/s11517-005-0012-2.

Fabietti, P. G., V. Canonico, M. Orsini-Federici, E. Sarti, and M. Massi-Benedetti (2007). "Clinical Validation of a New Control-Oriented Model of Insulin and Glucose Dynamics in Subjects with Type 1 Diabetes". *Diabetes Technol Ther* **9**:4, pp. 327–338. ISSN: 1520-9156. DOI: 10.1089/dia.2006.0030.

Facchinetti, A., G. Sparacino, and C. Cobelli (2007). "Reconstruction of glucose in plasma from interstitial fluid continuous glucose monitoring data: role of sensor calibration". *J Diabetes Sci and Technol* **5**, pp. 617–623.

Farmer, T. G., T. F. Edgar, and N. A. Peppas (2009). "Effectiveness of Intravenous Infusion Algorithms for Glucose Control in Diabetic Patients Using Different Simulation Models." *Ind Eng Chem Res* **48**:9, pp. 4402–4414. ISSN: 0888-5885. DOI: 10.1021/ie800871t.

FDA (2015). *Mobile Medical Applications. Guidance for Industry and Food and Drug Administration Staff*. Tech. rep. 1741. FDA.

Finan, D. A., C. Palerm, F. J. Doyle, D. E. Seborg, H. Zisser, W. C. Bevier, and L. Jovanovic (2009). "Effect of input excitation on the quality of empirical dynamic models for type 1 diabetes". *AIChE Journal* **55**:5, pp. 1135–1146.

Finan, D. A., F. J. Doyle, C. C. Palerm, W. C. Bevier, H. C. Zisser, L. Jovanovic, and D. E. Seborg (2009). "Experimental evaluation of a recursive model identification technique for type 1 diabetes." *J Diabetes Sci and Technol* **3**:5, pp. 1192–202. ISSN: 1932-2968.

Fogt, E. J., L. M. Dodd, E. M. Jenning, and A. H. Clemens (1978). "Development and evaluation of a glucose analyzer for a glucose-controlled insulin infusion system (Biostator)". *Clin Chem* **24**:8, pp. 1366–1372. ISSN: 0009-9147.

Freckmann, G., A. Baumstark, N. Jendrike, E. Zschornack, S. Kocher, J. Tschiananga, F. Heister, and C. Haug (2010). "System Accuracy Evaluation of 27 Blood Glucose Monitoring Systems According to DIN EN ISO 15197". *Diabetes Technol Ther* **12**:3, pp. 221–231.

Galvanin, F., M. Barolo, S. Macchietto, and F. Bezzo (2009). "Optimal Design of Clinical Tests for the Identification of Physiological Models of Type 1 Diabetes Mellitus". *Ind Eng Chem Res* **48**:4, pp. 1989–2002. ISSN: 0888-5885. DOI: 10.1021/ie801209g.

Galvanin, F., M. Barolo, and F. Bezzo (2011). "Online redesign of clinical tests for the identification of type 1 diabetes models in the presence of continuous glucose monitoring systems". In: *Proc. 18th IFAC World Congress*. Milano, pp. 8328–8333.

Gani, A., A. V. Gribok, Y. Lu, W. K. Ward, R. A. Vigersky, and J. Reifman (2010). "Universal glucose models for predicting subcutaneous glucose concentration in humans". *Trans Info Tech Biomed* **14**:1, pp. 157–165. ISSN: 1089-7771. DOI: 10.1109/TITB.2009.2034141.

Gani, A., A. V. Gribok, S. Rajaraman, W. K. Ward, and J. Reifman (2009). "Predicting Subcutaneous Glucose Concentration in Humans : Data-Driven Glucose Modeling". *IEEE Trans Biomed Eng* **56**:2, pp. 246–254.

García-López, J. M., M. González-Rodriguez, M. Pazos-Couselo, F. Gude, A. Prieto-Tenreiro, and F. Casanueva (2013). "Should the amounts of fat and protein be taken into consideration to calculate the lunch prandial insulin bolus? Results from a randomized crossover trial." *Diabetes Technol Ther* **15**:2, pp. 166–71. ISSN: 1557-8593. DOI: 10.1089/dia.2012.0149.

Gentilcore, D., R. Chaikomin, K. L. Jones, A. Russo, C. Feinle-Bisset, J. M. Wishart, C. K. Rayner, and M. Horowitz (2006). "Effects of fat on gastric emptying of and the glycemic, insulin, and incretin responses to a carbohydrate meal in type 2 diabetes". *J Clin Endocrin Metabol* **91**:6, pp. 2062–2067. ISSN: 0021972X. DOI: 10.1210/jc.2005-2644.

Georga, E., V. Protopappas, A. Guillen, G. Fico, D. Ardigo, M. T. Arredondo, T. P. Exarchos, D. Polyzos, and D. I. Fotiadis (2009). "Data mining for blood glucose prediction and knowledge discovery in diabetic patients: the METABO diabetes modeling and management system." In: *Proc. IEEE EMBS 31st Annual Int. Conf. (EMBC2009)*. Minneapolis, pp. 5633–6. ISBN: 9781424432967. DOI: 10.1109/IEMBS.2009.5333635.

Georga, E. I., V. C. Protopappas, and D. I. Fotiadis (2011). "Glucose Prediction in Type 1 and Type 2 Diabetic Patients Using Data Driven Techniques". In: Funatsu, P. K. (Ed.). *Knowledge-Oriented Applications in Data Mining*. InTech. Chap. 17. ISBN: 978-953-307-154-1.

Georga, E. I., V. C. Protopappas, D. Polyzos, and D. I. Fotiadis (2012). "A Predictive Model of Subcutaneous Glucose Concentration in Type 1 Diabetes Based on Random Forests". In: *Proc. IEEE EMBS 34th Annual Int. Conf. (EMBC2012)*, pp. 2889–2892. ISBN: 9781457717871.

Georga, E. I., V. C. Protopappas, D. Ardigò, D. Polyzos, and D. I. Fotiadis (2013). "A glucose model based on support vector regression for the prediction of hypoglycemic events under free-living conditions." *Diabetes Technol Ther* **15**:8, pp. 634–43. ISSN: 1557-8593. DOI: 10.1089/dia.2012.0285.

Gillespie, S. J., K. D. Kulkarni, and A. E. Daly (1998). "Using carbohydrate counting in diabetes clinical practice". *J Am Diet Assoc* **98**:8, pp. 897–905.

Goodwin, G. C., a. M. Medioli, D. S. Carrasco, B. R. King, and Y. J. Fu (2015). "A fundamental control limitation for linear positive systems with application to Type 1 diabetes treatment". *Automatica* **55**, pp. 73–77. ISSN: 00051098. DOI: DOI10.1016/j.automatica.2015.02.041.

Grant, M. and S. Boyd (2014). *CVX: matlab software for disciplined convex programming, version 2.1*. http://cvxr.com/cvx.

GroupHealth (2015). https://provider.ghc.org/open/. Accessed Oct 13, 2015.

Gustafsson, F. (2000). *Adaptive Filtering and Change Detection*. John Wiley & Sons, Hoboken, New Jersey, USA.

Hanas, R. and G. John (2010). "2010 consensus statement on the worldwide standardization of the hemoglobin A1C measurement." *Diabetes care* **33**:8, pp. 1903–4. ISSN: 1935-5548. DOI: 10.2337/dc10-0953.

Handelsman, Y., Z. T. Bloomgarden, G. Grunberger, and et al. (2015). "AACE / ACE Guidelines American Association of Clinical Endocrinologists and American College of Endocrinology – Clinical Practice Guidelines for Developing a Diabetes Mellitus Comprehensive Care Plan – 2015". *Endocr Pract* **21 (Suppl)**:April, pp. 1–87.

Hastie, T. J. and R. J. Tibshirani (1990). *Generalized additive models*. Vol. 43. CRC Press, Boco Raton, Florida.

Heinemann, L, C Weyer, M Rauhaus, S Heinrichs, and T Heise (1998). "Variability of the Metabolic Effect of Soluble Insulin and the Rapid-Acting Insulin Analog Insulin Aspart". *Diabetes Care* **21**:11, pp. 1910–1914.

Heinemann, L. (2002). "Variability of Insulin Absorption and Insulin Action". *Diabetes Technol Ther* **4**:5, pp. 673–682.

Heinemann, L. and D. B. Muchmore (2012). "Ultrafast-acting insulins: state of the art." *J Diabetes Sci Technol* **6**:4, pp. 728–42. ISSN: 1932-2968. DOI: 10.1177/193229681200600402.

Hejlesen, O. K., S Andreassen, R Hovorka, and D. A. Cavan (1997). "DIAS–the diabetes advisory system: an outline of the system and the evaluation results obtained so far." *Comput Meth Prog Biomed* **54**:1-2, pp. 49–58. ISSN: 0169-2607.

HemoCue Glucose 201+ Analyzer (2012). http://www.hemocue.com/.

Henriksson, F, C. D. Agardh, C Berne, J Bolinder, F Lönnqvist, P Stenström, C. G. Ostenson, and B Jönsson (2000). "Direct medical costs for patients with type 2 diabetes in Sweden." *J Intern Med* **248**:5, pp. 387–96. ISSN: 0954-6820.

Herrero, P, P. C, E Dassau, and et al (2008). "A glucose absorption model library of mixed meals for in silico evaluation of artificial beta-cell control algorithms". *J Diabetes Sci Technol* 2, A70.

Herrero, P., J. Bondia, C. C. Palerm, J. Vehí, P. Georgiou, N. Oliver, and C. Toumazou (2012). "A simple robust method for estimating the glucose rate of appearance from mixed meals." *J Diabetes Sci Technol* **6**:1, pp. 153–62. ISSN: 1932-2968.

Hildebrandt, P, K Birch, L Sestoft, and A Vølund (1984). "Dose-dependent subcutaneous absorption of porcine, bovine and human NPH insulins." *Acta Med Scand* **215**:1, pp. 69–73. ISSN: 0001-6101.

Hlebowicz, J., G. Darwiche, O. Björgell, and L.-O. Almér (2007). "Effect of cinnamon on postprandial blood glucose, gastric emptying, and satiety in healthy subjects." *Am J Clin Nutr* **85**:6, pp. 1552–6. ISSN: 0002-9165.

Hoeting, J. A., D. Madigan, A. E. Raftery, and C. T. Volinsky (1999). "Bayesian model averging: a tutorial". *Stat Sci* **14**:4, pp. 382–417.

Home, P. D. (1997). "Insulin Therapy". *International Textbook of Diabetes Mellitus*, pp. 899–928.

Hönes, J., P. Müller, and N. Surridge (2008). "The Technology Behind Glucose Meters: Test Strips". *Diabetes Technol Ther* **10**:s1, S–10–S–26. ISSN: 1520-9156. DOI: 10.1089/dia.2008.0005.

Hovorka, R., F. Shojaee-Moradie, P. V. Carroll, L. J. Chassin, I. J. Gowrie, N. C. Jackson, R. S. Tudor, A. M. Umpleby, and R. H. Jones (2002). "Partitioning glucose distribution/transport, disposal, and endogenous production during IVGTT." *Am J Physiol Endocrinol Metab* **282**:5, E992–1007. ISSN: 0193-1849. DOI: 10.1152/ajpendo.00304.2001.

Hovorka, R., V. Canonico, L. J. Chassin, U. Haueter, M. Massi-Benedetti, M. O. Federici, T. R. Pieber, H. C. Schaller, L. Schaupp, T. Vering, and M. E. Wilinska (2004). "Nonlinear model predictive control of glucose concentration in subjects with type 1 diabetes". *Physiol Meas* **25**:4, pp. 905–920. ISSN: 0967-3334. DOI: 10.1088/0967-3334/25/4/010.

Hovorka, R., L. J. Chassin, M. Ellmerer, J. Plank, and M. E. Wilinska (2008). "A simulation model of glucose regulation in the critically ill." *Physiol Meas* **29**:8, pp. 959–78. ISSN: 0967-3334. DOI: 10.1088/0967-3334/29/8/008.

Huckvale, K., S. Adomaviciute, J. T. Prieto, M. K.-S. Leow, and J. Car (2015). "Smartphone apps for calculating insulin dose: a systematic assessment". *BMC Medicine* **13**:1, p. 106. ISSN: 1741-7015. DOI: 10.1186/s12916-015-0314-7.

Humalog™ (2012). http://www.humalog.com/.

IAEA (1996). *INSAG-10. Defence in Depth in Nuclear Safety*. Tech. rep.

IAEA (2009). *Specific Safety Guide No. SSG-2. Deterministic Safety Analysis for Nuclear Power Plants*. Tech. rep.

IAEA (2010). *Specific Safety Guide No. SSG-3. Development and Application of Level 1 Probabilistic Safety Assessment for Nuclear Power Plants*. Tech. rep.

IDF (2011). *2011 Guideline for Management of PostMeal Glucose in Diabetes*. ISBN: 2930229810.

IDF (2014). *Diabetes atlas*. https://www.idf.org/sites/default/files/Atlas-poster-2014_EN.pdf. sixth edition.

Jenkins, D. J. A., T. M. S. Wolever, R. H. Taylor, H Barker, H Fielden, J. M. Baldwin, A. C. Bowling, H. C. Newman, A. L. Jenkins, and D. V. Goff (1981). "Glycemic index of foods: a physiological basis for carbohydrate exchange". *Am J Clin Nutr* **34**:3, pp. 362–366.

Jensen, K., C. Pedersen, and L. Larsen (2007). "Diasnet mobile: A personalized mobile diabetes management and advisory service". In: *Second Workshop on Personalization for E-Health*. Vol. 1.

Johansen, K, P. A. Svendsen, and B Lørup (1984). "Variations in renal threshold for glucose in Type 1 (insulin-dependent) diabetes mellitus." *Diabetologia* **26**:3, pp. 180–2. ISSN: 0012-186X.

Johansson, R. (2009). *System Modeling & Identification*. KFS AB.

Jones, T. W., P. Paul, R. S. Sherwin, D. E. A., O. Peter, F. Frazer, G. Byrne, S. Stick, and W. V. Tamborlane (1998). "Decreased epinephrine responses to hypoglycemia during sleeep". *N Engl J Med* **338**:23, pp. 1657–1662.

Joslin Diabetes Center (2015). Accessed Oct 13, 2015.

Kahn, C. R. (1997). "Insulin Receptors and Insulin Signaling in Normal and Disease States". *International Textbook of Diabetes Mellitus*, pp. 437–467.

Kanderian, S. S., S. Weinzimer, G. Voskanyan, and G. M. Steil (2009). "Identification of intraday metabolic profiles during closed-loop glucose control in individuals with type 1 diabetes." *J Diab Sci Technol* **3**:5, pp. 1047–57. ISSN: 1932-2968.

Keenan, D. B., J. J. Mastrototaro, G. Voskanyan, and G. M. Steil (2009). "Delays in minimally invasive continuous glucose monitoring devices : a review of current technology". *J Diabetes Sci and Technol* **3**:5, pp. 1207–1214.

Keener, J. and J. Sneyd (2009). *Mathematical Physiology: II: Systems Physiology*. Interdisciplinary Applied Mathematics. Springer-Verlag New York. ISBN: 9780387793887.

Kildegaard, J, J Randlov, J. U. Poulsen, and O. K. Hejlesen (2007). "The impact of non-model-related variability on blood glucose prediction". *Diabetes Technol Ther* **9**:4, pp. 363–371. ISSN: 1520-9156. DOI: 10.1089/dia.2006.0039.

Kirchsteiger, H., G. C. Estrada, S. Pölzer, E. Renard, and L. Del Re (2011). "Estimating Interval Process Models for Type 1 Diabetes for Robust Control Design". In: *Proc. IFAC World Congress 2011*. Milano, pp. 11761–11766.

Kirchsteiger, H., R. Johansson, E. Renard, and L. Del Re (2014). "Continuous-time interval model identification of blood glucose dynamics for type 1 diabetes". *Int J Control* **0**:January 2015, pp. 1–13. ISSN: 0020-7179.

Kolter, J. Z. and M. A. Maloof (2003). "Dynamic weighted majority: a new ensemble method for tracking concept drift". In: *Proc IEEE Int Conf on Data Mining*. IEEE Computer Society, Los Alamitos, CA, USA, pp. 123–130. ISBN: 0-7695-1978-4. DOI: http://doi.ieeecomputersociety.org/10.1109/ICDM.2003.1250911.

Kovatchev, B. P., D. J. Cox, L. A. Gonder-Frederick, and W. L. Clarke (1997). "Symmetrization of the Blood Glucose Measurement Scale and Its Applications". *Diabetes Care* **20**, pp. 1655–1658.

Kovatchev, B. P., C. King, M. Breton, S. Anderson, and W. Clarke (2006). "Clinical assessment and mathematical modeling of the accuracy of continuous glucose sensors (cgs)". In: *Proc. IEEE EMBS 28th Annual Int. Conf. (EMBC2006)*. New York, pp. 71–74.

Kovatchev, B. P., D. Shields, and M. Breton (2009). "Graphical evaluation of continuous glucose sensing time lag". *Diabetes Technol Ther* **11**:3, pp. 139–143.

Kovatchev, B. P., D. J. Cox, L. S. Farhy, M. Straume, L. Gonder-Frederick, and W. L. Clarke (2000). "Episodes of severe hypoglycemia in type 1 diabetes are preceded and followed within 48 hours by measurable disturbances in blood glucose". *J Clin Endocrin Metabol* **85**:11, pp. 4287–4292. ISSN: 0021972X. DOI: 10.1210/jc.85.11.4287.

Kovatchev, B., M. Straume, D. Cox, and L. Farhy (2000). "Risk analysis of blood glucose data: a quantitative approach to optimizing the control of insulin dependent diabetes". *J Theor Med* **3**, pp. 1–10.

Kovatchev, B., C. Breton, C. Dalla Man, and C. Cobelli (2008). *In Silico model and computer simulation environment approximating the human glucose/insulin utilization*. Tech. rep. Food and Drug Administration Master File MAF 1521.

Laguna, A., P. Rossetti, F. Ampudia-Blasco, J. Vehi, and J. Bondia (2010). "Optimal design for individual model identification based on ambulatory continuous glucose monitoring in patients with type 1 diabetes". In: *Proc UKACC Int Conf Control 2010*, pp. 1–6. DOI: 10.1049/ic.2010.0349.

Lam, T. K., A Carpentier, G. F. Lewis, G van de Werve, I. G. Fantus, and A Giacca (2003). "Mechanisms of the free fatty acid-induced increase in hepatic glucose production". *Am J Physiol Endocrinol Metab* **284**:5, E863–73. ISSN: 0193-1849. DOI: 10.1152/ajpendo.00033.2003.

Landin-Olsson, M. (2002). "Latent Autoimmune Diabetes in Adults". *Ann N Y Acad Sci* **958**:1, pp. 112–116. ISSN: 1749-6632. DOI: 10.1111/j.1749-6632.2002.tb02953.x.

Lane, J. D., M. N. Feinglos, and R. S. Surwit (2008). "Caffeine increases ambulatory glucose and postprandial responses in coffee drinkers with type 2 diabetes". *Diabetes Care* **31**:2, pp. 221–222. ISSN: 01495992. DOI: 10.2337/dc07-1112.

Lantus™ (2012). http://www.lantus.com/.

Leal, Y., W Garcia-Gabin, and J. Bondia (2010). "Real-time glucose estimation algorithm for continuous glucose monitoring using autoregressive models". *J Diabetes Sci and Technol* **4**:2, pp. 391–403.

Lee, H., B. A. Buckingham, D. M. Wilson, and B. W. Bequette (2009). "A closed-loop artificial pancreas using model predictive control and a sliding meal size estimator." *J Diabetes Sci and Technol* **3**:5, pp. 1082–90. ISSN: 1932-2968.

Lehmann, E. D. (1994). "AIDA : an interactive diabetes advisor". *Comp Meth Prog Biomed* **2607**:93, pp. 183–203.

Lehmann, E. D. and T Deutsch (1992). "A physiological model of glucose-insulin interaction in type 1 diabetes mellitus". *J Biomed Eng* **14**, pp. 235–242.

Lehmann, E., I. Hermanyi, and T. Deutsch (1994). "Retrospective validation of a physiological model of glucose-insulin interaction in type 1 diabetes mellitus". *Med Eng Phys* **16**:4, pp. 351–352. ISSN: 13504533. DOI: 10.1016/1350-4533(94)90064-7.

Levemir™ (2012). http://www.levemir.com/.

Linkura AB (2015). https://www.linkura.se/.

Littlestone, N. and M. K. Warmuth (1994). "The weighted majority algorithm". *Inform Comput* **108**:2, pp. 212–261.

Livesey, G., P. D. G. Wilson, J. R. Dainty, J. C. Brown, R. M. Faulks, M. A. Roe, T. A. Newman, J. Eagles, F. A. Mellon, and R. H. Greenwood (1998). "Simultaneous time-varying systemic appearance of oral and hepatic glucose in adults monitored with stable isotopes". *Am J Physiol Endocrinol Metab* **275**:4, pp. 717–728. ISSN: 0002-9513.

Lonergan, T., A. L. Compte, M. Willacy, J. G. Chase, G. M. Shaw, C. E. Hann, T. Lotz, J. Lin, and X.-W. Wong (2006). "A pilot study of the SPRINT protocol for tight glycemic control in critically Ill patients." *Diabetes Technol Ther* **8**:4, pp. 449–62. ISSN: 1520-9156. DOI: 10.1089/dia.2006.8.449.

Lu, Y., S. Rajaraman, W. K. Ward, R. A. Vigersky, and J. Reifman (2011). "Predicting human subcutaneous glucose concentration in real time: a universal data-driven approach." In: *Proc. IEEE EMBS 33rd Annual Int. Conf. (EMBC2011)*. Boston, pp. 7945–8. ISBN: 9781424441228. DOI: 10.1109/IEMBS.2011.6091959.

Luijf, Y. M., A. C. van Bon, J. B. Hoekstra, and J. H. Devries (2010). "Premeal injection of rapid-acting insulin reduces postprandial glycemic excursions in type 1 diabetes." *Diabetes care* **33**:10, pp. 2152–5. ISSN: 1935-5548. DOI: 10.2337/dc10-0692.

Lv, D., M. D. Breton, and L. S. Farhy (2013). "Pharmacokinetics modeling of exogenous glucagon in type 1 diabetes mellitus patients." *Diabetes Technol Ther* **15**:11, pp. 935–41. ISSN: 1557-8593. DOI: 10.1089/dia.2013.0150.

Maahs, D. M., P. Calhoun, B. A. Buckingham, H. P. Chase, I. Hramiak, J. Lum, F. Cameron, B. W. Bequette, T. Aye, T. Paul, R. Slover, R. P. Wadwa, D. M. Wilson, C. Kollman, and R. W. Beck (2014). "A randomized trial of a home system to reduce nocturnal hypoglycemia in type 1 diabetes". *Diabetes Care* **37**:7, pp. 1885–1891. ISSN: 19355548. DOI: 10.2337/dc13-2159.

Makroglou, A., J. Li, and Y. Kuang (2006). "Mathematical models and software tools for the glucose-insulin regulatory system and diabetes: an overview". *Appl Num Math*, pp. 559–573.

Man, C. D., F. Micheletto, D. Lv, M. Breton, B. Kovatchev, and C. Cobelli (2014). "The UVA/PADOVA Type 1 Diabetes Simulator: New Features." *J Diabetes Sci Technol* **8**:1, pp. 26–34. ISSN: 1932-2968. DOI: 10.1177/1932296813514502.

MathWorks (2012). *Matlab™*. www.mathworks.com. URL: {www.mathworks.com}.

Medtronic (2012). http://www.medtronic-diabetes.se/.

Mitsis, G. D. and V. Z. Marmerelis (2014). "Data-driven modeling for diabetes". In: Mitsis, G. D. et al. (Eds.). Lecture Notes in Bioengineering. Springer-Verlag Berlin Heidelberg. Chap. 1. Data-Driven and Minimal-Type Compartmental Insulin-Glucose Models: Theory and Applications, pp. 1–35.

Mokan, M., A. Mitrakou, T. Veneman, C. Ryan, M. Korytkowski, P. Cryer, and J. Gerich (1994). "Hypoglycemia unawareness in IDDM". *Diabetes Care* **17**:12, pp. 1397–1403. DOI: 10.1016/S0168-8227(11)70020-1.

Morrow, L., D. B. Muchmore, M. Hompesch, E. A. Ludington, and D. E. Vaughn (2013). "Comparative pharmacokinetics and insulin action for three rapid-acting insulin analogs injected subcutaneously with and without hyaluronidase." *Diabetes care* **36**:2, pp. 273–5. ISSN: 1935-5548. DOI: 10.2337/dc12-0808.

Mudaliar, S. R., F. A. Lindberg, M. Joyce, P. Beerdsen, P. Strange, A. Lin, and R. R. Henry (1999). "Insulin Aspart (B28 Asp-Insulin): A Fast-Acting Analog of Human Insulin". *Diabetes care* **22**:9, pp. 1501–1506.

Natali, A., A. Gastaldelli, S. Camastra, A. M. Sironi, E. Toschi, A. Masoni, E. Ferrannini, and A. Mari (2000). "Dose-response characteristics of insulin action on glucose metabolism: a non-steady-state approach". *Am J Physiol Endocrinol Metab* **278**:5, E794–E801.

National Security Agency (2015). https://www.nsa.gov/ia/_files/support/defenseindepth.pdf.

Nationella Programrådet Diabetes (2014). *Behandlingsstrategi Typ 1-diabetes*. Ed. by A. Petersson. 5334.

Nauck, M. A., B. Baller, and J. J. Meier (2004). "Gastric inhibitory polypeptide and glucagon-like peptide-1 in the pathogenesis of type 2 diabetes." *Diabetes* **53 Suppl 3**:December, S190–6. ISSN: 0012-1797.

Naumova, V, S. V. Pereverzyev, and S Sivananthan (2012). "A meta-learning approach to the regularized learning-Case study: blood glucose prediction." *Neural Netw* **33**, pp. 181–93. ISSN: 1879-2782. DOI: 10.1016/j.neunet.2012.05.004.

New, J. P., R. Ajjan, A. F. H. Pfeiffer, and G. Freckmann (2015). "Continuous glucose monitoring in people with diabetes: the randomized controlled Glucose Level Awareness in Diabetes Study (GLADIS)". *Diabet Med* **32**, pp. 609–617. ISSN: 07423071. DOI: 10.1111/dme.12713.

NICE guideline (2015). *Type 1 diabetes in adults: diagnosis and management*. http://www.nice.org.uk/guidance/ng17. Published 26 August 2015.

NIH online (2015). http://diabetes.niddk.nih.gov/dm/pubs/medicines_ez/insert_C.aspx. Accessed Oct 13, 2015.

Novo Nordisk (2014). http://www.novonordisk.com/diabetes/public/diabetestools/insulins/default.asp. Accessed Dec 30, 2014.

Novolog™ (2015). http://www.novolog.com/. Accessed Nov 9, 2015.

Nucci, G and C Cobelli (2000). "Models of subcutaneous insulin kinetics. a critical review". *Comp Meth Prog Biomed* **62**, pp. 249–257.

Nussey, S. and S. Whitehead (2001). *Endocrinology: An Integrated Approach*. BIOS Scientific Publishers Limited.

O'Connell, M. a. and H. R. Gilbertson (2008). "Optimizing Postprandial Glycemia in Pediatric Patients With Type 1 Diabetes Using Insulin Pump Therapy". *Diabetes care* **31**:8. DOI: 10.2337/dc08-0306.Clinical.

Ohlsson, H, L. Ljung, and S. Boyd (2010). "Segmentation of ARX-models using sum-of-norms regularization". *Automatica* **46**:6, 1107—1111.

Oza, N. (2005). "Online bagging and boosting". In: *Systems, Man and Cybernetics, 2005 IEEE Int. Conf. on*. Waikaloa, HI, 2340 –2345 Vol. 3.

Palerm, C., H Zisser, W. Bevier, and L Jovanovič (2007). "Prandial insulin dosing using run-to-run control". *Diabetes Care* **30**:5. DOI: 10.2337/dc06-2115.A.

Palerm, C. C. and B. W. Bequette (2007). "Hypoglycemia detection and prediction using continuous glucose monitoring-a study on hypoglycemic clamp data." *J Diabetes Sci Technol* **1**:5, pp. 624–9. ISSN: 1932-2968.

Palerm, C. C., J. P. Willis, J. Desemone, and B. W. Bequette (2005). "Hypoglycemia Prediction and Detection Using Optimal Estimation". *Diabetes Technol Ther* **7**:1, pp. 3–14.

Pappada, S. M., B. D. Cameron, P. M. Rosman, R. E. Bourey, T. J. Papadimos, W. Olorunto, and M. J. Borst (2011). "Neural network-based real-time prediction of glucose in patients with insulin-dependent diabetes." *Diabetes Technol Ther* **13**:2, pp. 135–41.

Percival, M., W. Bevier, and Y Wang (2010). "Modeling the effects of subcutaneous insulin administration and carbohydrate consumption on blood glucose". *J Diabetes Sci Technol* **4**:5, pp. 1214–1228.

Percival, M., Y. Wang, B. Grosman, E. Dassau, H. Zisser, L. Jovanovič, and F. Doyle (2011). "Development of a multi-parametric model predictive control algorithm for insulin delivery in type 1 diabetes mellitus using clinical parameters". *J Proc Control* **21**:3, pp. 391–404. ISSN: 09591524. DOI: 10.1016/j.jprocont.2010.10.003.

Pérez-Gandía, C, A Facchinetti, G Sparacino, C Cobelli, E. J. Gómez, M Rigla, A. D. Leiva, and M. E. Hernando (2010). "Artificial Neural Network Algorithm for Online Glucose". *Diabetes Technol Ther* **12**:1, pp. 81–88.

Perriello, G., P. De Feo, E. Torlone, C. Fanelli, F. Santeusanio, P. Brunetti, and G. B. Bolli (1991). "The dawn phenomenon in Type 1 (insulin-dependent) diabetes mellitus: magnitude, frequency, variability, and dependency on glucose counterregulation and insulin sensitivity". *Diabetologia* **34**:1, pp. 21–28.

Plank, J., A. Wutte, G. Brunner, A. Siebenhofer, B. Semlitsch, R. Sommer, S. Hirschberger, and T. R. Pieber (2002). "A direct comparison of insulin aspart and insulin lispro in patients with type 1 diabetes." *Diabetes Care* **25**:11, pp. 2053–7. ISSN: 0149-5992.

Plank, J., M. Bodenlenz, F. Sinner, C. Magnes, E. Görzer, W. Regittning, L. A. Endahl, E. Draeger, M. Zdravkovic, and T. Pieber (2005). "A Double-Blind, Randomized, Dose-Response Study Investigating the Pharmacodynamic and Pharmacokinetic Properties of the Long-Acting Insulin". *Diabetes Care* **28**:5, pp. 1107–1112.

Plougmann, S. r., O. Hejlesen, B. Turner, D. Kerr, and D. Cavan (2003). "The effect of alcohol on blood glucose in Type 1 diabetes—metabolic modelling and integration in a decision support system". *Int J Med Inform* **70**:2-3, pp. 337–344. ISSN: 13865056. DOI: 10.1016/S1386-5056(03)00038-8.

Poolsup, N., N. Suksomboon, and A. Kyaw (2013). "Systematic review and meta-analysis of the effectiveness of continuous glucose monitoring (CGM) on glucose control in diabetes". *Diabetol Metabol Syndr* **5**:1, p. 39. ISSN: 1758-5996. DOI: 10.1186/1758-5996-5-39.

Prigeon, R. L., M. E. Røder, D Porte, and S. E. Kahn (1996). "The effect of insulin dose on the measurement of insulin sensitivity by the minimal model technique. Evidence for saturable insulin transport in humans." *J Clin Invest* **97**:2, pp. 501–7. ISSN: 0021-9738. DOI: 10.1172/JCI118441.

Puckett, W. R. (1992). *Dynamic Modeling of Diabetes Mellitus*. Ph.D. thesis. Department of Chemical Engineering, University of Wisconsin-Madison, Madison.

Raftery, A. E., T. Gneiting, F. Balabdaoui, and M. Pololakowski (2005). "Using Bayesian Model Averaging to Calibrate Forecast Ensembles". *Mon Weather Rev* **133**, pp. 1155–1174.

Raftery, A. E., M. Kárný, and P. Ettler (2010). "Online prediction under model uncertainty via dynamic model averaging: application to a cold rolling mill". *Technometrics* **52**:1, pp. 52–66.

Raftery, A. E. and S. Lewis (1992). "How many iterations in the gibbs sampler?" In: *In Bayesian Statistics 4*. Oxford University Press, pp. 763–773.

Ramotowska, A. and A. Szypowska (2014). "Bolus calculator and wirelessly communicated blood glucose measurement effectively reduce hypoglycaemia in type 1 diabetic children – randomized controlled trial." *Diabetes Metab Res Rev* **30**:2, pp. 146–153.

Rave, K. (2006). "Renal glucose excretion as a function of blood glucose concentration in subjects with type 2 diabetes–results of a hyperglycaemic glucose clamp study". *Nephrol Dial Transplant* **21**:8, pp. 2166–2171. ISSN: 0931-0509. DOI: 10.1093/ndt/gfl175.

Rave, K., S. Bott, L. Heinemann, S. Sha, R. H. Becker, S. A. Willavize, and T. Heise (2005). "Time-Action Profile of Inhaled Insulin in Comparison With Subcutaneously Injected Insulin Lispro and Regular Human Insulin". *Diabetes care* **28**:5, pp. 1077–1082.

Rebrin, K and G. M. Steil (2000). "Can interstitial glucose assessment replace blood glucose measurements?" *Diabetes Technol Ther* **2**:3, pp. 461–72. ISSN: 1520-9156.

Regional Ethical Review Board in Lund (2014). Accessed Dec 30, 2014.

Revert, a., R. Calm, J. Vehi, and J. Bondia (2011). "Calculation of the Best Basal–Bolus Combination for Postprandial Glucose Control in Insulin Pump Therapy". *IEEE Trans Biomed Eng* **58**:2, pp. 274–281. ISSN: 0018-9294. DOI: 10.1109/TBME.2010.2058805.

Revital, N and P Moshe (2014). "Artificial pancreas: fuzzy logic and control of glycemia". *Curr Opin Endocrinol Diabetes Obes* **21**:4, pp. 251–6.

Rizza, R., L. J. Mandarino, and J. E. Gerich (1981). "Dose-response characteristics for effects of insulin on production and utilization of glucose in man". *Am J Phys Endocrinol Metab* **240**:6, E630–E639.

Rossetti, P., F. J. Ampudia-Blasco, A. Laguna, A. Revert, J. Vehì, J. F. Ascaso, and J. Bondia (2012). "Evaluation of a Novel Continuous Glucose Monitoring-Based Method for Mealtime Insulin Dosing—the iBolus —in Subjects with Type 1 Diabetes Using Continuous Subcutaneous Insulin Infusion Therapy: A Randomized Controlled Trial". *Diabetes Technol Ther* **14**:11, pp. 1043–1052. ISSN: 1520-9156. DOI: 10.1089/dia.2012.0145.

Roy, A. and R. S. Parker (2006a). "Dynamic Modeling of Free Fatty Acid, Glucose, and Insulin: An Extended "Minimal Model"". *Diabetes Technol Ther* **8**:6, pp. 617–626.

Roy, A. and R. S. Parker (2006b). "Mixed meal modeling and disturbance rejection in type i diabetes patients". In: *Proc. IEEE EMBS 28th Annual Int. Conf. (EMBC2006)*. New York, pp. 323–326.

Roy, A. and R. S. Parker (2006c). "Mixed meal modeling and disturbance rejection in Type I diabetic patients". *Proc. IEEE EMBS 28th Annual Int. Conf. (EMBC2006)*, pp. 323–326. ISSN: 05891019. DOI: 10.1109/IEMBS.2006.260372.

Roy, A. and R. S. Parker (2007). "Dynamic Modeling of Exercise Effects on Plasma Glucose and Insulin Levels". *J Diabetes Sci and Technol* **1**:3, pp. 338–347.

Salzsieder, E, G Albrecht, U Fischer, and E.-J. Freyse (1985). "Kinetic Modeling of the Glucoregulatory System to Improve Insulin Therapy". *IEEE Trans Biomed Eng* **BME-32**:10, pp. 846–855.

Salzsieder, E, L Vogt, K.-D. Kohnert, P Heinke, and P Augstein (2011). "Model-based decision support in diabetes care." *Comput Meth Prog Biomed* **102**:2, pp. 206–18. ISSN: 1872-7565. DOI: 10.1016/j.cmpb.2010.06.001.

Schmelzeisen-Redeker, G., A. Staib, M. Strasser, U. Müller, and M. Schoemaker (2013). "Overview of a novel sensor for continuous glucose monitoring." *J Diabetes Sci Technol* **7**:4, pp. 808–14. ISSN: 1932-2968. DOI: 10.1177/193229681300700402.

Schmidt, S. and K. Nørgaard (2014). "Bolus calculators." *J Diabetes Sci Technol* **8**:5, pp. 1035–1041.

Schvarcz, E, M Palmér, J Aman, M Horowitz, M Stridsberg, and C Berne (1997). "Physiological hyperglycemia slows gastric emptying in normal subjects and patients with insulin-dependent diabetes mellitus." *Gastroenterology* **113**:1, pp. 60–6. ISSN: 0016-5085.

Senseonics (2015). http://senseonics.com/uncategorized/senseonics-rubin-medical-partner-scandinavia-commercialize-cgm-product.

Shapira, G., O. Yodfat, A. HaCohen, P. Feigin, and R. Rubin (2010). "Bolus guide: a novel insulin bolus dosing decision support tool based on selection of carbohydrate ranges." *J Diabetes Sci and Technol* **4**:4, pp. 893–902. ISSN: 1932-2968.

Shashaj, B, E Busetto, and N Sulli (2008). "Benefits of a bolus calculator in pre- and postprandial glycaemic control and meal flexibility of paediatric patients using continuous subcutaneous insulin infusion (CSII)." *Diabet Med* **25**:9, pp. 1036–42. ISSN: 1464-5491. DOI: 10.1111/j.1464-5491.2008.02549.x.

Shoelson, S. E. and P. A. Halban (1994). "Insulin Biosynthesis and Chemistry". *Joslin's Diabetes Mellitus*, pp. 29–55.

Shumway, R. H. and D. S. Stoffer (1982). "An approach to time series smoothing and forecasting using the EM algorithm". *J Time Ser Anal* **3**:4, pp. 253–264. ISSN: 01439782. DOI: 10.1111/j.1467-9892.1982.tb00349.x.

Siler, S. Q., R. A. Neese, M. P. Christiansen, M. K. Hellerstein, Q Scott, and M. P. Chris (1998). "The inhibition of gluconeogenesis following alcohol in humans". *Am J Physiol* **275**, E897–E907.

Smart, C. E., K. Ross, J. A. Edge, B. R. King, P. McElduff, and C. E. Collins (2010). "Can children with Type 1 diabetes and their caregivers estimate the carbohydrate content of meals and snacks?" *Diabetic Medicine* **27**:3, pp. 348–353. ISSN: 07423071. DOI: 10.1111/j.1464-5491.2010.02945.x.

Sorensen, J. T. (1985). *A physiologic model of glucose metabolism in man and its use to design and assess improved insulin therapies for diabetes*. PhD thesis. Department of Chemical Engineering, Massachusetts Institute of Technologhy, Cambridge.

Sparacino, G., F. Zanderigo, S. Corazza, A. Maran, A. Fachinetti, and C. Cobelli (2007). "Glucose concentration can be predicted ahead in time from continuous glucose monitoring sensor time-series". *IEEE Trans Biomed Eng* **54**:5, pp. 931–937.

Srinivasan, A., J. B. Lee, E. Dassau, and F. J. Doyle (2014). "Novel Insulin Delivery Profiles for Mixed Meals for Sensor-Augmented Pump and Closed-Loop Artificial Pancreas Therapy for Type 1 Diabetes Mellitus". *J Diabetes Sci Technol* **8**:5, pp. 957–968. ISSN: 1932-2968. DOI: 10.1177/1932296814543660. URL: http://dst.sagepub.com/lookup/doi/10.1177/1932296814543660.

St John, A., W. A. Davis, C. P. Price, and T. M. E. Davis (2010). "The value of self-monitoring of blood glucose: a review of recent evidence". *J Diabetes Complicat* **24**:2, pp. 129–41. ISSN: 1873-460X.

Ståhl, F (2003). *Diabetes Mellitus Modelling Based on Blood Glucose Measurements*. Master Thesis TFRT-5703. Dept. Automatic Control, Lund University, Sweden.

Ståhl, F. (2012). *Diabetes Mellitus Glucose Prediction by Linear and Bayesian Ensemble Modeling*. Licentiate Thesis TFRT--3255--SE. Department of Automatic Control, Lund University, Sweden.

Ståhl, F. and R. Johansson (2009). "Diabetes mellitus modeling and short-term prediction based on blood glucose measurements". *Math Biosci* **217**, pp. 101–117.

Stork, A. D., H. Kemperman, D. W. Erkelens, and T. F. Veneman (2005). "Comparison of the accuracy of the Hemocue glucose analyser with the Yellow Springs Instrument glucose oxidase analyser, particularly in hypoglycemia". *Eur J Endocrionol* **153**, pp. 275–281.

Takagi, T. and M. Sugeno (1985). "Fuzzy identification of system and its applications to modelling and control". *EEE Trans Syst Man Cybern Syst* **SMC-15**, pp. 116–132.

Taniguchi, C. M., B. Emanuelli, and C. R. Kahn (2006). "Critical nodes in signalling pathways: insights into insulin action". *Nat Rev Mol Cell Bio* **7**:2, pp. 85–96. ISSN: 1471-0072. DOI: 10.1038/nrm1837.

The DIAdvisor Consortium (2012). *Final publishable summary report*. http://cordis.europa.eu/results/home_en.html.

The Swedish National Board of Health and Welfare (2009a). *Folkhälsorapporten 2009*. http://www.socialstyrelsen.se/.

The Swedish National Board of Health and Welfare (2009b). *Öppna jämförelser av hälso- och sjukvårdens kvalitet och effektivitet jämförelser mellan landsting 2009*. http://www.socialstyrelsen.se/.

Tonyushkina, K. and J. H. Nichols (2009). "Glucose meters: a review of technical challenges to obtaining accurate results." *J Diabetes Sci Technol* **3**:4, pp. 971–80. ISSN: 1932-2968.

Toumaz (2012). http://www.toumaz.com.

Turksoy, K., E. S. Bayrak, L. Quinn, E. Littlejohn, D. Rollins, and A. Cinar (2013). "Hypoglycemia Early Alarm Systems Based on Multivariable Models". *Ind Eng Chem Res* 52, pp. 12329–12336.

Turner, B. C., E. Jenkins, D. Kerr, R. S. Sherwin, and D. A. Cavan (2001). "The Effect of Evening Alcohol Consumption on Next-Morning Glucose Control in Type 1 Diabetes". *Diabetes Care* **24**:11, pp. 1888–1893. ISSN: 0149-5992. DOI: 10.2337/diacare.24.11.1888.

U.S. NRC Fire Protection (2015). http://www.nrc.gov/reactors/operating/ops-experience/fire-protection/defense-in-depth.html.

Vaddiraju, S., D. J. Burgess, I. Tomazos, F. C. Jain, and F. Papadimitrakopoulos (2010). "Technologies for continuous glucose monitoring: current problems and future promises." *J Diabetes Sci and Technol* **4**:6, pp. 1540–62. ISSN: 1932-2968.

Van Cauter, E, K. S. Polonsky, and A. J. Scheen (1997). "Roles of circadian rhythmicity and sleep in human glucose regulation." *Endocrin Rev* **18**:5, pp. 716–38. ISSN: 0163-769X.

Van den Berghe, G, P Wouters, F Weekers, C Verwaest, F Bruyninckx, M Schetz, D Vlasselaers, P Ferdinande, P Lauwers, and R Bouillon (2001). "Intensive Insulin Therapy in Critically Ill Patients". *N Engl J Med* **345**:19, pp. 1359–1367.

Vashist, S. (2013). "Continuous Glucose Monitoring Systems: A Review". *Diagnostics* **3**:4, pp. 385–412. ISSN: 2075-4418. DOI: 10.3390/diagnostics3040385.

Vella, A., G. Bock, P. D. Giesler, D. B. Burton, D. B. Serra, M. L. Saylan, B. E. Dunning, J. E. Foley, R. A. Rizza, and M. Camilleri (2007). "Effects of Dipeptidyl Peptidase-4 Inhibition on Gastrointestinal Function, Meal Appearance, and Glucose Metabolism in Type 2 Diabetes". *Diabetes* **56**:May, pp. 1475–1480. DOI: 10.2337/db07-0136.A.V..

Veneman, T., A. Mitrakou, M. Mokan, P. Cryer, and J. Gerich (1993). "Induction of Hypoglycemia Unawareness by Asymptomatic Nocturnal Hypoglycemia". *Diabetes* **42**:September, pp. 1233–1237.

VivoMetrics (2012). http://vivonoetics.com/products/sensors/lifeshirt/.

Voulgari, C., S. Pagoni, S. Paximadas, and A. I. Vinik (2012). ""Brittleness" in diabetes: easier spoken than broken." *Diabetes Technol Ther* **14**:9, pp. 835–48. ISSN: 1557-8593. DOI: 10.1089/dia.2012.0058.

Walsh, J., R. Roberts, and T. Bailey (2010). "Guidelines for Insulin Dosing in Continuous Subcutaneous Insulin Infusion Using New Formulas from a Retrospective Study of Individuals with Optimal Glucose Levels". *J Diabetes Sci Technol* **4**:5, pp. 1174–1181. ISSN: 1932-2968.

Walsh, J., R. Roberts, and L. Heinemann (2014). "Confusion Regarding Duration of Insulin Action: A Potential Source for Major Insulin Dose Errors by Bolus Calculators." *J Diabetes Sci Technol* **8**:1, pp. 170–178. ISSN: 1932-2968.

Walsh, R. and R. Roberts (2012). *Pumping Insulin*. 5th ed. Torrey Pines Press, 1030 West Upas Street.

Warren, R. E. and B. M. Frier (2005). "Hypoglycaemia and cognitive function". *Diabetes Obes Metab* **7**:5, pp. 493–503. ISSN: 1462-8902. DOI: 10.1111/j.1463.

Wild, S., G. Roglic, A. Green, R. Sicree, and H. King (2004). "Global Prevalence of Diabetes Estimates for the year 2000 and projections for 2030". *Diabetes Care* **27**:5, pp. 1047–1053.

Wilinska, M. E., L. J. Chassin, H. C. Schaller, L. Schaupp, T. R. Pieber, and R. Hovorka (2005). "Insulin kinetics in type-1 diabetes: continuous and bolus delivery of rapid acting insulin". *IEEE Trans Biomed Eng* **52**:1, pp. 3–12.

Wilinska, M. E., L. J. Chassin, C. L. Acerini, J. M. Allen, D. B. Dunger, and R. Hovorka (2010). "Simulation environment to evaluate closed-loop insulin delivery systems in type 1 diabetes." *J Diab Sci Technol* **4**:1, pp. 132–44. ISSN: 1932-2968.

Wolpert, H. A., A. Atakov-Castillo, S. A. Smith, and G. M. Steil (2013). "Dietary Fat Acutely Increases Glucose Concentrations and Insulin Requirements in PatientsWith Type1 Diabetes". *Diabetes care* **36**:April, pp. 810–816. DOI: 10.2337/dc12-0092..

Wood, I. S. and P. Trayhurn (2003). "Glucose transporters (GLUT and SGLT): expanded families of sugar transport proteins". *Br J Nutr* **89**:01, p. 3. ISSN: 0007-1145. DOI: 10.1079/BJN2002763.

Worthington, D. R. L. (1990). "The use of models in the self-management of insulin-dependent diabetes mellitus". *Comp Meth Prog Biomed* **32**, pp. 233–239.

Worthington, D. R. L. (1997). "Minimal Model of Food Absorption in the Gut". *Med Inform* **22**:1, pp. 35–45.

Yale, J.-F. (2004). "Nocturnal hypoglycemia in patients with insulin-treated diabetes." *Diabetes Res Clin Pract* **65 Suppl 1**, S41–6. ISSN: 0168-8227. DOI: 10.1016/j.diabres.2004.07.007.

Yellow Springs Instrument (2012). http://www.ysilifesciences.com/.

Yki-Järvinen, H. (1990). "Acute and chronic effects of hyperglycaemia on glucose metabolism". *Diabetologia* **33**:10, pp. 579–585.

Zecchin, C., A. Facchinetti, G. Sparacino, G. De Nicolao, and C. Cobelli (2011). "A new neural network approach for short-term glucose prediction using continuous glucose monitoring time-series and meal information". *Proc. IEEE EMBS 33rd Annual Int. Conf. (EMBC2011)*, pp. 5653–5656. DOI: 10.1109/IEMBS.2011.6091368.

Ziegler, R., D. A. Cavan, I. Cranston, K. Barnard, J. Ryder, C. Vogel, C. G. Parkin, W. Koehler, I. Vesper, B. Petersen, M. a. Schweitzer, and R. S. Wagner (2013). "Use of an insulin bolus advisor improves glycemic control in multiple daily insulin injection (MDI) therapy patients with suboptimal glycemic control: first results from the ABACUS trial." *Diabetes care* **36**:11, pp. 3613–9. ISSN: 1935-5548. DOI: 10.2337/dc13-0251.

Zisser, H., L. Robinson, W. Bevier, E. Dassau, C. Ellingsen, F. J. Doyle, and L. Jovanovic (2008). "Bolus calculator: a review of four "smart" insulin pumps." *Diabetes Technol Ther* **10**:6, pp. 441–4. ISSN: 1520-9156. DOI: 10.1089/dia.2007.0284.

Zisser, H., C. C. Palerm, W. C. Bevier, F. J. Doyle, and L. Jovanovic (2009). "Clinical update on optimal prandial insulin dosing using a refined run-to-run control algorithm." *J Diabetes Sci Technol* **3**:3, pp. 487–91. ISSN: 1932-2968.